

VOL. 4
No. 22

METEOROLOGICAL MONOGRAPHS

PUBLISHED BY THE AMERICAN METEOROLOGICAL SOCIETY

Topics in Engineering Meteorology

by

**J. M. Biggs, G. S. Vincent,
A. K. Blackadar, H. E. Cramer,
E. P. Segner, E. Cohen, C. C. Bates and
M. A. Kohler, S. A. Changnon, F. A. Hoff
and R. G. Semonin, M. K. Thomas,
R. W. Gerdel, H. A. Murphy,
R. A. Boyd, I. Solomon and
W. C. Spreen, O. L. Stokstad,
and F. E. Legg**

MAY 1960

METEOROLOGICAL MONOGRAPHS

BOARD OF EDITORS

Assistant Editor

THOMAS A. GLEESON
Florida State University

Editor-in-Chief

WERNER A. BAUM
Florida State University

Assistant to the Editor

WHEATON M. COWARD, JR.
American Meteorological Society

Associate Editors

DAVID ATLAS
A. F. Cambridge Research Center

GERALD L. BARGER
U. S. Weather Bureau

LOUIS J. BATTAN
University of Arizona

FREDERIC A. BERRY
Aerometric Research Inc.

ROSCOE R. BRAHAM, JR.
University of Chicago

RICHARD A. CRAIG
Florida State University

GEORGE P. CRESSMAN
U. S. Weather Bureau

A. NELSON DINGLE
University of Michigan

GORDON E. DUNN
U. S. Weather Bureau

ROBERT G. FLEACLE
University of Washington

F. N. FRENKIEL
J. Hopkins Applied Physics Lab.

W. LAWRENCE GATES
University of California at L.A.

JOSEPH J. GEORGE
Eastern Air Lines

MAURICE H. HALSTEAD
Navy Electronics Laboratory

BERNHARD HAURWITZ
University of Colorado

SEYMOUR L. HESS
Florida State University

HENRY G. HOUGHTON
Mass. Institute of Technology

WOODROW C. JACOBS
Library of Congress

HELMUT E. LANDSBERG
U. S. Weather Bureau

JAMES E. MILLER
New York University

JEROME NAMIAS
U. S. Weather Bureau

HANS NEUBERGER
Pennsylvania State University

CHESTER W. NEWTON
University of Chicago

HANS A. PANOFSKY
Pennsylvania State University

NORMAN G. PHILLIPS
Mass. Institute of Technology

RICHARD J. REED
University of Washington

HERBERT RIEHL
University of Chicago

HENRY STOMMEL
Woods Hole Ocean. Instn.

VERNER E. SUOMI
University of Wisconsin

HARRY WEXLER
U. S. Weather Bureau

METEOROLOGICAL MONOGRAPHS, a serial publication of the American Meteorological Society, serves as a medium for original papers, survey articles, and other material in meteorology and closely related fields; it is intended for material which is better suited in length or nature for publication in monograph form than for publication in the *Journal of Meteorology*, in the *Bulletin of the American Meteorological Society* or in *Weatherwise*. A METEOROLOGICAL MONOGRAPH may consist of a single paper or of a group of papers concerned with a single general topic.

INFORMATION FOR CONTRIBUTORS

Manuscripts for the METEOROLOGICAL MONOGRAPHS should be sent directly to the Editor: Werner A. Baum, Florida State University, Tallahassee, Florida. Manuscripts may be submitted by persons of any nationality who are members or nonmembers of the Society, but only manuscripts in the English language can be accepted. Every manuscript submitted is reviewed and in no case does the editor advise the author as to acceptability until at least one review has been obtained. Authors will receive galley proof but not page proof.

Manuscripts. The manuscript must be complete and in final form when submitted. It must be original typewritten copy on one side only of white paper sheets $8\frac{1}{2} \times 11$ inches, consecutively numbered; double spacing and wide margins are essential. Carbon copy and single spacing are not acceptable.

Each manuscript may include the following components, which should be presented in the order listed. Of these, the table of contents; title, author's name and affiliation; abstract; text; references; and legends are obligatory.

1. Title page. This will be prepared by the editor if the manuscript is accepted for publication.

2. Preface or foreword. A preface may be contributed by the sponsors of the investigation, or by some other interested group or individual. The preface should indicate the origin of the study and should present other facts of general interest which emphasize its importance and significance.

3. Table of contents. Chapter, section, and subsection headings should all be listed in the table of contents.

4. Title, author's name and affiliation. The affiliation should be stated as concisely as possible and should not constitute a complete address. The date of receipt of the manuscript is supplied by the editor.

5. Abstract. This should summarize the principal hypotheses, methods, and conclusions of the investigation. It should not include mathematical symbols or references to equation numbers, since the abstract is sometimes quoted verbatim in abstracting or reviewing journals.

6. Text. For one of a group of papers which together constitute a MONOGRAPH, it is sufficient to divide the text into sections, each with a separate heading, numbered consecutively. The section heading should be placed on a separate line, flush with the margin, and should not be underlined. Subsection headings, if needed, should be located at the beginning of certain paragraphs and underlined.

7. References. References should be arranged alphabetically and designated by numbers. The numbers are enclosed by brackets in the text but not in the alphabetical listing. When two or more references are involved, separate the numbers by semicolons: thus, "previous investigations [3; 12; 27] have shown . . ."

Each reference listed should be complete and in the following form. For an article: author(s), year, title of article, title of serial publication (underlined), volume

METEOROLOGICAL MONOGRAPHS

Volume 4

May 1960

Number 22

Topics in Engineering Meteorology

by

**J. M. Biggs, G. S. Vincent,
A. K. Blackadar, H. E. Cramer, E. P. Segner,
E. Cohen, C. C. Bates and M. A. Kohler,
S. A. Changnon, F. A. Hoff and R. G. Semonin,
M. K. Thomas, R. W. Gerdel, A. H. Murphy,
R. A. Boyd, I. Solomon and W. C. Spreen,
O. L. Stokstad, and F. E. Legg**

**PUBLISHED BY THE AMERICAN METEOROLOGICAL SOCIETY
45 BEACON ST., BOSTON 8, MASS.**

ISBN 978-1-940033-39-6 (eBook)

DOI 10.1007/978-1-940033-39-6

METEOROLOGICAL MONOGRAPHS

BOARD OF EDITORS

Assistant Editor

THOMAS A. GLEESON
Florida State University

Editor-in-Chief

WERNER A. BAUM
Florida State University

Assistant to the Editor

WHEATON M. COWARD, JR.
American Meteorological Society

Associate Editors

DAVID ATLAS
A. F. Cambridge Research Center

GERALD L. BARGER
U. S. Weather Bureau

LOUIS J. BATTAN
University of Arizona

FREDERIC A. BERRY
Aerometric Research Inc.

ROSCOE R. BRAHAM, JR.
University of Chicago

RICHARD A. CRAIG
Florida State University

GEORGE P. CRESSMAN
U. S. Weather Bureau

A. NELSON DINGLE
University of Michigan

GORDON E. DUNN
U. S. Weather Bureau

ROBERT G. FLEAGLE
University of Washington

F. N. FRENKIEL
J. Hopkins Applied Physics Lab.

W. LAWRENCE GATES
University of California at L.A.

JOSEPH J. GEORGE
Eastern Air Lines

MAURICE H. HALSTEAD
Navy Electronics Laboratory

BERNHARD HAURWITZ
University of Colorado

SEYMOUR L. HESS
Florida State University

HENRY G. HOUGHTON
Mass. Institute of Technology

WOODROW C. JACOBS
Library of Congress

HELMUT E. LANDSBERG
U. S. Weather Bureau

JAMES E. MILLER
New York University

JEROME NAMIAS
U. S. Weather Bureau

HANS NEUBERGER
Pennsylvania State University

CHESTER W. NEWTON
University of Chicago

HANS A. PANOFSKY
Pennsylvania State University

NORMAN G. PHILLIPS
Mass. Institute of Technology

RICHARD J. REED
University of Washington

HERBERT RIEHL
University of Chicago

HENRY STOMMEL
Woods Hole Ocean. Instn.

VERNER E. SUOMI
University of Wisconsin

HARRY WEXLER
U. S. Weather Bureau

METEOROLOGICAL MONOGRAPHS, a serial publication of the American Meteorological Society, serves as a medium for original papers, survey articles, and other material in meteorology and closely related fields; it is intended for material which is better suited in length or nature for publication in monograph form than for publication in the *Journal of Meteorology*, in the *Bulletin of the American Meteorological Society* or in *Weatherwise*. A METEOROLOGICAL MONOGRAPH may consist of a single paper or of a group of papers concerned with a single general topic.

TABLE OF CONTENTS

	PAGES
Part I: Wind and Structural Engineering	
<i>Introductory Remarks</i>	J. M. BIGGS 1
<i>Introductory Remarks</i>	G. S. VINCENT 2
<i>A Survey of Wind Characteristics below 1500 feet</i>	A. K. BLACKADAR 3-11
<i>Use of Power Spectra and Scales of Turbulence in Estimating Wind Loads</i>	H. E. CRAMER 12-18
<i>Estimates of Minimum Wind Forces Causing Structural Damage in the Dallas Tornado</i>	E. P. SEGNER 19-24
<i>Wind Loads on Towers</i>	E. COHEN 25-42
Part II: Meteorology and Hydrologic Engineering	
<i>Introductory Remarks</i>	C. C. BATES AND M. A. KOHLER 43
<i>A Method for Determining Dry-Period Probabilities as Applied to Illinois</i>	S. A. CHANGNON 44-49
<i>An Investigation of Flood-Producing Storms in Illinois</i>	F. A. HUFF AND R. G. SEMONIN 50-55
Part III: Environmental Engineering	
<i>Introductory Remarks</i>	M. K. THOMAS 56
<i>Snow Drifting and Engineering Design</i>	R. W. GERDEL 57-64
<i>Meteorology and Heating Load Requirements</i>	A. H. MURPHY 65-68
<i>Studies on Daylight Availability</i>	R. A. BOYD 69-79
Part IV: Transportation Engineering	
<i>Computation of the Distribution of Maximum Allowable Gross Takeoff Weights for Aircraft</i>	I. SOLOMON AND W. C. SPREEN 80-88
<i>The Climatic Environment as a Factor in Building Roads and Airport Pavements</i>	O. L. STOKSTAD 89-91
<i>Weathering Tests of Portland-Cement Concrete for Highways</i>	F. E. LEGG 92-98

EDITOR'S PREFACE

The articles contained in this MONOGRAPH are based on presentations made at the Second National Conference on Applied Meteorology: Engineering, held under the sponsorship of the American Meteorological Society in Ann Arbor, Michigan in September 1958.

The Society and the editor are greatly indebted to Dr. Donald J. Portman of the University of Michigan who was Chairman of the Program Committee for the Conference. Dr. Portman encouraged participants to submit manuscripts, and collected and collated them. Without his generous expenditure of time and energy, this MONOGRAPH would not have become available.
W. A. B.

PART I: Wind and Structural Engineering

INTRODUCTORY REMARKS

(Morning Session, 9 September 1958)

J. M. Biggs

Massachusetts Institute of Technology

This conference provides a unique opportunity for an exchange of ideas between two groups—namely, meteorologists and structural engineers, who have radically different backgrounds and points of view but at least one important interest in common. Both are interested in the nature of the wind, although the interest is for completely different reasons. Perhaps a few introductory remarks by a structural engineer will help the meteorologists to understand the problems and needs of the engineer.

The structural engineer is interested in the wind because it is an important cause of loading on many structures. Some of the most notable structural failures have been due to wind. The wind problem with regard to structures may be separated into two parts: the static problem, and the dynamic problem.

As far as static loads are concerned (these are important on tall buildings, radio and television towers, long-span bridges, etc.), the structural designer needs to know the maximum wind velocity and wind directions to be expected at a given site. This involves not only the basic wind velocity for the area but also such things as probability of occurrence, variation with height, the spatial distribution of gust velocities, and the local effects of topography. Once the wind characteristics are known, the engineer can determine the loading with reasonable accuracy. There is available a considerable quantity of wind-tunnel data which, in the aggregate, provide a basis for the determination of loads on a particular structure. However, these data are useless unless the wind velocity and direction are known.

The dynamic problem is structurally more complicated. However, given the dynamic characteristics of the wind load, it is possible to determine the dynamic response of the structure. There are two

aspects of the dynamic problem: self-induced vibration, and the dynamic effect of gusts. The former, which may occur in tall stacks, transmission lines, suspension bridges, etc., results from vortex formations around the structure and is most serious in a perfectly steady wind. Since each structure has one or more critical wind velocities at which self-induced vibration may be severe, the important meteorological data required are the probabilities of occurrence of such velocities.

The dynamic effect of gusts is probably not important for most structures, but our knowledge in this area is extremely limited. If the duration of the gust is small compared to the natural period of the structure, the latter may not feel the full loading associated with the maximum gust velocity. The same may be true if the depth of the structure is less than the length of the gust. On the other hand, if the time required for the gust to reach its maximum velocity is small compared to the natural period, the stresses in the structure may be even greater than those due to the maximum velocity considered statically. For these reasons, the time variation of the velocity is important but the engineer has very little information on this subject.

The engineers certainly do not expect the meteorologists to provide immediate answers to all of their questions. However, it is probable that in many cases the information is available but the engineer does not know where it may be located. In other cases, perhaps the required data could be easily obtained by meteorologists, but they do not know that it is needed by the engineer. It is for these reasons that this conference provides an unusual opportunity for both meteorologists and structural engineers. The papers to be presented will help to bridge the gap between the two groups.

INTRODUCTORY REMARKS

(**Afternoon Session, 9 September 1958**)

George S. Vincent

Bureau of Public Roads

In attacking the problem of the effect of wind on structures, our approach is necessarily divided. No single mind, so to speak, comprehends the available knowledge of the nature of the wind and at the same time its effect upon a structure. The structural engineer can gain a conception of the wind only through its observed effects on a given structure in a given instance. In the past, specifications and codes defining design wind loads have often been developed by computing what uniform pressure would have been required to wreak the observed havoc on a particular structure. The meteorologist, however, knows that this presents a very unreal picture of the invisible structure of the wind. The truer concept might indicate a wind which would have an entirely different effect on a slightly different structure than might be computed on the basis used in the engineer's analysis.

On the other hand, the meteorologist, with his

superior comprehension of the character of the wind, may be at a loss to know which of its characteristics are most significant in relation to a structure under consideration.

A conference of this kind brings these two aspects of man's knowledge of the wind into closer relation. The papers in this particular group are addressed primarily to the meteorologists. They show the engineer's attempts to study the effects of wind on specific structures and may serve to suggest to the meteorologists those characteristics of the wind and those elements of his own knowledge which come closest to bear upon the engineering problems described.

Other sessions of the conference will serve to acquaint the structural engineer with the resources which the meteorologist can bring to bear upon the engineer's problem of wind forces, but this is a matter to be considered elsewhere in this publication.

A SURVEY OF WIND CHARACTERISTICS BELOW 1500 FT

Alfred K. Blackadar

The Pennsylvania State University¹

ABSTRACT

A survey is given of the important observational and theoretical generalizations of the wind distribution up to about 500 ft, including work by Prandtl, Deacon, Monin and Obukhov, and Ellison. The vertical distribution of peak gust velocities is also discussed. Some of the less precise theories of the wind distribution above 500 ft are also described.

1. Introduction

The wind distribution in the lowest layers of the atmosphere enters into many practical problems of interest to civil engineers. The number and variety of these applications is probably exceeded only by the great variety of problems which a civil engineer is called upon to solve. Wind is known to be the principal consideration in the design of elevated highways (Biggs, Namyet, and Adachi, 1956) and is a major consideration in the design of many types of bridges. The erection of broadcasting towers to heights of 1500 ft or more has focussed attention on the need for greater knowledge of the wind profiles up to these levels. In addition to these obvious applications, the wind characteristics are involved directly or indirectly in such problems as air pollution, the blow-up of forest fires (Byram, 1954), irrigation, evaporation from reservoirs, design of airports, flood control, wind erosion, and the design of installations for generating electric power from the wind (Putnam, 1948).

The greatest source of data about the wind comes from routine surface observations, most of which are made at a height of about 30 ft. Other information is available at intervals of a thousand feet from balloon observations made four times daily at a smaller number of stations in the United States. To fill the gaps in time and space, it is necessary to have a detailed theory of the wind distribution so that extrapolations or interpolations of the mean distribution can be made. In addition, the variations of gust structure are needed, and for some problems, particularly that of air pollution, it is becoming increasingly evident that the spectral distribution of the wind variations must be thoroughly understood.

The height of 30 ft has been mentioned as roughly the height at which most wind observations are made. It is also a rather critical level in the theory of the wind distribution, and the approach which is used

differs somewhat according to whether one is required to interpolate between the 30-ft level and the ground or to extrapolate from 30 ft in the upward direction.

In this article, some of the results are given which are applicable below 400 or 500 ft, where a relatively large number of observational data have been presented by many authors. After this, the theory of the wind at greater heights will be briefly reviewed along with a description of two phenomena which illustrate the great complexity of this problem.

2. Adiabatic profile below 30 ft

Under adiabatic conditions, the wind profile below 30 ft is distributed logarithmically with height according to the formula

$$u = \frac{1}{k} \sqrt{\frac{\tau_0}{\rho}} \ln \left(\frac{z}{z_0} \right). \quad (1)$$

This formula was derived by Prandtl (1932). In this formula, u is the wind speed at height z , k is the Karman constant which has a value close to 0.4, ρ is the air density, τ_0 is the drag of the wind per unit area on the surface, and z_0 is a roughness parameter with dimension of height.

The logarithmic profile has been thoroughly tested at many different localities and has been found to be completely satisfactory under neutral conditions. Once z_0 has been determined at a given location, a single observation of the wind at any height within the layer determines the surface stress and enables one to calculate the wind speed at any other height up to at least 30 ft and sometimes considerably more. The value of z_0 has been measured at many different locations, and a list of typical values reported by different authors is given in table 1.

Over land, the value of z_0 depends only on the nature of the surface. It may usually be assumed to be constant at a fixed location unless the surface characteristics change (for example, when long grass is flattened at high wind speeds). The value of z_0 usually

¹ College of Mineral Industries Contribution No. 59-47.

TABLE 1. Roughness parameter z_0 for various surfaces.

Surface	z_0 (cm)
Scrub oak, average 30-ft height ¹ (Brookhaven)	100.0
Long grass ² (60–70 cm) 1.5 m sec^{-1} at 2 m	9.0
6.2 m sec^{-1} at 2 m	3.7
Mown grass ² (3 cm)	0.7
Natural snow surface ²	0.1
Sun baked sandy alluvium ²	0.03
Smooth mud flat ²	0.001
Ocean surface, ³ $10\text{--}15 \text{ m sec}^{-1}$	0.0021
Light wind	0.0010

¹ Panofsky (personal communication).² Deacon (1949).³ Deacon, Sheppard, and Webb (1956).

is found to be a little more than 1/10 the height of the effective surface obstacles, but not all obstacles are equally effective. The drag is caused by pressure differences between the upwind and downwind sides of the obstacles and is partly connected with the ability of the obstacles to dissipate the energy of the air flow around or through them. Gently sloping features are less effective than smaller abrupt obstacles. The smallness of z_0 over water indicates that typical long-wave shapes are ineffective obstacles and that the drag is caused mostly by smaller and steeper ripples.

When the obstacles are very high (for example, trees and buildings), a somewhat better fit of the winds to the logarithmic law is possible if a constant value is subtracted from each measured height. This value is called the *zero-plane displacement*, and its introduction represents an additional parameter which must be determined for the location.

Over water, the roughness parameter changes with the wind speed because of the sensitivity of the surface to the wind. This behavior is of practical importance since, under neutral conditions, the roughness parameter determines the surface drag occurring with a given wind speed at the anemometer level. Thus, the roughness parameter enters into any attempt to predict lake or ocean movements from the wind. With short fetches of the wind, there is general agreement that the effective roughness (z_0) increases with wind speed and, for a given speed, it increases with the fetch distance. Less clear is the behavior of z_0 with the wind speed when the fetch is sufficient for the development of a full wave spectrum. Neumann (1956), by using only data for long fetches, has found the drag coefficient, and therefore z_0 , decreasing with increasing wind speed, a behavior which he explained by supposing that the ripples located in the troughs between the larger waves are sheltered from the wind and cease to exert a drag on it. A more recent study by Deacon, Sheppard, and Webb (1956), some results of which are included in table 1, contradicts this conclusion. It is

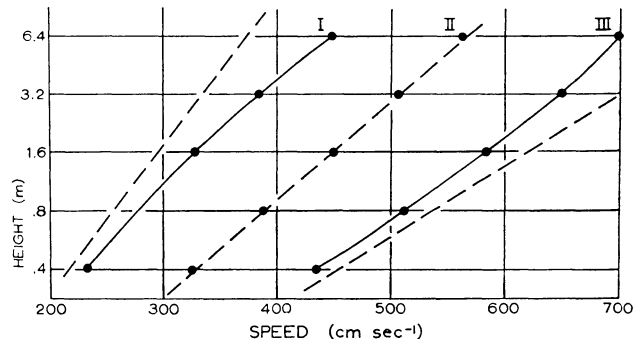


FIG. 1. Hourly average wind speed observed at O'Neill, Nebraska on 22 August 1953 by the Johns Hopkins University Group at (I) 0435, (II) 0635, and (III) 1235 local time. Dashed lines are computed from the Prandtl formula using τ_0 observed with a Sheppard-type drag plate and roughness parameter $z_0 = 0.84 \text{ cm}$.

obvious that more good observations of wind profiles over the ocean are needed.

Since the surface obstacles on a water surface are moving, it appears more logical that the wind in the Prandtl formula should be the wind speed measured relative to the motion of the effective surface ripples. Such a revision is not necessary, but it may prove to be more convenient. It is easily shown that if c is the ripple speed and if the Prandtl law is valid for the relative wind

$$u - c = \frac{1}{k} \sqrt{\frac{\tau_0}{\rho}} \ln \frac{z}{z_0};$$

then the Prandtl law in the form of (1) is also satisfied by changing only the roughness parameter in such a way that

$$\ln z_0 = -kc(\rho/\tau_0)^{1/2} \ln z_0'.$$

Since the roughness parameter is presumably calculated from the wind profile itself, the correct value of the surface stress is derived regardless of whether the ripple speed is taken into account or not. It is of interest that z_0' , which presumably is more directly associated with the surface obstacles, is always larger than z_0 . Hunt (1958) found from studies of Lake Heffner observations that by choosing an appropriate ripple speed (about 65 cm sec^{-1}) z_0' is a constant equal to about 1.5 cm. The equivalence of a uniform horizontal displacement of the coordinate system to a change of surface roughness was first pointed out by Ellison (1957) and is applicable to non-neutral conditions also.

3. The diabatic wind profile near the ground

In fig. 1, values of wind speed observed at O'Neill, Nebraska over short grass are plotted against height on a logarithmic scale. Profile I was observed at 0435

local time, about an hour before sunrise when the temperature increased strongly with height (stable). Curve II was observed at 0635, about one hour after sunrise when the lapse rate was approximately adiabatic. Curve III was observed at 1235 local time under strongly superadiabatic or unstable conditions. This figure illustrates the following generally accepted generalizations concerning the wind profile under widely varying lapse rates:

(1) The profile is well represented by the Prandtl equation only when the lapse rate is adiabatic.

(2) Near the ground, the wind shear is greatest under unstable conditions (day), whereas at increasingly higher levels there is an increasing tendency for greatest shear at night.

(3) Under non-neutral conditions, the Prandtl distribution is approached more and more closely as one approaches the surface.

The most widely used formula for the wind profile under non-neutral conditions is that of Deacon (1949),

$$u = \frac{1}{k} \sqrt{\frac{\tau_0}{\rho}} \frac{1}{1-\beta} \left[\left(\frac{z}{z_0} \right)^{1-\beta} - 1 \right], \quad (2)$$

in which β is a new parameter which is less than one with stability and more than one with instability. This equation can be expanded in a power series of which the Prandtl equation represents the first-order term which is approached as $\beta \rightarrow 1$. Other wind-profile formulas have been suggested by Lettau (1949), Halstead (1952), Panofsky (1952), and by Monin and Obukhov (1954).

As an interpolation formula, Deacon's equation gives satisfactory results when the parameters are determined by fitting wind observations. There is, however, a tendency for the departure of β from unity to increase with increasing height, so that the formula should not be used for extrapolation above the lowest 5 or 10 m. A more stringent test is provided by whether or not the formula when used with observed values of surface stress and roughness parameter is still capable of correctly predicting the wind profile. Rider (1954) has found the relation between wind speed and surface stress satisfactory for unstable but not under stable conditions, and Panofsky (1952) has also found poor agreement between observed and predicted stresses. Deacon (1949) observed a relationship between β and the Richardson number which would be useful in calculating the wind profile from gross-meteorological parameters. However, Davidson and Barad (1956) failed to find a unique relationship between β and the Richardson number in the lowest layers at O'Neill, Nebraska under stable conditions and concluded that β depends also on the wind profile up to at least 500 m.

Monin and Obukhov (1954) have suggested from principles of similarity that the logarithmic wind shear function

$$S = \frac{k}{u^*} \frac{\partial u}{\partial \ln z} \quad (3)$$

is a universal function of the dimensionless ratio z/L , where L is defined by

$$L = u^{*3} c_p \rho T / kgH. \quad (4)$$

In this equation, c_p is the specific heat at constant pressure, T the absolute temperature, g the acceleration of gravity, H the turbulent flux of heat in the upward direction, and u^* stands for $(\tau_0/\rho)^{1/2}$. For the adiabatic case, S is unity. For small z/L , S can be determined by a power-series expansion of which the first terms are

$$S = 1 - \frac{\alpha z}{L}. \quad (5)$$

By vertical integration of S , one then gets the velocity distribution for small z/L —

$$u = \frac{u^*}{k} \left(\ln \frac{z}{z_0} - \frac{\alpha z}{L} \right). \quad (6)$$

This representation has the realistic property of giving the logarithmic distribution close to the ground and thus permits the surface stress to be calculated correctly from low-level wind data. Recent studies by Panofsky, Blackadar, and McVehil (1959) indicate that α is about 4.5 for small values of z/L . A satisfactory representation of wind profiles is possible over the range from small negative values of z/L to the largest positive superadiabatic values normally encountered below 100 ft by using 0.6 for α as suggested by Monin and Obukhov.

A still better prediction of the wind profile is obtained by finding S from the equation

$$S^4 + \frac{\gamma z}{L} S^3 = 1, \quad (7)$$

suggested by Ellison (1957), rather than from (5). The constant γ is assumed to be universal and must be determined empirically. In practice, L is difficult to obtain, since the heat flux is seldom measured. Therefore, it is necessary to replace γ/L by an equivalent ratio γ'/L' where L' is evaluated from the relation

$$L' = - u^* \theta \frac{\partial u}{\partial z} / kg \frac{\partial \theta}{\partial z}, \quad (8)$$

θ being the potential temperature. In this case, γ' appears to have the value 18 according to recent work

(Panofsky, Blackadar, and McVehil, 1959). To what height Ellison's formula is a successful representation is not yet known. Under unstable conditions at Brookhaven, which is a rather rough site, satisfactory predictions of the mean wind profile are given up to the top of the tower at 125 m. It thus appears that Ellison's theory has considerable applicability above the arbitrary 30-ft level.

4. Wind profiles up to about 500 ft above flat country

Most attempts to summarize the wind distribution above the lowest 10 m have been based upon the power law distribution

$$\frac{u}{u_1} = \left(\frac{z}{z_1} \right)^p \quad (9)$$

with the subscript 1 referring to some level within the layer and p a parameter which is independent of height. The two parameters p and u_1 can be ascertained empirically from wind observations at two heights. DeMarrais (1959) has compared the efficiency of this expression to a two-parameter logarithmic law,

$$u = a \log z + b, \quad (10)$$

at Brookhaven. With suitable choice of parameters, this logarithmic expression gives profiles which are quite similar to the power-law profiles, but, as an interpolation formula for use under a wide variety of different meteorological conditions, the power law is superior.

Since observations of wind at two heights are not usually available, it is necessary to be able to relate the exponent p to environmental conditions. Many such studies have indicated that p depends principally upon the vertical gradient of temperature and the roughness of the surface. Over smooth open country, a value close to 1/7 is usually found with neutral lapse rate; for example, Scrase (1930) found 0.13; Giblett *et al* (1932), 0.143; Frost (1947), 0.15; and Deacon (1955), 0.16. At Brookhaven, Long Island, where the terrain is covered fairly uniformly with scrub oak 25 to 30 ft high, DeMarrais (1959) found an average value of 0.28 under an adiabatic lapse rate. The largest values occurred with upwind fetch over wooded ground; smaller values were observed in winds from one direction with more grass cover. Values of 0.23 and 0.22 have been reported at Quickborn, Germany and Akron, Ohio (see Deacon, 1955) where the terrain is described as gently rolling with many bushes and small trees.

These values are the ones which should be applied under conditions of extreme wind speeds as the vertical lapse rate is then usually very close to the adiabatic rate. They apply to the distribution of the mean speed

over something like a five-minute interval and not to the wind speeds which occur during gusts. For example, Sherlock (1953) found that the winds during the storm of 19 January 1933 fitted the exponent 1/7 over level open country. At Brookhaven, Long Island, Singer and Smith (1953) reported that the exponent p was 0.274 during the unusually severe storm of 25 November 1950, a value which agrees closely to the average value of 0.28 observed there under adiabatic conditions.

The increase of the exponent p with increasing roughness results in a decreasing wind shear close to the surface and a relative increase in the main portion of the layer. The decreased shear close to the surface reflects the greater increase of turbulence close to the surface. Power laws with exponents 1/7 and 2/7 respectively can be closely approximated by the Prandtl logarithmic profiles with z_0 equal to 11 cm and 1.2 m respectively. These values appear reasonable for flat open country in the first case and for wooded land at Brookhaven in the second case, and indicate that the roughness has an important effect on the profile up to at least 400 ft during adiabatic conditions.

There is a fairly large number of observations which indicate that p increases with increasing stability. Values as low as 0.01 and 0.02 have been observed by Giblett *et al* (1932) and Ali (1932) during superadiabatic conditions; for such values, the wind is nearly independent of height. Under stable conditions, values as high as 0.85 have been reported by Best (1935) and Ali (1932). Averages for different lapse rates determined by Frost (1947) at Cardington (smooth grassland) between 25 and 400 ft, and averages determined by DeMarrais (1959) from data observed between 36 and 410 at Brookhaven, which is largely wooded, are compared in fig. 2. Besides the increase of p with increasing stability with both kinds of terrain, it appears that the effect of roughness is most conspicuous under neutral conditions and more or less disappears with increasing stability as the temperature gradient increases above about 2C per 100 m. The observed decrease of exponent with instability indicates that negative temperature gradients have a selective effect near the top of the layer, where the increased turbulent mixing reduces the wind shear. This effect is opposite to that of surface roughness which reduces the wind shear near the ground.

DeMarrais also found that when the vertical temperature gradient is held constant, the exponent tends to increase with increasing wind speed at a fixed level. This effect is strongest under superadiabatic (unstable) conditions and disappears with stable lapse rates. This behavior of the wind is completely explained by assuming that wind tends to

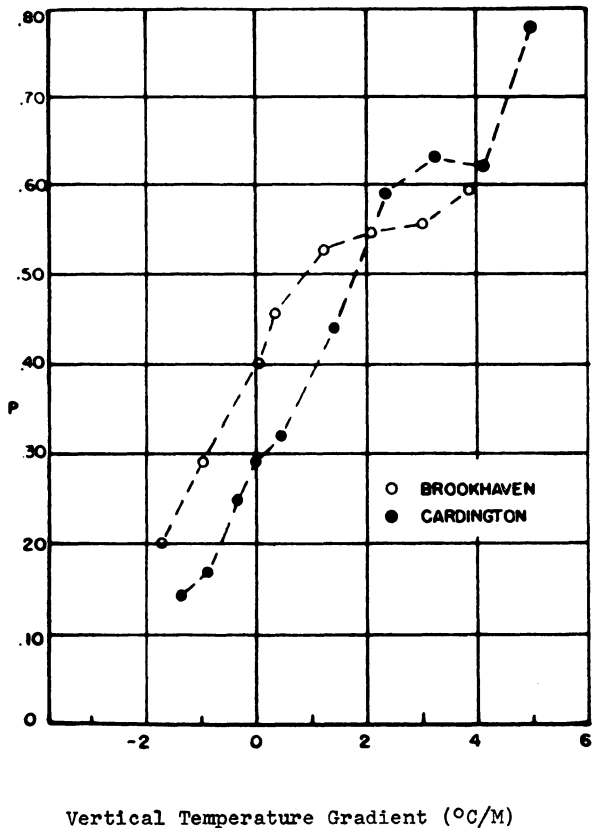


FIG. 2. Power-law wind profile exponent p vs. vertical temperature gradient at Brookhaven and Cardington.

increase the selective effect of roughness on the distribution of turbulence near the surface.

Since the exponent p is given by $\partial \ln u / \partial \ln z$, eq (3) gives the relation

$$p = u^* S / k u. \quad (11)$$

Given L' , z_0 , and the height z , one can determine p from Ellison's eq (7) during unstable and slightly stable conditions. Calculations confirm the empirical findings that p increases with increasing surface roughness and increasing stability and that p tends to approach the neutral value appropriate for the surface roughness when the wind speed increases (Panofsky, Blackadar, and McVehil, 1959).

When there is a strong horizontal temperature gradient, there must be a rapid change in the geostrophic wind vector with height. Although its effect on the vertical-wind distribution is greatest at higher levels, a horizontal temperature gradient should have noticeable effect on the value of the power law exponent below 400 ft. This effect does not appear to have been studied in this height range.

5. Vertical distribution of gust velocities

The design of structures must make allowance for the maximum wind speed which will be encountered

at each level during gusts. Only gusts which last for about 5 sec or longer need to be considered, since shorter gusts have too small a size to develop substantial loads on structures.

Sherlock (1953) and Deacon (1955) have pointed out that the air in the large gusts with excess speed is usually descending. It is reasonable, therefore, to picture the gusts as masses of air descending from much higher levels, tending to maintain the large velocities of those levels. They form an efficient mechanism for transporting momentum downward toward the ground to compensate for the loss manifested by the surface drag. In the case of large gust-masses which descend rapidly through large vertical distances, the velocity decreases downward less rapidly than does the average velocity. Thus it is that the peak wind speed in the gusts is usually observed to increase more slowly with height than does the mean wind speed.

Significant analyses of gust velocities up to at least 250 ft have been made by Sherlock (1953), Singer and Smith (1953), and by Deacon (1955). Table 2 summarizes the findings of these authors.

TABLE 2. Comparison of data for peak wind speeds.

Source	Exponent		
	Mean velocity	Peak gusts	30-ft gust factor
Sherlock (level, open country)	0.143	0.080	1.5
Deacon (level, open country)	0.16	0.085	1.47*
Singer and Smith (30' woods)	0.274	0.127	2.00**

* Extrapolated down from value 1.44 at 40 ft.

** Extrapolated down from value 1.94 at 37 ft.

The gust factor is defined as the ratio of the average peak gust speed during a five-minute period to the mean wind speed during this period. Some of the differences between values cited by different authors in table 2 may arise because of differences in the duration of gusts considered, but the principal factor appears to be the terrain. In rough terrain, the gust factor is large for two reasons: the wind is gustier, and the mean wind which makes up the factor's denominator is smaller. The gust factor decreases with height mostly as a result of the increase of mean speed. With strong mean winds, the gust amplitude (that is, the peak minus lull) remains roughly constant up to 500 ft at least.

As indicated before, the peak gust speeds increase less rapidly with height than does the mean. This

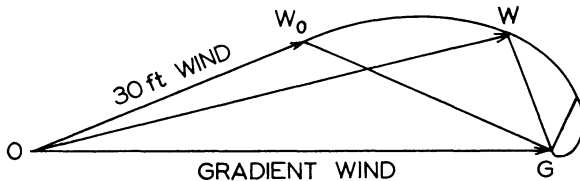


FIG. 3. The Ekman spiral wind hodograph.

fact is reflected in the smaller values of the power-law exponent which pertain to the peak speeds. The table indicates that it is probably unwise to attempt to adopt a single value of this exponent but rather to try to choose a value consistent with the kind of surface which prevails in the vicinity of the wind-observation point. It appears that use of the value 0.0805 recommended by Sherlock would tend to underestimate the peak wind speeds aloft at many sites.

6. Wind distribution above 300 ft

At about 300 ft, we begin to leave empiricism behind and pass into a region where the number of theoretical wind distributions exceeds the number of detailed observations of the wind distribution. The simplest of several theoretical distributions is that derived by Ekman, who originally applied the theory to calculate the drift currents in the ocean. When it is applied to the atmosphere, the theory is based on the assumptions (1) that the motions are steady and unaccelerated, (2) that the pressure gradient is independent of elevation, and (3) that the eddy viscosity is constant. The wind distribution which prevails in this case is shown by the vector diagram in fig. 3. The vector OG is the gradient wind, which would prevail in the absence of viscosity, and which is approached at great heights above the surface. The vector OW_0 is the actual wind at the base of the uniformly viscous layer, in practice usually assumed to be somewhere near 30 ft. The wind at any higher level is obtained by rotating the vector GW_0 to the right through an angle proportional to the height so as to determine a new point W and, thus, the wind vector OW prevailing at this height. The ratio of the angle to the height is inversely proportional to the square root of the eddy viscosity and is strongly influenced by the stability. During the day, in air masses which are being heated from below, the eddy viscosity is large; consequently, the wind changes rather slowly with elevation. At night, or in stable atmospheres, the converse is generally true, in which case the gradient wind tends to be approached at a lower level. Under typical daytime conditions, the gradient-wind direction is usually closely approached at a height of the order of 2000 to 3000 ft.

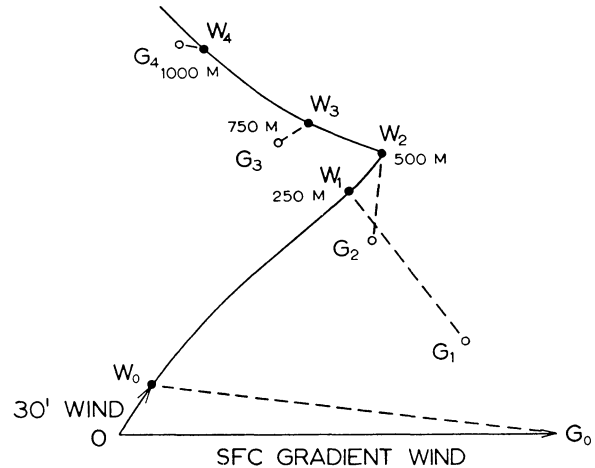


FIG. 4. Example of the height variation of the wind with a strong horizontal temperature gradient.

The assumption of constant eddy viscosity has frequently been questioned, and several indirect determinations indicate a considerable variation with height; usually a maximum is displayed at a height of 500 ft more or less. Köhler (1933) has treated theoretically the case in which the eddy viscosity is proportional to the height raised to an arbitrary exponent. The solutions which apply to the various exponents are in every case spirals which are superficially similar to the Ekman spiral of fig. 3; qualitatively, the departure from the Ekman spiral is such that the wind varies more rapidly with height where the viscosity is smaller and less rapidly with height (compared to the Ekman spiral) where the viscosity is greater. Generally, the structure and distribution of turbulence is not known sufficiently well to warrant the refinements introduced by Köhler.

Many fine examples of wind spirals resembling the distribution of fig. 3 have been observed by pilot-balloon techniques (*cf.* Mildner, 1932), but most examinations of routine pilot-balloon observations in the lowest 3000 ft reveal strange, varied, and sometimes bizarre distributions displaying little or no resemblance to any of the theoretical wind spirals. There are several reasons for this disagreement: (1) inadequate sampling of the winds at the reported level by the pilot balloon, (2) the presence of a horizontal temperature gradient which results in the superposition of a vertical gradient of the wind, and (3) the occurrence of large accelerations, both sporadic and periodic in nature, which introduce certain phenomena of considerable importance to engineers, airmen, and forest-fire fighters. The vertical distribution of eddy viscosity is probably a negligible factor in explaining this disagreement.

Sampling inadequacies are usually greatest in un-

stable air masses, owing to the presence of large eddies which exert a sustained effect on a rising balloon. In extreme cases, as for example in the vicinity of thunderstorms, the prevailing circulation of the atmosphere may be completely overwhelmed by a local convective circulation.

Horizontal variations of temperature are of frequent occurrence in temperate latitudes, especially in winter. These gradients cause a variation of horizontal pressure gradient with height, and thereby cause the wind in the free atmosphere to vary in direction and speed from one elevation to another. In the simplest case (the Ekman spiral), the disturbing effects of friction and temperature gradient are independent of each other, and the combined effect can be obtained by adding both disturbances together vectorially. An example of the modification of the wind by this cause is given in fig. 4. It differs from fig. 3 in the introduction of a temperature gradient of 1°C per 30 km, a value often observed in winter; and appropriate modification of lower boundary condition has also been made. The presence of a temperature gradient almost always masks or greatly distorts the frictional spiral, and it probably explains in great part why the theoretical spiral is so seldom seen on wind hodographs in temperate latitudes. The effect on wind speed is greatest when the isotherms are parallel to the isobars. With a given pressure gradient, the wind shear is greatest when the high temperature and high pressure coincide and least when they are opposed.

7. The low-level jet

The wind distributions discussed in the last section have been predicated on the existence of a steady-state flow. Over a continental land surface subjected to a strong periodic heating and cooling, steady-state flow does not become established, and, instead, some very striking phenomena are sometimes observed. One of these is the low-level jet which is best developed over the Great Plains.

This phenomenon has been studied critically by Lettau (1954) and Blackadar (1955, 1957). It is best developed at night. The wind speed increases very rapidly to a maximum at the top of the nocturnal inversion which is usually between 1000 and 3000 ft above the surface. At this level wind speeds of 60 or 70 kn are frequently observed, and it has been found that these are supergeostrophic; that is, they exceed the equilibrium wind speed for the pressure gradient existing at that level. The strong low-level jets occur only with a wind from the southerly quadrant. Beneath the jet, enormous values of wind shear are usually encountered. During a series of kite ascents at Drexel, Nebraska on 18 March 1918 in which detailed wind observations were obtained, the mean wind

was observed to increase from 5 kn to 70 kn through a vertical distance of 780 ft.

The phenomenon results from the sudden relaxation of frictional restraint at about the time of sunset. During the day convection causes a downward flow of momentum which is not entirely compensated from above. As a result, the wind at around 2000 ft above the ground is retarded from its equilibrium value. As evening approaches, convection ceases, and the air at these levels is free to accelerate under the influence of the unbalanced Coriolis and pressure-gradient forces. The resulting motions can be studied by referring to the equations of horizontal frictionless motion,

$$\left. \begin{aligned} \frac{du}{dt} &= 2\omega \sin \varphi v - \frac{1}{\rho} \frac{\partial p}{\partial x} \\ \frac{dv}{dt} &= - 2\omega \sin \varphi u - \frac{1}{\rho} \frac{\partial p}{\partial y} \end{aligned} \right\}, \quad (12)$$

in which u and v are the components of velocity in the x and y directions, ω the angular velocity of the Earth, φ the latitude, and p the pressure. Let u_g and v_g be the components of the geostrophic wind, which satisfy these equations in the special case when the accelerations vanish. Then, in terms of the geostrophic winds, the equations can be written in the form

$$\left. \begin{aligned} \frac{du}{dt} &= 2\omega \sin \varphi (v - v_g) \\ \frac{dv}{dt} &= - 2\omega \sin \varphi (u - u_g) \end{aligned} \right\}. \quad (13)$$

It will be assumed that the pressure gradient does not change with time. In order to solve and interpret the result most easily, consider the complex number defined by

$$W = (u - u_g) + i(v - v_g). \quad (14)$$

Then (13) can be rewritten in the form

$$\frac{dW}{dt} = - 2i\omega \sin \varphi W \quad (15)$$

which has as solution

$$W = W_0 e^{-ift} \quad (16)$$

in which f is the Coriolis parameter

$$f = 2\omega \sin \varphi.$$

The complex number W_0 represents the deviation from the geostrophic wind at the initial time, which for the present purpose may be taken to be the time of sunset. The changes of the wind which typically occur after

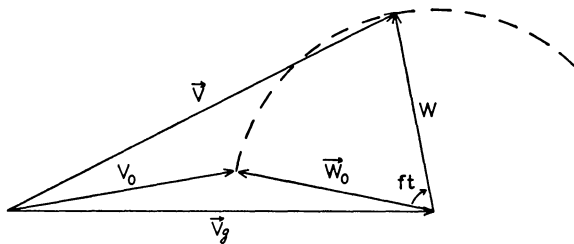


FIG. 5. Wind-vector variations with time in the absence of friction.
 \vec{V}_0 is the initial wind vector; \vec{V}_g is the geostrophic wind.

sunset can now be seen in fig. 5. According to (16), the geostrophic deviation vector \vec{W} rotates to the right without change of magnitude at an angular speed of f radians per second and if continued would perform a complete revolution in a period of one day divided by twice the sine of the latitude. The circle thus traced out marks the locus of the positions of the end of the wind vector as function of time. If the initial wind direction is close to the geostrophic wind direction, the maximum wind speed is reached after a period of about $t = \pi/f$, which in the range of latitudes of the United States varies from about 8 hr to 12 hr. At this time, the wind speed is greater than the geostrophic wind speed by an amount which is about equal to the initial retardation. The amplitude of the changes is generally a maximum at about 2000 ft above the ground. At higher levels, the amount of the retardation in the daytime is insufficient to initiate a large oscillation, whereas at lower levels there is too much turbulent mixing even at night. It is to be expected from theory that similar oscillations might be set up by a sudden change of pressure gradient or by abrupt changes in surface heating or cooling experienced by air as it crosses a coast line. Observations indicate that the wind actually traces out an elliptical path which results from the fact that the relaxation of friction is not abrupt (Buajitti and Blackadar, 1957).

It appears that the effect of the low-level jet on high structures has never been discussed. It has been pointed out by Byram (1954) that a jet profile is conducive to the establishment of a "chimney" above a forest fire which leads to the blow-up phenomenon and results in the scattering of flaming debris over a wide area. The very strong wind shear beneath the jet has also been the cause of a number of airplane accidents. The effect of shear on a landing aircraft has been described by Neyland (1956). As an airplane lets down through a layer with wind shear, it suffers a rapid loss of headwind. If not compensated for, this loss reflects a loss of airspeed, which may be disastrous if the original airspeed is close to the stalling speed of the airplane. The problem is especially serious with jet-type aircraft which must descend at near

stalling speed and which require several seconds to develop thrust.

REFERENCES

1. Ali, B., 1932: Variation of wind with height. *Quart. J. r. meteor. Soc.*, **58**, 285-288.
2. Best, A. C., 1935: Transfer of heat and momentum in the lowest layers of the atmosphere. *Geophys. Mem.*, **7**, No. 65, 66 pp.
3. Biggs, J. M., S. Namyot, and J. Adachi, 1956: Wind loads on girder bridges. *Trans. Amer. Soc. Civil Eng.*, **121**, 101-120.
4. Blackadar, A. K., 1955: The low-level jet phenomenon. *Inst. Aero. Sci. Preprint No. 519*. (Abstract in *Bull. Amer. meteor. Soc.*, **35**, p. 494.)
5. Blackadar, A. K., 1957: Boundary layer wind maxima and their significance for the growth of nocturnal inversions. *Bull. Amer. meteor. Soc.*, **38**, 283-290.
6. Buajitti, K., and A. K. Blackadar, 1957: Theoretical studies of diurnal wind variations in the planetary boundary layer. *Quart. J. r. meteor. Soc.*, **83**, 486-500.
7. Byram, G. M., 1954: *Atmospheric conditions related to blowup fires*. Stn. pap. No. 35, Southeast Forest Exper. Stn., Asheville, North Carolina.
8. Davidson, B. and M. L. Barad, 1956: Some comments on the Deacon wind profile. *Trans. Amer. Geophys. Union.*, **37**, 168-176.
9. Deacon, E. L., 1949: Vertical diffusion in the lowest layers of the atmosphere. *Quart. J. r. meteor. Soc.*, **75**, 89-103.
10. Deacon, E. L., 1955: Gust variation with height up to 150 m. *Quart. J. r. meteor. Soc.*, **81**, 562-573.
11. Deacon, E. L., P. A. Sheppard, and E. K. Webb, 1956: Wind profiles over the sea and the drag at the sea surface. *Austral. J. Phys.*, **9**, 511-541.
12. DeMarrais, G. A., 1959: Wind speed profiles at the Brookhaven National Laboratory. *J. Meteor.*, **16**, 181-190.
13. Ellison, T. H., 1957: Turbulent transport of heat and momentum from an infinite rough plane. *J. Fluid Mech.*, **2**, 456-466.
14. Frost, R., 1947: The velocity profile in the lowest 400 ft. *Meteor. Mag.*, **76**, 14-17.
15. Giblett, M. A., et al., 1932: The structure of wind over level country. Report on experiments carried out at the Royal Airship Works, Cardington. *Geophys. Mem.*, **6** (54), 119 pp.
16. Gifford, F. A., 1952: The breakdown of a low-level inversion studied by means of detailed soundings with a modified radiosonde. *Bull. Amer. meteor. soc.*, **33**, 373-379.
17. Halstead, M. H., 1952: The relationship between wind structure and turbulence near the ground. *Geophys. Res. Pap.* No. 19, 96-126.
18. Hunt, I. A., 1958: *Winds, wind set-ups, and seiches on Lake Erie, Part 1*. Second Natl. Conf. Applied Meteor., Engineering.
19. Köhler, H., 1933: Meteorologische Turbulenzuntersuchungen 1. *Kgl. Svenska Vetenskap. Handlingar*, Ser. 3, **13**, 1-54.
20. Lettau, H., 1949: Isotropic and non-isotropic turbulence in the atmospheric surface layer. *Geophys. Res. Pap.* No. 1, 86 pp.
21. Lettau, H., 1954: *Graphs and illustrations of diverse atmospheric states and processes observed during the seventh test period of the Great Plains Turbulence Field Program*. Occasional Rep. No. 1, Atmos. Anal. Lab., Geophys. Res. Dir., Cambridge, Mass.
22. Mildner, P., 1932: Über die Reibung in einer speziellen Luftmasse in den untersten Schichten der Atmosphäre. *Beitr. Physik fr. Atmos.*, **19**, 151-158.

23. Monin, A. S., and A. M. Obukhov, 1954: Osnovnye zakonomernosti turbulentnogo peremeshivaniia v prizemnom sloe atmosfery (Basic laws of turbulent mixing in the ground layer of the atmosphere). *Akad. Nauk SSSR, Leningrad, Geofiz. Inst., Tr.*, No. 24 (151), 163-187.
24. Neuman, G., 1956: Wind stress on water surfaces. *Bull. Amer. meteor. Soc.*, **37**, 211-217.
25. Neyland, L. J., 1956: Change without notice. *Flying Safety*, April, 16-20.
26. Panofsky, H. A., 1952: A comparison of different types of stress measurement. *Quart. J. r. meteor. Soc.*, **78**, 411-414. (See also discussion by E. L. Deacon, **79**, 164-167.)
27. Panofsky, H. A., A. K. Blackadar, and G. E. McVehil, 1959: *The diabatic wind profile*. (Unpubl. ms.).
28. Prandtl, L., 1932: Meteorologische Anwendung der Strömungslehre. *Beitr. Physik fr. Atmos.* (Bjerknes-Festschrift), **19**, p. 188.
29. Putnam, P. C., 1948: *Power from the wind*. Van Nostrand Publish. Co., New York, 224 pp.
30. Rider, N. E., 1954: Eddy diffusion of momentum, water vapor and heat near the ground. *Phil. Trans. r. Soc. London*, Ser. A, **246**, 481-501.
31. Scrase, F. J., 1930: Some characteristics of eddy motion in the atmosphere. *Geophys. Mem.*, **6**, No. 52.
32. Sheppard, P. A., 1958: Transfer across the earth's surface and through the air above. *Quart. J. r. Meteor. Soc.*, **84**, 205-224.
33. Sherlock, R. H., 1953: Variation of wind velocity with height. *Trans. Amer. Soc. Civil Eng.* **118**, 463-488.
34. Singer, I. A., and M. E. Smith, 1953: Variation of wind velocity and gusts with height. (Discussion of paper by R. H. Sherlock.) *Trans. Amer. Soc. Civil Eng.*, **118**, 491-493.

USE OF POWER SPECTRA AND SCALES OF TURBULENCE IN ESTIMATING WIND LOADS¹

H. E. Cramer

Massachusetts Institute of Technology

ABSTRACT

Estimates of wind forces on structures are traditionally based on the assumption that the wind speed is invariant with space and time. However, air flow within the lower layers of the atmosphere is almost always turbulent due to fluctuations in wind velocity that comprise a very broad spectrum of characteristic lengths and amplitudes. In view of the fundamental dynamic nature of the problem, ultimate resolution depends upon satisfactory knowledge of the spectra and cospectra of the wind-velocity fluctuations. Recent measurements of these properties of turbulent structure are summarized, and application of these data to the problem of estimating wind forces is discussed. It is suggested that estimates of maximum wind speeds associated with gusts may be conveniently based on the level of the mean wind speed, assuming that the fluctuations in wind speed are approximately Gaussian and that the average turbulent intensity is about 0.25. Until additional measurements of the basic properties of turbulent structure are available, it appears unlikely that the power-spectral-analysis techniques can replace the conventional steady-state procedure.

1. Introduction

Civil engineers have long recognized the need for satisfactory estimates of wind force. Recent advances in structural theory and past structural failures directly attributable to wind action emphasize the importance of accurate wind-loading information [3]. In conventional engineering practice, wind forces are treated as static loads. Although it is generally recognized that the problem is basically of a dynamic nature, this simplification is justified on the grounds that resonance frequencies of most structures do not coincide with orderly, large-amplitude fluctuations in wind velocity. Wind-loading factors used in current design specifications are principally based on estimates of maximum wind speed obtained from routine U. S. Weather Bureau observations of the "fastest-mile-of-wind" [22; 23] and on drag coefficients for structural members of various shapes determined from wind-tunnel experiments [2; 4]. This treatment rests on the assumption that the wind is steady; *i.e.*, characteristic properties of the flow are invariant with time and, in the plane of the horizon, with space. It is well known that the natural wind is not steady; fluctuations in wind velocity comprise a very broad spectrum of eddy sizes ranging from fractions of a centimeter to hundreds of kilometers. During the past decade, meteorologists have become increasingly interested in studying these fluctuations. Although much remains to be learned, many of the gross features of the structure of atmospheric turbulence have been established.

Ultimate resolution of the problem of predicting the wind forces on structures depends upon improved knowledge of the spectra and cospectra of velocity fluctuations. The purpose of this paper is to summarize the results of recent turbulence studies and to indicate possible applications of this information in determining wind loads on structures.

2. Basic concepts of turbulent structure

For purposes of orientation, it is desirable to outline some of the basic concepts employed by meteorologists in studying the structure of atmospheric turbulence. Due to the random nature of wind-velocity fluctuations, their characteristic properties are not easily described in terms of discrete wave motion. Rather, adequate description is achieved only by means of statistical measures. The wind velocity, V , measured at a fixed point, is considered to comprise a steady or slowly varying mean velocity, \bar{V} , and an irregular fluctuating component or deviation from the mean, V' . It is assumed that \bar{V} depends only upon the duration of the sampling interval, T ; the instant in time, t , at the midpoint of the sampling interval; and the height, z , above the earth's surface [25]. In symbols,

$$V = \bar{V} + V'$$

and

$$\bar{V}(T, t, z) = \frac{1}{T} \int_{t-T/2}^{t+T/2} V dt.$$

Experience demonstrates that the above definition for \bar{V} is most satisfactory when the duration of the sam-

¹ Research sponsored by the Geophysics Research Directorate, Air Force Cambridge Research Center, under Contract No. AF 19(604)-3460.

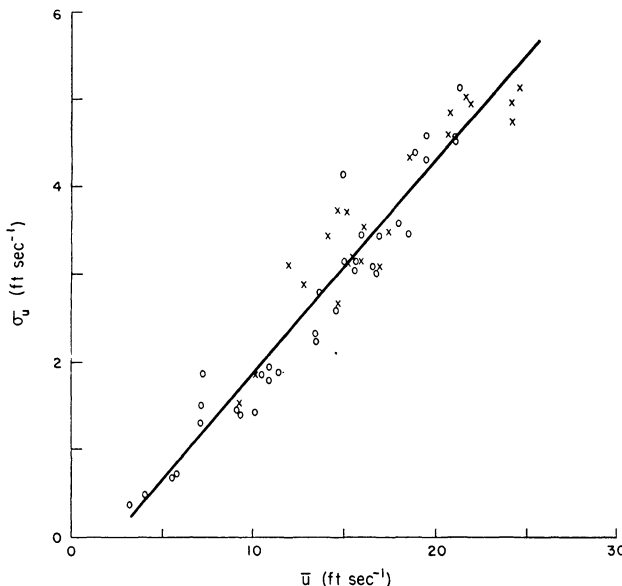


FIG. 1. Relationship between standard deviation of wind velocity and level of the mean wind speed for mechanical turbulence regime. Data based on 10-min samples of heated-thermocouple anemometer records obtained at height of 1.5 m during Great Plains Program [14]. Open circles refer to stable thermal stratification and symbol \times refers to unstable stratification. Intensity of turbulence indicated by slope of regression line is 0.24.

pling interval T is about 5 to 30 min. The direction of \bar{V} is customarily referred to the x -axis of a Cartesian coordinate system in which y is normal to the mean wind direction (in the plane of the horizon) and z is directed vertically. Orthogonal velocity components u , v , and w referred to the x , y , and z axes, respectively, are defined as follows:

$$u = \bar{u} + u'; \quad v = \bar{v} + v'; \quad w = \bar{w} + w'$$

and

$$\bar{u}' = \bar{v}' = \bar{w}' = \bar{v} = \bar{w} = 0.$$

The bars denote mean values for the period of sampling, T . The average amplitude of the fluctuations in wind velocity is expressed in terms of the standard deviation or rms value σ_v which is given by

$$\sigma_v^2 = \bar{V}^2.$$

Similar definitions apply in the case of the velocity components. The level or intensity of turbulence, I_V , is defined by the ratio of the average amplitude to the mean wind speed; *i.e.*,

$$I_V = \sigma_v / \bar{V}.$$

Characteristic dimensions of the fluctuations in wind velocity, or the scales of turbulence, are specified in terms of linear correlation coefficients, $R(s)$, that depend upon the covariance between simultaneous velocity measurements at pairs of fixed points, i , j , separated by a distance, s . For example, the alongwind

(longitudinal) correlation function, $R(x)$, is given by

$$R(x) = \bar{V}_i' \bar{V}_j' / \sigma_{V_i} \sigma_{V_j}.$$

As might be anticipated, the correlation tends to decrease from a theoretical value of unity for zero separation distance to a level of insignificance as the separation distance increases. The longitudinal scale of turbulence, $S(x)$, is defined by the integral

$$S(x) = \int_0^\infty R(x) dx.$$

This definition of scale, which has been confirmed in the wind tunnel [10], avoids the necessity for a detailed description of the geometry of a typical eddy. In practice, the upper limit of integration is taken at the point where the correlation function reaches a level of insignificance.

3. Probability distribution and turbulent intensity of fluctuations in horizontal wind speed

It has been established that probability distributions of wind velocity are approximately Gaussian for sampling intervals of the order of 10 min [1; 7; 12; 24]. Due to the influence of the earth's surface and the fact that wind speeds are bounded at zero, frequency distributions of horizontal wind speed are somewhat positively skew; however, this does not seriously alter the approximate Gaussian form of the distributions. It has also been established that the intensity of turbulence for the horizontal wind speed varies from about 0.05 to 0.40 depending upon the level of the mean wind speed, thermal stratification, surface roughness parameters, and height above ground. Within the layer of mechanical turbulence (which extends from ground level to a height of about 10 times the average height of surface-roughness elements) and in the presence of low or moderate wind speeds, the intensity of turbulence is about 0.25 in all thermal stratifications [7; 14]. In unstable stratification, this value for the intensity of turbulence applies to a very deep layer ($z \leq 1500$ ft). The data presented in fig. 1 are based on 10-min records from heated-thermocouple anemometers located at a height of 1.5 m above a smooth surface; the slope of the regression line is about 0.25. Satisfactory data for high mean wind speeds are not available. It appears likely that the intensity of turbulence decreases with increasing mean wind speeds in excess of about 30 mph and may be about 0.15 for mean wind speeds > 100 mph. In any event, the assumption of a value of 0.25 for the intensity of turbulence seems conservative for both moderate and extremely high mean wind speeds.

Since the probability distribution of horizontal wind speed is approximately Gaussian, estimates of the

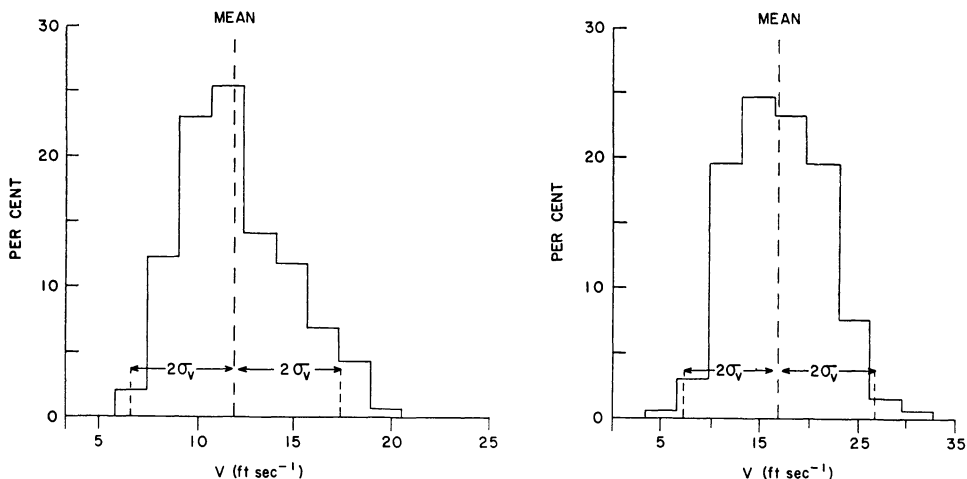


FIG. 2. Sample frequency distributions of wind velocity at height of 2 m above rough surface. Diagram at left refers to 5-min sampling period and a turbulent intensity of 0.22; diagram at right refers to 10-min sampling interval and turbulent intensity of 0.29.

extreme range in wind speed likely to be experienced during sampling intervals of the order of 10 min are conveniently obtained by reference to the areas and ordinates of the normal-error curve. The only information required is the level of the mean wind and either the standard deviation or the turbulent intensity. For general use, an intensity of 0.25 appears to provide a comfortable margin of safety at high wind speeds that should adequately compensate for any skewness in the distribution. Mean wind speeds are readily available from U. S. Weather Bureau records or may be estimated on the basis of experience. Two examples of the frequency distribution of wind velocity are presented in fig. 2; the data refer to heated-thermocouple-anemometer observations at a height of 2 m above a rough surface. As shown in the figure, about 95 per cent of the data points are included within two standard deviations of the mean; all data points are included within three standard deviations of the mean. Sample estimates of the extreme range in horizontal wind speed for various confidence levels are presented in table 1. A useful rule-of-thumb for estimating gust velocities involves multiplying the

mean wind speed by the factor 1.62; this limit should include about 99 per cent of the cases.

An alternative technique for estimating maximum wind speeds involves the application of the extreme-value theory [11] to available gust data. The principal objection to this procedure and, also, to that proposed by Sherlock [23] is the doubtful quality of the measurements. Conventional anemometers do not provide representative measures of maximum wind speeds; they are designed to provide satisfactory estimates of the mean wind for minimum sampling intervals of the order of 1 or 2 min. In addition, most anemometers blow down at wind speeds of the order of 100 mph due to failure of support structures; reliable observations for mean wind speeds of this order are consequently very scarce. Until satisfactory data are available, it seems reasonable to base estimates of maximum gust velocities on relationships already established at low and moderate wind speeds.

4. Power spectra and cospectra of atmospheric turbulence

The above discussion has been concerned with average properties of turbulence for sampling intervals of the order of 10 min. These gross statistics are non-selective; *i.e.*, contributions from all scales of turbulence are lumped together and no information is provided on the relative contribution of various frequencies to the total variance or covariance. For many practical applications, including determination of the dynamic response of structures to wind forces, it is necessary to have a knowledge of these relative contributions as a function of the frequency. Techniques for the selective (frequency-sensitive) analysis of velocity fluctuations are available from communica-

TABLE 1. Estimates of the extreme range in horizontal wind speed for 10-min sampling intervals. Entries are based on the assumptions that the fluctuations in wind speed are normally distributed and that the intensity of turbulence is 0.25.

\bar{V} (mph)	Confidence level		
	90 per cent ($\bar{V} \pm 1.65\sigma_V$) mph	95 per cent ($\bar{V} \pm 2.0\sigma_V$) mph	99 per cent ($\bar{V} \pm 2.58\sigma_V$) mph
20	12-28	10-30	7-33
40	25-56	20-60	14-66
80	48-112	40-120	28-132
120	70-170	60-180	43-197

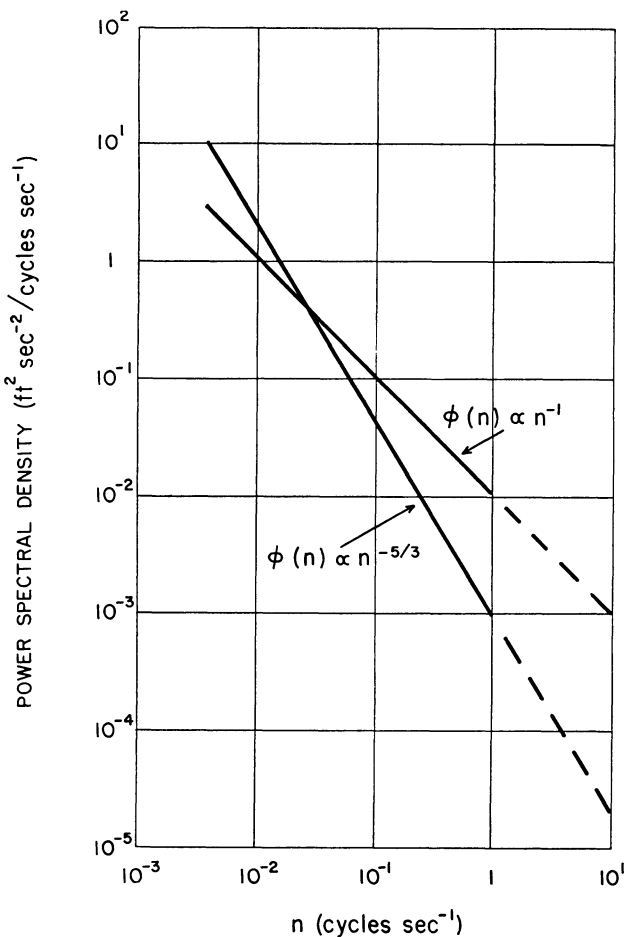


FIG. 3. Limiting values of the power spectrum of horizontal wind speed for frequency band from 1 to 10^{-3} cycles sec $^{-1}$. Data are adjusted for mean wind speed of 1 ft sec $^{-1}$ and turbulent intensity of 0.25. Dashed lines show extension of spectra to 10 cycles sec $^{-1}$. Calculations assume a cutoff frequency at 1/300 cycles sec $^{-1}$ based on 10-min sampling period.

tions theory [5]. These techniques involve calculation of the power spectrum or power-spectral-density function, $\phi(n)$, which has a simple physical interpretation: the integral of $\phi(n)$ between any two frequencies, n_1, n_2 , represents the contribution of all frequencies within the band from n_1 to n_2 to the total variance, σ_v^2 . It follows that

$$\sigma_v^2 = \int_0^\infty \phi(n) dn.$$

In the case of local variations in wind velocity measured at a point, power-spectral densities are obtained from the Fourier transform of the autocovariance function for stationary time series. Selective analysis of scale data utilizes the Fourier transform of the covariance function relating simultaneous time sequences of wind velocity measured at pairs of points [8].

Sufficient data are available to permit a description of the gross properties of the power-spectral-density

function for atmospheric turbulence [6; 9; 13; 15; 17; 18; 28]. Within the frequency range from about 10 to 10^{-3} cycles sec $^{-1}$, power spectra for the horizontal components of wind velocity are closely approximated by a power law expression of the type

$$\phi(n) \propto n^{-p},$$

where the absolute value of the exponent varies in the extreme between 0 and 2. At frequencies > 1 cycle sec $^{-1}$, the turbulence is approximately isotropic and the exponent is about $-5/3$ for all three velocity components. At frequencies < 1 cycle sec $^{-1}$ and at wave lengths larger than the height above ground, power spectra for the various components behave quite differently [9; 17]. The vertical component, for example, contains relatively little low-frequency energy. The power spectrum for the longitudinal or alongwind component tends to follow the $-5/3$ law in all thermal stratifications and, therefore, contains relatively large amounts of energy at low frequencies. In the presence of unstable thermal stratification, the low-frequency energy in the power spectrum for the lateral or crosswind component exceeds that for the alongwind component; in the presence of stable thermal stratification, the shape of the power spectrum for the lateral component at low frequencies is similar to the shape of the w -spectrum. This behavior of the power spectrum for the lateral component of wind velocity is in part explained by the elongation of mechanical eddies in the direction of the mean flow; large convective eddies are of approximately equivalent extent both along and across the direction of the flow. At suitable distances above ground level in all thermal stratifications, the power spectrum of horizontal wind speed tends to follow the $-5/3$ law within the frequency range from 10 to 10^{-3} cycles sec $^{-1}$. Close to ground level, at heights from about 1 to 10 times the vertical dimensions of surface-roughness parameters, a somewhat smaller absolute value of the exponent applies. This is accounted for by the tendency for larger eddies to be broken into smaller elements by the obstructions; energy is thus added to the high-frequency end of the spectrum and subtracted from the low-frequency end. In the limit, the result is a spectrum in which the power-spectral density is inversely proportional to the frequency (see figs. 3, 4).

Limiting forms of the power spectrum for horizontal wind speed are presented in fig. 3. The solid lines are drawn so that the integral of the power-spectral density between 1 and 1/300 cycles sec $^{-1}$ is $0.0625\bar{V}^2$ for $\bar{V} = 1$ ft sec $^{-1}$. This relationship follows from the value of 0.25 assumed for the intensity of turbulence. Extension of the spectra to 10 cycles sec $^{-1}$ is indicated by the dashed lines; there is some question about the

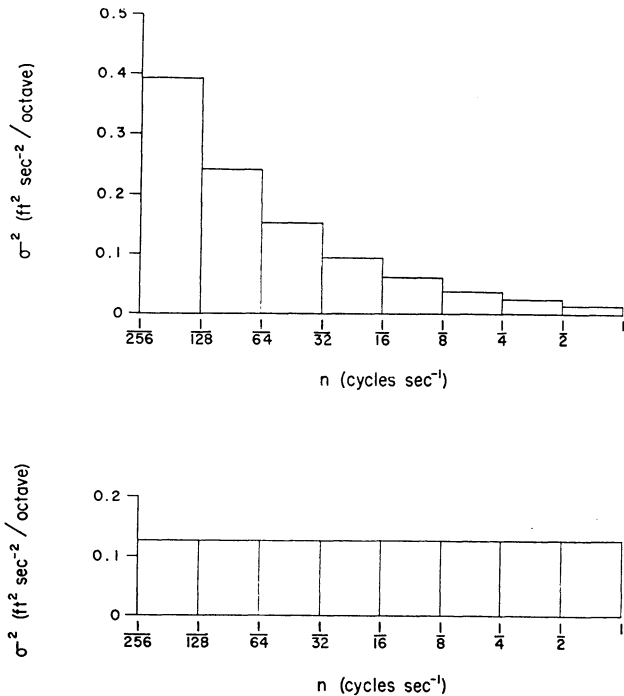


FIG. 4. Fraction of total variance or power contributed in each octave of the spectral band from 1 to 1/256 cycles sec⁻¹ for $n^{-5/3}$ (upper diagram) and n^{-1} (lower diagram) power spectra. Total variance is set equal to unity.

validity of this extension for the n^{-1} spectrum, since the $-5/3$ law supposedly applies within this region. In constructing the figure, it has been assumed that the mean wind speed is measured over a 10-min sampling interval and that frequencies $< 1/300$ cycles sec⁻¹ do not contribute significantly to the total variance. In the event that the spectral gap at about 10⁻³ cycles sec⁻¹ found by Van der Hoven [28] is established as a characteristic feature of the spectrum, the low-frequency cutoff in fig. 3 would have to be set at about 1/200 cycles sec⁻¹. An alternative representation of these power spectra is shown in fig. 4 where the frequency band from 1 to 1/256 cycles sec⁻¹ is divided into octaves. In this case, the ordinate represents the percentage contribution of each octave to the total variance which has been set equal to unity. Ordinates are obtained from the product of the spectral density and the frequency at the midpoint of each octave. The upper diagram of fig. 4 shows quite clearly the relatively large concentration of energy at low frequencies implied by the $-5/3$ law; the lower diagram shows the characteristic form of the n^{-1} spectrum in which the mean square amplitude of the fluctuations is invariant with frequency.

Characteristic features of the power spectrum of the vertical-velocity component have recently been described by Panofsky and McCormick [18]. They show that the shape of the power spectrum tends to be invariant with thermal stratification, height above

ground level, and surface roughness if the product of spectral density and frequency, $n\phi_w(n)$, is plotted against the ratio, f , of the height above ground level and the wave length, \bar{V}/n . In symbols,

$$n\phi_w(n) \propto nz/\bar{V} = f,$$

where z is the height. The position of the maximum shifts toward lower frequencies with increasing height above ground; also, the level of turbulence or absolute values of the variance changes markedly with surface roughness, thermal stratification, and height above ground. The following expression is suggested for general use [18]:

$$n\phi_w(n) = \frac{0.2 V_1^{2f}}{(1 + 4f)^2 \log^2 z_1/z_0},$$

where the subscript 1 denotes a height of about 3 ft over smooth terrain and about 30 ft over very rough surfaces, and z_0 is a roughness length which varies from about 0.03 to 3 ft depending upon the surface. The above expression is considered adequate in all thermal stratifications at heights < 40 ft; it applies at much greater heights (perhaps up to 1500 ft) in the presence of thermal instability. The validity of the formula at frequencies > 1 cycle sec⁻¹ is open to question, since the $-5/3$ law should apply within this range.

Analysis of wind forces on structures requires, in addition to a knowledge of the power spectrum of atmospheric turbulence, information on the characteristic lengths or scales of turbulence. Data of this type are needed in evaluating the effects of yaw and lift. Appropriate quantities are derived from the co-spectra of wind-velocity fluctuations measured simultaneously at pairs of points located at various separation distances along the axes of the conventional Cartesian coordinate system. Few direct measurements of the Eulerian space spectra (as distinguished from the Eulerian time spectra discussed above) are available. Practically the only data available are those obtained by the Massachusetts Institute of Technology during Project Prairie Grass [8]. These observations comprise 20-min records of wind velocity from five instrument assemblies (bivanes equipped with heated-thermocouple anemometers) located at a height of 2 m above a smooth surface and oriented either parallel or normal to the prevailing wind direction at separation distances of 6, 12, 24, and 48 m. The procedure for securing scale estimates is similar to that used in wind-tunnel investigations [10] except that, instead of dealing with linear correlation coefficients based on the entire length of record, the coefficients utilized are functions of frequency. The co-spectral correlation function, $R_{cos}(n, s)$, is defined

by the relation

$$[R_{cos}(n, s)]^2 = [COV(n, s)]^2 / \phi_i(n) \phi_j(n),$$

where $COV(n, s)$ is the cospectral density; $\phi_i(n)$, $\phi_j(n)$ are power-spectral densities identified with the time sequences at positions i, j ; and s is the separation distance between appropriate pairs of positions. The scale estimate, $S(n)$, for a frequency band centered at frequency n is given by the integral

$$S(n) = \int_0^\infty R_{cos}(n, s) ds$$

where the upper limit of integration is, in practice, taken as the separation distance at which the correlation function reaches a level of insignificance.

Results of the selective analysis of the Prairie Grass data, which refer to the frequency domain from about 0.5 to 0.01 cycle sec⁻¹, may be summarized as follows: scale spectra of the orthogonal components of wind direction are dominated by fluctuations in the alongwind and crosswind components; the maximum horizontal extent of fluctuations in the vertical component was less than the minimum separation distance of 6 m used in the experiments. At high frequencies, there is approximate equality in all thermal stratifications in the crosswind and alongwind scales for both u and v . Alongwind scales for both components increase at about the same rate as the frequency decreases, the scale for the lateral velocity component being somewhat larger at low frequencies than the scale for the longitudinal component. In the presence of thermal instability, the crosswind scales for both components are approximately equal to the alongwind scales over the entire frequency range. In the presence of stable stratification, the alongwind scales for both u and v greatly exceed the crosswind scales at low frequencies. This is an approximately linear relationship between the scale estimates for both velocity components and inverse wave number $k^{-1} = \bar{V}/n$. This is not unexpected, since the data have previously been used to demonstrate the validity of Taylor's hypothesis relating time and space spectra [26]. Panofsky *et al* [17] have shown that the substitution $x = \bar{V}/n$ holds for distances < 300 ft over a smooth surface. The results of the scale analysis are indicated in fig. 5 which presents the regression lines for the alongwind and crosswind estimates of both velocity components as functions of k^{-1} . It is of interest to note that the alongwind scale estimates are from three to five times smaller than the half wave lengths indicated by the abscissa (scale estimates refer to half cycles rather than complete cycles). This difference may be explained by a simple geometric argument. In the case

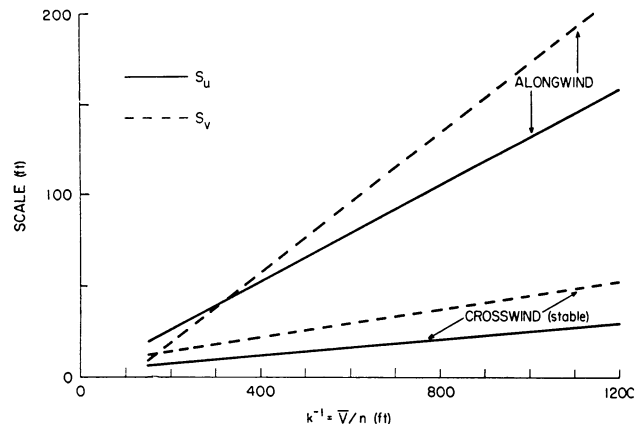


FIG. 5. Alongwind and crosswind scales of turbulence for the u - and v -components of wind velocity as functions of inverse wave number. Crosswind scales for both components in unstable stratification are not shown but are approximately the same magnitude as the alongwind scales.

of eddies that are elongated in the direction of flow, the continual turning of the wind in the azimuth plane results in a low "collection efficiency" for a grid oriented along the mean flow; projections of the characteristic lengths on the grid principally reflect the cross wind dimensions of the eddies for angular deviations greater than about 10 deg from the mean direction.

5. Application of power-spectral analysis in determining wind loadings

As pointed out by Zbrożek [29], power-spectral analysis makes it unnecessary to define the waveform for a typical single gust; instead, it is only necessary to specify the shape of the power-spectral-density function for atmospheric turbulence. Once the form of the power spectrum is established, calculation of the dynamic response of structures to wind forces is a comparatively simple matter. This approach has been widely used by aeronautical engineers, and many of their techniques appear to be adaptable to civil engineering problems. Three elements are involved in determining the structural load produced by wind forces [27]: the input spectrum, defined by the power-spectral density of atmospheric turbulence, $\phi_V(n)$; the frequency response function of the structure $T(n)$, defined in terms of the steady-state-load-response amplitude for a unit sinusoidal gust as a function of the forcing frequency; and the output spectrum, $\phi_L(n)$, defined in terms of the load. The basic relationship between output and input spectra for linear systems is given by the expression

$$\phi_L(n) = |T(n)|^2 \phi_V(n),$$

where $|T(n)|^2$ is the square of the modulus of the structure frequency response function. The variance

of the load, σ_L^2 , is obtained from the integral

$$\sigma_L^2 = \int_0^\infty \phi_L(n) dn = \int_0^\infty |T(n)|^2 \phi_V(n) dn.$$

Under certain simplifying assumptions (*i.e.*, the turbulence is locally stationary and Gaussian, and the shape of the input spectrum is invariant with the level or intensity of turbulence), it is possible to deduce the probability that a given load will be exceeded. Rice [20; 21] and Press *et al* [19] have derived the appropriate expressions for use in connection with aircraft design.

6. Concluding remarks

This brief survey of existing knowledge of the structure of atmospheric turbulence is intended only to point out the potential usefulness of power-spectral analysis in determining the dynamic wind load on structures. It is evident that much remains to be learned about the basic properties and mechanisms of turbulence, particularly at high levels of mean wind speed. Due to the nature of the problem, this improved understanding can only be achieved through extensive empirical investigations. Until satisfactory data are available, power-spectral techniques cannot be expected to take the place of conventional steady-state procedures. It is hoped that the potential advantages offered by this new approach to load problems will stimulate both civil engineers and meteorologists to see that the necessary experiments are carried out.

Acknowledgments. The author is indebted to Dr. F. A. Record and Dr. A. Fleisher for helpful discussions of the contents of the manuscript.

REFERENCES

- Best, A. C., 1935: *Transfer of heat and momentum in the lower layers of the atmosphere*. Geophys. Mem., No. 65, 40–66.
- Biggs, J. M., 1954: Wind loads on truss bridges. *Trans. Amer. Soc. Civil Eng.*, **119**, 879–898.
- , 1958: Wind forces on structures; introduction and history. *J. Struct. Div., Proc. Amer. Soc. Civil Eng.*, **84**, No. ST 4.
- , S. Namyot, and J. Adachi, 1956: Wind loads on girder bridges. *Trans. Amer. Soc. Civil Eng.*, **121**, 101–124.
- Blackman, R. B., and J. W. Tukey, 1958: The measurement of power spectra from the point of view of communications engineering. *Bell Sys. Tech. J.*, **37**, 185–288 and 485–569.
- Bushnell, R. H., and P. O. Huss, 1958: A power spectrum of surface winds. *J. Meteor.*, **15**, 180–183.
- Cramer, H. E., 1952: Preliminary results of a program for measuring the structure of turbulent flow near the ground. *Geophys. Res. Pap.* No. 19, AFCRC, 187–205.
- , 1959: Measurements of turbulence structure near the ground within the frequency range from 0.5 to 0.01 cycles sec⁻¹, in *Advances in geophysics*, 6, *atmospheric diffusion and air pollution*. New York and London, Academic Press, 75–96.
- Cramer, H. E., and F. A. Record, 1955: Power spectra of the eddy velocity components. *J. Meteor.*, **12**, 146–151.
- Dryden, H. L., G. B. Schubauer, W. C. Mock, Jr., and H. K. Skramstead, 1937: *Measurements of the intensity and scale of wind-tunnel turbulence and their relation to the critical Reynold's number of spheres*. Natl. Advis. Comm. Aero. Rep. No. 581, 32 pp.
- Gumbel, E. J., 1935: Les valeurs extrêmes des distributions statistiques. *Ann. de l'Inst. de H. Poincaré*, **5**, 115–158.
- Hesselberg, T., and E. Bjorkdal, 1929: Über das Verteilungsgesetz der Windunruhe. *Beitr. Physik. fr. Atmos.*, **15**, 121–133.
- Lappe, U. O., B. Davidson, and C. B. Notess, 1959: *Analysis of atmospheric turbulence spectra obtained from concurrent airplane and tower measurements*. Inst. Aero. Sci. Rep. No. 59–44, 33 pp.
- Lettau, H., and B. Davidson, 1957: *Exploring the atmosphere's first mile*. London, Pergamon Press, 578 pp.
- MacCready, P. B., 1953: Structure of atmosphere turbulence. *J. Meteor.*, **10**, 434–449.
- Panofsky, H. A., H. E. Cramer, and V. R. K. Rao, 1958: The relation between Eulerian time and space spectra. *Quart. J. r. meteor. Soc.*, **84**, 270–273.
- Panofsky, H. A., and R. J. Deland, 1959: One-dimensional spectra of atmospheric turbulence in the lowest 100 meters in *Advances in geophysics*, 6, *atmospheric diffusion and air pollution*. New York and London, Academic Press, 41–64.
- Panofsky, H. A., and R. A. McCormick, 1959: *The spectrum of vertical velocity near the surface*. Inst. Aero. Sci. Rep. No. 59–6, 12 pp.
- Press, H., M. T. Meadows, and I. Haddock, 1956: A re-evaluation of data on atmospheric turbulence and airplane gust loads for application in spectral calculations. Natl. Advis. Comm. Aero. Rep. 1272.
- Rice, S. O., 1944: Mathematical analysis of random noise. *Bell Sys. Tech. J.*, **23**, 282–332.
- , 1946: Mathematical analysis of random noise. *Bell Sys. Tech. J.*, **24**, 46–156.
- Sherlock, R. H., 1951: Analyzing winds for frequency and duration. *Meteor. Monogr.*, **1**, No. 4, 42–49.
- , 1958: Wind forces on structures: Nature of the wind. *J. Struct. Div., Proc. Amer. Soc. Civil Eng.*, **84**, No. ST 4.
- Shiotani, M., 1950: Turbulence in the lowest layers of the atmosphere. *Sci. Rep. Tohoku Univ., Series 5, Geophys.*, **2** No. 3, 167–201.
- Sutton, O. G., 1953: *Micrometeorology*. New York, McGraw-Hill Co., p. 250.
- Taylor, G. I., 1938: The spectrum of turbulence. *Proc. r. Soc. London A*, **164**, p. 476.
- Thorson, K. R., and Q. R. Bohne, 1959: *Application of power spectral methods in airplane and missile design*. Inst. Aero. Sci. Rep. No. 59–42, 34 pp.
- Van der Hoven, I., 1957: Power spectrum of horizontal wind speed in the frequency range from 0.0007 to 900 cycles per hour. *J. Meteor.*, **14**, 160–164.
- Zbrozek, J. K., 1958: Some effects of atmospheric turbulence on aircraft. *Weather*, **13**, 215–227.

ESTIMATES OF MINIMUM WIND FORCES CAUSING STRUCTURAL DAMAGE IN THE DALLAS TORNADO¹

E. P. Segner, Jr.

A. & M. College of Texas

ABSTRACT

The minimum wind velocities required to produce some of the structural failures that occurred during the Dallas tornado of 2 April 1957 have been determined. Data on the wind velocities were obtained from an analysis of many types of structures. In each case, the minimum or, in a few cases, the maximum wind velocities were computed based upon reasonable sequences or modes of failure. Although the results are limited by the assumptions required by the analysis, it is felt that they have considerable value as an indication of the relative magnitude of the wind velocities involved.

1. Introduction

In selecting items for engineering analysis from the great number of interesting and unique occurrences present, consideration was given to choosing only those for which sufficient and pertinent information was available to make the engineering estimate reasonable and reliable. Naturally, some of the sites yielded an estimate much more trustworthy than others, due to the extent of the damage and obvious sequence of events, the helpfulness of the eye-witness reports, the type and quality of construction, and the availability of wind-tunnel data. Another factor which had to be considered was whether or not the damage resulted from actual wind forces or from flying objects. This, in some cases, was impossible to determine. It is necessary to keep in mind the factors which have been mentioned and realize that, in each case, the velocities are probably somewhat in error and represent only a reasonable estimate at best.

2. Collapse of two walls of a service station located on the corner of Stewart and Edgfield Streets in Southeast Dallas (item no. I) (Fig. 1)

The walls A and B were blown outward at this location. Both walls were constructed of 8-inch concrete blocks and had a clear ceiling height of 12 ft. The minimum computed velocity needed to collapse walls A and B was approximately 92 mph. Of course this assumes sound original construction, which may or may not have been present, as the general character of masonry construction makes pin-point analysis

impossible. This is especially true where combined bending and axial loading is involved.

3. Overturning of a small empty storage tank at Davisson Oil Co., 1616 Singleton Blvd. (item no. II) (Figs. 2 and 3)

This tank was overturned and was seen by eyewitnesses to roll for over 100 ft along the ground after overturning. This analysis determined only the minimum wind velocity required to overturn, and it assumed the legs were not anchored. The minimum wind velocity required to produce this overturning action was between 55 and 65 mph; however, it should be kept in mind that the tank actually was blown along the ground for some distance after overturning, which might possibly indicate that a much higher wind velocity was present. Since the legs were not anchored, the tank may have been subject to gust action.

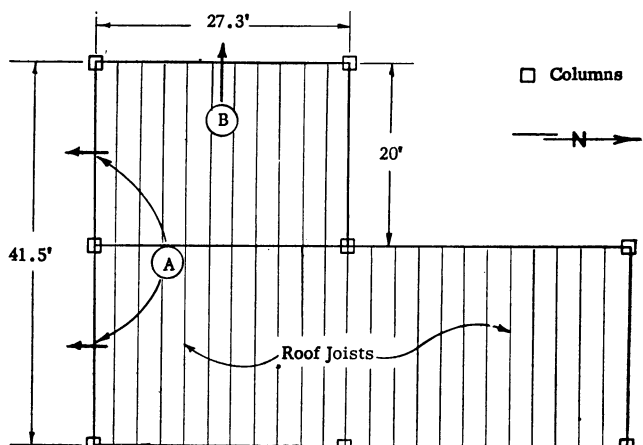


FIG. 1. Plan view of building.

¹ Presented before the Second National Conference on Applied Meteorology: Engineering, held in Ann Arbor, Michigan, September 9-11, 1958, under the joint sponsorship of the American Meteorological Society and the American Society of Civil Engineers.

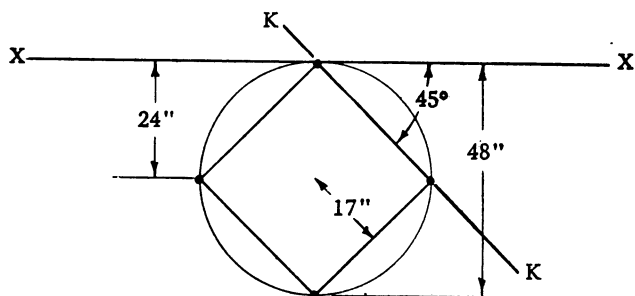


FIG. 2. Plan view of tank.

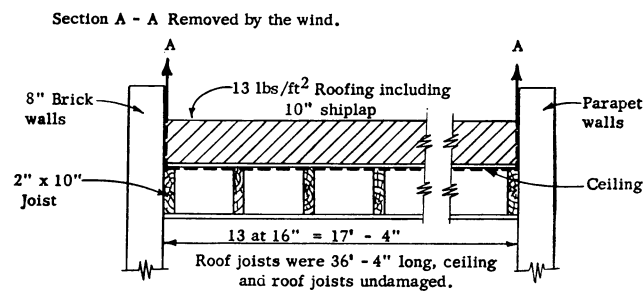
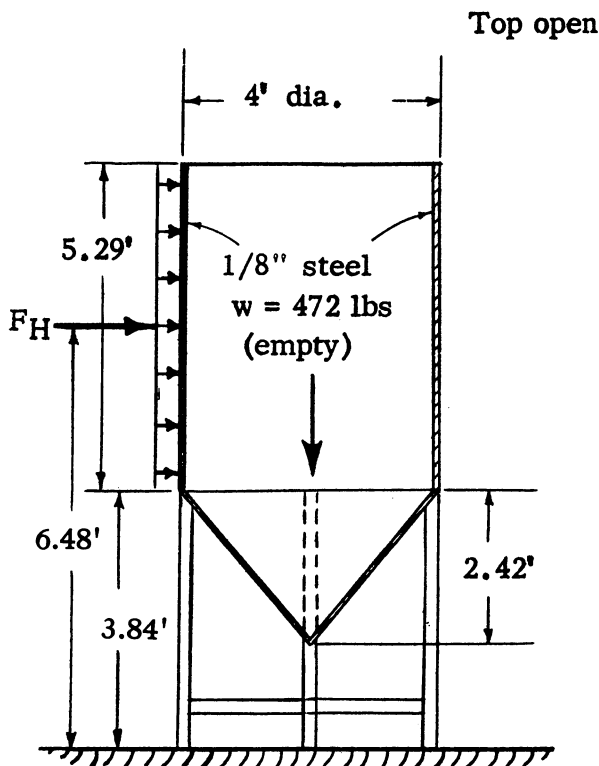


FIG. 4. Elevation of roof section.

FIG. 3. Elevation view of tank. Support consists of 4 legs and horizontal braces. All are $1\frac{1}{2}'' \times 1\frac{1}{2}'' \times \frac{3}{16}''$ angles.

4. Removal of the flat roof of a building owned by Mr. A. Ragland, located at 3013 Navarro, on the corner of Navarro and Singleton Blvd. (item no. III) (Fig. 4)

In this item, the built-up roof of the two-story building was completely blown off, including the 10-inch shiplap. The roofing material was unusually heavy for this type of construction, being approximately 13 psf. Neither the supporting roof joists below nor the ceiling carried by the roof joists were damaged. Thus, it appears that only negative external wind pressure was involved. In the analysis, only 50 per cent of the attaching 20d common nails were assumed to be effective in resisting this uplift, since

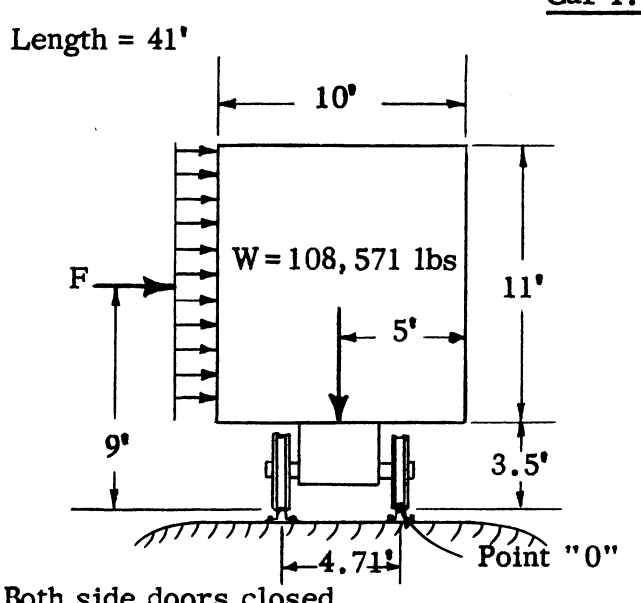


FIG. 5. End view of car I.

the roof joists themselves were not damaged. It should be kept in mind that this is only an approximation at best, but it is considered to be reasonable in view of the information available; therefore, the minimum wind velocity required to cause failure, in the manner described, was computed to be at least 179 mph. Of course, the chief error involved in these calculations relates to the type of end connection involved and its particular manner of failure.

5. Overturning of railroad freight cars at record crossing switch on the east side of the Trinity River (item no. IV) (Figs. 5 and 6)

At this location, several railway freight cars were overturned by the force of the tornado.

Car 1 was overturned sideways to the west, and at the time of overturning it had a gross weight, without the trucks, of approximately 108,600 lb. Both of its side doors were closed. The minimum velocity required was 128 mph.

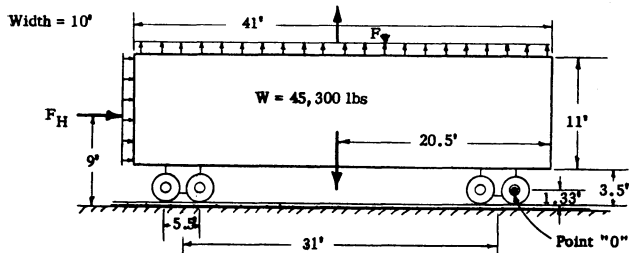


FIG. 6. Elevation of car IV.

Car 2, with both of its doors open, remained in an upright position on the track, and it had a loaded gross weight of 119,300 lb at the time. This does not include the weight of its trucks, which weighed a total of 10,000 lb. The minimum velocity required to overturn was 144 mph; therefore, if the assumptions made are correct, it can be concluded that the horizontal wind in the vicinity of the cars 1 and 2 was between 128 and 144 mph.

Car 3 remained upright on the track directly south of car 2 and was of similar position and weight; therefore, the horizontal wind velocity was less than 144 mph.

Car 4 was reported by an eye-witness to have been located south of car 6 and to have overturned endwise with a center rotation about one end. This car was empty and had a gross weight of approximately 45,300 lb, excluding the weight of the trucks which remained on the ground. The doors on each side of the car were open. It should be kept in mind that the values obtained from the analysis of this item were very approximate in nature, since the shape factors used in the calculations are only estimated average values and vary greatly with the shape and relative size of each structure. Exact values can be determined only by wind-tunnel tests for the particular item concerned. The minimum velocity required to produce this overturning action was calculated to be 217 mph.

Car 5 was empty and had a gross weight of 45,300 lb, excluding the weight of the trucks which were left on the ground as the car turned sideways to the east. Only one of its doors was definitely known to have been open; therefore, the other door was assumed to have been closed. The minimum computed wind velocity was 83 mph.

Car 6, with both of its doors open at the time, was overturned sideways to the east and had a gross weight of 119,300 lb. The minimum horizontal velocity required to overturn it was 144 mph.

Car 7 had a loaded gross weight, including its trucks, of 72,400 lb, and it overturned sideways to the east. Both of its doors were closed. The minimum computed velocity was 105 mph.

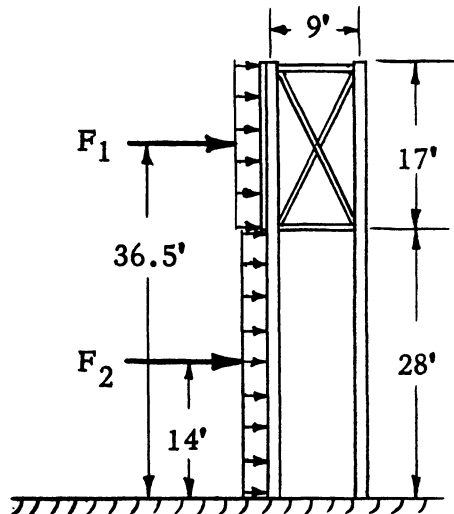


FIG. 7. End elevation of sign.

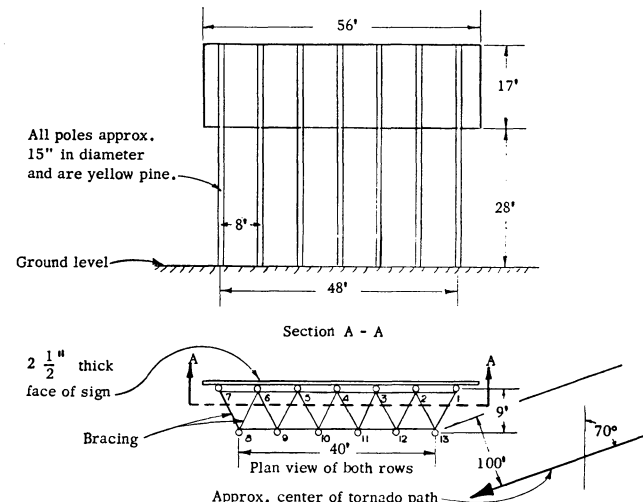


FIG. 8. Top view and rear elevation of sign.

Car 8 had a loaded gross weight, including weight of its trucks, of 135,600 lb, and it remained in an upright normal position. The door on the west side was open while the door on the east side was closed. The minimum computed velocity needed to produce overturning was 143 mph since it remained upright. Since both doors were not closed, it should be remembered that the exactness of any calculations would be very approximate without wind-tunnel tests.

6. Structural collapse of a 45-ft elevated signboard located on the west side of Harry Hines Blvd. in the 7400 block (item no. V) (Figs. 7 and 8)

This structure consisted of 13 poles extending 45 ft above ground. The horizontal bracing was in the elevation between 28 ft and 45 ft only, above the

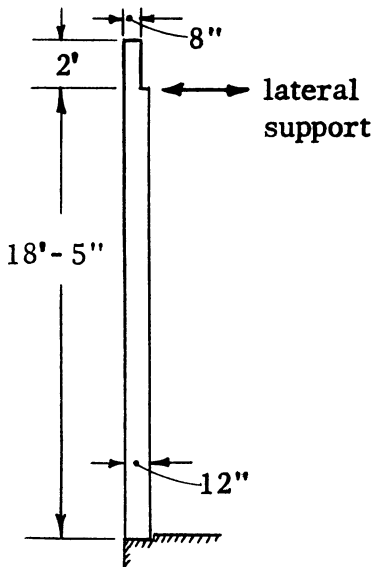


FIG. 9. Elevation of wall.

ground level, and was of unknown character. Since the dispensation of the bracing was approximated, the exact sequence of failure was unknown. Therefore, several conceivable sequences of failure were considered with the lowest minimum velocity computed being 302 mph. In this case, it was assumed that the bracing and face of the billboard itself failed first, and then each pole, stripped of all other components of structure, failed independently due to the wind pressure of its own vertical surface along its full height.

In view of this high value of the minimum wind velocity, and considering the other minimum velocities computed for different situations, it would seem very doubtful that a single mode of failure occurred. Rather, it is more likely that a combination of failures actually took place, thus making possible a reduced velocity to account for the damage. The possibility of destruction from flying objects should not be overlooked because of the distance from the damage and proximity of other structures which were not severely damaged. Another consideration to be noted is that, if the calculated velocity of 302 mph is regarded as a reasonable value, the velocity of the wind at the ground level could have been much less since the large resisting face of the sign was between 28 and 45 ft above the ground.

7. Structure failure of 12-inch masonry walls on three sides of Renard Linoleum and Rug Company, 2335 Burbank Street (item no. VI) (Figs. 9 and 10)

In this structure, three of the four vertical walls failed as shown with the wall "D" remaining intact. All walls were 12-inch masonry construction consisting of 8-inch light-weight concrete block interlaced

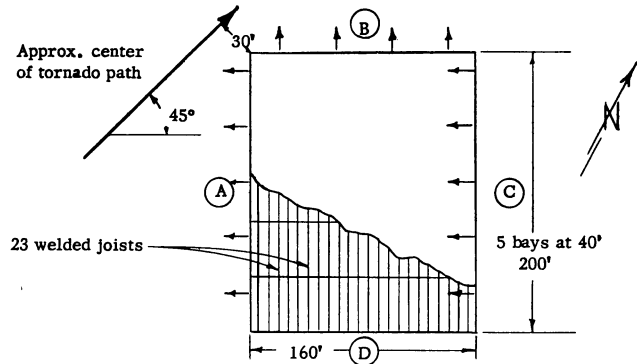


FIG. 10. Plan view of building.

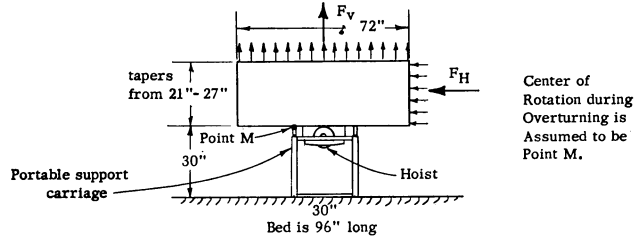


FIG. 11. Front elevation of truck bed.

by 4-inch brick. The clear height of all walls was 18 ft-5 inch. The computed minimum velocities needed to collapse walls A and C was 107 mph, while that of wall B was 109 mph. Of course, these values assume no secondary failure of either wall which might occur if failure of all walls were not simultaneous. In addition, it might be noted that, if a so called "down-draft" existed in the vicinity of this building, this downward vertical pressure on the roof would have enabled the walls to have withstood a much greater pressure differential before failing than the figures indicate. Of course the magnitude, or even the existence of this factor, is not known; therefore, it cannot be considered here.

8. Overturning of an empty truck bed and attached hoist at corner of Denton Road and Wyman Street (item no. VII) (Fig. 11)

This item consists of a 3-yd truck bed and its attached hydraulic hoist which was overturned by the wind force while resting on a portable support carriage about 30 inch off the ground. The bed and the hoist were overturned about an axis parallel to its longitudinal axis. In the analysis, the wind force was considered to have been composed of vertical uplift as well as horizontal pressure. In interpreting the results obtained by this method, it should be kept in mind that this value is only approximate in nature since estimated shape factors were used. No horizontal slippage was possible. Based on this analysis, the

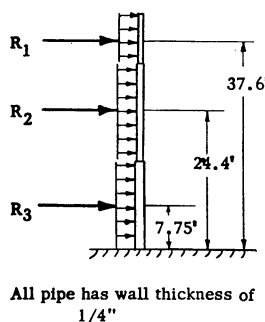


FIG. 12. Dimensions of flag pole.

minimum wind velocity required to overturn the truck and attached hoist was approximately 123 mph.

9. The yielding of a flag pole in front of the Johnson & Johnson Company, 9000 Denton Drive (item no. VIII) (Figs. 12 and 13)

This flag pole was located in front of the Johnson & Johnson Administrative Building, located on the east side of Denton Drive. The pole was composed of three telescoped sections of pipe having a total height of 42 ft. The pole was embedded in concrete for a length of 6 ft which was undisturbed by the tornado. This, coupled with the fact that the stresses in the portion of the pole above the ground remained in the elastic range, as evidenced by its straightness when measured afterwards, would seem to indicate that all of the

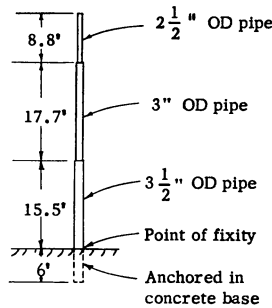


FIG. 13. Stress distribution in pole.

permanent deformation occurred at its base—that is, at the top of the concrete base. The final angle of deviation off the vertical was 1 deg 30 min. If one assumes a yield point steel stress of 35,000 psi, the minimum wind velocity required to produce this stress would be between 115 and 133 mph. It might be added that the writer feels that these values are quite accurate and can be taken as being very reliable as an indication of minimum wind velocities encountered.

10. Roof damage to Johnson & Johnson Company warehouse located at 9000 Denton Drive (item no. IX) (Fig. 14)

This item consists of a hole in the roof of the Johnson & Johnson Company warehouse which was the result of either external negative pressure or

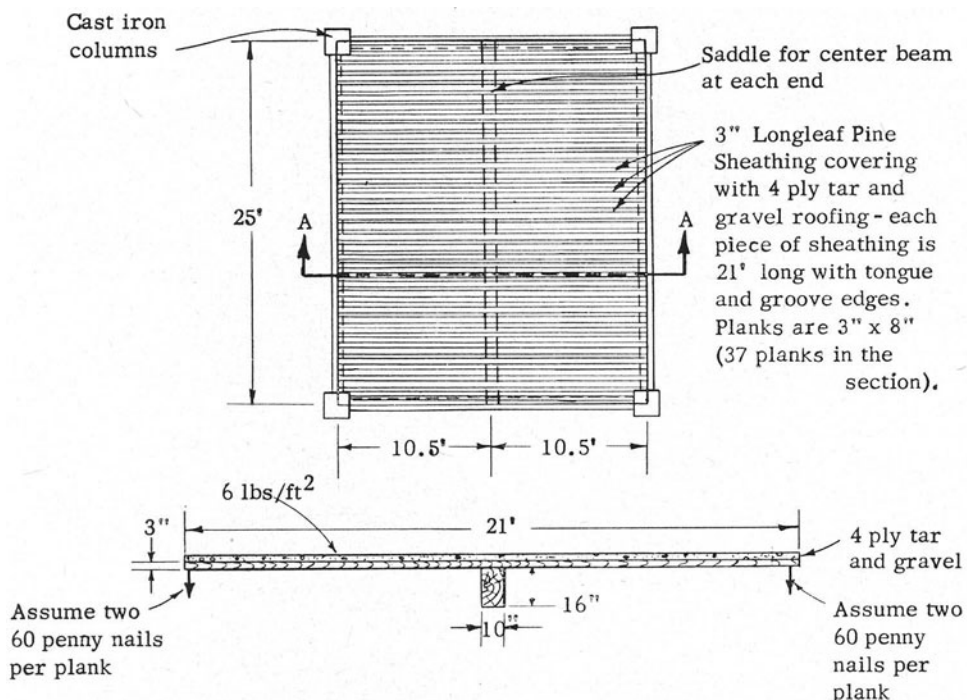


FIG. 14. Plan and elevation views of roof.

internal pressure. The roof section considered was approximately 21×25 ft. The roof portion consisted of 3-inch longleaf pine sheathing covered with a 4-ply tar-and-gravel roofing. In the analysis, only 50 per cent of the nails at each end of each sheathing plank were assumed to be effective in pullout. The minimum pressure differential to cause failure of the roof section

above was approximately equivalent to a wind velocity of 189 mph; however, this value would be subject to great change with any change in the type of connection failure assumed. Since the exact type of connection failure is unknown, this value must be considered, at best, only a rough estimate; however, it is probably correct within 25 per cent.

11. Summary of estimated wind velocities in Dallas tornado

Item No.	Location	Item description	Estimated velocities (mph)
1.	Corner of Stewart and Edgefield Sts.	Service station wall collapse (12" high). (a) collapse outward of south 8" concrete block wall. (b) collapse outward of west 8" concrete block wall.	91.6 (min) 92.2 (min)
2.	1616 Singleton Blvd.	Overturning of 48" diam empty tank on 3'-10" legs. (a) with single leg as center of rotation. (b) with pair of adjacent legs as center of rotation	65.5 (min) 55.2 (min)
3.	Corner of Navarro and Singleton Blvd.	Uplift of roof section from flat-roofed 2-story structure.	179 (min)
4.	Record crossing on east side of Trinity River.	Overturning, or near overturning, of 8 railway freight cars. Car I. Car II. Car III. Car IV. Car V. Car VI. Car VII. Car VIII.	128 (min) 144 (max) 144 (max) 217 (min) 83 (min) 144 (min) 105 (min) 143 (max)
5.	7400 Block of Harry Hines Blvd.	Failure of 13 pole, 45' elevated signboard. Independent failure of each pole assumed critical.	(very doubtful) 302 (min)
6.	2335 Burbank	Structural failure of 12" concrete block walls—18' ht. (a) southwest wall outward. (b) northwest wall outward. (c) northeast wall inward.	107.4 (min) 109.3 (min) 107.4 (min)
7.	Corner of Denton Rd. and Wyman St.	Overturning of empty truck bed and hoist.	123 (min)
8.	9000 Denton Rd.	Yielding of flag pole in front of Johnson and Johnson Co. (a) assuming elastic action. (b) assuming plastic action.	115 (min) 133 (min)
9.	9000 Denton Rd.	Removal of roof section from Johnson and Johnson Warehouse.	189 (min)

Acknowledgments. The author would like to acknowledge the support and assistance given him by the Department of Oceanography and Meteorology at A. & M. College of Texas. He is particularly indebted to Professor Stuart G. Bigler. If the reader would like a more detailed report including calculations, he may secure the full formal report that was prepared jointly by Professor Bigler and the writer for the Department of Oceanography and Meteorology at A. & M. College

of Texas entitled *The Dallas Tornado of 2 April 1957—Scientific Report No. 2*. This research was conducted through the Texas A. & M. Research Foundation and sponsored by the U. S. Weather Bureau under Contract No. Cwb-9116. The assistance of the Texas Engineering Experiment Station, College Station, Texas, with manuscript preparation also is gratefully acknowledged.

WIND LOAD ON TOWERS

Edward Cohen

Ammann & Whitney, New York City

ABSTRACT

The two basic types of towers are briefly described with their diversity in form, construction, and function illustrated by a number of recently constructed structures.

The general theory of wind pressure for aerostatic effects and the empirical-shape factors reported for common structural members are presented. Composite shape factor-solidity ratio relations for square and triangular towers are derived through the use of test data on trusses for aerostatic drag, shielding, and yaw effects. The validity of these relations as reasonably conservative design tools is confirmed by a comparison with test results. Various foreign and American codes are compared relative to aerostatic wind-loading recommendations on tower structures.

Vibration of towers in the direction of the wind and the dynamic behavior of cylindrical elements normal to the wind stream are examined. Recently reported test data on aerodynamic-lift (lateral force) coefficients are presented, and recommendations are made for the dynamic design of cylindrical tower structures. The types of guy oscillation due to wind action and possible means of their suppression are indicated.

Design loadings as well as design procedures for determining maximum stresses and deflections are discussed. The safety of tower structures is discussed, and the additional data required for an accurate estimate of safety are described.

1. Introduction

a. General description

Towers are basically of two general types, (1) free-standing towers which are fixed at their foundations and act as vertical cantilevers, and (2) guyed towers which are supported laterally by guys attached at one or more levels. The grandfather of our modern steel towers is the Eiffel Tower (fig. 1), built to a height of 984 ft for the Paris World's Fair of 1889. The tower is free standing and has a total weight of 7700 tons. It is still the tallest structure in Europe. From an apartment atop the tower, Gustave Eiffel conducted some of the first high altitude studies of the wind.

Eiffel predicted that "my tower will stand a thousand years." Modern towers must be amortized much sooner. Many towers now being built by both military and civilian agencies may become functionally obsolete in less than 10 to 25 yr.

The next tallest structure in Europe is a guyed television tower (fig. 2) completed in 1956 at Stein-kimmen, Germany [21; 41]. The structure rises to a height of 977 ft but weighs only 240 tons. In the United States, towers of 1000 ft or more have become commonplace. A 3000-ft-high guyed antenna tower is now under consideration. The tallest existing structure in the world is the 1572-ft-high tower of Station KWTV in Oklahoma City¹.

While there are only two basic types of towers, their form and construction are subject to pronounced

variations as shown by the three towers mentioned above. The Eiffel Tower is a square tapered free-standing tower of intricately trussed framework. The shaft of the German tower is a steel tube 2 m in diam with wall thicknesses ranging from 6 mm to 10 mm. The Eiffel Tower has been observed to sway a maximum of 4.7 inches. The German Tower is expected to displace about 6.5 ft at the top under a wind of about 80 mph. The Oklahoma tower is a triangular truss, 12 ft on a side, built of solid rounds up to 8 inches in diam, heavy wide-flange column sections, and angle bracing.

Some other interesting examples of tower structures, recently completed or in construction, are the 696 ft free-standing television tower at Stuttgart, Germany [46], the BMEWS Radar Antenna [38], the Radio Liberation Network Directional Antenna, and the 600-ft-diameter radio telescope at Sugar Grove, West Virginia, [36], as shown in figs. 3, 4, 5, and 6, respectively.

The Stuttgart Tower consists of a 194-ft steel shaft on a reinforced concrete base with restaurants at the top of the concrete section. The BMEWS Radar Antenna is fabricated of high-strength nickel steel pipes for low-temperature service in the Arctic. The towers of the RLN Antenna provide vertical reactions for the counter-weights and screens, the longitudinal components of the screen catenaries being taken by the guys. The towers are essentially free standing for wind loads. The Sugar Grove Radio Telescope is capable of altitude rotation from the horizontal to the zenith while the entire structure can rotate up to 450

¹Since presentation of this paper, the title "world's tallest structure" has passed to the new 1619-ft-high guyed tower of WGAN-TV at Portland, Maine. See *Broadcast News*, 106, p. 28.

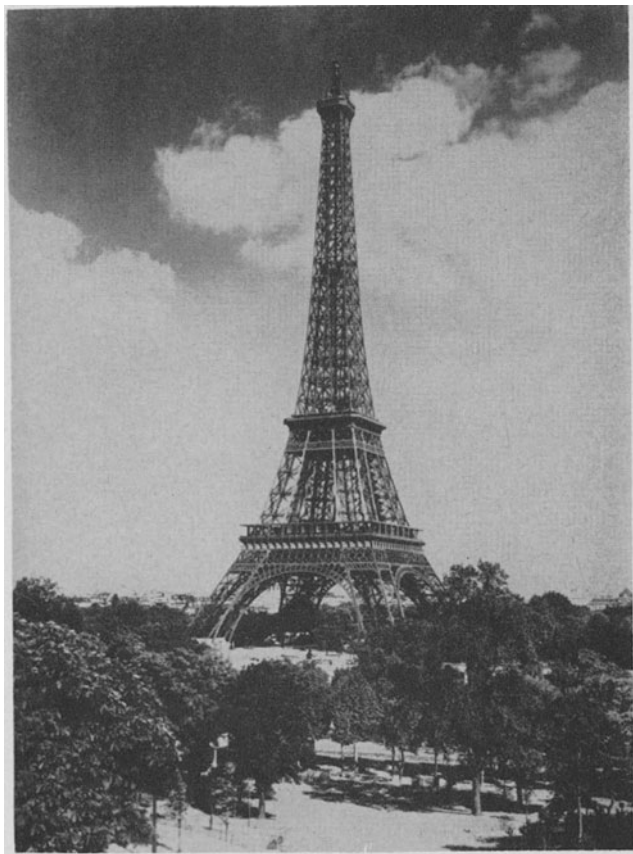


FIG. 1. 984-ft free-standing Eiffel Tower at Paris, France.
(Courtesy of French Govt. Tourist Office New York.)



FIG. 3. 690-ft free-standing television tower
at Stuttgart, Germany.

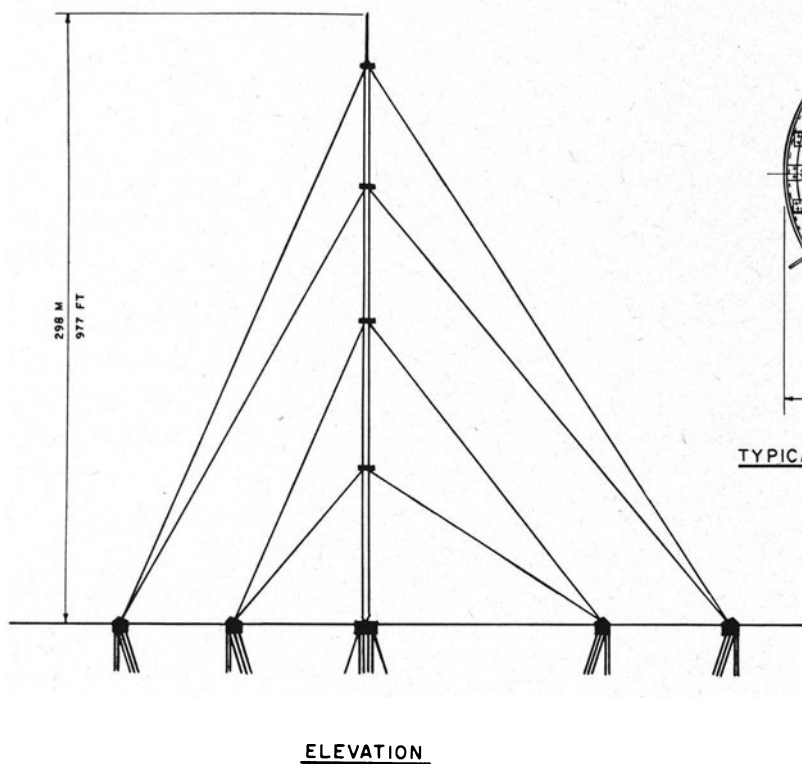
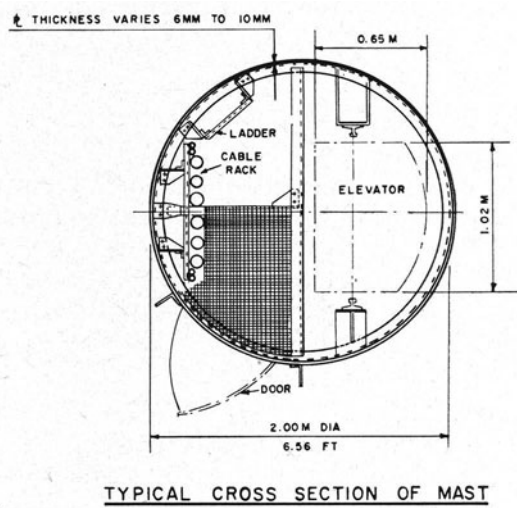


FIG. 2. 977-ft guyed television tower at Steinkimmen, Germany.



TYPICAL CROSS SECTION OF MAST

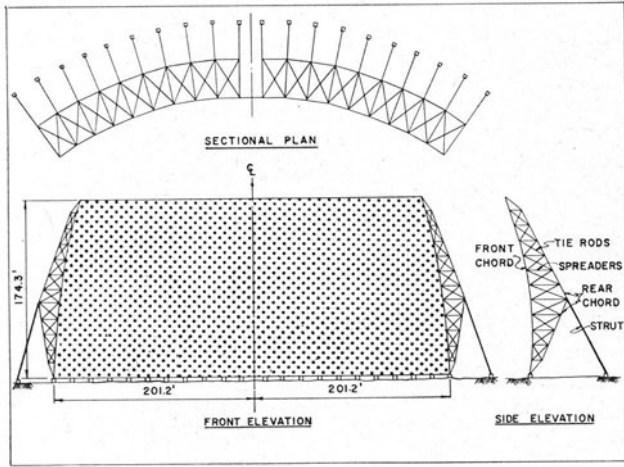


FIG. 4. BMEWS radar antenna.

deg in the horizontal plane. Close deflection tolerances were required for operational considerations.

b. Guyed towers

In recent years, the needs of the television industry, of national defense, etc. for towers of great height has resulted in a great increase in the construction of multilevel guyed towers (figs. 7 and 8). By supporting the structural shaft at suitable intervals with high-strength wire-strand guys, a highly economical structure results when space is available to provide adequate anchors for the guys at ground level.

Although most multilevel guyed towers in this

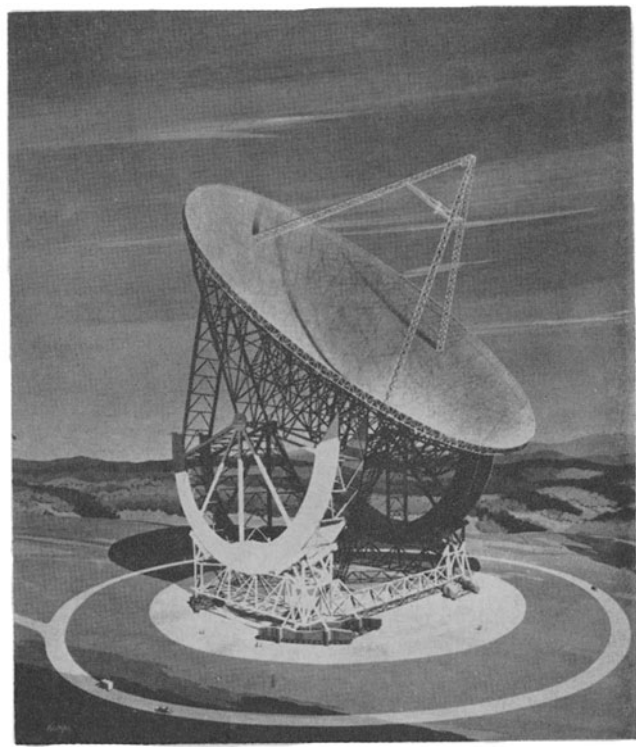


FIG. 6. 600-ft-diam radio telescope at Sugar Grove, West Virginia now under construction. (Courtesy of Grad, Urbahn and Seelye.)

country have trussed structural steel shafts of triangular cross-section as shown in fig. 8, others have been built as square-box trusses, circular shafts of steel plate or concrete, and timber-box trusses. The

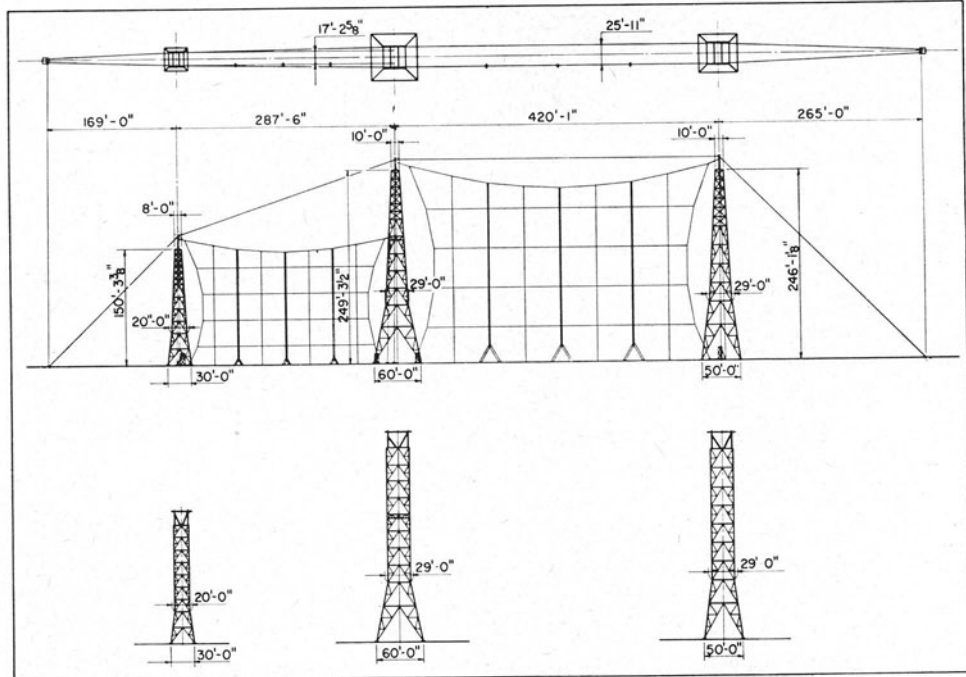


FIG. 5. Radio liberation network directional radio antenna.

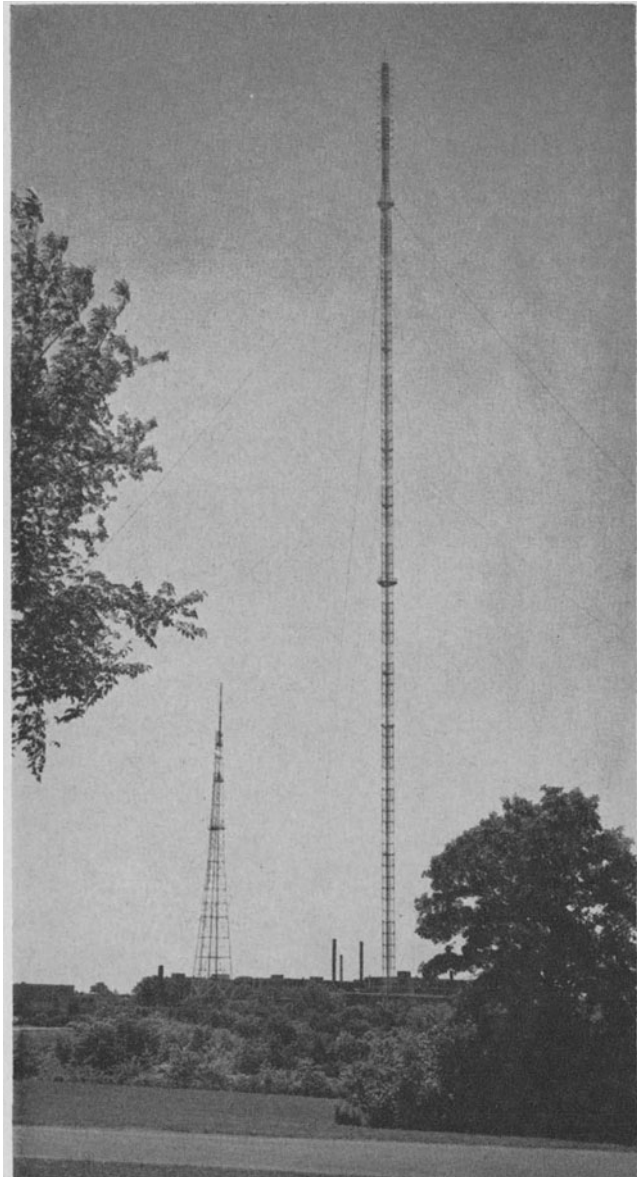


FIG. 7. Guyed and free-standing television towers at Milwaukee, Wisconsin. (Milwaukee Journal Photo.)

square and triangular types have four and three vertical faces respectively which are trusses with vertical chords, each chord being common to two faces. The shapes for the individual members are usually chosen based on their availability and adaptability to the manufacturing processes of the fabricator. Members of high-strength material and circular cross section have the initial advantage that the wind loading on the tower and the guys is substantially reduced by their use.

To reduce sag and increase stiffness, the guys usually receive a substantial initial stress (*i.e.*, pre-stress) during installation. The points of attachment of the guys at shaft and anchorage are also located to equalize, as nearly as possible, the moments at the

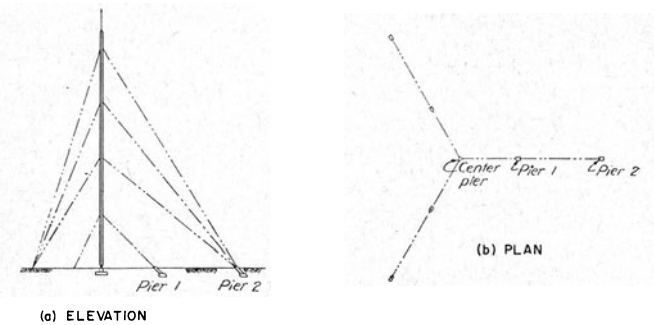


FIG. 8. Multilevel guyed tower with triangular shaft.

guy points and at midspan or to produce a linear displacement of the shaft under wind loading.

Although towers are usually made symmetrical, economies are sometimes possible by careful orientation with respect to drag coefficients and wind directions where it is well known that the maximum winds in different directions are substantially different [31].

c. Design loads

The primary loads on towers are those due to (a) the dead weight of the structural members and any associated apparatus (b) wind velocity and (c) ice load. The source and magnitude of the loads due to the dead weight of the structure are self-evident and readily computed. The loads due to wind velocity are greatly affected by the shape of the tower and, in the case of non-circular trussed towers, by the orientation of the tower to the direction of the wind, the ratio of the solid area to the total enclosed area of a vertical face, and the cross-sectional shape of the individual members of the tower. The ice load is doubly important because it increases both the wind area and the vertical load. Most specifications note that it should be considered but make only general recommendations and do not differentiate between design velocities for winter and summer wind storms.

Before computing the loads due to wind velocity, it is first necessary to determine a design wind at the specific location of the tower. Because wind velocities vary throughout the country, each locality will have a design wind which is consistent with past experience in the given area. Wherever possible, charts of probable wind frequency in various directions should be used to determine the design loads. These should be used with caution where the period of record is short. Where the towers are located so that a failure might be expected to involve loss of life or extensive property damage, the design frequency of the storm for design by conventional allowable stress methods should not be greater than once in 100 yr; for design by ultimate strength procedures, a period of 150 yr appears

reasonable. Where the towers are in isolated areas, the frequency may be increased and the design velocity and pressure reduced accordingly. It should be noted that a 100-yr velocity has a 50 per cent probability of occurring in a 50-yr period and a 10 per cent probability of occurring in a 10-yr period.

Although there is no assurance that the 100- or 150-yr storm will not occur within the year following construction, it does evaluate, even for the individual owner, the "calculated risk" which he is assuming. It is suggested that the rates of insurance for wind damage might well be based on the estimated frequency of the design wind velocity.

The design wind must be described by the following three characteristics:

1. basic wind velocity,
2. gust factors, and
3. variation with height.

2. Wind loads and drag coefficients [6]

a. General theory

The basic concept of the transformation of wind velocity into pressure may be obtained from Bernoulli's general law for an ideal fluid.

If the airstream is brought to rest by a surface normal to the wind, the overpressure on the surface, the pressure above that in the free airstream, may be taken as

$$q = \rho V^2/2, \quad (1)$$

where ρ = air density at the design ambient temperature and atmospheric pressure

and V = wind velocity

or

$$q = 0.002558 V^2 \text{ lb/sq ft}, \quad (1a)$$

where V = wind velocity in miles per hour

and $\rho = 0.002378 \text{ lb sec}^2/\text{ft}^4$ at 59F and 29.92 inches Hg.

When the temperature drops to 0F, the pressure corresponding to a given velocity is increased by 13 per cent. At an elevation of 1000 ft above sea level, the pressure for a given velocity is reduced by about 3.5 per cent by the reduction in air density.

The wind force, W , on a finite object or structure of area, A , is modified by an aerodynamic coefficient, called the shape factor " C ", which depends on the geometrical properties of the object such that

$$W = C \cdot q \cdot A. \quad (2)$$

This force may be divided into two parts, W_D and W_L , the drag force in the direction of the wind and the

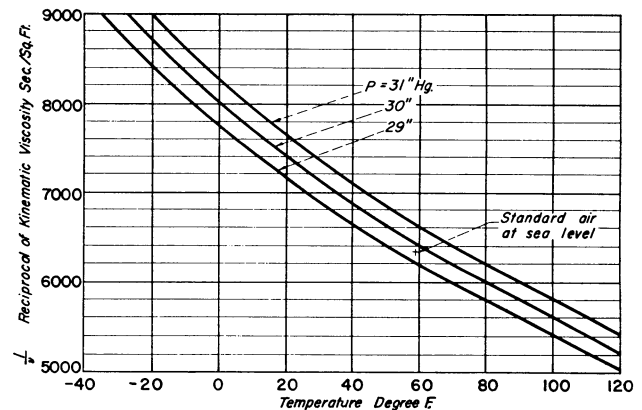


FIG. 9. Reciprocal of kinematic viscosity of air.

lift force in the direction normal to the wind respectively. The corresponding coefficients are designated C_D and C_L .

The coefficients for cylinders and other rounded elements are greatly affected by Reynold's number. Reynold's number is the ratio of the inertial force to the viscous force which a fluid stream exerts on a body, and is given by

$$R = VD/\nu, \quad (3)$$

where ν = kinematic viscosity of the air and D = characteristic dimension or diameter.

R varies greatly with the atmospheric pressure and the temperature [37] because of the variation of the kinematic viscosity (fig. 9).

b. Individual members

Considerable data are available on shape factors for common structural elements [3; 18; 19; 40]. The coefficients listed in fig. 10, applicable to elements with short and average lengths are functions of the slenderness ratio λ , defined as

$$\lambda = \frac{L}{a}, \quad (4)$$

where "L" is the length of the member normal to the windstream and "a" is the characteristic width of the member.

The simplified variation of the shape factors as a function of slenderness ratio is illustrated by the chart in the lower left hand corner of fig. 10. For very short members with values of the slenderness ratio λ less than or equal to λ_0 , the shape factors are constant (columns 4 and 6 of fig. 10). For elements of average length where λ is greater than or equal to λ_0 , the linear formulas for the shape factors are to be used (columns 5 and 7 of fig. 10).

For an I-beam with wind blowing parallel to the web, the theoretical lift coefficient is zero. The value

1. PROFILES	2. α	3. λ_0	4. For $\lambda = \lambda_0$ C_x^0 & C_z^0	5. For $\lambda \geq \lambda_0$ C_x & C_z	6. For $\lambda = \lambda_0$ C_n^0 & C_t^0	7. For $\lambda \geq \lambda_0$ C_n & C_t
	0°	8	$C_x^0 = 1.17$ $C_z^0 = 1.23$	$C_x = 1.85 - 5.44 \frac{1}{\lambda}$ $C_z = 2.20 - 7.76 \frac{1}{\lambda}$		$C_t = C_x$ $C_n = C_z$
	45°	20	$C_x^0 = 0.79$ $C_z^0 = 1.10$	$C_x = 0.95 - 3.2 \frac{1}{\lambda}$ $C_z = 1.80 - 14 \frac{1}{\lambda}$	$C_t^0 = 0.22$ $C_n^0 = 1.34$	$C_t = 0.60 - 7.63 \frac{1}{\lambda}$ $C_n = 1.95 - 1.2 \frac{1}{\lambda}$
	135°	12	$C_x^0 = 1.24$ $C_z^0 = 0$	$C_x = 1.90 - 7.92 \frac{1}{\lambda}$ $C_z = 0$	$C_t^0 = 0.88$ $C_n^0 = C_t^0$	$C_t = 1.35 - 5.62 \frac{1}{\lambda}$ $C_n = C_t$
	180°	12	$C_x^0 = 1.20$ $C_z^0 = 0.12$	$C_x = 1.94 - 8.9 \frac{1}{\lambda}$ $C_z = 0.30 - 3.16 \frac{1}{\lambda}$		$C_t = C_x$ $C_n = C_z$
	315°	9	$C_x^0 = 1.65$ $C_z^0 = 0$	$C_x = 2.64 - 8.91 \frac{1}{\lambda}$ $C_z = 0$	$C_t^0 = 1.17$ $C_n^0 = C_t^0$	$C_t = 1.87 - 6.31 \frac{1}{\lambda}$ $C_n = C_t$
	0°	20	$C_x^0 = 1.32$ $C_z^0 = 0$	$C_x = 2.25 - 18.5 \frac{1}{\lambda}$ $C_z = 0$		$C_t = C_x$ $C_n = C_z$
	45°	11	$C_x^0 = 1.16$ $C_z^0 = 0.67$	$C_x = 1.70 - 5.94 \frac{1}{\lambda}$ $C_z = 0.93 - 2.75 \frac{1}{\lambda}$	$C_t^0 = 1.30$ $C_n^0 = 0.346$	$C_t = 1.86 - 6.15 \frac{1}{\lambda}$ $C_n = 0.545 - 2.26 \frac{1}{\lambda}$
	90°	8	$C_x^0 = 0.52$ C_z^0 negl.	$C_x = 0.64 - 0.96 \frac{1}{\lambda}$ C_z negligible		$C_n = C_x$ $C_t = C_z$
	135°	20	$C_x^0 = 0.94$ $C_z^0 = 0.54$	$C_x = 1.66 - 14.4 \frac{1}{\lambda}$ $C_z = 0.86 - 6.4 \frac{1}{\lambda}$	$C_t^0 = 1.05$ $C_n^0 = 0.285$	$C_t = 1.78 - 14.7 \frac{1}{\lambda}$ $C_n = 0.565 - 5.65 \frac{1}{\lambda}$
	180°	17	$C_x^0 = 1.22$ $C_z^0 = 0$	$C_x = 1.85 - 10.7 \frac{1}{\lambda}$ $C_z = 0$		$C_t = C_x$ $C_n = C_z$
	0°	12	$C_x^0 = 1.22$ $C_z^0 = 0$	$C_x = 1.92 - 8.4 \frac{1}{\lambda}$ $C_z = 0$		$C_t = C_x$ $C_n = C_z$
	45°	11	$C_x^0 = 1.10$ $C_z^0 = 0.70$	$C_x = 1.86 - 8.36 \frac{1}{\lambda}$ $C_z = 0.93 - 2.53 \frac{1}{\lambda}$	$C_t^0 = 1.28$ $C_n^0 = 0.283$	$C_t = 1.98 - 7.72 \frac{1}{\lambda}$ $C_n = 0.66 - 4.14 \frac{1}{\lambda}$
	90°	9	$C_x^0 = 0.534$ $C_z^0 = \pm 0.5$	$C_x = 0.90 - 3.3 \frac{1}{\lambda}$ $C_z = 0$		$C_n = C_x$ $C_t = C_z$
<p><u>NOTE:-</u></p> <p>These values hold for very short elements where $\lambda = l/a$ is smaller than or equal to λ_0 (col. 4 & 6) and for elements of average length where λ is greater than λ_0 (col. 5 & 7). The first term of the second member of the expressions listed in cols. 5 & 7 is extrapolated from the coefficient for $\lambda = \infty$.</p>						

FIG. 10. Shape factors for short common structural shapes.

PROFILES	Coefficients			PROFILES	Coefficients			PROFILES	Coefficients		
	C_t	C_n	C'_n		C_t	C_n	C'_n		C_t	C_n	C'_n
	1.88	0	0		1.50	1.50	1.50		0	1.88	1.88
	1.57	0	0		1.50	1.50	1.50		0	1.87	1.87
	2.07	0	0		1.40	0.70	1.40		0	0.75	1.58
	2.00	—	—		1.8	0.10	—		0	0.10	—
	2.00	0	0		1.80	0.65	1.36		0	0.80	1.68
	1.25	0	0		1.15	1.60	1.75		0	1.30	1.51
	2.05	0	0		1.85	0.60	1.40		0	0.60	1.39
	1.79	0	0		1.60	0.40	0.93				
	1.70	2.15	2.15		1.70	1.70	1.70				
	1.90	0.3	0.3		1.35	1.35	1.35		1.60	0.10	0.20
					0.70	1.70	1.70		1.55	0.70	1.40
	1.98	1.00	2.00		1.30	0.20	0.40		0.25	0.80	1.60
	2.00	0.09	0.18		1.80	0.80	1.60		2.00	1.75	3.50
	1.30	0	0		0.50	1.05	2.28		0.93	0.70	1.52
	1.50	0	0		1.50	0.15	0.30				
	1.65	0	0		0.90	0.90	0.90				
	1.55	0	0		1.20	0.75	0.69		1.60	2.15	1.98
	2.01	0	0		1.10	2.40	2.22				

NOTE :-

The listed values are valid only for very long structural members. The coefficients C_t and C_n are to be used with the areas of the incident surfaces shown in the first column on the extreme left. The coefficients C'_n are to be used with the areas of the surfaces normal to the direction of n .

* A small variation in the direction of the wind causes a significant increase in C_n . In these cases the choice of C_n values lies on the conservative side.

FIG. 11. Shape factors for very long common structural shapes and built-up members.

Flow Direction →	$\frac{b}{a}$	$\frac{r}{a}$	$C_d \text{ at } R=10^5$	Flow Direction →	$\frac{b}{a}$	$\frac{r}{a}$	$C_d \text{ at } R=10^5$
	1:1	0.50	1.0*		1:2	0.021	1.8
	1:2	—	1.6		1:2	0.167	1.7
	2:1	—	0.6		1:1	0.015	1.5
	1:2	0.021	2.2		1:1	0.235	1.5
	1:2	0.250	1.5		2:1	0.042	1.1
	1:1	0.021	2.0		2:1	0.333	1.1
	1:1	0.333	1.0		1:1	0.021	1.2
	2:1	0.042	1.4		1:1	0.250	1.1
	2:1	0.500	0.4		1:1	0.021	2.0
	1:1	0.250	1.3				

* Other Experiments Indicate 1.2

FIG. 12. Drag coefficient C_d for cylinders.

of 0.50 is shown to cover the possibility of a slight change in wind direction.

Shape factors for very long structural members are listed in fig. 11. The coefficients for square, rectangular, or flat-plate elements with average or short lengths may be obtained by multiplying the coefficients given for these shapes in fig. 11 by a reduction factor for solid plates. The reduction factor, K_i , is given as a function of the slenderness ratio by the curve for $\phi = 1.0$ (solid plate) in fig. 17. In the absence of more precise data, this curve may be generally used for shapes consisting of flat surfaces with sharp-edged intersections.

All coefficients are given for the long axis normal to the wind and are modified by the effects of yaw [40].

They are modified also by the presence of a ground plane.

When a flat plate is inclined to the direction of the wind, as shown in fig. 11, the center of pressure acting normal to the plate does not coincide with the geometric center. At a yaw of 40 deg, the resultant is located at approximately 0.30 of the width from the near end.

Delany and Sorensen [9] have reported on drag characteristics of prismatic and other configurations, as shown in fig. 12. Their tests indicate that all shapes with sufficiently rounded edges experience a sharp decrease in drag in the critical Reynold's number region similar to the cylinder. On the other hand, the drag

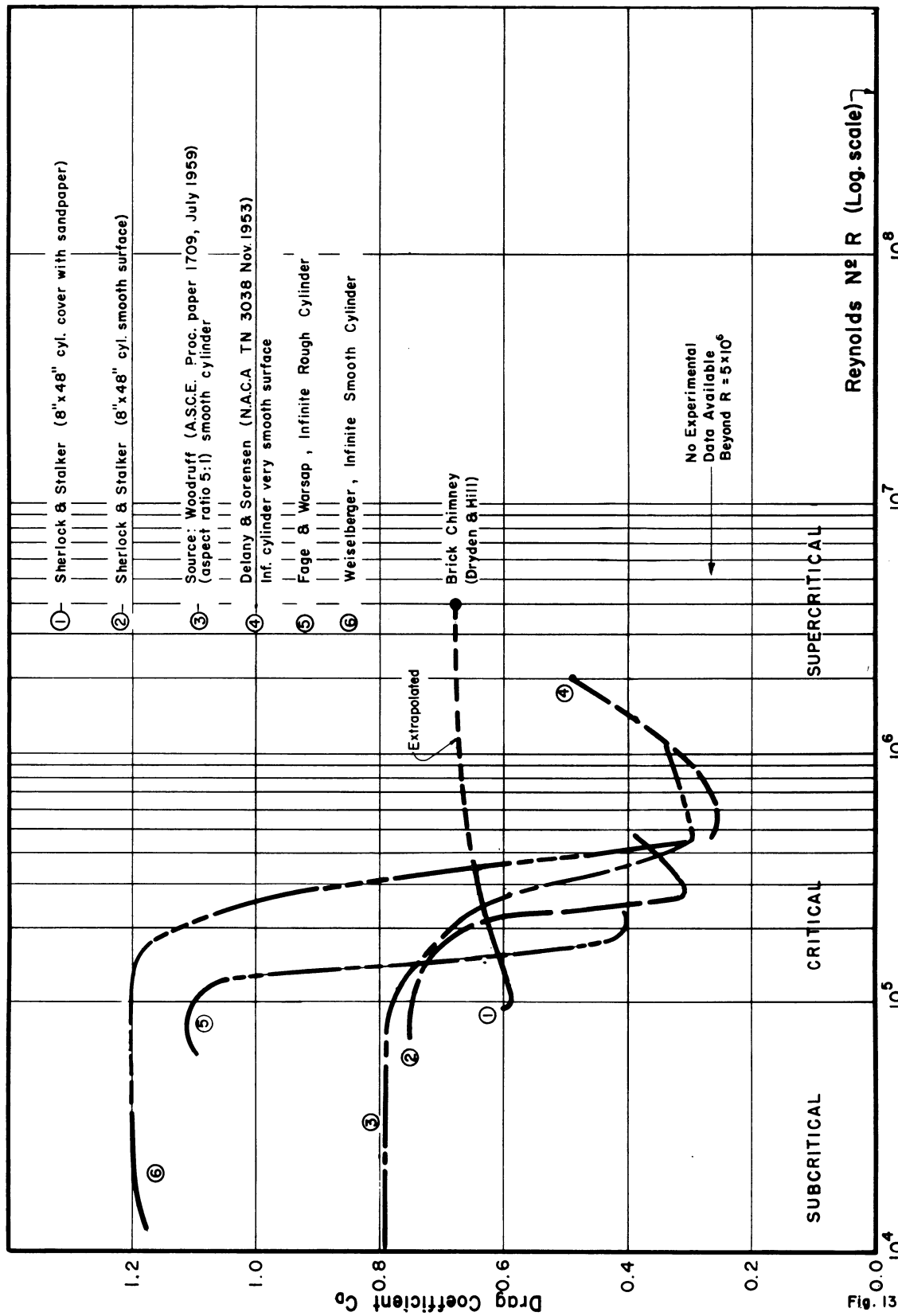


FIG. 13. Data on drag coefficients for a cylindrical metal stack.

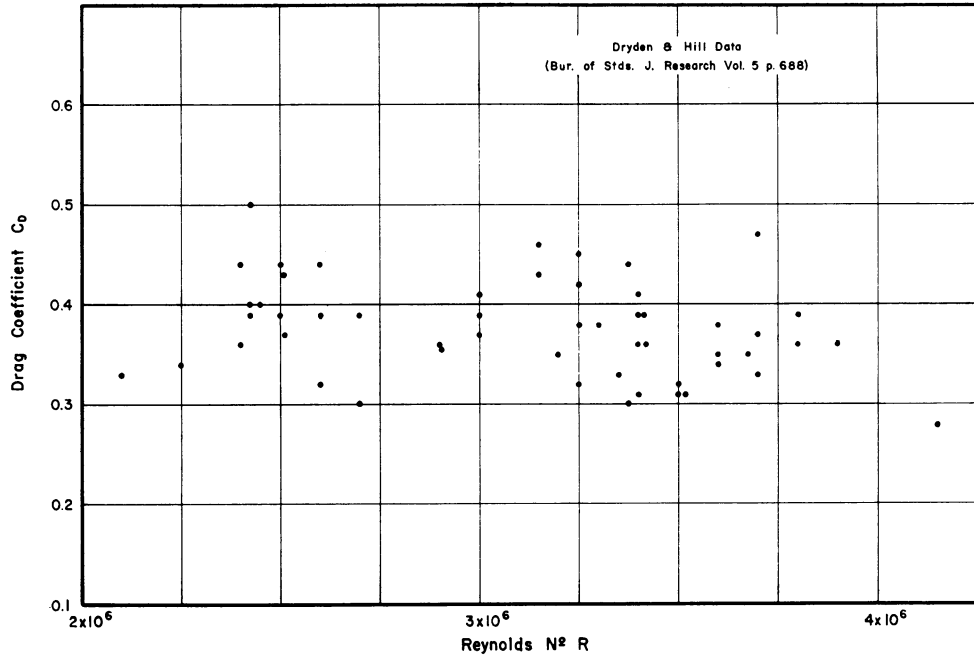
DRAG COEFFICIENT C_d FOR A CYLINDRICAL METAL STACK

FIG. 14. Drag coefficients for poles, ropes, wires, reservoirs, stacks, and masts.

of sharp-edged members appears to be independent of Reynold's number.

A drag coefficient of 1.2 is used for very long circular elements about which the air flow at design wind velocity occurs in the sub critical or critical Reynolds number region (*i.e.*, $R \leq 500,000$). For R higher than 500,000, a shape factor of 0.50 appears to be a conservative value for smooth cylinders. However, the lower value should be used with care. For example, at a velocity of 100 mph, a temperature change from 0F to 100F and a barometric pressure change from 31 inches Hg to 29 inches Hg will mean that the limiting diameter for the reduced shape factor goes from 5.0 inches to 7.7 inches.

Reported experimental results of the drag coefficients of rough and smooth cylindrical bodies as a function of R are presented in fig. 13. Included is the curve for a smooth cylinder with a slenderness ratio λ equal to 5. This curve shows that in the subcritical range the slenderness ratio has an important influence on the drag of smooth cylinders. For this cylinder with an L/d equal to 5, its drag factor is two-thirds that of a very long cylinder.

More data on drag coefficients of a smooth cylindrical stack with a diameter of 10 ft and a height of 30 ft, resting on a roof and tested in natural winds, are shown in fig. 14. Recommendations of the Swiss Code [40] are summarized in fig. 15.

Attention should be drawn to the influence of roughness on the drag of cylinders in both the subcritical and supercritical range. The data on fig. 13 indicate that the drag of rough cylinders is substan-

tially higher than that of smooth cylinders in the supercritical region. On the other hand, smooth cylinders seem to have somewhat higher drag effects than rough cylinders at subcritical Reynold's numbers.

It should be noted that the drag factors for cylindrical bodies assume relatively large values at Reynold's numbers below 100, where the drag-factor—Reynold's number curve begins a steep ascent. Although the drag factors are very high, the wind velocity is negligible. Therefore, this laminar flow region is not usually critical for design.

c. Trusses

Although the determination of the total wind force on a truss is theoretically more involved than summing up the forces that would have been applied to the various members if they had been isolated pieces, the correlation of test results yields simple relationships if the drag coefficients are given in terms of the solidity ratio, ϕ , the solid area divided by the enclosed area of the total truss, as shown in fig. 16 for a plane frame work made up of flat members.

It is interesting to note that the drag coefficient drops as low as 1.45 for normal incidence and ϕ between 0.4 and 0.8.

The curves in fig. 16 are for trusses of infinite length. The reduction factor, K_i , for trusses of finite length are shown in fig. 17 as a function of the slenderness ratio and the solidity ratio. Numerous tests [14; 15; 19; 27] on the variation of drag coefficients of plates as a function of their slenderness, generally

agree quite well with the curve for $\phi = 1.0$ (solid plate).

The above curves were first determined by O. Flachsbart and H. Winter [18; 19] from numerous tests performed at Gottingen. Many of the test results were presented in English by J. W. Pagon [25]. They are obtained from wind-tunnel tests on trusses with members of various structural shapes (flats) and different sizes of connections. Tests in the United States [2; 39; 47], England [45; 48; 49], and France [14; 15; 16] are in general agreement with the data shown.

Although only limited data are available, the current practice of using $2/3$ as the ratio of load between trusses of round members and those of structural (or flat) members appears to be somewhat on the safe side.

$W_D = C_D \cdot q \cdot A$ $A = d \cdot L$	R	$< 5 \times 10^5$	$> 5 \times 10^5$
	COEF	C_D	C_D'
SMOOTH WIRES, RODS, PIPES	1.2	0.5	
ROUGH WIRE RODS	1.2	0.7	
FINE WIRE CABLES	1.2	0.9	
THICK WIRE CABLES	1.3	1.1	

SLENDERNESS $L/d =$	25	7	1
UPRIGHT CYLINDER $W_D = C_D \cdot q \cdot A$			
C_D FOR $R > 500,000$ $A = dL$			
X SECTION & ROUGHNESS	C_D	C_D	C_D
Smooth Surface Metal, Timber, Concrete	0.55	0.5	0.45
Rough Surface Round Ribs $h = 2\% d$	0.9	0.8	0.7
Very Rough Surface Sharp Ribs $h = 8\% d$	1.2	1.0	0.8
Smooth Rough Surface Sharp Edges	1.4	1.2	1.0

FIG. 15. Geometric and drag characteristics of models of various cross sections.

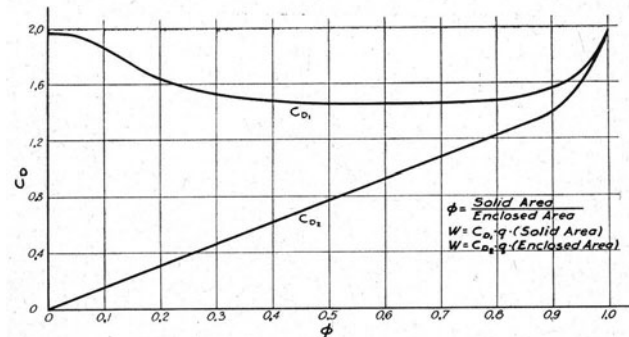


FIG. 16. Variation of shape factors for plane trusses as a function of solidity ratio.

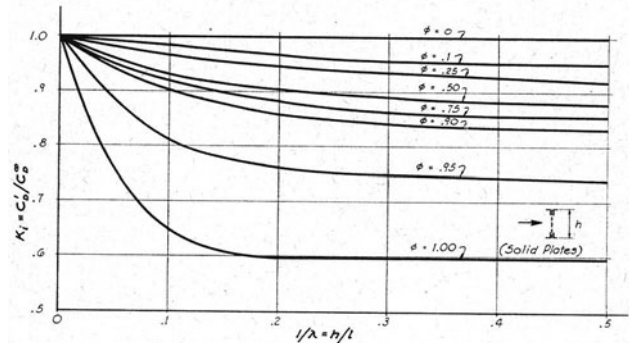


FIG. 17. Reduction as function of slenderness for trusses and plates.

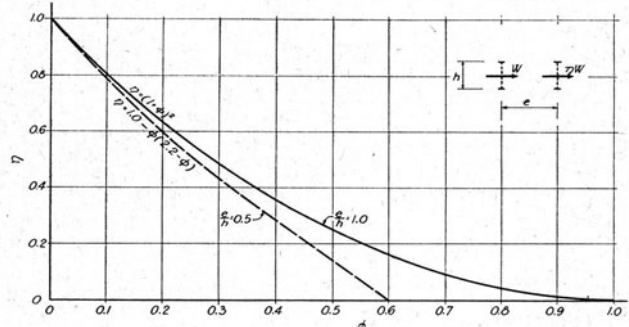


FIG. 18. Shielding coefficient ratio for parallel trusses.

d. Shielding effect

When two members or trusses of height, h , are placed a distance, e , one behind the other, the wind forces acting on the leeward member or truss are reduced by the shielding effect of the windward structure and may even become negative as shown on tests run with plates set close together [14; 15]. The ratio of the load on the leeward truss to that on the windward truss is given by the shielding coefficient, η .

For $e/h = 1.0$, Flachsbart proposed the following formulas [18; 19] for

$$\eta = K(1 - \phi)^2, \quad (5)$$

with $K = 1.0$ for lattices covering one another, and $K = 1.2$ for lattices off-set by half a panel.

The following formula is indicated for $e/h = 0.50$

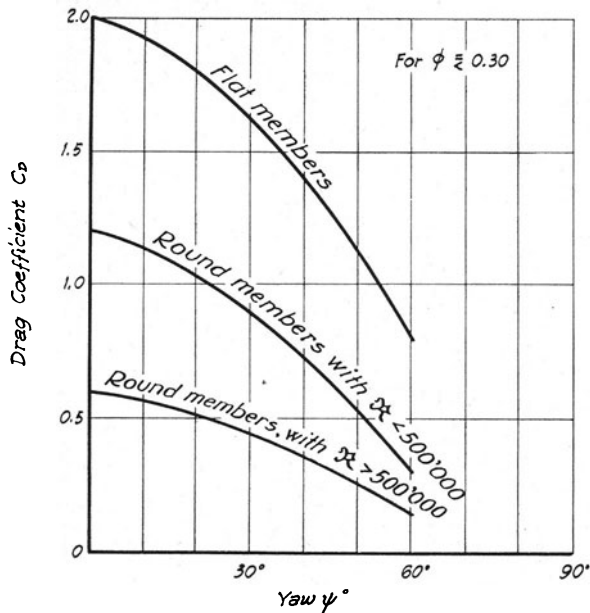


FIG. 19. Drag coefficients for trusses as function of yaw.

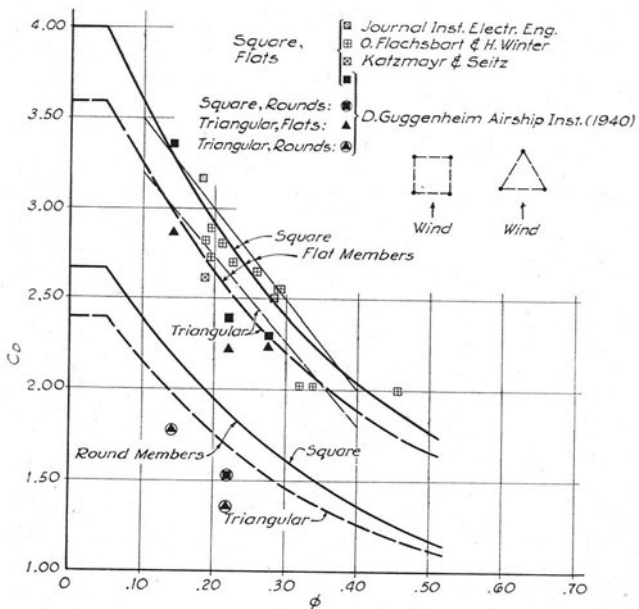


FIG. 20. Composite shape factors for trussed towers (wind normal to a face).

in the Swiss Code [40]:

$$\eta = 1.0 - \phi(2.2 - \phi). \quad (6)$$

The relationships are shown graphically in fig. 18.

The same factors may be used for trusses and towers with flat (or structural) members or with round members if $R < 5 \times 10^5$. If the Reynolds number is bigger than 5×10^5 , a value of 0.95 is recommended for any value of ϕ for frame work with round members.

e. Influence of yaw

The effect of the yaw or skew angle, ψ , formed by the wind direction and the normal to the surface under

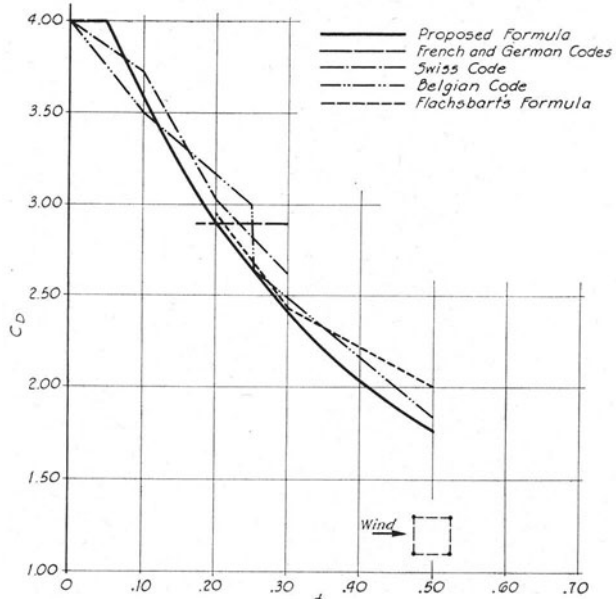


FIG. 21. Comparison of composite shape factors for trussed towers.

consideration, is shown in fig. 19 as given in the Swiss code [40].

The influence of yaw is also affected by the slenderness ratio.

The curve for trusses with flat members is given for a drag coefficient at zero incidence $C_D^0 = 2$. For other values of C_D^0 , the ratios C_D^ψ/C_D^0 remain the same as for $\phi \leq 0.3$. The values for trusses with round members are as shown independent of ϕ , for $\phi \leq 0.3$.

f. Square tower

A square tower, for wind blowing normal to a face, may be treated as a two-truss structure as the drag forces on the side faces are negligible [18; 19]. According to tests performed in England [48], the drag forces on the side faces may even be negative and vary between -3.6 per cent and +5 per cent of the total drag force.

Therefore, from the data previously established, it is possible to obtain a "composite" shape factor of the following type for a square tower:

$$C_{DT} = C_D(1 + \eta), \quad (7)$$

C_{DT} = shape factor of the tower as a whole,

C_D = shape factor of the front face, and

η = shielding coefficient given by (5).

Such a curve, modified for low values of ϕ , can be written also as

$$C_{DT} = 4.0 \quad \text{for } 0 < \phi < 0.05, \quad (8)$$

$$C_{DT} = 6.8\phi^2 - 8.8\phi + 4.4 \quad \text{for } 0.05 < \phi < 0.45. \quad (9)$$

For values of ϕ near unity, the total drag force will approach the value for a square prism.

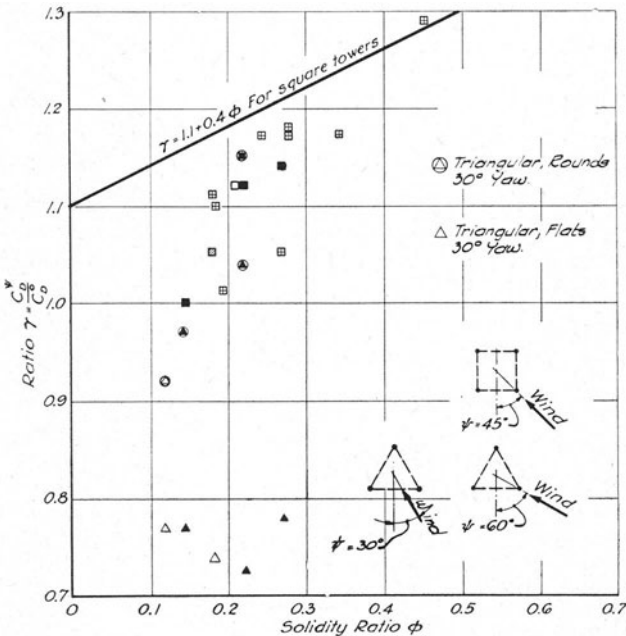


FIG. 22. Drag coefficients for towers as function of yaw.
(See Fig. 20 for tests notation.)

A simpler relationship may be developed for design purposes in the range of

$$0.1 < \phi < 0.4 : \quad C_{DT} = 4.0 - 5\phi. \quad (10)$$

As shown in fig. 20, both curves have good agreement with the test data. The minimum value for C_{DT} should not be less than that for a solid square tower of the same slenderness coefficient.

Fig. 21 shows a comparison with current codes.

Since the shielding effects of trusses with round and flat members are essentially the same [40] for $R < 500,000$, the drag coefficients for square towers with round members may be taken as $\frac{2}{3}$ of the coefficients for square towers with flat members, as in the case of a single truss. For a square tower with a combination of flat and round members, a weighted average as a function of the ratio of the flat areas to round areas seems to be a reasonable approach.

The maximum drag force for a square tower occurs when the wind is blowing along a diagonal [18; 22]. A conservative formula for the increase in drag force at a yaw of 45 deg is given by

$$\gamma = 1.1 + 0.4\phi. \quad (11)$$

This relationship may be assumed to be independent of the type of members, flat or round. The relationship is shown in fig. 22 along with available test data. For double (angle or other) member trusses, γ should be increased by 10 per cent [43].

g. Triangular tower

A "composite" shape factor may also be determined for triangular towers with wind blowing normal to a

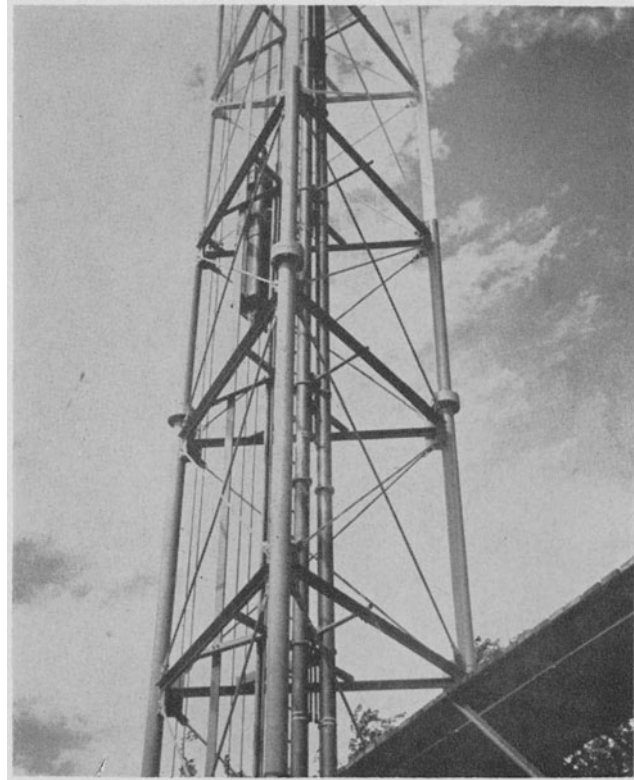


FIG. 23. Conduits and elevator system for multilevel guyed towers at Milwaukee, Wisconsin (fig. 7).

face by using a ratio $e/h = 0.50$ for computing the shielding effect on the leeward bracing. In addition, the drag on the two shielded faces is further reduced as a result of yaw, as follows:

$$C_{DT} = C_D(1 + 2\gamma\cos\psi), \quad (12)$$

where γ = reduction coefficient for a truss due to yaw.

For $\psi = 60^\circ$ and $\gamma = 0.80$, we obtain

$$C_{DT} = C_D(1 + 0.8\gamma). \quad (13)$$

Following the same procedure as for a square tower,

$$C_{DT} = 3.60 \text{ for } 0 < \phi < 0.05, \quad (14)$$

and

$$C_{DT} = 5.7\phi^2 - 7.4\phi + 3.9 \quad \text{for } 0.05 < \phi < 0.45. \quad (15)$$

For design purpose,

$$C_{DT} = 3.65 - 4.65\phi \quad \text{for } 0.1 < \phi < 0.40. \quad (16)$$

The curves covering the above equations are shown in fig. 20. For small values of ϕ , the values obtained above are conservative, particularly if the truss is made up of heavy chords and light lattice members. Few test data are available for triangular towers, particularly concerning the influence of yaw. From the available data, it appears that the biggest drag force is obtained when the wind is blowing normal to a face, as shown in fig. 22. Although formulas similar to (15) and (16) can be derived for yaws of 60 to 90 deg,

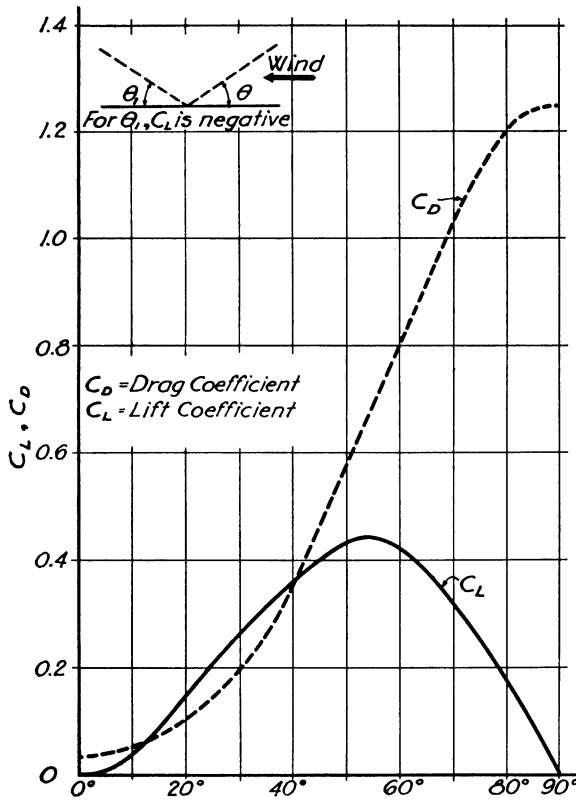


FIG. 24. Drag and lift coefficients for guys.

they should be used with caution until confirming test data become available.

C_{DT} for towers with round members may be taken as $\frac{2}{3}$ of the values for towers with flat members for corresponding values of ϕ . Although test data are not available for towers with round members for large values of ϕ , it appears reasonable that the total drag force will approach the values for solid sections of the same shape as the tower.

h. Slenderness ratio

Although guyed towers usually have a high slenderness ratio, reductions from the coefficients shown due to a finite slenderness ratio can be considered for high values of the solidity ratio ϕ . The reductions shown for single trusses in fig. 17 may be applied.

i. Effect of additional members such as pipes, ladders, etc.

In addition to the structural members of the tower itself, most towers support conduits, pipes, ladders, lift rails, etc. either on their faces or in the interior as shown in fig. 23. The influence of shielding on, or as a result of, such members is usually neglected, and wind loads are computed from the shape factors and projected area for the individual pieces.

j. Guys

The drag and lift coefficients [7; 11] for guys are shown in fig. 24 as a function of the yaw. The angle of attack, θ , is the angle in space between the wind and

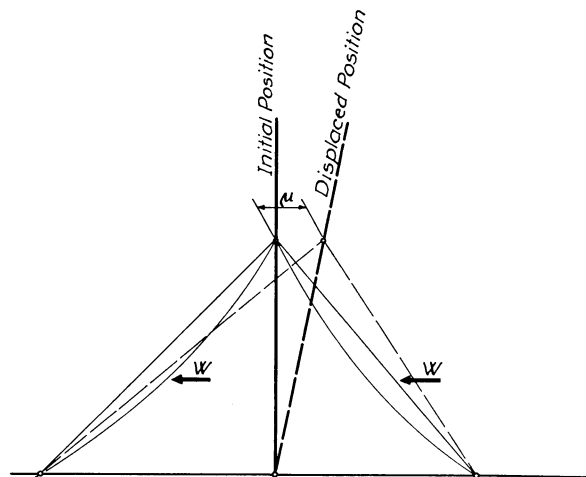


FIG. 25. Effects of wind on guys.

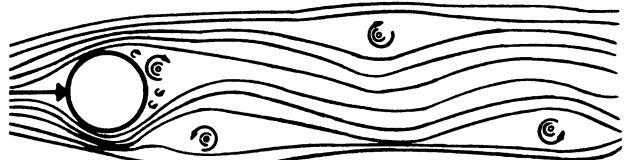
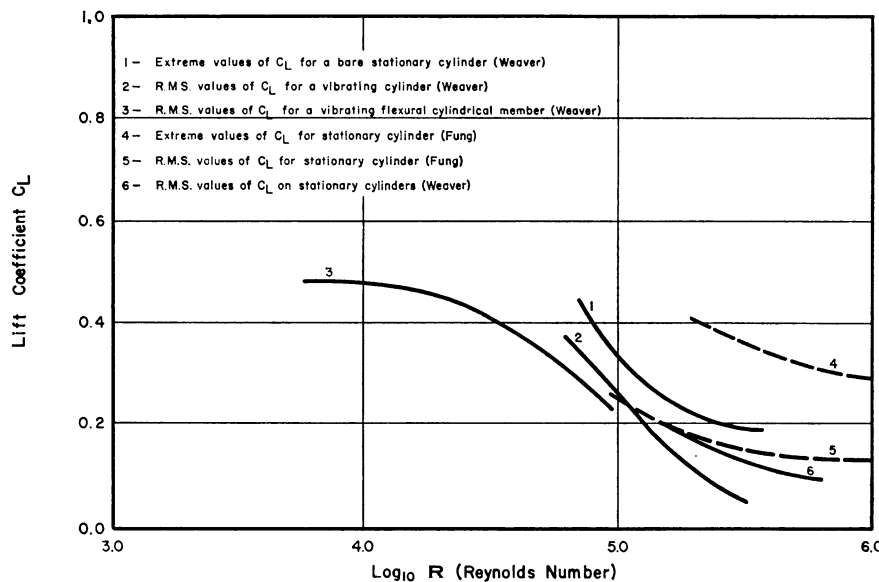


FIG. 26. Karman vortex wake (after Vincent).

the guy. The lift is in the direction formed by the intersection of the plane of the guy and the plane normal to the wind. The drag is in the direction of the wind. These forces are combined with the weight of the guy to form a resultant force acting on the guy. The plane of the guy will rotate from the vertical to the plane of the resultant force. If we consider a windward and a leeward guy pair in a plane parallel to the wind with their intersection fixed in space, the net force at the connection will be into the wind. If the joint is released horizontally, it will move into the wind until the horizontal components in the windward and leeward guys are equalized as shown in fig. 25.

k. Dynamic effects (general)

Although a succession of periodic gusts can induce tower oscillations in the direction of the resulting variation in applied load, there is only limited confirming data [44] in this connection. If the gust frequency approaches a natural frequency of the structure, damage or failure may result. Two towers erected in the Far East to avoid a natural frequency between 4 and 8 sec were undamaged by numerous typhoons although previous towers had collapsed successively, apparently from the effects of resonance. Slender towers of high solidity or of cylindrical section will also be subject to Karman vortex effects (fig. 26) as are the individual members of all framed towers. Although almost all towers contain members which are in resonance with some vortex shedding frequency, experience with bolted truss steel towers indicates that failure does not usually result. Failures at connections

FIG. 27. Lift (lateral force) coefficient C_L for oscillating and stationary cylinders.

have been reported for welded aluminum towers under low temperature conditions.

A number of investigators [10; 12; 20; 24; 26; 28; 35] have concentrated attention on the lateral response of oscillating cylindrical elements. This motion arises due to the formation of lateral lobes of unbalanced negative pressure as the air stream passes around a cylindrical object. The studies just cited show that energy is fed continuously, at first, into the oscillating element from the air stream as indicated by the steady buildup in the amplitudes of lateral motion. The buildup reaches a maximum, and then the oscillations subside fairly rapidly. This cycle of amplitude buildup and decay repeats itself characteristically as long as the element is excited by a steady wind stream. The decay may be attributed to a possible phase shift in the formation of the lateral lobes of unbalanced negative pressure as the amplitude of the vibration increases.

Experimental data [35] have been made available recently on "extreme" and "root mean square" dynamic lateral force or lift coefficients, C_L , as a function of Reynold's number R . The curves of C_L vs. R are shown on fig. 27. It should be noted that C_L for vibrating members decreases sharply from a value of 0.5 for $R \leq 20,000$ to a value less than 0.1 for $R \sim 400,000$. Curves of C_L for stationary cylinders [20] have also been included. These indicate that values of C_L for stationary cylinders are larger than those for oscillating cylinders.

Laboratory data on C_L for oscillating cylinders at Reynold's numbers greater than 400,000 seem to be unavailable. This information is needed for the dynamic design of large cylindrical structures where values of R exceeding 10,000,000 may be encountered.

Weaver [35] has proposed the use of root-mean-square values of C_L in the analysis of cylindrical

vibrating members subjected to lateral wind forces of random amplitude and constant frequency ($R < 300,000$). When both the amplitude and frequency of the exciting wind force are random ($R > 300,000$), the analysis still makes use of the root-mean-square values of C_L but must deal with power input rather than energy input per cycle. This is necessary because power is a function of both the amplitude and frequency of the exciting force whereas energy depends only on amplitude. The characteristic power-frequency function, or "power spectrum" required in the analysis, is obtained empirically. The ordinate of the "power spectrum" at a particular frequency is termed the "power spectral density" for the given frequency. A high spectral density indicates a high response at resonance. The entire analytical approach rests upon the basic mathematical theory of stochastic processes [8].

It should be noted that some tests have been conducted which indicate that flexible cylindrical bodies, subjected to wind excitation, vibrate laterally at their natural frequencies in the supercritical region ($R > 300,000$) [24; 26; 28]. On this basis, dynamic analysis, employing a conservatively selected value of C_L , may serve as a designer's guide for estimating the damped resonant response until data required for a more exact treatment become available.

Power spectra for the evaluation of the dynamic response of towers in the direction of the wind are also becoming available [32].

l. Dynamic effects (guys)

Wind vibration of guys may occur in two essentially different forms. Both are caused by steady winds with a maximum response resulting from a transverse wind blowing across the guy. In both, the energy of the wind is imparted to the suspended guy, causing it to vibrate in a series of loops. The amplitude of vibration

builds up until a condition is reached where the energy input of the wind is balanced by the energy dissipation of the guy. While this has been the classic explanation of the phenomena, there is the possibility that a phase shift between the dynamic lift forces and the motion of the guy is either wholly or partly responsible for the limitation of the movement.

One type of vibration, known as "galloping" or "dancing," may develop if a coating of sleet or sheet ice forms. Usually this deposit does not shape itself uniformly around the periphery of the guy. The coating changes the aerodynamic properties of the guy and makes "self excited" vibrations possible. These are generally low frequency oscillations with a small number of loops. Up to the present time, it has not been common practice to investigate the possibility of the harmful motion of the guys due to random excitation during final designs. However, procedures [5] have been presented recently which indicate the analytical lines that must be followed. In order to render any computations of stress and strain meaningful, a correlation of the analytical results with field experience will have to be made.

The other type of vibration which can occur may be termed "resonant forced" vibration. It is induced by the formation of vortices in the wake of the guy, which develop in a manner to produce unbalanced forces normal to the wind stream. This motion is characterized by high-frequency oscillations or "sing-

ing." Steidel [33] submits evidence that vortex disturbances of the guys at Reynold's numbers above 400,000 may be weak and aperiodic.

"Dancing" can be alleviated in some cases by careful installation of weights of such mass and spacing as to change the dynamic characteristics of the system. Unless properly designed and installed, they may be harmful [13]. "Singing" can be minimized by the use of vibration dampers which absorb and dissipate the energy delivered by the wind [34], thus preventing resonant vibration. One type of damper (fig. 28) consists of resiliently supported weights which continuously absorb the energy of the incipient vibrations, thus preventing the building up of amplitude and stress in the guys.

Damage due to guy vibration is usually the result of fatigue in insulators or connections. The writer knows of no failures due to "dancing" of uninsulated guys.

Although an accurate analysis of structures subject to aerodynamic vibrations is often difficult, the adequacy of any such structure should be carefully reviewed either by comparison with experience of similar structures or by using the analytical methods available in conjunction with sound engineering judgment.

3. Design procedure and conclusion [1; 4; 7; 17; 23; 29]

After determination of the loading, tower design follows the general methods of structural analysis. Guyed towers are treated as continuous beam-columns on elastic supports. First the guys are analyzed to determine the stiffness of the supports at the guy levels—*i.e.* the force developed per unit displacement of the guy points. The shaft is then analyzed as a beam on elastic supports taking into account the effects of axial load and the displacements of the supports. Such an analysis yields a reliable estimate of the stresses throughout the structure under a given wind velocity. The design wind velocity varies with height, and pattern-type loading is used as shown in fig. 29 to cover the effects of gusts as described by Professor Sherlock [31].

By conventional-design methods, the guy and member sizes are proportioned to reduce the stresses to values allowed by the applicable codes. For structural steel the allowable stress is approximately 6/10 of the yield stress or $\frac{1}{3}$ of the breaking strength. For guys, the allowable stress is usually taken between $\frac{1}{4}$ and $\frac{1}{3}$ of the breaking strength of the strands. The guy anchorages are proportioned to resist 2 times the computed loads. In a well designed and constructed free-standing (cantilever) tower, the factor of safety against wind load increases somewhat from top to bottom because of the increase in fixed dead load. The taller the tower, the greater this effect. Near the top

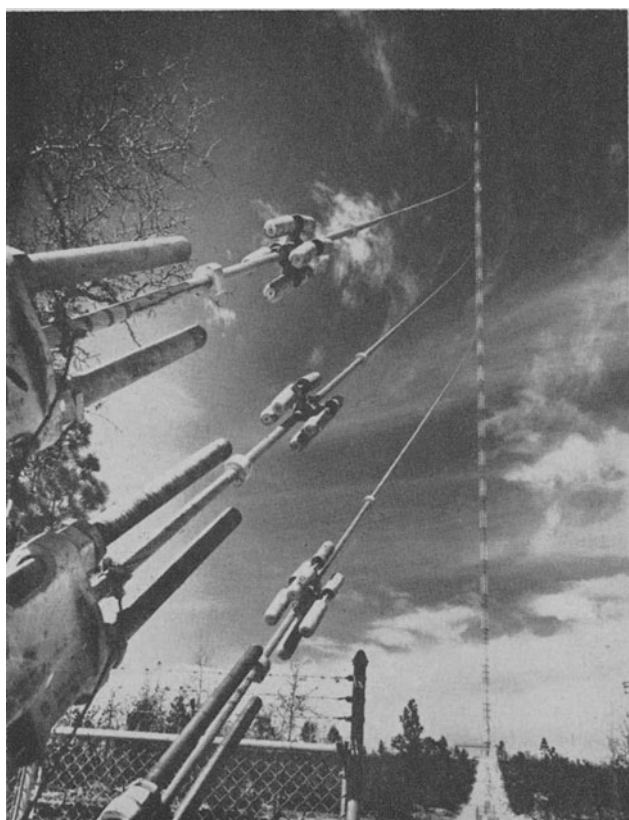


FIG. 28. Stock-bridge-type vibration dampers for tower guys (Roebling Co. photograph).

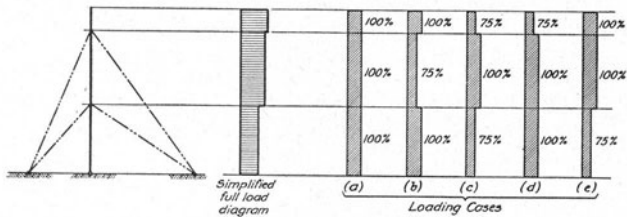


FIG. 29. Wind loads for tower guyed at 2 levels.

of tower, the factor is close to that defined by the allowable stress. This is borne out by actual failures which normally occur substantially above the base.

In guyed towers, the effect of dead load is similar. In addition, the factor of safety against collapse by wind is further increased by the prestress caused by the initial tensions in the guys. The higher the initial tension, the greater this effect. Where the tower is guyed at several levels, additional factors of safety are obtained by redistribution of moments along the tower away from overstressed areas except for the cantilever sections. Because of the need to satisfy the usual specification requirement for reversal of wind directions, the shaft will be fully developed for the design load in a given direction only at either the guy points or at the mid-spans.

Thus, if the tower is designed with similar ratios of allowable stress to yield stress in all parts, the actual factors of safety for the various parts will be different and will be lowest in the cantilever section. This is again borne out by actual failures, many of which start by collapse of the cantilever sections. As the cantilever section of a guyed tower is also the only section subject to tension and stress reversal, a reduced allowable stress for the cantilever section may be justified with conventional design methods.

Although the present practice which limits the "working" stress in the guys to $\frac{1}{3}$ of the breaking strength is safe, it does not assure designs of uniform strength and stiffness among competing designs unless the deflection of the mast under load and the minimum initial tension in the guys are also specified. It can be shown that variations in the initial tension and working stress over a wide range do not directly affect the safety of the tower.

A partial list of wind failures compiled by an insurance company [42] lists over 40 failures in civilian radio and TV transmission towers between 1940 and 1954. Data are undesirably meager in many instances, and they state that there have been numerous other incidents regarding which they have not received data. Only one failure is listed as a result of being struck by the vortex of a tornado.

This appears incongruous. On one hand, towers are designed with substantial factors of safety over and above that required to cover variations in material and workmanship. On the other hand, we find that failures are not uncommon. The answer appears to lie, at least partly, in the differences between the design

wind loads and the actual wind loads to which the towers were subjected. These differences stem from two sources, (a) prediction of the magnitude and variation with height of wind and gust velocities and (b) evaluation of drag and lift coefficients.

The evaluation of the former is outside the normal scope of the structural engineer. However, it may be pertinent to point out the type of information he needs and the general direction which his design procedures are taking.

Although the conventional "allowable stress" design methods have been outlined and are used in the great majority of cases, ultimate strength and plastic-limit design methods are also being used. In these cases, wind frequencies are needed in various directions to establish the ultimate loads to which the collapse strength of the structures can be made equal. For structures where operation is dependent upon maintaining a given configuration within fixed limits, the frequency of a lower velocity wind is needed in order to assure operation over any fixed per cent of the time. This can normally be established at a high percentage with a relatively low wind velocity.

At present, such data are not available. Therefore, even where the drag coefficients and structural design are precise, there is no readily available reliable index of safety for the proposed loadings. It would be highly desirable to establish wind-velocity recommendations in various critical directions covering (a) maximum observed velocity (b) predicted 50-yr maximum (c) predicted 100-yr maximum (d) predicted 150-yr maximum, all with appropriate gust factors. The recommendations should be based on the most severe storm conditions which can be anticipated in a given region. To the extent that ice accretion greatly alters the aerodynamic characteristics of the structure, these data should not then be presented separately but should be included as a function of the maximum wind speed. The recurrence interval of the maximum "combined effect" is the engineering quantity desired.

It would be desirable to have more data on probable gust loadings obtained and analyzed for the purpose of establishing these factors as functions of duration, extent, basic wind velocity, height, topography, and locality or storm type in a manner where the structural designer can make a rational selection of these factors for any given design.

The structural engineer could then design an adequate structure for maximum loading consistent with the useful life of the structure and allow a margin of uncertainty only for variations in materials and workmanship and drag coefficients.

The above are not intended as complaints. The author recognizes that considerable progress is being made as shown by the excellent papers presented at this meeting. This is one of the rare opportunities when structural engineers can discuss with the

meteorologists the margins of safety or ignorance now required to cover the voids in the structural engineers' understanding of the ways of the wind.

REFERENCES

1. Alton, J., 1951: Masts and guys under wind action. *The Eng. J.*, **34**, 1096.
2. Biggs, J. M., 1954: Wind loads on truss bridges. *Trans. Amer. Soc. Civil Eng.*, **119**, 879–892.
3. Blanjean, L., 1949: *L'action du vent sur les constructions. Ossature Metallique*, **14**, 91–111.
4. Boursiere, M., 1954: *Le calcul des pylônes haubannes*. Le Genie Civil, **131**, 205–208.
5. Caughey, T., 1959: Response of a non-linear string to random loading. *J. App. Mech.*, **26**, 341–344.
6. Cohen, E., and H. Perrin, 1957: Design of multi-level guyed towers: wind loading. *J. Struct. Div. Amer. Soc. Civil Eng.*, **83**, 1355–1 thru 1355–29.
7. Cohen, E., and H. Perrin, 1957: Design of multi-level guyed towers: structural analysis. *J. Struct. Div. Amer. Soc. Civil Eng.*, **83**, 1356–1 thru 1356–29.
8. Crandall, S., 1958: *Random vibration*. Cambridge, Mass. Inst. Tech. Technology Press.
9. Delany, N., and N. Sorensen, 1953: *Low speed drag of cylinders of various shapes*, Natl. Advis. Comm. Aero. Tech. Note 3038, p. 7.
10. Dickey, W., and G. Woodruff, 1956: The vibrations of steel stacks. *Trans. Amer. Soc. Civil Eng.*, **121**, 1054–1070.
11. Diehl, W. S., 1930: *Engineering aerodynamics*, New York, Ronald Press Co.
12. Dockstader, E., W. Swiger, and E. Ireland, 1956: Resonant vibration of steel stacks. *Trans. Amer. Soc. Civil Eng.*, **121**, 1088–1109.
13. Edwards, A. T., and A. Madeyski, 1956: Progress report on the investigation of galloping of transmission line conductors (Includes extensive bibliography). *Trans. Amer. Inst. Elec. Eng.*, **75**, Part III, 666–685.
14. Eiffel, G., 1911: *Resistance de l'air and l'aviation*. Paris, Dunod.
15. Eiffel, G., 1914: *Resistance de l'air and l'aviation, Nouvelles recherches*. Paris, Dunod & Pinard.
16. Esquillan, M., 1947: *Les nouvelles règles francaises relatives à l'action de la neige et du vent sur les constructions*. Annales Institut Technique des Batiments et travaux publics, Series I, No. 38, Paris, Institut Technique des Batiments et Travaux Publics (publisher).
17. Fiesenheiser, March, 1957: How to approach the design of tall guyed towers. *Consulting Eng.*, **9**, 64–70.
18. Flachsbart, O., and H. Winter, 1934 and 1935: *Modelversuche über die Belastung Von Gitterfachwerken durch Wind Kräfte*. Stahlbau, No. 9, p. 65; No. 10, p. 73; No. 8, p. 65.
19. Flachsbart, O., 1932: Winddruck auf Vollwandige Bauwerke und Gitterfachwerke. *Publications Internat. Assn. Bridge Struct. Eng.*, **1**, 153–172.
20. Fung, Y., 1958: *Fluctuating lift and drag acting on a cylinder in a flow at supercritical Reynolds number*. Shock and Vibration Bull., No. 26, Part II, Washington, D. C., U. S. Naval Research Laboratory.
21. Herrnstadt, T., 1956: *The highest structure in the German Federal Republic*. Acier-Stahl-Steel, **21**, 499–502.
22. Katzmayr, and H. Seitz, May 1934: *Winddruck auf Fachwerkture von quadratischem Querschnitt*. Der Bauingenieur, **15**, 218–221.
23. Kolousek, V., 1947: Solution statique et dynamique des pylônes d'antennes haubannes. *Publications Internat. Assoc. Bridge Struct. Eng.*, **8**, 105–140.
24. Ozker, M., and O. Smith, 1956: Factors influencing the dynamic behavior of tall stacks under the action of wind. *Trans. Amer. Soc. Mech. Eng.*, **83**, 1381–1386.
25. Pagon, W. W., 1934 and 1935: Aerodynamics and the civil engineer. *Eng. News Record*, **112**, 41, 348, 456, 814; **114**, 582, 665, 742; **115**, 601.
26. Penzien, J., 1957: Wind induced vibrations of cylindrical structures. *J. Eng. Mech. Div. Amer. Soc. Civil Eng.*, **83**, 1141–1 thru 1141–17.
27. Prandtl, Flachsbart, and others, 1925–1930: *Ergebnisse der aerodynamischen Versuchsanstalt Ergebnisse*. Gottingen, 1–IV Lieferungen.
28. Price, P., 1956: Suppression of the fluid induced vibration of circular cylinders. *J. Eng. Mech. Div. Amer. Soc. Civil Eng.*, **82**, 1030–1 thru 1030–22.
29. Schott, G., F. Thurston, and P. Peacock, 1954: *Analysis of structural behavior of guyed antenna masts*. Natl. Res. Council of Canada—Div. Mech. Eng., Report MM-238.
30. Sherlock, R. H., 1958: Wind forces on structures: nature of the wind. *J. Struct. Div. Amer. Soc. Civil Eng.*, **84**, 1708–1 thru 1708–16.
31. Sherlock, R. H., 1953: Variation of wind velocity and gusts with height. *Trans. Amer. Soc. Civil Eng.*, **11**, 463.
32. Singer, J., and G. Rayner, 1957: *Analysis of meteorological tower data*. Brookhaven Natl. Lab. Rep., BNL 461. (T102) Physics and Mathematics.
33. Steidel, B., 1959: Strains induced in transmission line cables by aeolian vibration. *Proc. Society of Experimental Stress Analysis XVI*, No. 2, 109–118.
34. Sturm, R. G., 1936: Vibration of cables and dampers. *Elec. Eng.*, **55**, 455–465 and 673–688.
35. Weaver, W., Jr., 1959: *Experimental investigation of wind induced vibrations on antenna members*. Cambridge, Mass. Inst. Tech. Lincoln Lab. Group Reports, No. 75–4.
36. Tyrrell, 1959: The big dish. *Civil Eng.*, **29**, 792.
37. Wood, 1935: *Technical aerodynamics*. New York, McGraw-Hill Co.
38. —, 1959: Building the Arctic warning radar system. *Eng. News Rec.*, **163**, 26.
39. Vincent, G. S., 1953: *Investigation of wind forces on highway bridges*. Highway Res. Board Spec. Rep. 10, publication 272, Washington, D. C., National Research Council.
40. —, 1956: *Normen für die Belastungsannahmen, die Statistischen Berechnungen, die Abnahme, die Überwachung, und den Unterhalt der Bauten*. SIA No. 160, Zurich Schweiz. Ing. und Arch. Verein (publisher).
41. —, 1956: Radio and television mast at Steinkimmen. *Eng.*, **202**, 489.
42. Firemen's Mutual Insurance Company, 1954: Radio and television towers partial list of windstorm failures. New York, Factory Mutual Engineering Division, Stds. Dept. of FMIC (Unpublished date).
43. Ministere de la reconstruction et de l'urbanisme, 1947: *Regles définissant les effets de la neige et du vent sur les constructions*. Paris, published by Ministry of Reconstruction and Urbanism.
44. —, 1937: The action of typhoons on structures. *Eng.*, **164**, 499.
45. Woodhouse, W. B., 1929: Overhead electric lines. *J. Inst. Elec. Eng.*, **67**, 226.
46. —, 1958: Special purpose structures. *Trends*, **4**, 692.
47. —, 1940: Tests at Daniel Guggenheim Airship Institute, Akron. Unpubl.
48. —, 1935: Wind pressure on latticed towers. *J. Inst. Elect. Eng.*, **77**, 189–196.
49. Ower, E., 1948: *Wind resistance of lattice girder bridges*. London, Inst. of Civil Eng. and Inst. of Struct. Eng., 58 pp.
50. Deutscher Normenausschuss, 1938: *Windlast DIN 1055 Blatt 4*, Berlin, Beuth-Vertrieb GmbH.

PART II: Meteorology and Hydrologic Engineering

INTRODUCTORY REMARKS

Charles C. Bates

Office of Naval Research

and Max A. Kohler

U. S. Weather Bureau

The opening of the St. Lawrence Seaway means that the heavily industrialized coastline of the Great Lakes will experience an even greater concentration of economic wealth in the next few years. With the average water level for each lake being a key datum upon which coastal engineering designs and operations are based, a complete understanding and adequate warning of both short- and long-term deviations in these average levels must be at hand if loss of life and economic wealth are to be kept at a minimum. Several of the papers presented at one of the two sessions on Meteorology and Hydrologic Engineering reviewed the present state of our knowledge concerning natural fluctuations in water level within the Great Lakes basin. Inter-relations between precipitation, wind patterns, storm tracks, and lake levels were described in some detail, and indications were given as to where the state of present knowledge is inadequate.

The paper presented by Major Ira Hunt, and published in this Monograph, comprehensively describes the large-scale seiche action of Lake Erie. Through an unusually comprehensive statistical study by the Corps of Engineers concerning wind conditions both over and around the lake, Major Hunt has obtained a reliable stress coefficient for the set-up equation. This type correction, neglected by earlier workers who used misleading wind values from onshore, permits the wind set-up to be computed for specific points over the lake, and excellent correlations were obtained with the observed lake levels. However, the shallow, island-filled western end of Lake Erie creates a highly variable energy absorber, and Major Hunt notes that the

present-day prediction accuracy of seiche-decay rates is still unsatisfactory.

The other session on Meteorology and Hydrologic Engineering comprised a series of papers on various aspects of precipitation as pertaining to engineering design and operational problems. This series of papers was particularly appropriate to a joint meeting of the American Meteorological Society and the American Society of Civil Engineers, since precipitation constitutes one of the more obvious phases of the hydrologic cycle falling within the common ground of meteorology and hydrology. Many aspects of design rest to a considerable degree upon analyses of precipitation data, particularly in the case of water control and utilization structures. Moreover, any improvement in the reliability of precipitation forecasts will provide direct benefits through more efficient operation of hydraulic structures.

Two of the papers presented at this session are included in the Monograph. Although both describe studies of precipitation over the State of Illinois, one concerns the probabilities of specified dry periods, while the other treats flood-producing storms. The drought studies reported by Mr. Changnon demonstrate the use of high-speed electronic computers to process tremendous quantities of climatological data in a minimum of time. It is interesting to note, also, that the storm studies reported by Messrs. Huff and Semonin utilize radar data for improved definition of storm pattern. There is every reason to expect that the more elaborate and dependable radar of the future will be invaluable for such purposes.

A METHOD FOR DETERMINING DRY-PERIOD PROBABILITIES AS APPLIED TO ILLINOIS

Stanley A. Changnon, Jr.

Illinois State Water Survey

ABSTRACT

A method to rapidly calculate dry-period probabilities from long-term climatological records utilizing machine techniques is presented. Fifty-five years of daily rainfall records entered on IBM cards can be processed in 32 hr to give the probability for each date to occur in continuous dry periods of 1, 2, 3 days or longer. Dryness, or lack of daily rainfall, has been defined at four levels: 0.10 in, 0.25 in, 0.50 in, and 1.00 in per calendar day with daily probabilities computed simultaneously for each level.

The results of analyses, as applied to data from three widely separated locations in Illinois, reveal that significant regional and seasonal variations in probabilities for dryness exist. In general, the highest probabilities for dryness occur during the colder half-year with a secondary high in July. Lowest probabilities for dryness occur in the spring months and mid-August. Considerable fluctuation in the probability values occur during each month, especially for the 0.10- and 0.25-in-per-day values.

1. Introduction

Because many activities in the functioning of agriculture and industry require relatively dry periods that persist for two or more consecutive days, information for predicting the most likely rain-free periods is economically beneficial. To determine the probability for the occurrence of dry periods in Illinois, a study was initiated utilizing rainfall data entered on IBM cards [1]. Records of daily rainfall were available from 60 U. S. Weather Bureau Stations in Illinois, each with over 50 yr of nearly continuous daily rainfall observations entered on daily-summary IBM cards. Fifty-four of these stations were cooperative substations, and the remaining six were first-order stations.

To define drought or even dryness as it relates to every field of interest has always been a difficult climatological problem. In the present study, dryness has been defined simply as the lack of various rainfall amounts on any day. The daily precipitation amounts entered in the cards and used in this analysis were based on calendar day totals measured once daily, usually at 1700 CST. No adjustment was made to alter the probabilities for dryness due to possible differences between calendar-day and maximum 24-hr amounts. Huff [2], in studying excessive daily precipitation in Illinois, found that, on the average, the maximum 24-hr amounts exceeded calendar-day amounts by a factor of 1.13. This suggests that the computed probabilities for dryness in this study would have been somewhat lower if data other than calendar-day amounts had been available for analysis. However, very few maximum-period precipitation records are available in Illinois, or elsewhere in the United States,

since a large preponderance of the useful long-term precipitation records have been collected at cooperative substations which only have calendar-day amounts. Furthermore, any alterations in probabilities for dryness which might be produced by using maximum-period amounts should be evenly distributed throughout the year, making little or no relative change in the comparative probabilities from day-to-day or month-to-month.

Four different amounts of rain were selected as the delimiting criteria or levels for the dryness analyses. These were 0.10 in, 0.25 in, 0.50 in, and 1.00 in per day. For any level, a day with less than the amount at the given level was considered dry. The length of a dry period was determined by the number of consecutive dry days. A dry period at any of the four levels was considered broken with the occurrence of a day with a rainfall amount greater than the level. These four levels were chosen so that agricultural, engineering, and hydrological interests could find a level suitable to their operational requirements. Agriculturally, the 0.10- and 0.25-in amounts per day relate to the daily water requirements of most plants, while data based on the 0.50- and 1.00-in amounts per day have application in industry and hydrology.

2. Methodology

The analysis was accomplished largely by machine processing of IBM cards. The method of card analysis required only three passes of the cards through the IBM Calculator, two passes on the IBM Statistical Machine, and a single pass on the IBM Sorter [1]. The process required each card to have 20 blank columns for insertion of calculated information.

Briefly, the method of machine-card analysis for a single station follows this procedure. First, on a chronological pass through the Calculator, each card is marked as being wet or dry for the 0.10- and 0.25-in levels. At the same time, the number of continuous wet or dry days in both levels was being counted and, as each continuous period ended, the number of days was punched into a "period-ending" card. A similar pass through the Calculator was required for the 0.50- and 1.00-in levels. A third pass of the cards through the Calculator in reversed chronological order entered the number of continuous days per period for each day into the daily cards. The cards were sorted into months on the Statistical Machine and then sorted by dates on the Sorter. At the completion of the machine analysis, the Statistical Machine print-out for each of the four rainfall levels listed the number of times during the period of record each date had occurred in wet and dry periods of one-day, two-days, three-days, or longer duration. For one station with 20,000 cards, or approximately 55 yr of record, the IBM analysis required 32 hr.

This method eliminates need for a high-speed computer which often is not available to those wishing to do a similar study. Furthermore, the machines required for this analysis can be found in most IBM-machine installations.

3. Analysis procedures

Analyses were made for selected stations in Illinois to ascertain the areal variations in dry-period probabilities. Records from three U. S. Weather Bureau cooperative substations representing northern, central, and southern Illinois were processed to provide samples of the data from areas known to have relatively different rainfall climates [3]. The annual average rainfall in Illinois increases southward from 32 in in northeastern Illinois to 35 to 37 in in central Illinois and to over 46 in in southern Illinois. Most of this increase in rainfall to the south is attributed to the colder half-year rainfall, since during the warmer half-year the average rainfall in Illinois is almost uniformly distributed, ranging from 20 in in northern Illinois to 24 in in southern Illinois. During the six colder months, October through March, the average precipitation varies from 12 in in northern Illinois to 23 in in southern Illinois.

The three stations selected for comparison of dry probabilities are Aurora in northern Illinois with an average of 34.13 in per year, Urbana in central Illinois with 36.05 in average per year, and Mt. Vernon in southern Illinois with 41.02 in of average annual precipitation.

4. Probability for a 3-day dry period at the 0.10-in level

The curves for the probability of a date being in a continuous three-day dry period, with dry defined as less than 0.10 in in 24 hr, are shown in fig. 1. The data were smoothed by three-day moving averages. The cycles or fluctuations in the 0.10-in probability curves for the three Illinois stations are quite similar. The major differences appear in the magnitude of the probabilities on the same dates. As expected, the colder half-year probabilities for dryness are in general higher than those during the warmer half-year, and the northern- and central-area stations have higher probabilities in the colder half-year than do the southern stations.

During April, May, and June, the probabilities for dryness are lowest for the year, a trend that may be expected because these three months have the highest monthly rainfall averages and also average more days with rainfall amounts greater than 0.10 in than do the other nine months. However, an increasing tendency for dryness begins in late June and reaches a maximum probability in late July. This dryness period is followed by a sudden decrease to the minimum during the middle of August. This August minimum appears on all four levels of dryness classification, indicating the possible presence of an August rain occurrence singularity. This same feature in August was found in studies of dry-period probabilities for east-central Missouri [4]. In general, the probability curves increase rapidly during the middle of August and maintain a high probability for dryness into September and the colder half-year months.

All months except November have at least one period of high and one of low probability for dryness which allow selectivity within any month for choosing the best opportunity for dryness. Another surprising feature of these data shown in fig. 1 is the abruptness of the changes in probabilities from day to day. The dry-period probability curves for the central and northern Illinois stations have many similarities which are not found in the southern Illinois data. For instance, at Urbana and Aurora, the period of highest probabilities during the year is late January and early February, while the highest probability at Mt. Vernon is reached in October.

Close examination of the probability curves in fig. 1 reveals that there are four distinct periods or, as labeled, four seasons during which similar conditions appear to be in existence. These seasons do not closely coincide with those commonly referred to as climatic seasons. The winter season extends from 7 December to 13 April and is characterized by probability curves

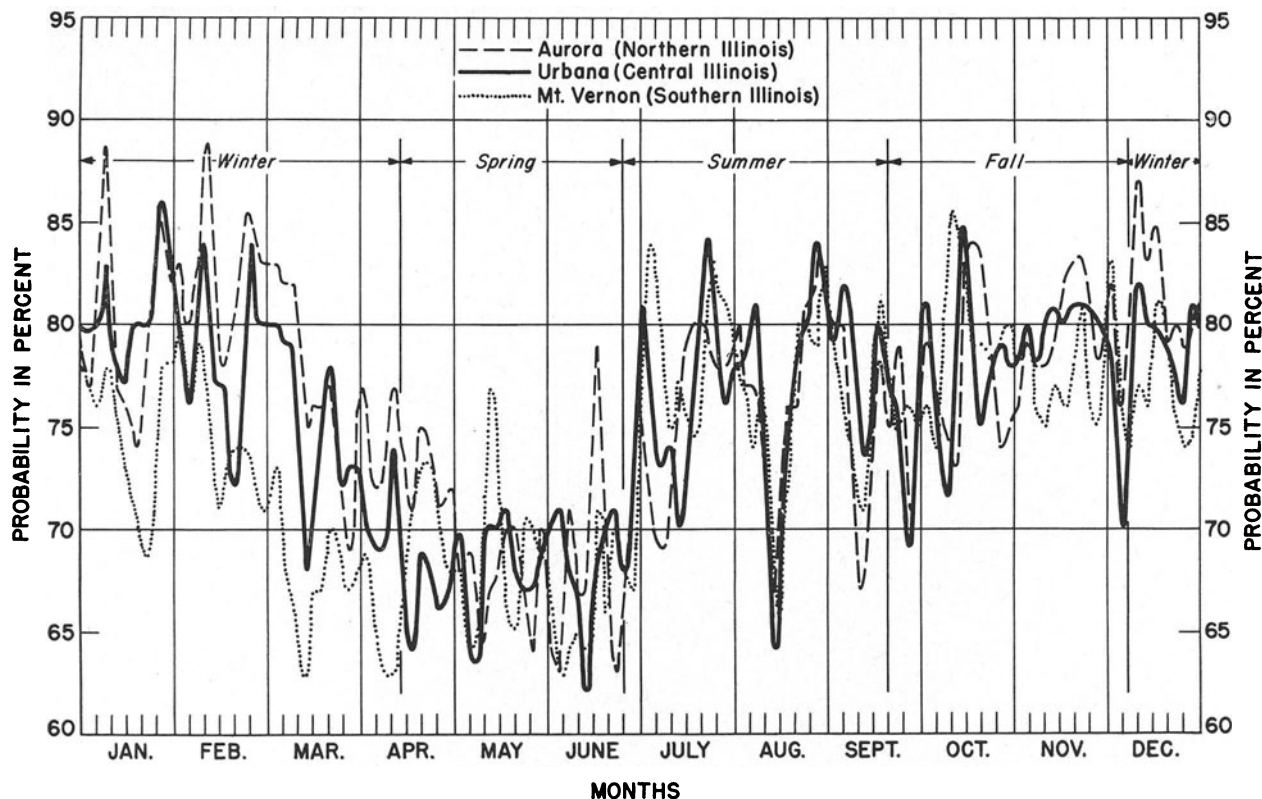


FIG. 1. Probability for a 3-day-or-longer dry period. Dry defined as less than 0.10 in per day.

with harmonious fluctuations. During these four months, Aurora in the north has the highest probabilities, Urbana in central Illinois averages 5 percentage points lower, and Mt. Vernon in the south has the lowest values throughout this entire season. This north-to-south decrease reflects the steep north-south gradient in average rainfall during these months with four-month averages of 7.59 in at Aurora, 9.47 in at Urbana, and 12.60 in at Mt. Vernon.

Beginning about 14 April, these conditions change and the curves lose their accordant as well as their latitudinal characteristics. The fluctuations in the probability curve for Mt. Vernon are not in agreement with the others. Other notable features during this spring period are the 10 to 15 May period of high probabilities at Mt. Vernon and the 18 to 23 June peak at Aurora. The northward movement of rain-producing conditions in Illinois from 14 April to 25 June brings discordant fluctuations in the probabilities of the three locations but, at each station, periods of dryness can be selected in any month.

During the summer season, beginning 26 June and ending 20 September, weather patterns throughout Illinois are much the same, producing more probabilities of nearly equal magnitudes for the three stations than in any other season. However, the probability values for Aurora do not become nearly equal to those of Mt. Vernon and Urbana until the

end of July. These conditions feature sudden increases in the chances for dryness at the end of June and during late July and early August. All three curves have decided tendencies for decreases in probability to the previously mentioned "wet" period centered on 14 August.

From 21 September through 6 December, the fall season prevails, which is a transitional climatic period reflecting the type of discordant conditions existing in the spring season. However, some high and low probabilities occur almost simultaneously at the three stations. A high probability for dryness, highest of the year at Mt. Vernon, occurs in the middle of October, reaching a peak on 10 October in Mt. Vernon, 13 October in Urbana, and on 17 October at Aurora. In October, the Aurora and Urbana probability curves have similar tendencies, but the Mt. Vernon curve is not harmonious with them. November has the smallest range in probability values with a maximum difference during the month of only 3 per cent at Urbana, only 6 per cent at Mt. Vernon, and only 5 per cent at Aurora.

5. Probability for a 10-day dry period at the 0.25-in level

In fig. 2, the probability that a given day will be in a 10-day-or-longer dry period, with dry defined as less

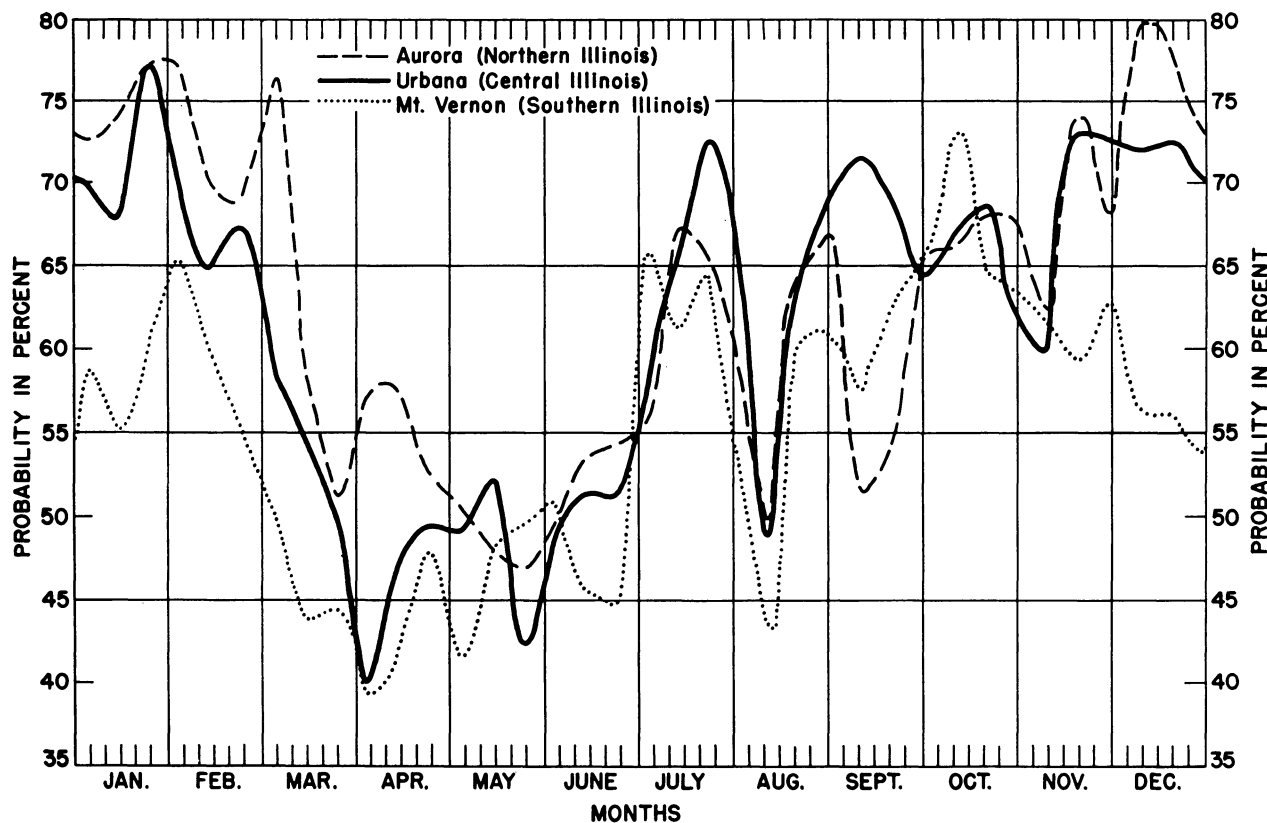


FIG. 2. Probability for a 10-day-or-longer dry period. Dry defined as less than 0.25 in per day.

than 0.25 in per day, is shown by curves for the three stations. The curves have been smoothed by 10-day moving averages. The general characteristics of the probability curves in fig. 2 are much the same as those shown in fig. 1. From early in December through the end of April, the latitudinal characteristic prevails with Aurora having the higher probabilities and Mt. Vernon having the lower probabilities for dryness. In general, the curves of the three stations have harmonious fluctuations during this four-month period.

Beginning in May, the curves fluctuate at different times, especially at Mt. Vernon where the probabilities are not in agreement with those at Aurora and Urbana. Again, as with the 0.10-in-level values, the probability values are lowest in May and June. Beginning in July, the summer season is in evidence with rather similar curve tendencies at all three stations featured by the low values in mid-August. By the first of September, the Urbana probability curve is not harmonious with the Aurora and Mt. Vernon curves, although the three curves again become somewhat similar in October and November. Aurora has its highest probabilities in December, while the highest at Urbana occur in late January, and at Mt. Vernon the most likely 10-day dry period during the year occurs in October. In most months, enough variability exists in the probability

values to permit a selection of dates in each month as most optimum for a 10-day-or-longer continuous period with less than 0.25 in of rain in any day.

6. Probability for dry periods at the 0.50- and 1.00-in levels

In fig. 3, the probability for each date being in a 30-day-or-longer period with less than 0.50 in rainfall on any day is shown as a series of three curves for the three stations. The data have been smoothed by 10-day moving averages. Much greater variation between stations in the range of the probability values occurs at this level during the year than at the 0.10- and 0.25-in levels. The latitudinal variation between the stations is also much greater. For instance, Aurora varies from a low of 22 per cent in May to 78 per cent in February, while Mt. Vernon varies from a low of 21 per cent in April to a high of only 48 per cent in February, a range of 27 percentage points as compared to 56 at Aurora. Values for the three stations are relatively the same from early May through mid-October.

The August low is not too apparent at Mt. Vernon but is evident in the Urbana and Aurora curves. The annual minimum values for the three stations occur

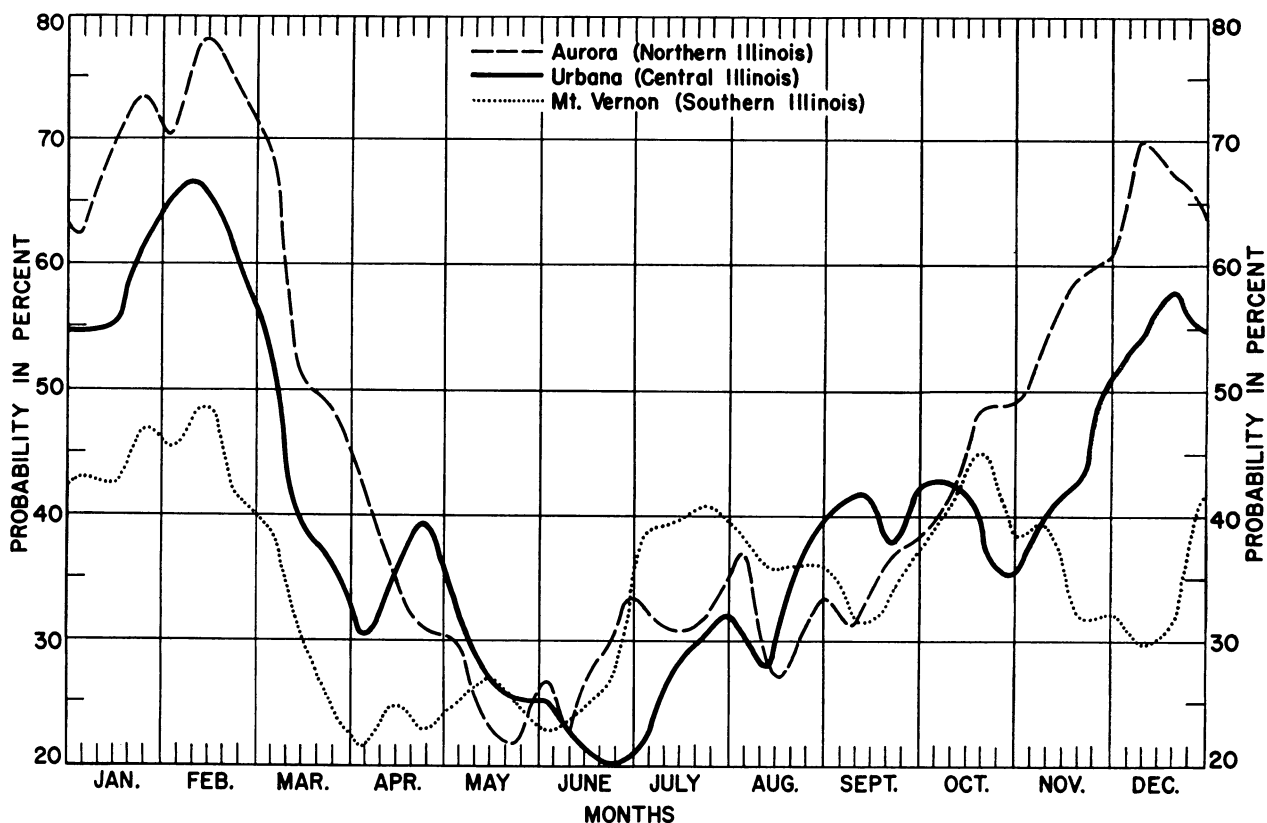


FIG. 3. Probability for a 30-day or longer dry period. Dry defined as less than 0.50 in per day.

in three different months. Mt. Vernon probabilities are lowest in April; Aurora probabilities, in May; and Urbana probabilities, in June. The six colder half-year months plus April have the distinguishing north-south decrease in values apparent in figs. 1 and 2. All stations have their maximum probabilities for the year in February. One interesting feature during these months is the period of low probability values at Mt. Vernon from 20 November to 20 December. Also, a sudden decrease in probability values occurs at Aurora during March. Chances are in 7 out of 10 yr that any of the first 5 days in March will be in a 30-day-or-longer 0.50-in dry period, while for the last 12 days of the month chances are that in only 5 out of 10 yr will these dates fall in a 30-day-or-longer 0.50-in dry period.

Fig. 4 gives the probabilities of a day being in a 60-day-or-longer period with less than 1.00 in rainfall on any day, which are shown as curves for each station smoothed by 10-day moving averages. As in fig. 3, the dominating feature is the one large cycle during the year composed of the high winter probabilities and the low summer probabilities. At Aurora, from mid-January until 8 March, the chances are 9 out of 10 for each date being in a 60-day-or-longer 1.00-in dry period. The annual range in the station probability values is quite large. At Aurora, the annual range extends from a low of 35 per cent in June to a

high of 93 per cent in January. All three stations reach their lowest probabilities in June and their highest values in either December or January. Only at Aurora does the mid-August wet cycle appear.

7. Conclusions

This method for determining dry-period probabilities by IBM machines can rapidly produce, in respect to the volume of data, for each date the frequency of occurrence in wet and dry periods of any length. Chances of each date being in a dry period, as defined by pre-selected levels of calendar-day rainfall, can easily be determined for any desired number of days. Another of the salient features of the method is that a high-speed computer is not required. Only IBM cards with daily rainfall amounts and a minimum number of IBM machines are required to accomplish the analysis.

Results of the analysis, as derived for three widely separated locations in Illinois, reveal that there is a great similarity between regions of the state in the seasonal distribution of dry periods. In general, only the magnitudes of probability values from the different regions vary seasonally. The higher probabilities for dryness normally occur in the colder half-year and the lowest in the April-June period. In July, the prob-

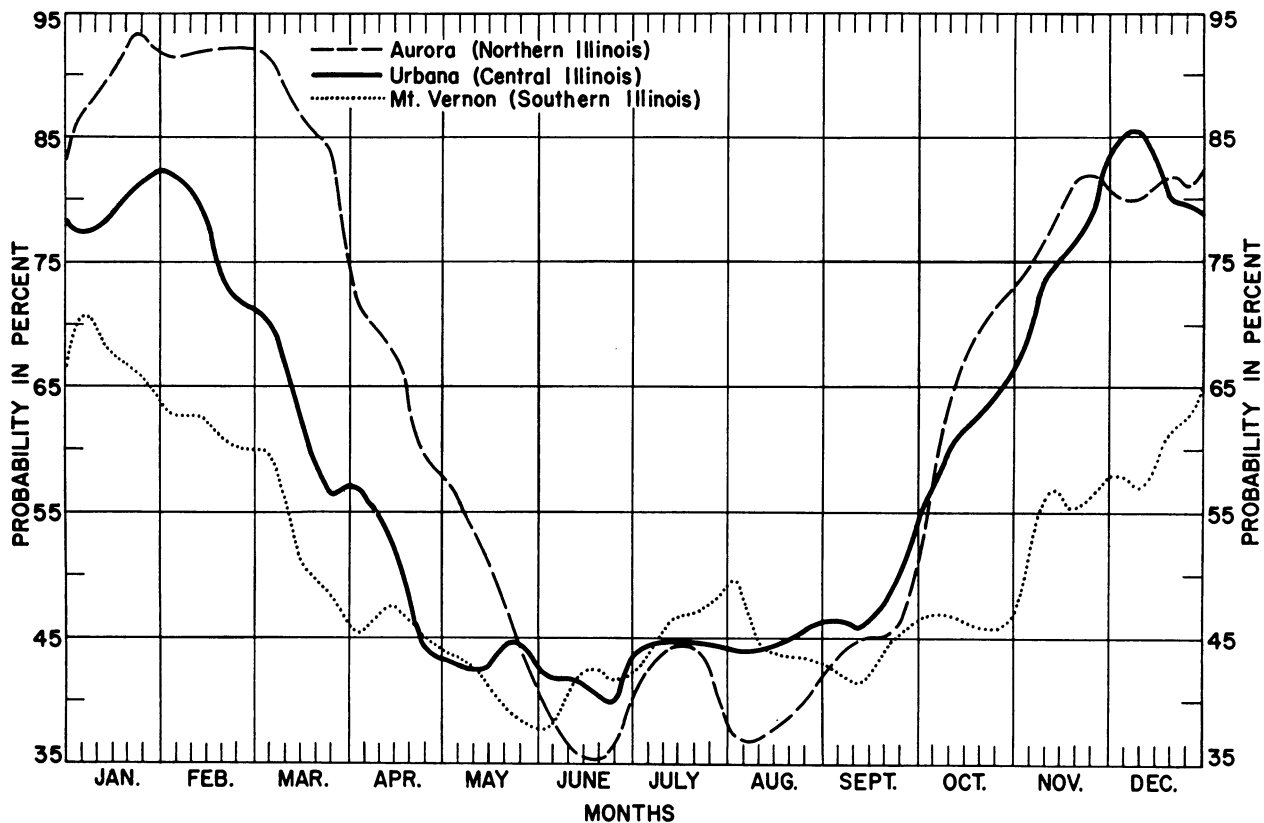


FIG. 4. Probability for a 60-day or longer dry period. Dry defined as less than 1.00 in per day.

abilities for dryness increase, followed by a short period in mid-August of low probabilities. At all four levels of dryness, the annual range in probability values is less at Mt. Vernon than at the other locations owing to the more even distribution of rainfall during the year in southern Illinois. The annual range in probability values is higher in the 1.00- and 0.50-in levels than in the 0.10- and 0.25-in levels.

At the 0.10- and 0.25-in-per-day levels of dryness, there are sudden changes in probability values from day to day. However, at the 0.50- and 1.00-in levels, the day-to-day changes are much less abrupt. At all four levels of dryness, it is possible to select for each month a period of days most likely to be dry. Therefore, outdoor activities and operations can be planned

to coincide with monthly or seasonal periods with better chances for dryness.

REFERENCES

1. Changnon, S. A., 1956: *Second progress report of the Illinois project in climatology*. Urbana, Ill., Ill. State Water Surv. Circ. 57, pp. 1-24.
2. Huff, F. A., and J. C. Neill, 1959: *Frequency relations for storm rainfall in Illinois*. Urbana, Ill., Ill. State Water Surv. Bull. 46, pp. 36-37.
3. Anon., 1930: *Climatic summary of the United States*. Washington, D. C., U. S. Dept. of Comm. Wea. Bur. Bull. W-Sect. 56-58, p. 2.
4. Decker, W. L., 1958: *Chances of dry periods in Missouri*. Columbia, Mo., Univ. Mo. Agric. Exper. Sta. Bull. 707, p. 8.

AN INVESTIGATION OF FLOOD-PRODUCING STORMS IN ILLINOIS

F. A. Huff and R. G. Semonin

Illinois State Water Survey

ABSTRACT

Meteorological conditions in major flood-producing storms of 1- to 10-day duration in Illinois are being analyzed. This paper presents the approach to the problem, progress to date, and preliminary results based on 2-day storms.

During 1914 to 1957, 262 storms of 2-day duration in which the mean rainfall over 10,000 sq mi was 1 in or greater were analyzed, and area-depth relations were determined for each storm. The seasonal distribution of storms was obtained and it was found that 51 percent occurred during the summer months. The most frequent area of occurrence was found to be southeastern Illinois. A study of the orientations of the major axes of the storms disclosed that 71 per cent of the storms were oriented within the sector from WSW-ENE to WNW-ESE. An investigation of synoptic conditions revealed that stationary fronts were associated with 27 per cent of the most intense storms. The distribution of 3-, 6-, and 12-hr rainfall maxima for the 28 heaviest storms during 1948 to 1958 was examined. For storms of 24 hr duration or less, the 3-hr maximum began most frequently between 0000 and 0300 CST; the 6-hr maximum, at the same time; and the 12-hr maximum, between 1800 and 2100. A brief description of a synoptic model of these storms which evolved during the progress of this investigation is presented.

1. Introduction

An investigation is being made in Illinois in an effort to obtain a more reliable definition of the time and space distribution of heavy rainstorms in the state. Analysis is being made of area-depth relations observed in major flood-producing storms of 1-to 10-day duration during the period 1914 to 1957, the orientation of these storms, the seasonal variations in their occurrence, their regional variations within the state, and the synoptic weather features associated with them. Special attention is being given to storms occurring during the period 1948 to 1957, when radar data and extensive field-survey data on rainfall were compiled.

This paper is concerned with the approach to the problem, progress to date, and preliminary results of analysis. The discussion of preliminary results will be restricted to those obtained from the study of 2-day storm periods.

2. Approach to problem

The primary sources of data used in the study are the publications of climatic data for first-order and cooperative stations of the U. S. Weather Bureau [1]. Since 1948, the Illinois State Water Survey has augmented the Weather Bureau data on outstanding storms with data collected by radar and by detailed field surveys [2]. In selecting the storms for analysis, all records for the period 1914 to 1957 were examined, and those storms in which the maximum observed

rainfall exceeded a pre-determined value were selected for further analysis. Thus, in selecting 2-day storm periods for analysis, all storms were examined in which a maximum rainfall of 4 in or greater had been recorded at one or more stations within Illinois. Area-depth curves from plotted maps were then drawn for each of these storms. All storms in which the mean rainfall over 10,000 sq mi did not exceed 1 in were eliminated from further analysis. Thus, storms of small areal extent were eliminated from the study, since the gage density in the state has not been adequate to record all such storms or to permit accurate analysis of those which have been observed by the existing network [3]. Area-depth relations in the 262 storms satisfying the above conditions were computed for areas of 10 to 20,000 sq mi within and surrounding the storm area.

3. Analysis and results

Investigation of mathematical expressions indicated an excellent fit of the area-depth data with an equation of the form

$$\log R = K + L \cdot A^n$$

where R = mean rainfall depth; A = area; and K , L , and n are regression constants. This form of equation was suggested by Horton [4]. It was found that an excellent fit could be obtained for practically every storm by varying the exponent n from 0.3 to 0.6. All storms were fitted to an equation of this form, and mean rainfall values for areas of 10 to 20,000 sq mi

were determined from each derived curve for individual storms.

Next, the mean rainfall values for areas ranging from 10 to 20,000 sq mi were ranked, based upon the area-depth curves for the 44-yr period 1914 to 1957. These ranked data were then used to obtain area-depth frequency relations for Illinois.

As the density of raingages in Illinois has undergone considerable growth during the period covered in this study, a method was devised to adjust the area-depth curves derived from the hydroclimatic network. Comparisons were made between (1) area-depth relations obtained in storms for which detailed field-survey data were available and (2) the relations which were obtained for the same storms with Weather Bureau data only. The field-survey storms were analyzed using the available gage networks of the Weather Bureau during the periods 1914 to 1919, 1920 to 1929, 1930 to 1939, 1940 to 1949, 1950 to 1957. In this manner, transformation factors were determined for application to the area-depth relations obtained with Weather Bureau data. The values obtained after using the transformation factors were designated "modified" data. Table 1 shows results for

TABLE 1. Mean area-depth frequency relations for 2-day storms.

Area (sq mi)	Depth (in) for given return period (yr)					Deviation (per cent)
	2	5	10	25	50	
10	10.9	13.1	14.6	16.7	18.4	-19
100	9.2	11.2	12.5	14.2	15.5	-13
1,000	7.0	8.5	9.5	10.7	11.8	-9
5,000	5.1	6.1	6.9	7.9	8.6	-8
10,000	4.2	5.1	5.7	6.5	7.2	-7
20,000	3.4	4.1	4.6	5.3	5.8	-7

2-day storms obtained with the modified data, along with the deviation of the unmodified rainfall values, obtained from use of Weather Bureau data alone. Results presented in subsequent tables are based also upon the modified data.

The deviations for 2-day storm periods range from approximately seven per cent for an area of 20,000 sq mi to 19 per cent for an area of 10 sq mi (table 1).

Seasonal distribution of storms. As part of the Illinois study, investigation is being made of the seasonal

TABLE 2. Distribution of 2-day storms by seasons.

Season	Number of storms for given 10-sq-mi mean rainfall (in)					Per cent of total storms
	Over 9.9	8.0-9.9	6.0-7.9	5.0-5.9	Combined	
Winter	1	5	8	5	19	7
Spring	5	8	31	7	51	20
Summer	22	35	66	11	134	51
Fall	9	21	23	5	58	22

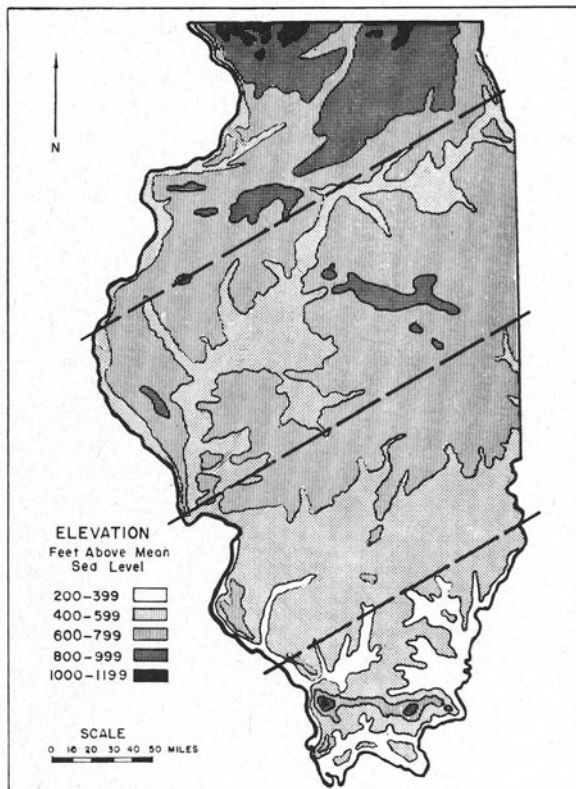


FIG. 1. Illinois topographic map with sectional divisions.

distribution of severe rainstorms. Table 2 shows the distribution of the 2-day storms, based upon various levels of maximum rainfall, as indicated by the 10-sq-mi mean rainfall. Reference to this table shows that heavy storms are far more frequent in summer, June through August, than in any of the other three seasons. Over 50 per cent of the storms occur during this season, with approximately 20 per cent in the spring and fall seasons, and only 7 per cent during winter. Winter includes the months of December, January, and February, while spring and fall include March through May and September through November, respectively.

Geographical distribution of storms. The state was divided into four sections of approximately homogeneous storm rainfall climate, as determined by a previous Water Survey study [5]. These sections are shown in fig. 1, together with the topographic features of the state. These sections have been designated the Northwest, North Central, South Central, and Southeast sections. The North Central section is the largest and the Southeast is the smallest among the four regions.

Table 3 shows the distribution of 2-day storms by section and storm magnitude. As considerable differences in the areal sizes of the four sections exist, the equivalent probability per unit area of a storm of a given magnitude being centered in each of the sections is given in table 4. Thus, after normalizing for area,

TABLE 3. Distribution of 2-day storms by sections.

10-sq-mi mean rainfall (in)	Number of storms				
	North- west	North- central	South- central	South- east	Total
Over 9.9	7	10	10	10	37
8.0-9.9	15	18	17	19	69
6.0-7.9	27	35	34	32	128
5.0-5.9	6	4	9	9	28
Total	55	67	70	70	262

TABLE 4. Comparative probability of given storm being centered on unit area in various sections.

10-sq-mi mean rainfall (in)	Probability (per cent)			
	North- west	North- central	South- central	South- east
Over 9.9	17	14	22	47
8.0-9.9	19	14	20	47
6.0-7.9	19	15	22	44
5.0-5.9	17	8	24	51
Average	18	13	22	47

TABLE 5. Two-day storm orientations.

Azimuth (degrees)	Per cent of storms for given 10-sq-mi mean rainfall				
	Over 9.9	8.0-9.9	6.0-7.9	5.0-5.9	Combined
180	0	0	0	0	0
190	0	0	0	0	0
200	0	0	0	0	0
210	2.9	5.2	2.8	4.8	3.6
220	0	0	3.7	0	1.8
230	2.9	3.4	3.7	9.4	4.1
240	8.8	12.2	11.1	28.6	12.7
250	14.7	22.4	15.7	14.3	17.1
260	6.0	12.2	7.4	19.0	9.5
270	11.8	8.6	14.8	0	11.3
280	14.7	10.3	12.0	0	10.9
290	2.9	8.6	10.3	14.3	9.0
300	20.6	10.3	7.4	4.8	10.0
310	2.9	1.7	2.8	0	2.3
320	2.9	3.4	3.7	4.8	3.6
330	6.0	1.7	2.8	0	2.7
340	0	0	0.9	0	0.5
350	2.9	0	0.9	0	0.9

Table 4 indicates that the probability of a storm of any given magnitude being centered on a unit area in the southeast section of the state is much greater than in any of the other sections.

Orientation of 2-day storms. Because the rainfall-runoff relations on specific watersheds are affected appreciably by the orientation of the storms causing the floods, investigation was made of the distribution of the orientation of the major axes of severe rainstorms in Illinois. Table 5 shows the distribution of the storm orientations for 2-day storms during 1914 to 1957, again classified according to the 10-sq-mi mean rainfall of each storm. In this table, azimuths are given only for the 180 deg ranging from 180 to 360.

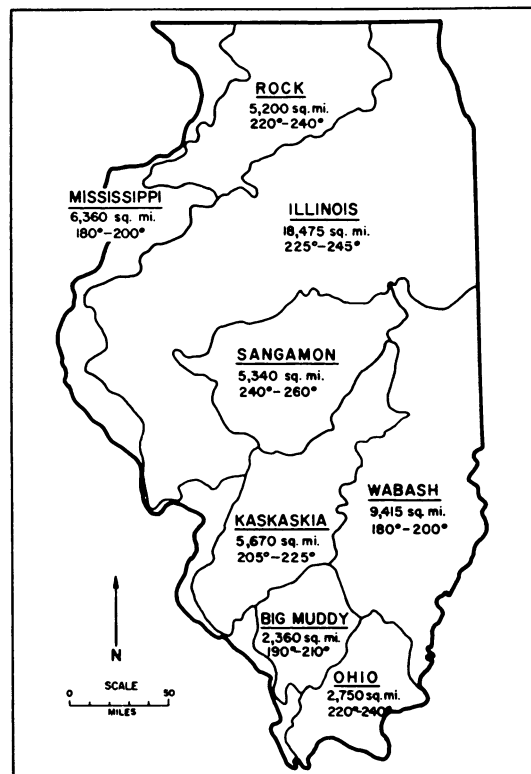


FIG. 2. Principal watersheds and optimum storm orientations.

Thus, a storm with an azimuth of 200 deg indicates that its major axis is orientated on a line from 200 deg to 20 deg. Table 5 indicates that 71 per cent of the Illinois storms have their major axes on azimuths from 235 to 295 deg. Fig. 2 shows the major watersheds in the state of Illinois, their areas, and the optimum orientation of storms for flooding on these watersheds. Reference to this figure shows that the Sangamon River Watershed has the most favorable orientation among the several basins for flooding. Of course, a number of other factors, in addition to basin orientation with respect to storm movement, are instrumental in determining the magnitude and frequency of basin floods.

Synoptic weather types. Another part of the program is a study of the synoptic weather types associated with the severe rainstorms to learn the generalized conditions under which these storms occur. Such information is valuable to the flood forecaster and should be useful eventually in helping to define the space and time distribution of these storms. Northern Hemisphere and U. S. Weather Bureau daily synoptic maps were used for this purpose. Table 6 shows a general synoptic typing of the 2-day storms, again based on the magnitude of the 10-sq-mi mean rainfall. As would be expected, warm fronts and cold fronts account for the majority of the storms, about 70 per cent, with the rest being distributed among stationary fronts, air

TABLE 6. Distribution of 2-day storms by synoptic type.

Synoptic type	Number for given 10-sq-mi mean rainfall (in)					
	Over 9.9	8.0-9.9	6.0-7.9	5.0-5.9	Com-	Per cent of total
Warm front	12	25	45	11	93	35
Cold front	8	23	47	11	89	34
Stationary front	10	6	14	2	32	12
Air mass	7	7	9	2	25	10
Miscellaneous	0	8	13	2	23	9

mass storms, and miscellaneous situations. Most of the cold fronts were slow moving with wave formations, and much of the rain undoubtedly occurred in pre-frontal squall lines. In table 6, miscellaneous includes occlusions, decaying hurricanes, and isolated lows without fronts.

An interesting feature of this table is the relatively high number of stationary fronts with outstanding severe storms, those in which the 10-sq-mi mean rainfall exceeded 9.9 in. Thus, stationary fronts accounted for 27 per cent of these heavier storms as compared to 12 per cent of the total storms. The synoptic phase of the investigation is still far from completed. Detailed analysis of storms during recent years, for which radar and field-survey data are available, is planned in an effort to determine more about the synoptic characteristics of severe rainstorms.

Diurnal rainfall distribution. Table 7 shows the diurnal distribution of maximum precipitation for periods of 3, 6, and 12 hr in the most severe rainstorms during 1948 to 1958. A total of 28 storms was included in this analysis. The data were grouped according to starting time of the 3-hr, 6-hr, or 12-hr maxima. It was found that the occurrence of the heaviest amounts takes place predominantly during the night. This is particularly true for storms of 24 hr or less duration and for the heaviest of the severe storms. Thus, all the 3-hr and 6-hr maxima in storms of 24 hr or less duration started between 1800 and 0230 CST. Dividing these storms into two groups, based upon the magnitude of the 10-sq-mi mean rainfall, it was again found that all of the 3-hr and 6-hr maxima began between 1800 and 0230 in the heaviest storms, while the 12-hr maxima fell between 1500 and 0200. When storms which had intermittent rainfall over a period exceeding 24 hr were examined, the distribution was found to be much more scattered and occurred over the entire day, as can be seen in table 7. Although the distribution was scattered over the entire day, the majority of the most intense rainfall periods did occur at night. Results presented in this table indicate a diurnal effect of considerable importance in the development and sustenance of unusually severe rainstorms.

TABLE 7. Diurnal distribution of 3-, 6-, and 12-hr rainfall maxima in severe storms, 1948 to 1958.

Time of day (CST)	Number of cases for given storm duration					
	24 hr or less			Over 24 hr		
	3 hr	6 hr	12 hr	3 hr	6 hr	12 hr
1800-2059	2	5	5	2	3	2
2100-2359	4	2	4	2	3	3
0000-0259	6	6	3	3	4	3
0300-0559	1	0	0	2	1	1
0600-0859	0	0	0	1	0	2
0900-1159	0	0	0	1	1	0
1200-1459	0	0	0	2	3	3
1500-1759	0	0	1	2	0	1
Median Occurrence range	0030 2000- 0330	2330 1800- 0230	2200 1500- 0200	0300 Entire day	0100 Entire day	0000 Entire day
Time of day (CST)	Number of cases for given group and period					
	Heaviest group			Second heaviest group		
	3 hr	6 hr	12 hr	3 hr	6 hr	12 hr
1800-2059	3	5	6	1	3	1
2100-2359	5	4	4	1	1	3
0000-0259	5	5	3	4	5	3
0300-0559	1	0	0	2	1	1
0600-0859	0	0	0	1	0	2
0900-1159	0	0	0	1	1	0
1200-1459	0	0	0	2	3	3
1500-1759	0	0	1	2	0	1
Median Occurrence range	2330 1800- 0330	2130 1800- 0230	2130 1500- 0200	0330 Entire day	0200 Entire day	0130 Entire day

4. Synoptic characteristics of severe rainstorms

The 3-cm radar records, collected by the State Water Survey during the five years 1953 to 1957 were analyzed to obtain measurements of precipitation areas appearing as lines on the plan position indicator. A line was defined as being composed of at least five precipitation echoes separated by no less than 10 mi or a solid echo 50 mi or more in length. The results of this study indicated, among other things, that echoes appear to be grouped in lines approximately two-thirds of the time that echoes are observed by 3-cm radar, and lines were observed in nearly every heavy rainstorm during 1953 to 1957. The line-echo phenomenon is sometimes associated with synoptic frontal systems, but it is also frequently detected in air-mass situations. Therefore, any model devised for the formation and sustenance of squall lines should be independent of, but not preclude, the presence of frontal structures.

Twice-daily upper-air soundings were obtained for the past five years for Green Bay, Wisconsin; Rantoul (later Peoria), Illinois; Columbia, Missouri; and Nashville, Tennessee. Computations of precipitable water content for the layer from the surface to 400 mb

were made with the electronic digital computer at the University of Illinois.

These computations show a sharp increase in the precipitable water content during periods preceding squall-line formation and associated with the area of squall-line initiation. Several flood-producing storms in Illinois during the period 1953 to 1957 were examined for moisture conditions. It was found that pockets of relatively high moisture content existed within large areas of moist air and the pockets were of the same order of magnitude in size as the squall lines observed at a later time.

As an example, the St. Louis storm of 14 June 1957, in which 12-hr amounts exceeding 12 in were recorded, was associated with a precipitable water content of 2.26 in at Columbia, Missouri. Assuming little change of moisture charge with time, this amount would have been advected into the St. Louis area at the beginning of the storm. However, the importance of the 2.26 in is not apparent unless the range of values of precipitable water for June is considered. It has been found from frequency curves of precipitable water amounts, obtained from five years of soundings at Columbia, Missouri, that 2.26 in will occur less than one per cent of the time during June.

Another feature of soundings, to be considered in the production of squall lines and flood-producing storms, is the magnitude of the Showalter stability index. As expected, these storms are associated with negative stability indices. The analysis of the stability index will often indicate relatively unstable air over broad areas, as exemplified by the entire Midwest. It appears, therefore, that another mechanism is necessary before "line" phenomena can occur in a broad area of thermodynamically unstable atmosphere.

The third feature to consider is the hydrodynamics of the atmosphere. Admittedly, one cannot entirely separate the thermodynamics and hydrodynamics of the atmosphere, but in this discussion they are considered independently. From the analysis of severe rainstorms during 1953 to 1957, a relative wind maximum at 850 mb was found to be associated with the squall lines producing heavy rains. The wind maximum has a tendency to produce cyclonic vorticity leading to hydrodynamic instability to the left, following the motion of the stream of air. This vorticity is due to shear alone and may be enhanced by cyclonic curvature of the wind maximum. At the same time, horizontal convergence due to wind speed exists downstream from the wind maximum center. The combination of the instability due to horizontal shear and the vertical impetus provided by the horizontal convergence creates an area favorable for squall-line formation.

Assume now that in a homogeneous air mass over

the Midwest, free of any frontal interruptions, the atmosphere is thermodynamically unstable. However, the degree of instability is not sufficient to produce any organized vertical motion. Widely scattered showers may prevail with local afternoon heating.

A wind maximum is formed in the area and produces cyclonic vorticity to the left and horizontal convergence into the stream flow. These factors add to the slightly unstable situation existing, and, according to the authors' hypothesis, thunderstorms develop in localized places along the line of maximum instability. From this hypothesis it follows that, depending on local conditions, thunderstorms could develop, either simultaneously or at widely separated times, along a line. The motion and persistence of the line is a result of the large-scale motion of the wind maximum, which is dependent on the movement and development of systems in the neighborhood of the 850-mb level.

Unusually severe rainstorms tend to occur most frequently at night. This tendency is logical and strongly supported by observations in Illinois. Convective systems (squall lines or zones) which have developed during the afternoon, aided by diurnal heating, develop frequently into widespread and intense systems by late afternoon or early evening. Thus, when such well-developed systems, laden with moisture, move into a zone of instability, as previously described, unusually heavy rainstorms are likely to occur.

5. Summary

Area-depth frequency relations are being investigated in Illinois for storm periods of 1 to 10 days. It has been found that an excellent fit of the area-depth data is obtained with an equation of the form

$$\log R = K + LA^n$$

by varying the exponent n from 0.3 to 0.6.

An examination of the seasonal distribution of storms indicates that 52 per cent occur during the summer months. Investigation of the geographical distribution of these storms shows that the most frequent area of occurrence is in southeastern Illinois. It was found that the orientation of the major axes of the storms is most frequently from WSW-ENE to WNW-ESE.

Classification of general synoptic types revealed that stationary fronts account for 27 per cent of the most intense storms, although they were associated with only 12 per cent of the total number of storms investigated. A study of the diurnal rainfall distribution indicates a strong trend for maximization of the storm rainfall during the night.

Results presented in this paper are of a preliminary nature. The study will continue since much remains to be accomplished.

REFERENCES

1. Anon.: *Climatological data, Illinois 1914-57*. U. S. Dept. of Comm., Wea. Bur., Washington, D. C.
2. Huff, F. A., R. G. Semonin, S. A. Changnon, and D. M. A. Jones, 1958: *Hydrometeorological analysis of severe rain-*
3. Changnon, S. A., 1958: *Usefulness of supplemental field data in mapping severe rainstorms of short duration*. Trans. of the Ill. Acad. Sci., **51**, 17-23.
4. Horton, R. E., 1924: *Discussion on distribution of intense rainfall*. Trans. Amer. Soc. Civil Eng., **87**, 578-585.
5. Huff, F. A., and J. C. Neill, 1959: *Frequency relations for storm rainfall in Illinois*. Ill. State Water Surv. Bull. 46, Urbana, Ill., 3-5.

PART III: Environmental Engineering

INTRODUCTORY REMARKS

Morley K. Thomas

Meteorological Services of Canada

Traditionally, meteorologists are concerned with theoretical meteorology and weather forecasting, while engineers are responsible for the best practical and economic use of men and material. It has only been in the past decade that these two professions have got together to use applied meteorology in the broad field of practical engineering as it applies to design, construction, and maintenance.

In retrospect, it may seem difficult to understand why the engineering aspects of applied meteorology have been so slow to develop. In the past, the meteorologist has tended to supply average or normal weather data, and the engineer, a practical man who must arrive at answers for all his problems, has incorporated only these values into his design and operational equations. However, in the past two decades the meteorologists have made great progress in opening up the field of applied meteorology through the proper use of climatological analysis. This has been made possible by combining the application of statistical methods with the use of modern data-processing equipment. Miller's paper on area time frequencies for design in which he uses low temperatures in Alaska is a good example of this recent and useful combination.

Although some applied meteorologists might claim that environmental engineering should include all the engineering aspects of applied meteorology, the meteorological applications of structural and hydrologic engineering are becoming important specialized fields in their own right, and papers on these subjects appear in different sections. Perhaps one of the most practical applications of environmental engineering has been the control of enclosed atmospheres, or (as the application is more commonly known) heating, ventilating, and air conditioning. Representing this

application, Murphy's paper on meteorology and heating load requirements contains determinations and discussions of correlation coefficients between heating requirements and various meteorological parameters.

While the application of environmental engineering to enclosed space is fairly well developed, its application in the use of free-atmosphere conditions for the benefit of man is underdeveloped. For example, many northern areas are plagued each year with the problem of accumulating and drifting snow, and there are many papers in the literature concerning snow removal and the prevention of drifting. In contrast, the paper by Gerdel in this section shows how snow-drift-control procedures may be adopted to a constructive, rather than to a simple protective, program.

Failure of meteorologists in the past to provide engineers with sufficient data and information has arisen partially from the lack of certain basic observations. With this in mind, the operational papers in this section are complemented by one on solar radiation. Boyd describes a study made on daylight availability at Ann Arbor, Michigan and correlates the resulting data with theoretical considerations and climatological data.

Applied meteorology is today an underdeveloped but most promising division of meteorology. Through the training of engineers in applied meteorology and of meteorologists in the practical needs of engineering, through coordinated research by both professions in environmental engineering, and through the joint sponsorship of meetings and conferences, those working in the environmental-engineering aspects of applied meteorology will be making a major contribution to our economy and well-being. The papers that follow will present tangible evidence of useful and varied work in progress.

SNOW DRIFTING AND ENGINEERING DESIGN

R. W. Gerdel

Climatic and Environmental Research Branch,
U. S. Army Snow Ice and Permafrost Research Establishment

(Manuscript received 2 January 1960)

ABSTRACT

The results of field experiments and observations on drift snow accumulation in the vicinity of Arctic bases show that it is possible to design buildings and facilities and to lay out bases and depots in Polar regions which will largely control drifting snow. It is possible, also, to make use of drifting snow in the construction of some facilities.

Design criteria for Arctic construction, which will reduce snow drifting to a minimum, include the following:

- (1) elevation of buildings above the ground surface to permit free flow of wind-borne snow beneath the structure,
- (2) orientation of buildings and base layout to minimize coalescence of drifts, and
- (3) elevation of roadways and air strips to provide self clearing of the traffic surface.

Drifting snow may be accumulated by suitable catchment fences and utilized to construct elevated roads, air strips, and hardstands on the Polar Ice Caps, where loss of seasonal precipitation by melting is negligible.

Efforts are being made to develop snow-simulating materials suitable for scale-model tests in a wind tunnel. It appears that there must be a scaled relationship between the physical properties of the simulator and the prototype snow.

1. Introduction

Recent recognition of the strategic importance of the Polar regions has been followed by an expanded construction program for both military and civilian facilities in the Arctic. In the far north, persistently drifting snow imposes a severe handicap on air and ground transportation and creates a major maintenance problem where buildings and supporting facilities must be kept operational. The impediments imposed by drifting snow are particularly severe where design and construction of Arctic facilities have been based upon plans applicable to the temperate zones where heavy snowfall accompanied by drifting of sufficient magnitude to cause a breakdown in transportation and the facilities deemed essential to modern civilization occur only periodically.

On the high Polar Ice Caps, such as those covering Greenland and the Eastern portion of the Canadian Arctic Archipelago, blowing and drifting snow is an almost continuous phenomenon. In the Arctic, where total precipitation may be less than 12 water-equivalent inches in a year, drifts 8 ft high may form when snow-bearing winds meet man-made obstacles. On the high Polar Ice Caps where there is no alleviation by melting, facilities, if not properly designed, are quickly and permanently covered by drifts. Rolled or compacted snow landing strips for aircraft are made hazardous by the rapid development of finger-drifts which are not visible to the pilot. Such drifts may cause the collapse of the wheel carriage on one side of

a landing aircraft, and some ski-equipped aircraft have been wrecked by drifts on prepared snow and ice runways.

Snow-drift-control practices in the temperate zone have been developed primarily to simplify winter maintenance of highways and railroads. Two approaches are commonly used to prevent the development of snow drifts where they may form major obstacles to transportation. One method involves the use of design and construction practices which will reduce the volume of drift accumulation. The other method is based upon the use of temporary or permanent drift catchment devices.

By using sawdust and flake mica to simulate snow in a wind tunnel, Finney [3] established the value of proper elevation, side-slope gradient and orientation of roadways to provide an inherent self-clearing capacity. Rikhter [5] showed that in Russia the top of symmetrically elevated railway embankments and other properly designed elevated structures remained clear of snow in areas where drifting created a serious maintenance problem. Bekker [2] reported on a survey of snow-control practices in Germany and discussed the importance of proper highway design as a means of controlling drift formation. Snow-drift fences and vegetative barriers, the most common forms of drift catchment devices, have been used for many years and in many countries to protect railroads and highways from accumulation of drifting snow. A combination of the two methods has been used by



FIG. 1. Typical Barchan sand dunes of the Southwestern United States. The prevailing wind is from the left, and the steep slope of the dune is on the lee side.

construction of ditches, which not only catch and hold snow, but, by proper design of the ditch bank slope, deflect drifting snow from critical areas.

Pugh and Price [4] have presented an excellent summary of the results of studies on snow-fence design conducted in England, Canada, the United States, Germany, Russia, and the Scandinavian countries.

Those who have studied snow drifting frequently cite the apparent similarity between drifting snow and drifting sand and refer to Bagnold's [1] comprehensive treatment of the problem of drifting sand. Although snow is moved by the wind in suspension, and by saltation as is sand, the similarity may be said to be limited to these basic transportation processes. Sand is affected little by temperatures or load pressures and not at all by metamorphic changes in the grains or alterations in the matrix. Snow, on the other hand, is subject to great morphological changes as the product of small changes in air temperature and by impact and loading pressures. The change in structure, size, and cohesion capacity of the snow grains influences their response to wind forces. A simple example of the difference in response of sand and snow to movement by wind is shown in the great difference between the form of the typical barchan sand dune and the typical sastrugi or skalver of the wind-formed snow surface. The steep face of the sand barchan is on the lee side of the dune, while the windward side has a gentle slope. On the Greenland Ice Cap and in the flat, treeless muskeg area of Northern Canada, the typical sastrugi snow-drift form has the gentle slope on the lee side with the windward side vertical or even undercut (figs. 1 and 2). It is not within the scope of this paper to discuss the thermodynamic and physical



FIG. 2. Sastrugi snow drifts characteristic of the flat muskeg and ice caps of the Arctic. This type of drift is produced by a combination of erosion and deposition of cold dry snow. The prevailing wind is from the left, as in the preceding photograph of Barchans. The Sastrugi, however, have the steep or undercut slope to the windward.

processes which affect the drifting pattern of snow. Regardless of the form of the drift pattern, both sand and very cold dry snow rapidly accumulate around any obstacles in the path of dunes or drifts fed by an unlimited supply of material moved by prevailing winds.

Where information is available on the intensity and direction of prevailing winds, annual precipitation, and seasonal temperature variations, established drift control methods may be utilized for protection and even directly applied to construction practices in the Polar regions.

2. Drift control through design of highways and aircraft runways and hardstands

One of the most frequently quoted sources of information on the adaptation of highway design to control of snow drifting is the Michigan Engineering Experimental Station Bulletin by Finney [3]. He reviewed and summarized the special highway-design features developed by various states in the Snow Belt to combat the snow-drift problem and attempted to evaluate construction practices by wind-tunnel studies of air flow and simulated-snow deposition around model-highway cross sections.

In actual practice, one of the most ideal methods for control of snow drifting appears to be to elevate the highway. The minimum height of the raised grade line must be determined from the local snowfall record. In some areas, snowfall and associated drifts accumu-

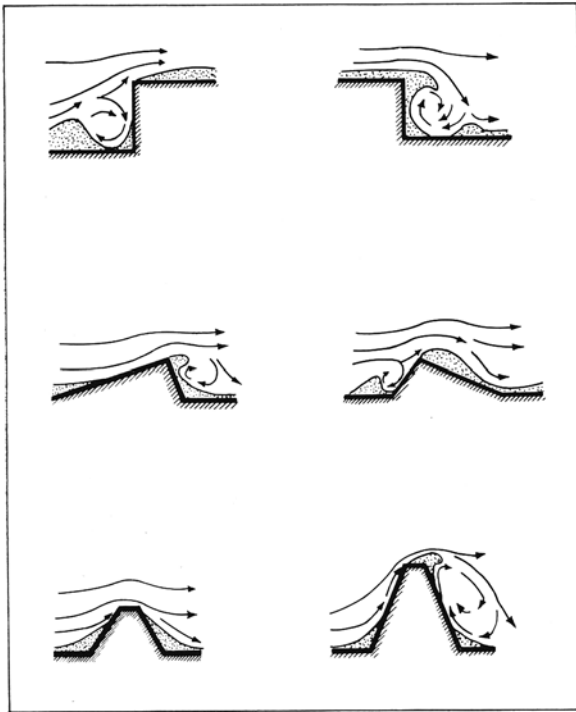
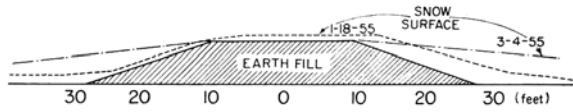


FIG. 3. Accumulation of drifting snow by some typical obstacles. (From Rikhter, 1945.) (a) Accumulation of snow at a sheer wall facing the wind. (b) Accumulation of snow at a sheer wall facing away from the wind. (c) Accumulation of snow around a narrow ridge with gradual windward slope and a steep leeward slope. (d) Accumulation of snow around a narrow ridge with a steep windward slope and a gradual leeward slope. (e) Accumulation of snow around a low ridge of symmetrical slope. (f) Accumulation of snow around a high ridge of symmetrical slope.

late all winter; in other areas, the snow deposited during a single storm may be largely dissipated by warm weather before the next snowfall. The efficient height of grade lines in the Snow Belt may be as little as 18 inches or more than 5 ft. To determine the most effective bank slope, which would reduce drift accumulation to a minimum, Finney tested 1:24 scale-model fill sections in the air stream of a wind tunnel using a mixture of flake mica and balsa-wood sawdust to simulate snow. He concluded that the most effective drift control on a four-foot fill was obtained with a side-slope gradient of 4 to 1.

In his study of the effect of embankment slope on the lee eddy area, he found that the surface boundary of the eddy area coincided with a 6-to-1 slope and that little drifting of simulated snow occurred on the embankment of models constructed with a 6-to-1 bank slope.

Rikhter [5] reported that in the eastern part of European Russia the top of railway embankments between 1 and 2 m high is blown clear of snow and that passenger-car highways elevated a meter or more are relatively free of blocking snow drifts. He does not present information on the most effective embankment slopes, although it may be implied from other portions



of his study on snow drifting that the gradients of both windward and leeward slopes may influence snow accumulation. A series of illustrations of drift accumulations from Rikhter's report is reproduced in fig. 3.

In the undeveloped and sparsely settled Polar regions, overland transportation is limited through most of the year to slow-moving tractors largely because of the enormous maintenance problem required in the almost continuous job of removing drifting snow from the highways which would support fast-moving wheeled vehicles. Over the Polar Ice Caps, tractors must now be used exclusively in all seasons for transportation over unprepared snow and ice surfaces. Aircraft runways at Arctic bases usually constructed with little or no raise of grade are subject to prolonged blocking by snow drifts. In spite of continuous, round-the-clock efforts at removal, drifting snow moved by the persistent Arctic winds even in the late spring and early summer may block highways and air strips for a continuous period of a week or, more at some of the Arctic military bases.

In order to determine the applicability of elevated traffic surfaces to possible improvement in transportation in the Arctic, a short test section of elevated roadway was constructed at the U. S. Army Snow Ice and Permafrost Research Establishment, Keweenaw Field Station, in the late summer of 1954. The fill was constructed normal to the prevailing winter winds in a level field on a portion of the Houghton County Airport, where there were no lee or windward obstructions for several thousand feet. The fill was raised to 6 ft above the adjacent field surface and constructed in three continuous, approximately 20-ft sections. One section was given a 2-to-1 slope, another a 3-to-1 slope, and the third a 4-to-1 slope.

By 7 February 1955, approximately midway through the snow season drift accumulation on both the windward and lee slopes of all three sections had reduced the embankment gradient to 9 to 1 (fig. 4).

Throughout the winter, the 20-ft-wide roadway was passable to wheeled automotive vehicles. The snow accumulation on the road surface was approximately 7 inches in mid winter, most of which blew off in a subsequent storm. During all of the late winter, the road surface was bare while normal snow depth averaged 21 inches on the surrounding level fields and an adjacent non-maintained air strip.

During the summer of 1955, the bank slope of the

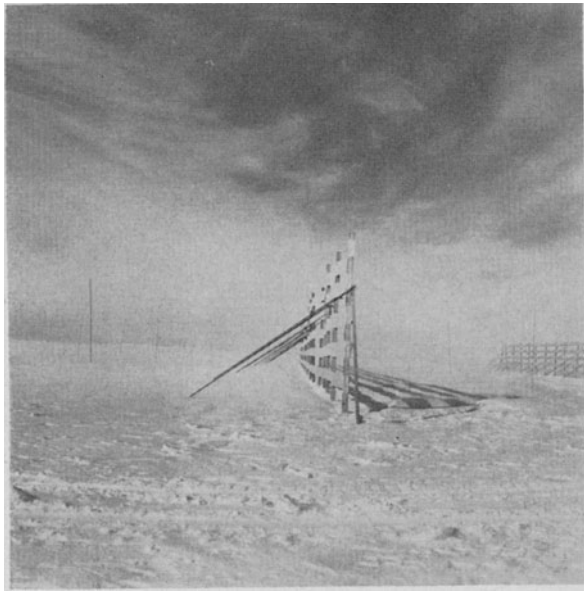


FIG. 5. One of several types of paper-strip drift fences erected on the Greenland Ice Cap. The bamboo poles are marked in feet and inches to facilitate measurement of drift accumulation.

entire 6-ft-high earth fill was converted to a 3-to-1 slope, and a short section of fill three feet high was added. The latter fill was given a 5-to-3 bank slope.

At the end of January 1956, snow accumulation on the windward and the lee slopes of both the 3- and 6-ft fills had converted the embankment gradients to approximately 9 to 1, duplicating the results obtained in the 1955 tests. The roadways were trafficable to wheeled automotive vehicles at the end of the 1956 snow season when the winter's accumulation on adjacent level areas was 27 inches.

In both seasons, there was little change in the embankment slope after the 9-to-1 gradient developed. This gradient which appeared to be optimum for the climatic conditions at the test site developed when about one half of the seasonal snow had fallen. Subsequent snowfall was blown over the 9-to-1 slopes and off the road surface of the 6-ft fill, apparently being deposited uniformly at a considerable distance downwind of the test road. There was a sufficient deposit of snow on the windward edge of the 3-ft fill in mid-January to impede two-way movement of wheeled traffic, indicating that, in an area where two to three feet of snow may be expected in a winter, a fill more than 3 ft high would be required to assure self clearing of the roadway.

The results of the U. S. Army Snow Ice and Permafrost Research Establishment studies indicate that it may be possible to construct elevated roadways for year-round use by wheeled vehicles, aircraft runways and hardstands in the Arctic and that even in areas of perpetual snow cover and persistent drifting such elevated surfaces may be self clearing if the important

meteorological parameters are taken into consideration in the development of design criteria.

3. Drift control by design and layout of structures

Drifts accumulate to the lee and windward of objects which interfere with the free flow of snow-laden winds. The drifts on the lee side of low obstructions, such as large crates, oil drums, vehicles, and small buildings, may extend horizontally more than ten times the height of the obstacle. The length of the lee drift is proportionally less for high structures than for small, low obstacles. High buildings which extend well above the zone of blowing snow tend to deflect the moving snow to the sides, creating a different lee-drift pattern than that produced by low obstructions over which the snow may be blown. The orientation of structures, with respect to the direction of the prevailing snow-bearing wind, determines the shape and volume of the accumulated drift.

When the air temperature is above -10°C , conditions are favorable for regelation or adhesion of snow particles, and an overhanging snow cornice may develop at the top of the lee wall of a structure. Roof area and wall configuration determine the size and shape of the snow cornice which may grow large enough to cause collapse of the structure.

The most rapid growth of snow drifts usually occurs to the lee and windward of narrow obstacles oriented normal to the prevailing wind; however, a drift will extend farther downwind of a narrow structure oriented with the wind than leeward of a similar structure erected broadside to the prevailing wind.

The results of studies by U. S. Army Snow Ice and Permafrost Research Establishment at the Keweenaw Field Station near Houghton, Michigan and at the Ice Cap research site in Northern Greenland indicate that the idealized accumulation patterns presented by Rikhter [5] may be subject to considerable modification where drifting is associated with strong persistent winds, very low temperatures, and an unlimited supply of fine-grained snow.

Drifting snow is not deposited beneath objects supported above the surface. The wind appears to be accelerated as it moves beneath an elevated structure carrying the burden of the suspended snow a considerable distance downwind before it is deposited.

The Swedish slat snow fence described by Pugh and Price [4] is designed to take advantage of the potential wind acceleration between the surface and an elevated object. It is constructed of horizontal wood slats so spaced that when the snow accumulates to the top level of one slat there is a horizontal opening between the new surface and the next higher slat. More recently, foot-wide strips of a special treated paper have been used for the construction of temporary

drift-control fences. The paper strips are usually attached to posts with alternate one-foot horizontal openings (fig. 5), through which the accelerated wind spreads the lee drift over a large area, increasing the operational life of the drift-control barrier.

At its Greenland research site, U. S. Army Snow Ice and Permafrost Research Establishment has studied the effect of a solid barrier erected in contact with the snow surface and a paper-strip fence on drift accumulation. Both structures were 5 ft high and were erected normal to the prevailing wind. As shown in fig. 6, the solid barrier was completely inundated by drift snow 26 days after erection. The paper-strip fence which had an initial clearance of one foot between the lowest horizontal strip and the original snow surface still had an average clearance of almost one foot below the bottom strip at the end of the same 26-day period. The drifts to the windward and lee of the paper-strip fence contained as much snow as was accumulated around and over the solid barrier. Subsequent periods of drifting snow tended to fill up the trench which developed between the lee and windward drifts, but the open spaces between the strips effectively controlled the drift pattern for several months.

Roots and Swithinbank [6] describe the experience of the Norwegian-British-Swedish Antarctic Expedition of 1949-1952. From their studies of the layout of Maudheim, the expedition's headquarters in the Antarctic, they have made some specific recommendations applicable to the construction and operation of an Arctic base. The following is a condensation of some of their suggestions.

- a. Objects may be kept entirely free of snow by supporting them above the surface so the wind, accelerated beneath the object, will carry the suspended snow away and deposit it to the leeward.
- b. The ground plan should provide for all objects being placed with their long axis normal to the wind. The length of an object, which must be placed parallel to the wind, should be kept as short as possible.
- c. The upper surface of objects should be as smooth as possible and, if necessary, a false, flat, smooth roof should be erected above stacks of oil drums, crates, and other irregular-shaped containers.
- d. Where numerous separate structures and storage facilities must be distributed at random, spacing should be not less than 30 times the height of the objects in order to avoid coalescence of drifts.
- e. Where possible, objects should be placed along a line normal to the prevailing wind to avoid overlap of the lee drifts from one object and the windward drift of another object.

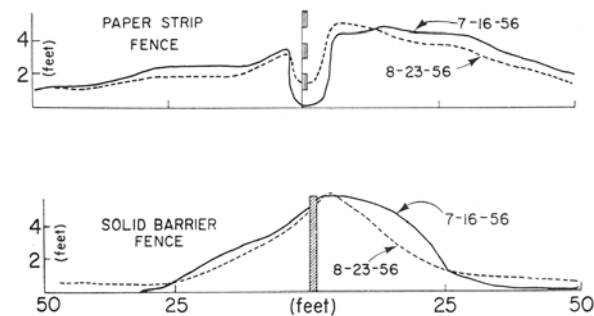


FIG. 6. Snow accumulation at paper-strip and solid-barrier drift fences, Greenland 1956.

- f. If it is desired to have objects deliberately buried beneath the snow, they should be placed in a compact group to insure rapid coalescence of drifts and subsequent complete coverage by normal accumulation of snow.

It appears that Roots and Swithinbank were among the first to recognize that the art of living in Polar regions and enjoying more of the amenities of civilization and less of the rigors of continuous snow shoveling requires deliberate planning to control and make use of the drifting snow rather than fighting it.

To the recommendations made by these authors should be added the requirements that, in areas where no melting occurs and where the surface is continuously raised by the annual accumulation of snow, provisions should be made for increasing the elevation of the structures to maintain an effective space beneath the buildings.

4. Utilization of drift-accumulation procedures for construction of roads and airstrips on permanent snow fields

The construction of an elevated road or airstrip on the permanent Polar Ice Cap would require the mechanical movement of enormous volumes of snow to produce the desired elevation of the trafficable surface. Since the surface and much of the subgrade must be compacted to a density of 0.6 or higher to attain the necessary supporting capacity, a volume of snow must be moved equal to about twice the size of the finished road or runway. The possibility of utilizing drift fences to deliberately accumulate a large volume of snow in a pattern that would permit processing with only limited equipment into a runway suitable for the landing of wheeled heavy aircraft on the Greenland Ice Cap was an outgrowth of some of the U. S. Army Snow Ice and Permafrost Research Establishment's early research on snow drifting and control methods. The need for a raised fill for construction of a runway is based not only upon the self-clearing capacity of the elevated surface but also upon the fact that, where the normal snow surface is processed and compacted to

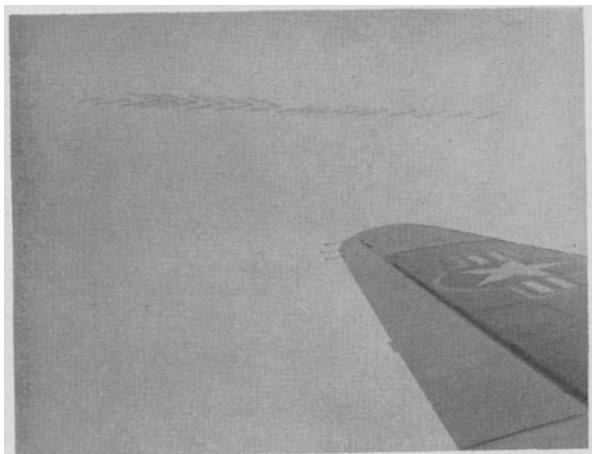


FIG. 7. Air photo of experimental drift fences designed to accumulate snow for an elevated aircraft landing strip on the Greenland Ice Cap.

a suitable bearing capacity, it is depressed below the surrounding area and is rapidly covered by new drift snow which requires additional processing. This second processed surface is soon buried beneath the normal seasonal snowfall which, in turn, must be processed to suitable bearing capacity.

Weather records from an installation maintained by the U. S. Air Force on the North Greenland Ice Cap from the Fall of 1953 through the Spring of 1957 provided information on the direction of prevailing winds and of snow-drifting storm winds. Although prevailing winds at this site some 200 mi east of Thule and at an elevation of 6800 ft are predominantly from the southeast, dictating the construction of a runway with a northwest-southeast axis, storm winds with blowing snow are predominantly from the south. By using this information and the experience gained from 2 yr of research on snow drifting by U. S. Army Snow Ice and Permafrost Research Establishment at the Ice Cap site, a pattern of drift-accumulation fences was erected

during the summer of 1957. It was hoped that these fences would produce a continuous drift about 2000 ft long, 200 ft wide, and with a surface 4 to 5 ft above the normal seasonal surface.

The first nine fences were 200-ft-long sections constructed with one-foot-wide paper strips spaced at one-foot intervals to provide a total height of 10 ft (fig. 5).

These fences were erected with their long axis in an E-W direction, normal to the direction of snow-bearing storm winds. They were staggered so the center line passing through all of the fences was oriented SE to NW, parallel to the direction of the prevailing winds. The second group of fences consisted of two, 200-ft sections, erected at right angles to each other and joined at the windward corner. The latter group of 6 fences was included in the plans to determine whether sufficient additional drift snow could be accumulated by interception of snow borne by both storm winds and prevailing winds to justify the more expensive and complicated construction. The pattern of the drift-catchment fences as completed on 8 August 1957 is shown in the aerial photograph, fig. 7.

The right-angle fences created a peculiar turbulence pattern that destroyed most of the paper strips shortly after erection and before any appreciable amount of snow was caught. The pattern of drift snow accumulated by the first 9 fences was measured on 21 May 1958, and a contour map was plotted. As shown in fig. 8, a fairly uniform drift 1,000 ft long and from two to more than 5 ft above the surrounding surface was accumulated between 8 August 1957 and 21 May 1958. During that period, precipitation amounted to 26 inches of snow of 0.33 mean density (8.58 water-equivalent inches) as measured at 4 accumulation stakes near the research site. The contour lines in fig. 8 were plotted to show the elevation above the 21 May 1958 surface.

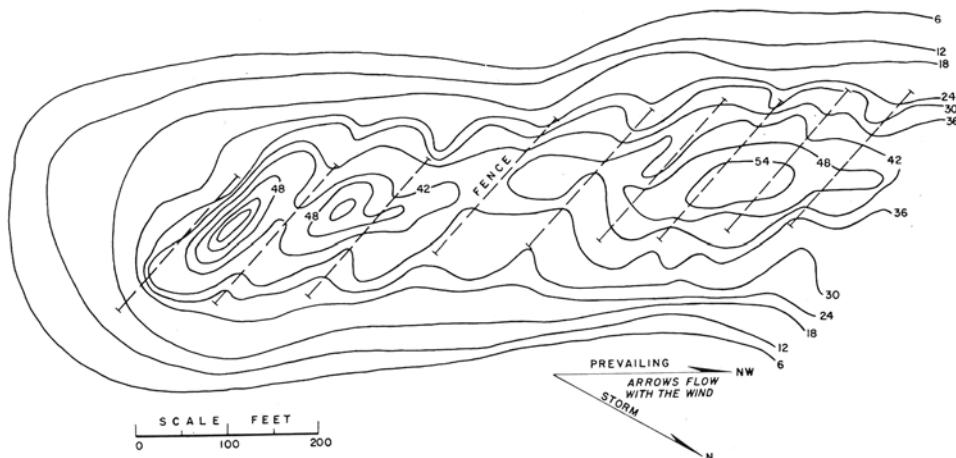


FIG. 8. Accumulation pattern developed between 8 August 1957 and 21 May 1958 by drift-fence installation on the Greenland Ice Cap. Dashed lines show position of fences.

The two top paper strips were destroyed some time during the winter, but all lower strips up to 6 ft above the 1957 surface appeared to be intact at the time of measurement. In two previous years, drift fences up to 6 ft high had survived the winter at the Ice Cap research site with no damage. It is not known whether a severe storm alone was the cause of destruction of the top paper strips on the 1957 fence or whether a ten-foot-drift fence is too high to survive normal winter storms at that site.

Initial plans took into consideration the possibility of removing the paper fence and the supporting posts and braces to permit leveling, processing, and compaction of the elevated snow surface. As discussed previously, the paper fences tested in prior years on the Greenland Ice Cap were not submerged by snow until the lee and windward drifts accumulated approximately to the height of the fence as shown in fig. 9. It would be possible to remove the fence and supports at the proper time and allow the remaining trough to fill prior to processing a trafficable surface on the elevated embankment.

The pattern of snow accumulated by the drift fences eliminates one of the major criticisms to an elevated aircraft runway. The bank gradients as developed in this experiment were on the order of 50 to 1, which would eliminate possible major damage to aircraft running off the side of the runway. Such gradients would be most uneconomical to produce with bulldozers, drag lines, or other standard road-building equipment, even if available.

The very satisfactory results obtained from this experiment in controlling and converting drifting snow to practical use justifies consideration of fence designs leading to a more simple procedure for installation and removal of the catchment barriers. The use of light-weight metal fences about 4 ft high and in 6-ft lengths would permit ready removal from the natural trough and re-erection on the crest of the lee drift to produce an optimum accumulation pattern. During the year or more that one elevated runway would remain reasonably clear of drift snow, the portable fence sections could be used to accumulate the necessary fill for another runway.

5. Discussion

Construction of facilities and the art of living in Polar regions may be simplified by making use of existing knowledge of the mechanics of drifting snow. Unfortunately, most of the available information is based upon empiricisms derived from brief experiences under limited conditions and upon the results of local field experiments which may not be applicable to other areas. The inability to maintain control over field experiments on drifting snow and the large number of

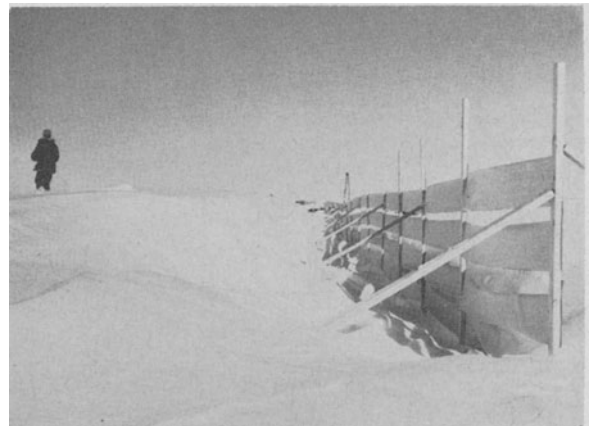


FIG. 9. A trough persists on each side of the paper-strip drift fence until lee and windward accumulations are as high as the fence.

variables, which may influence the results, prevents a rigorous study of the phenomenon and the development of specific design criteria from field studies.

Information leading to improved design of structures for drift control is needed to establish the following:

1. the optimum clearance between buildings and the ground surface,
2. optimum dimensions, width, length, and height of pile-supported structures,
3. maximum permissible obstructions in the form of piles, braces, and service conduits beneath an elevated building,
4. pitch and orientation of slope of roof with respect to prevailing and storm winds,
5. maximum width of elevated roads and aircraft runways which will insure optimum operational time,
6. influence of orientation with respect to prevailing winds on the self-clearing capacity of elevated trafficable surfaces,
7. radius and bank slopes for curves in roadways,
8. optimum spacing for drift-accumulating snow fences,
9. optimum density and optimum width and spacing of barrier material for snow fences,
10. optimum clearance between a snow fence and the ground or snow surface, and
11. relative value of vertical and horizontal barrier strips for snow fences.

Acquisition of such information demands a high degree of control of the environment, experimental structure design, and even of the snow itself. Previous efforts to attain this control by model studies in a wind tunnel failed to take into consideration the relationship between the physical properties of natural snow and the material used to simulate snow. Scale models

tested in a wind tunnel may be so small that they project entirely into the stream of moving simulated snow, whereas, in the field, the prototype would have most of its elevation above the layer of moving snow. The elastic properties of the simulating materials have been ignored; consequently, the relationship between the frequency and amplitude of the particles moving in saltation and the dimensions of the scale model being tested may be unrealistic. Little attention has been given to the relative threshold velocity of natural snow and the simulating materials.

As a means of acquiring the information essential to development of improved design criteria, U. S. Army Snow Ice and Permafrost Research Establishment has entered into a research contract with New York University to undertake wind-tunnel studies on the mechanics of drifting snow. During the first year of this contract, major emphasis has been devoted to the study of the characteristics of materials which may be used to simulate snow within the limits of the modeling capacity of the several tunnels available at the University.

The investigators have proceeded on the assumption that, in order to test scale-model structures with simulated snow in a small wind tunnel, the geometry of the paths of motion in relation to particle size must be the same for the simulating material and the prototype (snow). Preliminary studies indicate that a material suitable for use with one-twentyfifth-size scale models in a small wind tunnel may have to have a density several times that of a snow grain. They are developing methods for relating the simulating material to the prototype by measuring the comparative fall velocities of the model material and the actual snow grains by use of high-speed photographs of particles falling in a drop chamber. It is hoped that

the wind-tunnel studies will lead to the development of a scale-model blowing-snow environment which will permit rapid testing and development of design interior for use in the Polar regions.

Acknowledgments. Free use has been made of material contained in several project reports and a thesis submitted to the University of Washington in partial fulfillment of requirements for the Master Science degree by Mr. R. G. Baughman, who was project leader of the snow-drift studies conducted by U. S. Army Snow Ice and Permafrost Research Establishment at the Keweenaw Field Station and on the Greenland Ice Cap.

The several internal project reports and the thesis prepared by Mr. Baughman are in the process of being consolidated into a comprehensive report which will be published in the U. S. Army Snow Ice and Permafrost Research Establishment technical report series.

REFERENCES

1. Bagnold, R. A., 1941: *The physics of blown sand and desert dunes*. London, Methuen & Co. Ltd., 265 pp.
2. Bekker, M. G., 1951: *Snow studies in Germany*. Ottawa, Natl. Res. Council of Canada, Assoc. Comm. on soil and snow Mechanics, Tech. Memo. No. 20, 83 pp.
3. Finney, E. A., 1939: *Snow drift control by highway design*. East Lansing, Mich., Mich. Eng. Exper. Sta., Vol. 15, No. 2, Bull. No. 86, 56 pp.
4. Pugh, H. L. D., and W. I. J. Price, 1954: Snow drifting and the use of snow fences. *Polar record*, 7, 4-23.
5. Rikhter, G. D., 1945: *Snow cover, its formation and properties* (*Snezhnyi pokrov, ego formirovanie i svoistva*). Moskow-Leningrad, Izdatel' stvo AKADEMIIA NAUK SSSR. [Translated by William Mandel (1950) rev. ed., Translation 6, Snow Ice and Permafrost Research Establishment, Corps of Eng., U. S. Army, 66 pp.]
6. Roots, E. F., and C. W. M. Swithinbank, 1955: Snow drifts around buildings and stores. *Polar record*, 7, 380-387.

ENGINEERING METEOROLOGY: METEOROLOGY AND HEATING LOAD REQUIREMENTS^{1,2,3}

Allan H. Murphy

University of Michigan⁴

ABSTRACT

Temperature and other meteorological parameters, including wind velocity and solar radiation, have been examined to determine their individual and combined effects on fuel requirements. Regression methods established a correlation coefficient of 0.89 between standard degree-days and gas consumption for 147 days during the 1951-52 heating season. A temperature-refined and wind-adjusted degree-day yielded a correlation coefficient of 0.94, a material improvement in estimating the heating load.

1. Introduction

The economic importance to the public utilities of an accurate specification of the heating load received strong emphasis in several papers presented at the Hartford meetings a year ago (American Meteorological Society, 1957). The point most stressed was that, to operate with maximum efficiency, the utilities must maintain a delicate balance between consumer demands, production, and inventory. To maintain this balance, a quantitative expression must be developed relating the amount of heat supplied to a house and the meteorological parameters affecting heat losses and gains.

2. Physical relationships

The heat supplied to a house may be lost in either of two ways: (1) transmission losses through the confining surfaces, and (2) infiltration losses through cracks and openings. The temperature of the outside air, or more specifically the temperature difference between the ambient and conditioned air, plays an important role in both the transmission and infiltration heat losses. The amount of heat transferred through the confining surfaces is proportional to the inside-outside temperature difference, while infiltration losses can result from the pressure gradient established by the density (temperature) difference between the ambient and conditioned air. The force of the wind

on building surfaces can also establish a pressure differential which in turn causes infiltration into the building through openings in the windward surfaces.

The physical relationships between other meteorological parameters and the heating load are not as easily discerned. However, a sunny day would be expected to have a smaller heating load than a cloudy day with the same temperature and wind conditions. Although precipitation has been suggested as another variable to be considered, the fact that very little is known qualitatively or quantitatively about its effect suggests that it is of secondary importance.

3. Degree-day history

A quantitative relationship between the ambient air temperature and the heating load was first established by the American Gas Association in 1927. The AGA determined that the fuel consumption varied directly as the difference between 65°F and the mean ambient temperature. The value 65°F, which is roughly the equivalent of a daytime temperature of 75°F and a nighttime temperature of 55°F, was found to be the temperature above which heat was not required to maintain daytime temperatures of 68°F to 72°F within a house. Each degree that the average temperature falls below 65°F represents one "degree-day." This degree-day was a function of temperature alone with the mean ambient temperature being calculated from an average of the maximum and minimum.

More-recent studies have treated other parameters, such as wind and sunshine (Lacy, 1951; and Gold and Lacy, 1952). However, load-estimating curves often neglect these refinements—assuming, in effect, average wind and sky conditions.

In this paper, a quantitative estimate of the relative importance of temperature, wind, and solar radiation refinements of the degree-day will be given.

¹ Based on a thesis submitted in partial fulfillment of the requirements for the degree of Bachelor of Science in Meteorology at the Massachusetts Institute of Technology.

² Presented on 10 September 1958 at the Second National Conference on Applied Meteorology: Engineering, at Ann Arbor, Michigan.

³ Paper No. 6 on Topics in Applied Meteorology from the Meteorological Laboratory, University of Michigan, Ann Arbor, Michigan.

⁴ Present affiliation: Weather System Division, Research Department, The Travelers Insurance Company, Hartford, Connecticut.

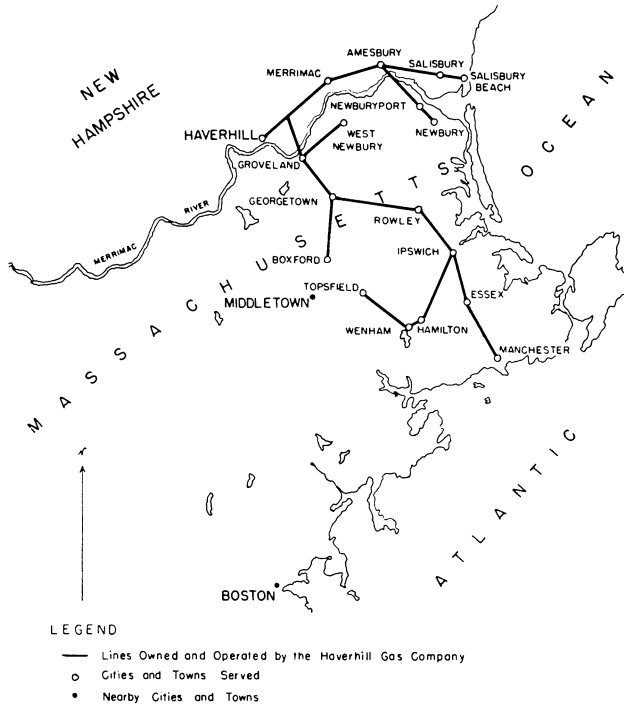


FIG. 1. — Lines owned and operated by the Haverhill Gas Company. ○ Cities and towns served. ● Nearby cities and towns.

4. Data

The heating-load data utilized in this study were obtained from the Haverhill Gas Company, Haverhill, Massachusetts. The Haverhill Gas Company serves a region consisting of seventeen communities in extreme northeastern Massachusetts (see fig. 1). The data consist of daily gas sendouts for 147 days during the 1951–52 heating season. The sendouts were read at 0730 each day and recorded in cubic feet.

Temperature (daily maximum and minimum only) and precipitation data from cooperative stations in the region were utilized, as well as hourly temperatures, wind speeds, and cloud data from Boston, Massachusetts and solar radiation data from Blue Hill Observatory, Milton, Massachusetts.

5. Statistical technique

The linear-regression technique was used to express the dependency of the heating load on the various meteorological parameters. A relationship of the form

$$\hat{Y} = a_0 + a_1 x_1 + a_2 x_2 + \dots + a_n x_n$$

was assumed, where \hat{Y} is the predicted heating load (dependent variable), x_1, x_2, \dots, x_n are the meteorological parameters (independent variables), and $a_0, a_1, a_2, \dots, a_n$ are the regression coefficients. Prior to its inclusion as a predictor, the values of each parameter in question were plotted *versus* the actual gas load as

a scatter diagram to determine if the relationship could be considered linear. Based on this somewhat insensitive but very simple test, linearity appeared to be a reasonable assumption for each predictor.

The appropriate values of the coefficients $a_0, a_1, a_2, \dots, a_n$, and correlation coefficients for each relationship tested were obtained from a least-squares solution by the Crout method (Crout, 1941).

6. Analysis and results

The gas data were first subjected to a t-test and then an F-test to determine if the means and variances, respectively, of the days of the week were comparable. The tests indicated that the means and variances of the individual days of the week were not significantly different at the one-per-cent level. As a result of these tests, all the data could be pooled together during the subsequent analysis.

Temperature. The first relationship examined was that between fuel consumption and Haverhill degree-days, DD_{HAV} (see table legend for definition). As previously noted, the gas sendouts were logged at 0730 each morning and the value recorded as the sendout for the previous day. Thus, to represent the temperature during the period covered by the sendout, Haverhill degree-days were computed by taking the average of the maximum temperature on the day of the sendout and of the minimum on the following morning. The least-squares solution yielded a correlation coefficient of 0.89 (see table 1, item 1).

Although the correlation coefficient gives a measure of the association of two variables, the square of the correlation coefficient, sometimes called the per cent reduction (or coefficient of determination), is a more meaningful term for this study. The per cent reduction expresses the percentage of the variance in the dependent variable (heating load) which is explained by the independent variable(s) (Haverhill degree-days in this case). The per cent reduction in this instance is 79 (see table 1, item 1).

As indicated by the map of northeastern Massachusetts (see fig. 1), Haverhill lies on the northwest edge of the territory served by the Haverhill Gas Company. Therefore, in order to utilize temperatures from a station whose location was more representative of the region served, a parameter DD_{MID} (see table legend) for Middletown, Massachusetts (see fig. 1) was calculated and correlated with the heating load. The correlation coefficient obtained was 0.90, and the per cent reduction was 81 (see table 1, item 2).

As noted previously, Boston is the closest station to the region in question which takes hourly and synoptic meteorological observations. Thus, to examine the possibility of obtaining an improved prediction using more than two temperatures, Boston data were

utilized. As a basis for comparison, the parameter DD_{BOS} (see table legend), computed as was DD_{HAV} , was correlated with the heating load. The correlation coefficient obtained was 0.89, and the per cent reduction was 79 (see table 1, item 3), not significantly different than the results obtained with similar variables for Haverhill and Middletown.

A degree-day parameter, $DD_{BOS}(5)$ (see table legend), determined by averaging the temperatures of the synoptic observations (0700, 1300, 1900, 0100, and 0700 local time) yielded a correlation coefficient of 0.92 and a per cent reduction of 84.5 when correlated with fuel consumption (see table 1, item 4). Then, hourly temperatures were used to compute another modified degree-day parameter ($DD_{BOS}(24)$, see table legend), which gave a correlation of 0.925 and a per cent reduction of 85.5.

Thus, it is evident that an improved specification of the heating load is possible by utilizing more than two temperature observations during the sendout period.

Wind. The mean wind speed for each sendout period, V_{BOS} (see table legend), was determined by averaging the speeds for the five synoptic observations just as was done with the Boston temperatures above.

When wind speed alone is plotted against the actual fuel consumption, there is some scatter; in general, however, as wind speed increases, fuel consumption increases. A correlation coefficient of 0.41 was obtained when wind speed and heating load were correlated (see table 1, item 6). Wind speed was then considered as the second independent variable and was added to the regression analysis.

The multiple correlation between \hat{Y} , the fuel consumption predicted from the equation

$$\hat{Y} = a_0 + a_1 DD_{MID} + a_2 V_{BOS},$$

and Y , the actual fuel consumption, yielded a correlation coefficient of 0.94 and a percent reduction of 88 (see table 1, item 11). This represents an increase of 7 in the per cent reduction over that obtained with the single predictor, DD_{MID} . Similar increases in the per cent reduction were noted when the wind factor was added to the other degree-day variables (see table 1, items 10, 12, 13, and 14).

Thus, it is readily evident that the inclusion of the wind factor has materially reduced the unexplained variance even in the situation where 85 per cent of the variance was explained by a modified degree-day alone (see table 1, items 5 and 14).

Solar radiation. Two variables which give a measure of the amount of sunshine were examined. When scatter diagrams of each were plotted against the heating load, considerable scatter was noted indicating weak relationships at best.

TABLE 1

Item	Independent variable(s)	Sample size N	Correlation coefficient r	Per cent reduction PR
1	DD_{HAV}	147	0.89	79
2	DD_{MID}	147	0.90	81
3	DD_{BOS}	147	0.89	79
4	$DD_{BOS}(5)$	147	0.92	84.5
5	$DD_{BOS}(24)$	147	0.925	85.5
6	V_{BOS}	147	0.41	17
7	C_{BOS}	147	-0.31	9.5
8	$I_{BL HLS}$	147	-0.29	8
9	P_{MID}	147	-0.04	0
10	$DD_{HAV} + V_{BOS}$	147	0.92	85
11	$DD_{MID} + V_{BOS}$	147	0.94	88
12	$DD_{BOS} + V_{BOS}$	147	0.92	85
13	$DD_{BOS}(5) + V_{BOS}$	147	0.945	89
14	$DD_{BOS}(24) + V_{BOS}$	147	0.95	90
15	$DD_{MID} + V_{BOS} + I_{BL HLS}$	147	0.94	88
16	$DD_{BOS}(5) + V_{BOS} + I_{BL HLS}$	147	0.945	89
17	$DD_{BOS}(5) + V_{BOS} + C_{BOS}$	147	0.95	90

Location subscripts:

HAV —Haverhill

BOS —Boston

MID —Middletown

BL HLS—Blue Hill Observatory

Key to independent variables:

DD_{HAV} —Haverhill degree-days, computed by using a mean temperature obtained by averaging the maximum and minimum on consecutive days (due to the time of gas sendout). For example, Sunday's average temperature would be obtained by averaging Sunday's maximum and Monday morning's minimum.

DD_{MID} —Middletown degree-days, computed as was DD_{HAV} .

DD_{BOS} —Boston degree-days, computed as was DD_{HAV} .

$DD_{BOS}(5)$ —Boston degree-days, computed by using a mean temperature obtained by averaging the temperatures of the synoptic observations, 0700, 1300, 1900, 0100, and 0700 local time.

$DD_{BOS}(24)$ —Boston degree-days, computed by using a mean temperature obtained by averaging the hourly temperatures, 0800 to 0700, inclusive.

V_{BOS} —Boston mean wind speed, computed by averaging the speeds at the synoptic observations, 0700, 1300, 1900, 0100, and 0700 local time.

C_{BOS} —Boston mean sunrise-to-sunset cloudiness.

$I_{BL HLS}$ —Total daily solar radiation received at Blue Hill Observatory, modified to take into account the variation of surface conductance with wind speed.

P_{MID} —Middletown daily precipitation amount.

A correlation between the sunrise-to-sunset cloudiness at Boston and the fuel consumption yielded a -0.31 correlation coefficient (see table 1, item 7). Although a low correlation, it indicates a tendency for the fuel consumption to increase as the cloudiness decreases, the opposite of the anticipated relationship. This correlation probably results from the association of clear and cold and of cloudy and mild weather in the region at that time of the year.

The second sunshine parameter investigated was the solar radiation measurements taken at Blue Hill Observatory. When this variable was correlated with

the heating load, a correlation coefficient of -0.29 resulted. Although the sign of the correlation coefficient indicates that an increase in solar radiation corresponds to a decrease in the heating load, it appears to contradict the result obtained with the cloudiness parameter above. Evidently, the tendency for maximum radiation to occur with partly cloudy skies is an important factor here.

In any case, neither of these measures of sunshine materially reduced the unexplained variance when added to the regression equation as a third independent variable (see table 1, items 15, 16, and 17). Furthermore, it is doubtful if either can be considered to be independent of temperature, a feature which should be realized if they are to add significantly to the regression analysis.

Precipitation. Correlations of both precipitation amounts and occurrence or non-occurrence of precipitation with heating load yielded correlation coefficients less than 0.05. For this reason, a precipitation parameter was not included in the multiple-regression analysis.

7. Conclusions

The results indicate that up to 90 per cent of the variance of the heating load can be explained with a temperature-refined and wind-adjusted degree-day. Each of the two refinements added materially to the improved specification. This is in general agreement with the emphasis placed upon "wind chill" in several investigations (Court, 1948, and Stone, 1943). Re-

duction of the error between estimated and actual fuel consumption is of obvious economic consequence to the space-heating industry.

Acknowledgments. The author wishes to express his appreciation to Dr. Thomas F. Malone, Director of Research, The Travelers Insurance Company, under whose guidance the original thesis work was completed, and to Mr. Harold W. Baynton of the Systems Division, Bendix Aviation Corporation for helpful suggestions pertaining to the content of this paper.

REFERENCES

1. American Gas Association, 1928: *House heating, 2nd ed., Industrial Gas Series*. New York, American Gas Assoc.
2. American Meteorological Society, 1957: *Weather problems in business and industry II, Proceedings of the first national conference on applied meteorology*. Hartford, Conn., Amer. Meteor. Soc., B1-B36.
3. Bryan, J., 1952: *Course notes, applied statistical methods*. Cambridge, Mass., Mass. Inst. Tech.
4. Court, A., 1948: Wind chill. *Bull. Amer. meteor. Soc.*, **29**, 487-493.
5. Crout, P. D., 1941: A short method for evaluating determinants and solving systems of linear equations with real or complex coefficients. *Trans. Amer. Inst. elect. Eng.*, **60**, 1235-1241.
6. Gold, E., and R. E. Lacy, 1952: Heating requirements of a house. *Meteor. Mag.*, **81** (960), 185-186.
7. Lacy, R. E., 1951: Variations of the winter means of temperature, wind speed and sunshine, and their effect on the heating requirements of a house. *Meteor. Mag.*, **80** (948), 161-165.
8. Stone, R. G., 1943: The practical evaluation and interpretation of the cooling power in bioclimatology. *Bull. Amer. meteor. Soc.*, **24**, 295-305 and 327-339.

STUDIES ON DAYLIGHT AVAILABILITY

R. A. Boyd

The University of Michigan

ABSTRACT

To utilize solar energy advantageously for the lighting and heating of buildings, additional data are required on the availability of daylight and solar heat for variously oriented surfaces and for numerous geographical locations. This study presents data on daylight availability at Ann Arbor, Michigan for the period March 1953 to March 1954 and correlates these data with theoretical considerations and climatological data as recorded by the U. S. Weather Bureau.

1. Introduction

Only meager data are available on the variability of exterior daylight intensities. References on this subject are widely scattered [1; 2; 3; 5; 6] and only a few of these [3; 5; 6] are available as illumination literature. To afford additional data in this direction, a study was undertaken on the availability of daylight at Ann Arbor, Michigan for a period to include all seasons, these findings then correlated with theoretical considerations and climatological data as recorded by the U. S. Weather Bureau. Measurements recorded are for the period March 1953 to March 1954.

2. Recording equipment

All measurements were made with a group of five photocells (fig. 1) mounted on the roof of the Daylighting Laboratory at The University of Michigan so that an unobstructed view of the sky could be obtained, the cells facing north, south, east, west, and toward the zenith. The supporting shield, painted flat black, reduced the light reflected from the "ground" to a minimum of approximately four per cent.

The photoelectric cells were model 856, as supplied by the Weston Electrical Instrument Corporation [4]. Each cell was equipped with a Viscor filter to provide it with the same spectral sensitivity as the human eye, and it was placed in a water-tight case. A metallic film filter and depolished flashed opal disc were sealed in place over the face of each cell.

A multipoint Speedomax Recorder, with appropriate shunts, was used for the recording. Each of the five circuits was provided with five shunts so that the Recorder response could be varied as the photocell response varied. The values of the shunts and the density of the metallic film filter for each cell were selected so that the Recorder response was directly proportioned to the illumination incident on the cell.

The photocell case and the opal disc were so de-

signed that the unit obeyed the cosine law of illumination. The maximum error of this corrected unit for undirectional illumination is four per cent, and that occurs for an angle of incidence of 80 deg. For measuring the illumination due to a uniform hemispherical source, such as a sky having a uniform brightness, this photocell has an error of less than one per cent.

The photocells were initially calibrated and periodically checked with 1000- and 5000-w incandescent lamps of known candlepower. For the higher intensities, corresponding to direct sunlight conditions, the photocells and metallic film filters were calibrated separately and then combined to avoid errors due to lack of application of the inverse-square law.

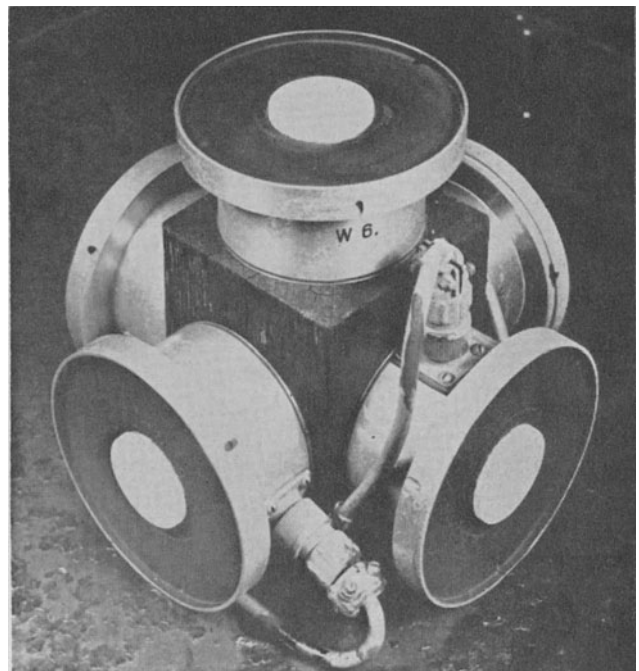


FIG. 1. Photocell arrangement (photograph).

3. Data recorded

Data were collected with weatherproof cells during most of the working days from 1 March 1953 to 1 March 1954 regardless of exterior weather conditions. The number of days in each month for which data are available are:

Month	Number of days
March 1953	18
April 1953	20
May 1953	19
June 1953	22
July 1953	22
August 1953	20
September 1953	19
October 1953	17
November 1953	20
December 1953	21
January 1954	19
February 1954	21
	238

4. Tabulation of data

Since the recorder provided approximately one intensity reading per photocell each minute, more data were collected on the recorder charts than could reasonably be analyzed for this study. Consequently, it was decided that foot-candle readings for each photocell would be selected on a 15-min-interval basis, from 8 am to 5 pm each day. Such a tabulation gave the intensity of daylight, in footcandles, every 15 min, on north, south, east, and west vertical surfaces and on a horizontal surface.

One aim of this study was to correlate the recorded intensities with the degree of cloudiness and percentage of possible sunshine as specified by the U. S. Weather Bureau. The nearest weather station to Ann Arbor is at Willow Run, which records the degree of cloudiness but not the percentage of possible sunshine. The U. S. Weather Bureau indicates the degree of cloudiness as tenths of the entire sky, 0 to 3 tenths being clear, 4 to

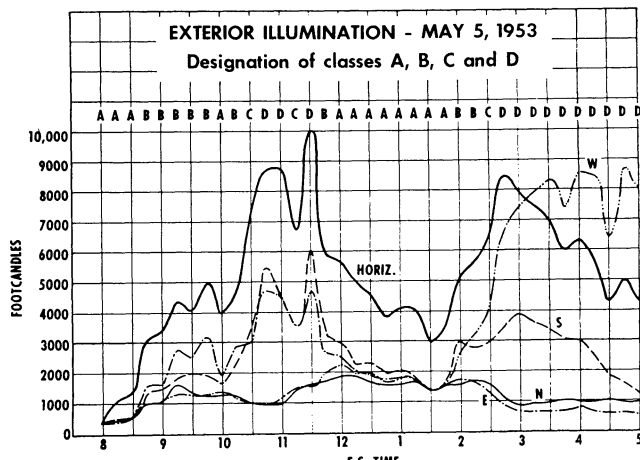


FIG. 2. Exterior illumination—5 May 1953. Designation of Classes A, B, C, and D.

7 tenths partly cloudy, and 8 to 10 tenths cloudy. These data were obtained for the entire year from the Weather Bureau Station at Willow Run.

An overcast sky is one for which the cloud formation is so dense that all vertical surfaces are equally illuminated. As the cloud density decreases, the sky brightness becomes non-uniform, and consequently the variation in vertical-surface illumination with orientation of the surface becomes greater.

In an attempt to obtain some correlation between the measured intensities and the degree of cloudiness, the readings were classified on the basis of the ratio of maximum-to-minimum vertical-surface illumination. The classes are as follows:

Class	Ratio $\frac{\text{max}}{\text{min}}$
A	1.0 to 1.5
B	1.5 to 2.5
C	2.5 to 3.5
D	>3.5

TABLE 1. Record of cloudiness.
8:00 am to 5:00 pm—March 1953 through February 1954

Month	Per cent of all days			Per cent of measured days			Sky cover		Per cent of readings			
	Cloudy	Partly cloudy	Clear	Cloudy	Partly cloudy	Clear	All days	Measured days	Class A	Class B	Class C	Class D
March	84	10	6	88	6	6	8.6	8.7	47	16	9	28
April	74	13	13	70	10	20	7.6	7.2	34	13	5	48
May	58	29	13	68	26	6	7.2	7.9	40	17	7	36
June	40	43	17	41	36	23	6.2	5.9	17	13	10	60
July	29	42	29	32	41	27	5.5	5.5	20	13	10	57
August	23	26	51	20	20	60	4.2	3.8	7	7	5	81
Sept.	20	37	43	16	42	42	4.3	4.2	10	10	4	76
Oct.	23	23	54	24	12	64	4.0	3.8	17	4	2	77
Nov.	53	17	30	55	15	30	6.3	6.3	37	11	6	46
Dec.	64	23	13	52	29	19	7.5	6.8	37	10	8	45
Jan.	74	16	10	84	5	11	8.2	8.7	70	6	4	20
Feb.	61	14	25	57	19	24	7.1	7.0	50	8	2	40
Avg	50	25	25	50	22	28	6.4	6.3	32	11	6	51

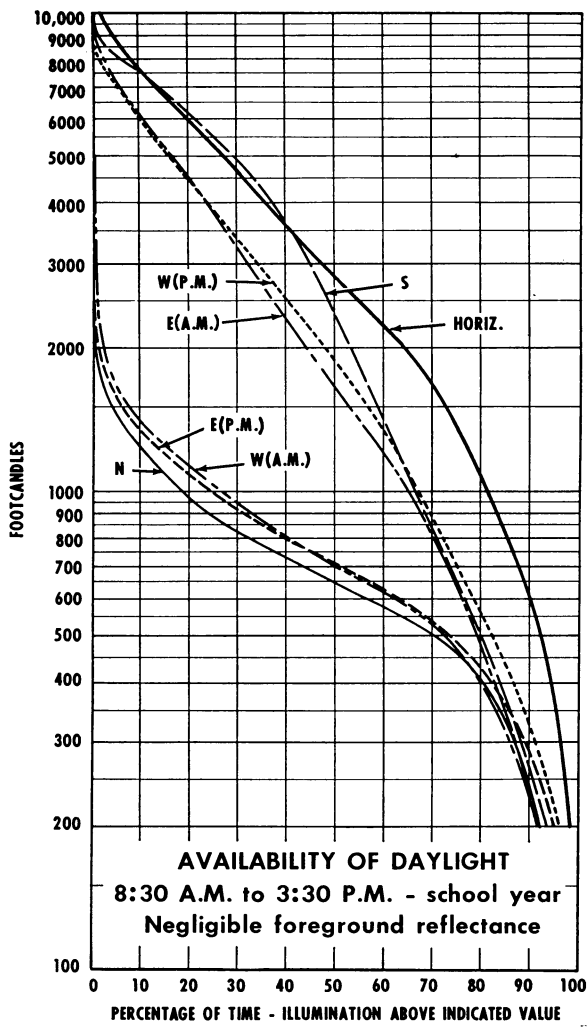


FIG. 3. Availability of daylight. 8:30 am to 3:30 pm—school year.
Negligible foreground reflectance.

The 5th of May 1953 was one of the days during which all four of these conditions existed. Fig. 2 shows the variation of the illumination on the four vertical surfaces and on the horizontal surface, with the readings marked according to the above classification. The readings were plotted as recorded; no attempt was made to account for light reflected to the vertical surfaces from a particular foreground.

Every reading, for the entire year, on the 15-min-interval basis, was classified in this manner. Table 1 shows a comparison, for each month, of the following:

1. Percentage of all days, designated as cloudy, partly cloudy, and clear by the U. S. Weather Bureau.
2. Percentage of all days for which recordings were made, designated as cloudy, partly cloudy, and clear by the U. S. Weather Bureau.
3. Sky cover, in tenths, for the entire month.
4. Sky cover, in tenths, for the days for which recordings were made.
5. Percentage of the total number of readings, 8 am to 5 pm, designated as being in classes A, B, C, and D.

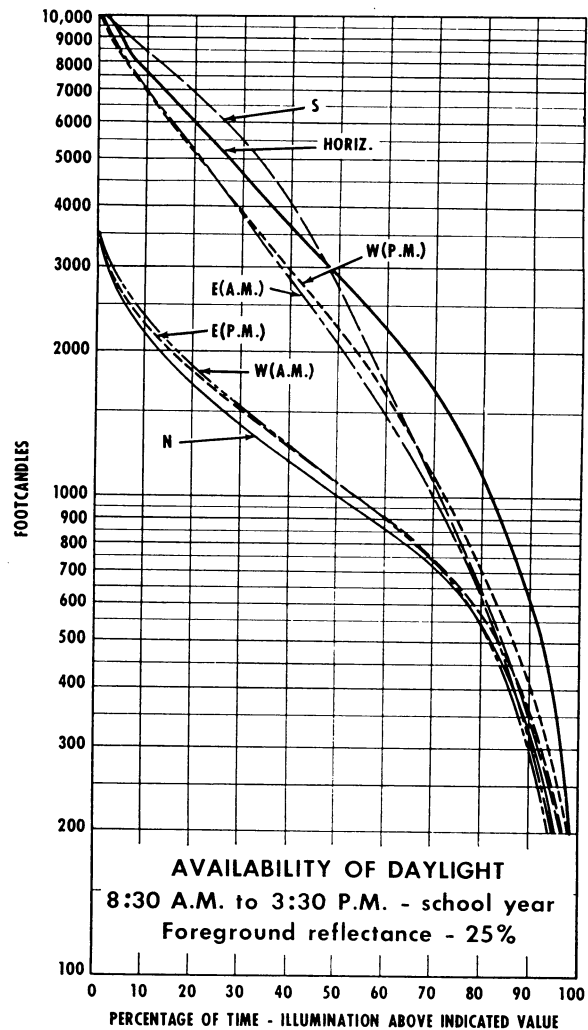


FIG. 4. Availability of daylight. 8:30 am to 3:30 pm—school year.
Foreground reflectance—25%.

This table indicates that the distribution of cloudy, partly cloudy, and clear days for the recorded periods is just about the same as for the entire year. The table also indicates that the days designated as cloudy by the U. S. Weather Bureau are not all overcast days. On the average, it takes the sum of Class A, Class B, and Class C conditions to equal approximately the percentage of days designated as cloudy.

To obtain maximum information from these data, they have been tabulated in several different ways. Each tabulation will be presented and explained in the following sections.

In the consideration of the increase in vertical-surface illuminations due to light reflected from a foreground, it has been assumed that (1) the quantities measured included a negligible amount due to ground reflection because of the black shield, and (2) for a foreground with a reflectance of 25 per cent, the increase in north, south, east, and west vertical-surface illuminations would equal 12.5 per cent of the horizontal-surface illumination.

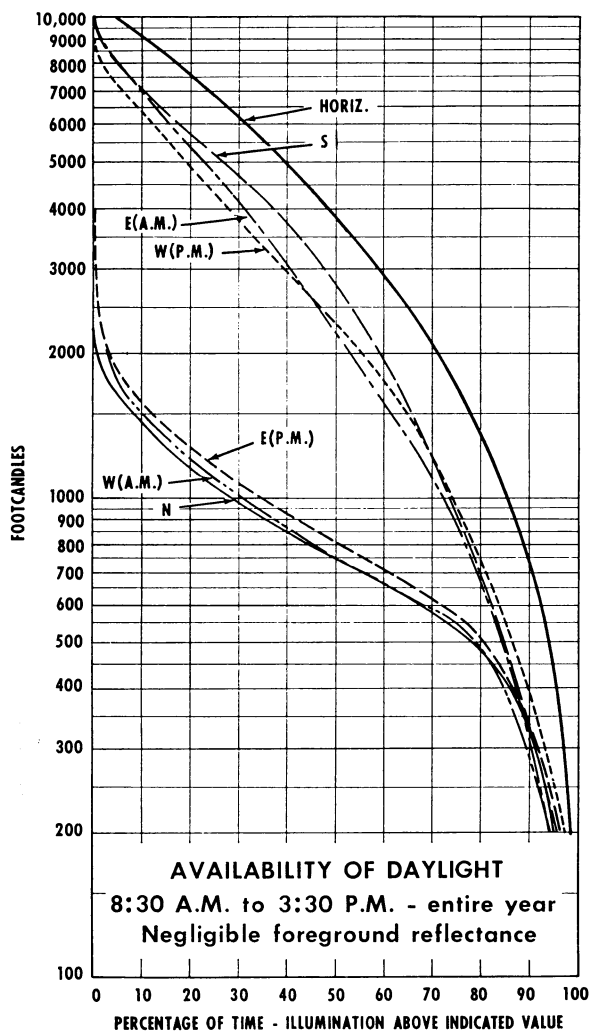


FIG. 5. Availability of daylight. 8:30 am to 3:30 pm—entire year.
Negligible foreground reflectance.

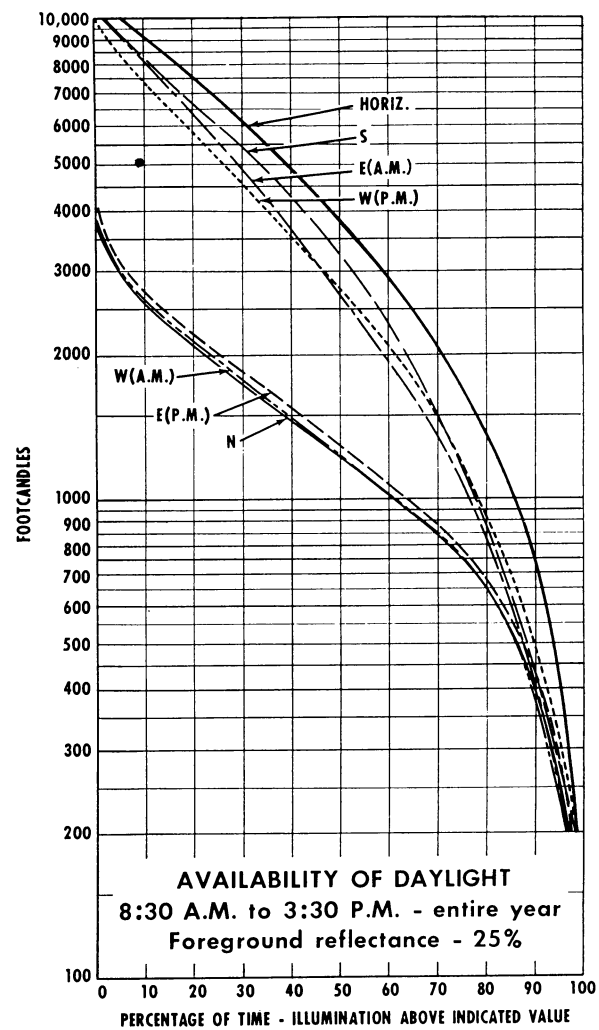


FIG. 6. Availability of daylight. 8:30 am to 3:30 pm—entire year.
Foreground reflectance—25%.

Time-intensity graphs. In the daylighting of schools, offices, small factories, shopping centers, and the like, it is of interest to know what percentage of the time of occupancy the exterior illumination of a particular surface is above a specific value. Such a presentation has been made for the periods 8:30 am to 3:30 pm for the *entire year*, for the *school year* (September through May), and for 8 am to 5 pm for the *entire year*. In plotting these data, the morning and afternoon values for east and west exposures have been kept separate. These data are presented in figs. 3 to 8 as follows:

Fig.	Coverage	Foreground reflectance
3	8:30 am to 3:30 pm—School year	Negligible
4	8:30 am to 3:30 pm—School year	25%
5	8:30 am to 3:30 pm—Entire year	Negligible
6	8:30 am to 3:30 pm—Entire year	25%
7	8:00 am to 5:00 pm—Entire year	Negligible
8	8:00 am to 5:00 pm—Entire year	25%

Average illumination. The average illuminations for classifications A, B, C, and D, for the period 8:30 am

to 3:30 pm were calculated for each month. These averages for each exposure, with and without consideration of ground-reflected light, are presented in table 2. This table also shows the average illumination for each exposure for the sum of Classes A, B, and C and for the sum of Classes A, B, C, and D; the averages are weighted on the basis of percentages of time involved.

The average illuminations for all conditions for the period 8:00 am to 5:00 pm are given in table 3, again with and without consideration of ground-reflected light.

Overcast and cloudy sky conditions. Overcast and cloudy sky conditions are of particular interest because it is generally considered that for these periods exterior illumination is inadequate for daylighting purposes. This opinion is prevalent in connection with the daylighting of schools. Table 4 shows the average external illuminations for each month for the school period 8:30 am to 3:30 pm for the overcast and cloudy sky

TABLE 2. Average illumination in footcandles.
Classes A, B, C, and D—8:30 am to 3:30 pm

	Class	Number of $\frac{1}{4}$ hr	Per cent of time	Horizontal	Foreground reflectance—Neg				Foreground reflectance—25%			
					North	South	East	West	North	South	East	West
January 1954	A	374	68	720	340	380	350	370	430	470	440	460
	B	37	7	1560	570	1190	720	900	770	1390	920	1100
	C	23	4	2750	730	1960	1190	940	1070	2300	1530	1280
	D	112	21	2740	730	4810	2000	1400	1070	5150	2340	1740
	Average Classes A, B, C			900	380	530	420	440	490	640	540	560
	Average Classes A, B, C, D			1300	450	1430	755	645	610	1590	920	810
	A	284	50	1140	550	610	550	590	690	750	690	730
	B	44	8	2600	860	1970	1330	1170	1180	2300	1650	1490
February 1954	C	12	2	2340	790	2230	1510	1160	1080	1520	1800	1450
	D	229	40	3370	580	5260	2340	1490	1000	5680	2760	1910
	Average Classes A, B, C			1390	600	830	690	670	770	1000	860	840
	Average Classes A, B, C, D			2180	590	2600	1350	1000	860	2870	1620	1270
March 1953	A	223	50	2200	890	1000	930	940	1170	1280	1200	1210
	B	15	3	3020	1040	1700	1320	1420	1420	2080	1700	1800
	C	52	12	4080	1110	3250	1940	1850	1620	3760	2450	2360
	D	158	35	5720	840	5330	3730	2010	1550	6040	4440	2720
	Average Classes A, B, C			2580	930	1450	1140	1130	1260	1770	1460	1450
April 1953	Average Classes A, B, C, D			3680	900	2810	2050	1440	1360	3270	2510	1900
	A	196	33	2590	990	1110	1030	1100	1310	1430	1350	1420
	B	91	16	4110	1230	2220	1670	1720	1740	2730	2180	2230
	C	28	5	5330	1240	3070	2220	2020	1910	3740	2890	2690
May 1953	D	272	46	6790	910	4520	3060	2830	1760	5370	3910	3680
	Average Classes A, B, C			3310	1080	1610	1330	1370	1490	2020	1740	1780
	Average Classes A, B, C, D			4910	1000	2950	2130	2040	1610	3660	2740	2650
June 1953	A	230	41	2740	1050	1170	1130	1150	1390	1510	1470	1490
	B	81	15	4270	1500	2160	1730	1740	2030	2690	2260	2270
	C	42	7	5500	1510	3060	2070	2430	2200	3750	2760	3120
	D	205	37	7870	1190	4220	2590	3350	2170	5200	3570	4330
	Average Classes A, B, C			3400	1210	1620	1380	1430	1630	2040	1800	1850
July 1953	Average Classes A, B, C, D			5050	1200	2580	1830	2140	1830	2210	2460	2770
	A	104	17	3260	1230	1540	1390	1320	1640	1950	1800	1730
	B	97	16	4770	1290	2270	1750	1750	1890	2870	2350	2350
August 1953	C	74	12	7570	1490	3580	2430	2500	2440	4530	3380	3450
	D	340	55	8450	1160	3920	3630	2910	2220	4980	4690	3970
	Average Classes A, B, C			4950	1320	2310	1800	1800	1940	2930	2420	2420
	Average Classes A, B, C, D			6880	1230	3200	2810	2410	2090	4060	3670	3270
September 1953	A	140	23	3240	1080	1490	1260	1330	1470	1880	1650	1720
	B	86	14	4610	1340	2290	1890	1830	1920	2870	2470	2410
	C	66	11	7540	1310	3510	2310	2390	2250	4450	3250	3330
	D	321	52	7930	1150	3270	3740	3060	2140	4460	4730	4050
	Average Classes A, B, C			4580	1210	2190	1680	1730	1780	2760	2250	2300
October 1953	Average Classes A, B, C, D			6320	1180	2850	2750	2420	1970	3640	3540	3210
	A	38	7	2910	1190	1440	1050	1320	1550	1800	1410	1680
	B	38	7	3500	1180	1980	1410	1470	1620	2420	1850	1910
August 1953	C	28	5	5250	1080	2610	1650	2340	1740	3270	2310	3000
	D	468	81	7650	1000	4610	3890	2430	1950	5560	4840	3380
	Average Classes A, B, C			3740	1160	1900	1320	1630	1630	2370	1790	2100
September 1953	Average Classes A, B, C, D			6910	1030	4100	3400	2280	1890	4960	4260	3140
	A	52	10	2480	970	1280	1140	1050	1280	1590	1450	1360
	B	59	11	2670	920	1620	1050	1400	1250	1950	1380	1730
October 1953	C	29	6	3810	990	2490	1390	1890	1470	2970	1870	2370
	D	377	73	6650	790	5680	3530	2540	1620	6510	4360	3370
	Average Classes A, B, C			2780	970	1700	1150	1370	1320	2050	1500	1720
	Average Classes A, B, C, D			5610	840	4610	2890	2220	1540	5310	3590	2920
October 1953	A	81	17	1200	510	570	560	560	660	720	710	710
	B	22	5	2000	720	1360	970	1220	970	1610	1220	1470
	C	9	2	2930	870	2500	1250	1730	1240	2870	1620	2100
	D	368	76	5210	650	6350	2980	2810	1300	7000	3630	3460
	Average Classes A, B, C			1500	610	920	730	810	800	1110	920	1000
October 1953	Average Classes A, B, C, D			4320	640	5050	2440	2330	1180	5590	2980	2870

TABLE 2 (*Continued*)

Class	Number of 1 hr	Per cent of time	Horizontal	Foreground reflectance—Neg				Foreground reflectance—25%				
				North	South	East	West	North	South	East	West	
November 1953	A	205	37	1130	510	640	550	600	650	780	690	740
	B	50	9	2040	740	1630	1140	1000	990	1880	1390	1250
	C	28	5	2470	720	2410	1460	920	1030	2720	1770	1230
	D	265	49	3080	560	5190	2360	1570	950	5580	2750	1960
	Average Classes A, B, C			1430	580	990	750	710	760	1170	930	890
December 1953	Average Classes A, B, C, D			2240	570	3050	1540	1130	850	3330	1820	1410
	A	211	39	820	370	470	420	440	470	570	520	540
	B	55	10	1590	600	1300	800	940	800	1500	1000	1140
	C	40	7	1980	660	1900	1030	1140	910	2150	1280	1390
	D	239	44	2350	510	4290	1660	1350	800	4580	1950	1640
Average Classes A, B, C				1100	460	790	570	620	600	930	710	760
	Average Classes A, B, C, D			1650	480	2330	1050	940	690	2540	1260	1150

TABLE 3. Average illumination in footcandles.
8:00 am to 5:00 pm

Month	Horizontal	Foreground reflectance—Neg				Foreground reflectance—25%			
		North	South	East	West	North	South	East	West
Jan. 1954	1140	420	1420	630	680	560	1560	770	820
Feb. 1954	2120	530	2640	1130	1300	790	2900	1390	1560
March 1953	3450	840	2530	1660	1680	1270	2960	2090	2110
April 1953	4560	860	2650	1900	2150	1430	3220	2470	2720
May 1953	4920	1110	2140	1850	2050	1720	2750	2460	2660
June 1953	6180	1120	2800	2750	2580	1890	3570	3520	3350
July 1953	6190	1130	2680	2770	2690	1900	3450	3540	3460
August 1953	6400	980	3750	3150	2710	1780	4550	3950	3510
Sept. 1953	5050	760	4260	2770	2660	1390	4890	3400	3290
Oct. 1953	3900	570	4660	2050	2510	1060	5150	2540	3000
Nov. 1953	2020	475	2720	1150	1230	730	2970	1400	1480
Dec. 1953	1470	420	2170	870	910	600	2350	1050	1090
Avg	3950	770	2870	1890	1930	1260	3360	2380	2420

TABLE 4. Average illumination.
Overcast and cloudy sky conditions—8:30 am to 3:30 pm

Month	Class A			Classes A + B + C			Class A H.S.I./V.S.I.	Classes A + B + C Neg grd
	Avg V.S.I.		Avg H.S.I.	Avg V.S.I.		Avg H.S.I.		
	Neg grd (FtC)	25% grd (FtC)	(FtC)	Neg grd (FtC)	25% grd (FtC)	(FtC)		
Jan. 1954	360	450	720	440	550	900	2.00	2.04
Feb. 1954	580	720	1140	700	870	1390	1.97	1.99
March 1953	940	1220	2200	1160	1480	2580	2.34	2.22
April 1953	1060	1380	2590	1350	1760	3310	2.44	2.45
May 1953	1130	1470	2740	1410	1830	3400	2.42	2.41
June 1953	1370	1780	3260	1810	2430	4950	2.38	2.73
July 1953	1290	1680	3140	1700	2270	4580	2.43	2.69
August 1953	1250	1610	2910	1500	1970	3740	2.33	2.49
Sept. 1953	1110	1420	2480	1300	1650	2780	2.24	2.14
Oct. 1953	550	700	1200	770	960	1500	2.18	1.95
Nov. 1953	580	720	1130	760	940	1430	1.95	1.88
Dec. 1953	430	530	820	610	750	1100	1.91	1.80
Average entire year	890	1140	2030	1130	1460	2640	2.22	2.23
Average school year	750	960	1670	940	1200	2040		

V.S.I.—Vertical-surface illumination.

H.S.I.—Horizontal-surface illumination.

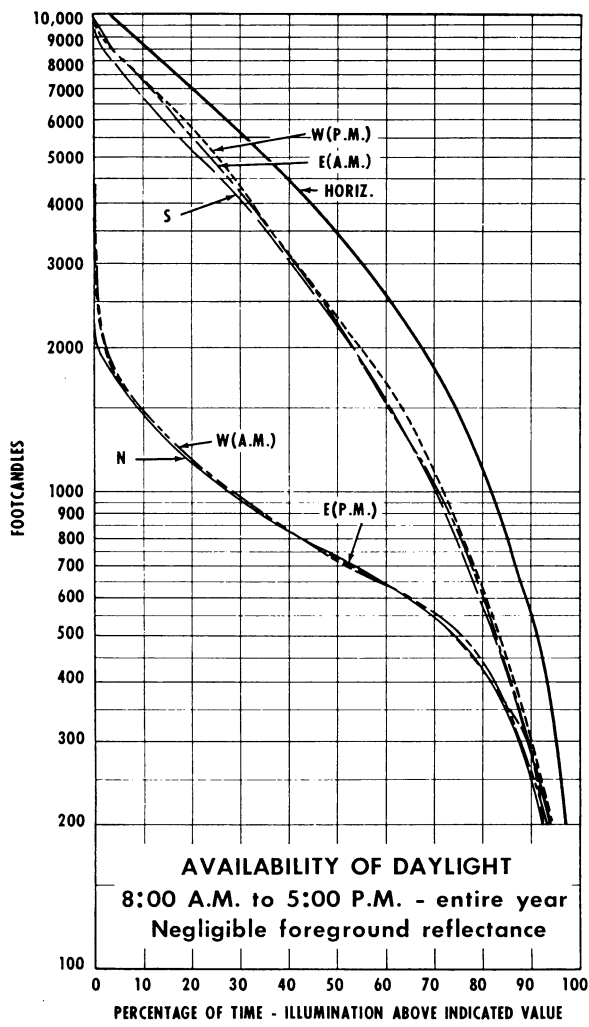


FIG. 7. Availability of daylight. 8:00 am to 5:00 pm—entire year.
Negligible foreground reflectance.

conditions. Overcast sky conditions are represented by Class A, and cloudy sky conditions by Classes A, B, and C. The vertical-surface illumination is given as the average of the values for north, south, east, and west exposures.

Table 4 also gives the ratio of horizontal-surface illumination to vertical-surface illumination for each month.

Sun and clear sky conditions. It is also of interest to consider the variation in exterior illumination for a cloudless day. One day each month was selected as being the best from this point of view, and the data were plotted. Four of these graphs are presented as follows:

Fig. 9, 20 March, 1953

Fig. 10, 23 June, 1953

Fig. 11, 28 September, 1953

Fig. 12, 16 December, 1953

These data were plotted without consideration of additional ground-reflected light.

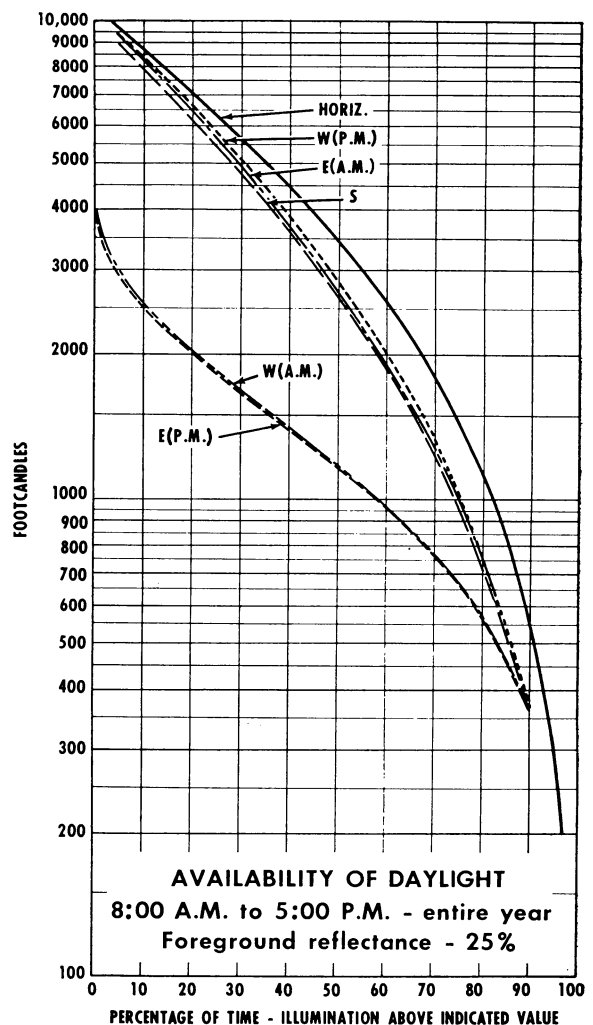


FIG. 8. Availability of daylight. 8:00 am to 5:00 pm—entire year.
Foreground reflectance—25%.

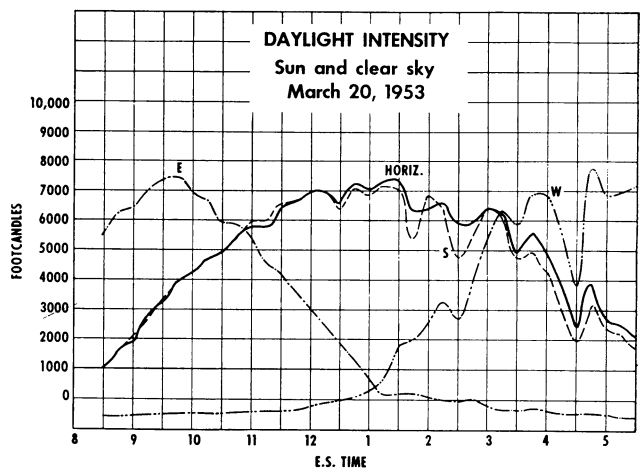


FIG. 9. Daylight intensity. Sun and clear sky. 20 March 1953.

As an indication of the total luminous energy that is incident directly on the specific surface during the period of one day, between the hours given, the area

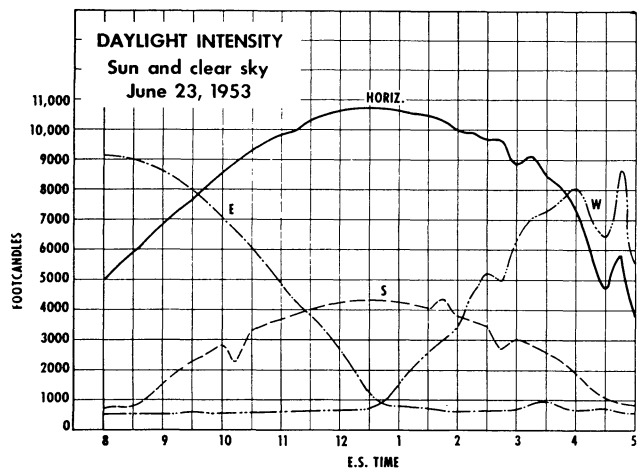


FIG. 10. Daylight intensity. Sun and clear sky. 23 June 1953.

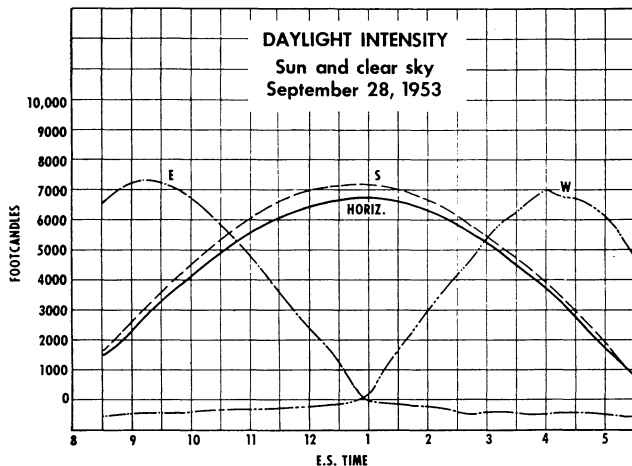


FIG. 11. Daylight intensity. Sun and clear sky. 28 September 1953.

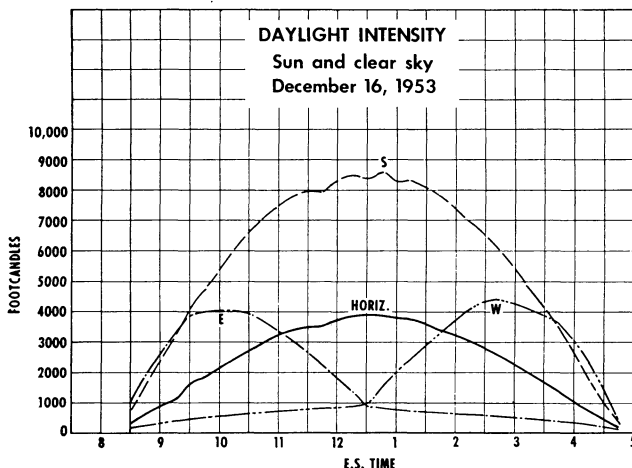


FIG. 12. Daylight intensity. Sun and clear sky. 16 December 1953.

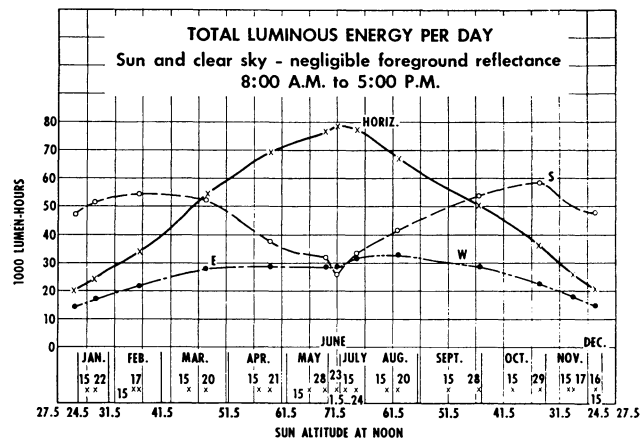


FIG. 13. Total luminous energy per day. Sun and clear sky—negligible foreground reflectance. 8:00 am to 5:00 pm.

AVERAGE NUMBER HOURS PER DAY - 8:00 A.M. to 5:00 P.M.
Illumination above 1000 and 2000 FTC.

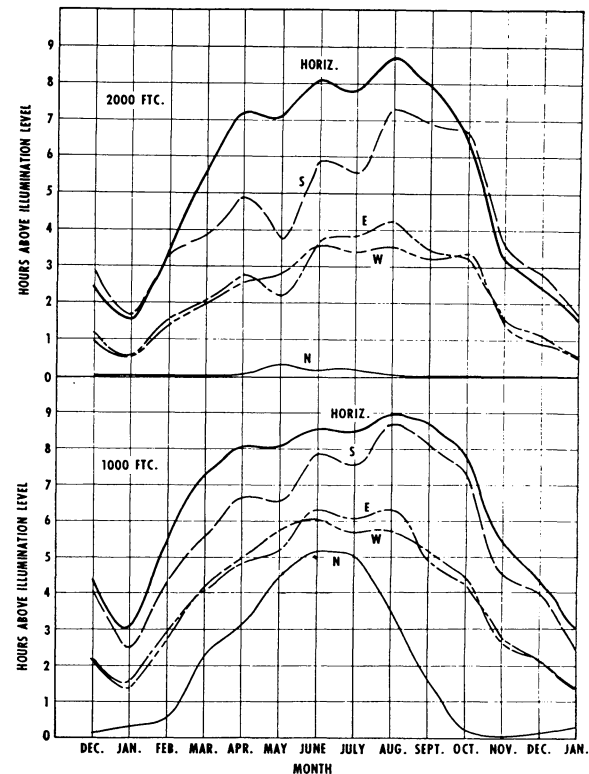


FIG. 14. Average number hours per day—8:00 am to 5:00 pm.
Illumination above 1000 and 2000 FtC.

under each of these curves was measured, and the results, in 1000 lumen-hours, are listed in table 5. In fig. 13, these same values of total luminous energy are plotted against noon-sun altitude for the day of measurement; the altitude scale is divided into two parts to separate the values for the two halves of the

TABLE 5. Total luminous energy.
1000 lumen-hours
Sun and clear sky—8:00 am to 5:00 pm

Date	South	East	West	Horizontal
22 Jan 1954	51.6	16.1	18.1	24.2
17 Feb. 1954	54.5	20.1	22.7	34.2
20 March 1953	52.1	30.4	27.5	54.3
21 April 1953	37.6	27.8	29.4	69.3
28 May 1953	31.8	33.0	24.5	76.5
23 June 1953	25.9	31.2	25.0	78.5
24 July 1953	33.2	34.7	29.7	77.7
20 August 1953	41.3	32.6	32.6	66.8
28 Sept. 1953	53.7	28.2	28.5	50.8
29 Oct. 1953	58.1	20.4	24.9	35.7
17 Nov. 1953	49.7	17.0	17.8	25.2
16 Dec. 1953	47.5	14.2	15.6	20.5

year. For convenience, the altitude scale is also divided into months with specific dates designated. The continuous curves are drawn to give some indication of the total luminous energy, 8:00 am to 5:00 pm, for any clear day of the year.

Exterior daylight intensities of 1000 and 2000 foot-candles. In a paper [6] on the availability of daylight at Port Allegany, Pennsylvania, data were presented showing the number of hours per day, between 8:00 am and 5:00 pm, that the illumination of particular surfaces was above 1000 and 2000 footcandles for each month. To allow direct comparison of these data with the data for Ann Arbor, a similar analysis has been made of the Ann Arbor data; the results are presented in fig. 14.

5. Discussion of results

Some previous papers [7] on the availability of daylight and solar radiation have attempted to relate the average intensity for cloudy days to the average intensity for cloudless days through the percentage of possible sunshine. In the absence of percentage of possible sunshine figures for Ann Arbor, approximate values have been obtained by averaging the available figures for East Lansing and Detroit. By utilizing these figures, an attempt will be made to relate cloudy day conditions to those for cloudless days.

From fig. 13, it is possible to determine the average illumination, I_0 , for each month, 8:00 am to 5:00 pm for each exposure, assuming that all days are cloudless or reasonably so. Then the average illuminations shown in tables 2 and 3 can be related to these to obtain the ratios listed in table 6, where R_1 is the ratio of the average illumination for strictly overcast sky conditions (Class A) to I_0 , R_2 is the ratio of the average illumination for cloudy sky conditions (Classes A, B, and C) to I_0 , and R_3 is the ratio of the average illuminations for all conditions to I_0 .

Angström [8] has suggested that an equation of the form $Q/Q_0 = a + bS$ represents the relation between sunshine, S (expressed as a fraction of the possible number of hours), and the ratio of the average radiation, Q , on a horizontal surface to the corresponding average radiation, Q_0 , during cloudless days, where a and b are constants. Using the data of table 6 for a

TABLE 6. Comparison of cloudy and cloudless days.
8:00 am to 5:00 pm

	Jan.	Feb.	Mar.	Apr.	May	June	July	Aug.	Sept.	Oct.	Nov.	Dec.
Per cent possible sunshine	31	44	38	43	52	70	75	76	75	70	40	32
Avg noon sun alt	27.5	35	46	57	66	70.5	69	62	51	40	30	25.5
Horizontal surface												
I_0	2700	3720	5500	7280	8250	8640	8560	7670	6250	4670	3110	2310
R_1	0.23	0.30	0.38	0.33	0.32	0.34	0.36	0.36	0.36	0.23	0.33	0.32
R_2	0.29	0.36	0.44	0.42	0.40	0.52	0.53	0.45	0.40	0.29	0.42	0.43
R_3	0.42	0.57	0.63	0.63	0.60	0.72	0.72	0.83	0.81	0.83	0.65	0.64
South vertical surface												
I_0	5600	5900	5640	4560	3600	3170	3420	4420	5450	6170	5840	5280
R_1	0.068	0.103	0.16	0.22	0.27	0.42	0.41	0.30	0.22	0.086	0.098	0.083
R_2	0.094	0.143	0.23	0.32	0.37	0.64	0.60	0.39	0.29	0.138	0.150	0.140
R_3	0.25	0.45	0.45	0.58	0.59	0.88	0.78	0.85	0.78	0.76	0.47	0.41
East or west vertical surface												
I_0	1800	2300	2900	3170	3170	3170	3360	3560	3330	2750	2080	1670
R_1	0.144	0.26	0.31	0.33	0.35	0.44	0.41	0.35	0.35	0.20	0.25	0.23
R_2	0.171	0.31	0.38	0.42	0.44	0.58	0.54	0.43	0.40	0.27	0.31	0.32
R_3	0.28	0.53	0.58	0.64	0.62	0.84	0.81	0.82	0.82	0.83	0.57	0.53
I_0^*	3200	4100	5000	5700	5600	5700	5000	6300	6000	5000	3670	2830
R_1^*	0.109	0.134	0.19	0.18	0.20	0.24	0.21	0.17	0.19	0.112	0.15	0.15
R_3^*	0.28	0.46	0.47	0.56	0.52	0.76	0.73	0.77	0.76	0.80	0.50	0.47

* For east in am or west in pm.

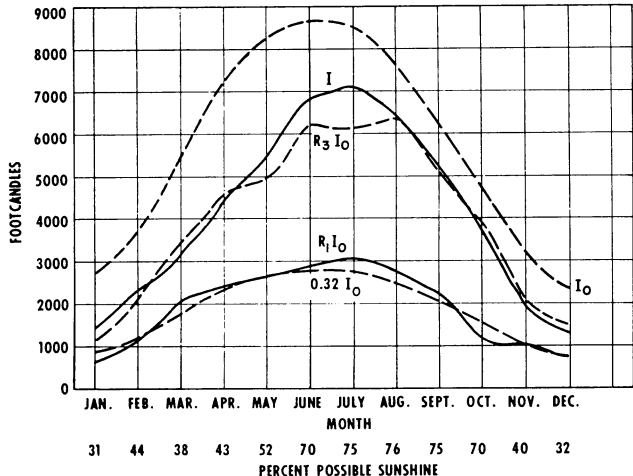


FIG. 15. Average illumination. Horizontal surface—8:00 am to 5:00 pm. Calculated and measured. $I = I_0(0.32 + 0.68S)$.

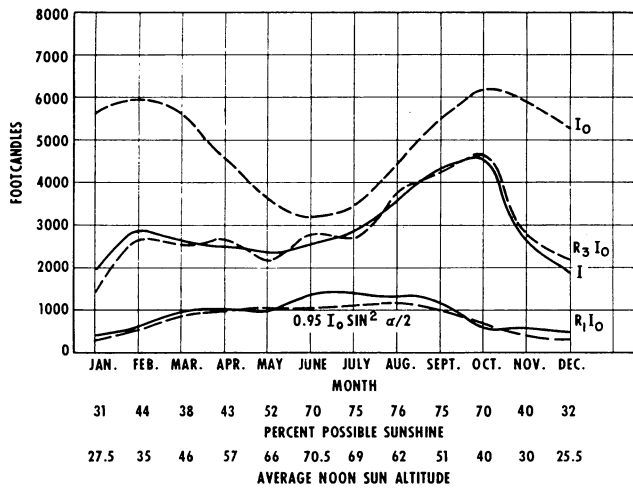


FIG. 16. Average illumination. South vertical surface—8:00 am to 5:00 pm calculated and measured. $I = I_0[S + 0.95(1 - S) \sin^2 \alpha/2]$.

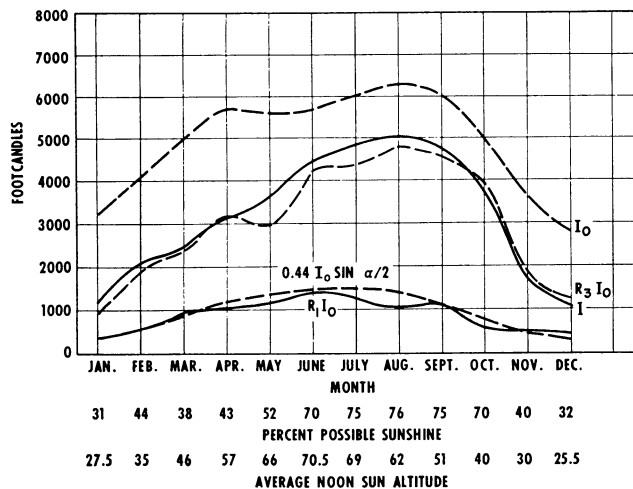


FIG. 17. Average illumination. East vertical surface in am. West vertical surface in pm. 8:00 am to 5:00 pm. Calculated and measured. $I = I_0[S + 0.44(1 - S) \sin \alpha/2]$.

horizontal surface, it appears that

$$I = I_0(0.32 + 0.68S) \quad (1)$$

is a reasonable expression, where I_0 is the average illumination for the month, assuming all days to be cloudless, and I is the average illumination for the month having 100 S per cent of possible sunshine. The values of I_0 , R_1I_0 , $0.32 I_0$, R_3I_0 , and I for the 12 months are shown in fig. 15. Setting $a = 0.32$ indicates that when $S = 0$ the sky is overcast and the average illumination is $0.32 I_0$. It appears that the agreement of $0.32 I_0$ to R_1I_0 and I to R_3I_0 is quite good, considering the uncertainty in S .

Reference to table 6 will indicate, however, that an equation of this form cannot be used to represent the conditions for a vertical surface since R_1 is not a constant or nearly so. An equation that represents fairly well the conditions for the south vertical surface is

$$I = I_0[S + 0.95(1 - S) \sin^2 \alpha/2], \quad (2)$$

where α is the average noon sun altitude for each month. The values of I_0 , R_1I_0 , R_3I_0 , $0.95 I_0 \sin^2 \alpha/2$, and I for the 12 months are shown in fig. 16.

A similar expression

$$I = I_0[S + 0.44(1 - S) \sin \alpha/2] \quad (3)$$

represents the conditions for east exposure in the forenoon and for west exposure in the afternoon; values of I_0 , R_1I_0 , R_3I_0 , $0.44 I_0 \sin \alpha/2$, and I are given in fig. 17.

Eqs (1), (2), and (3) represent fairly well the data of table 6 and were formed to give $I = I_0$ when $S = 1.0$, and average values for overcast sky conditions when $S = 0$. Eqs (2) and (3) are for direct light only and do not attempt to include an added vertical-surface component due to ground-reflected light.

Since total radiation intensities were not measured at Ann Arbor or Willow Run during the period the data of this paper were collected, these daylight intensities cannot be related to total radiation.

When the distribution of brightness of an overcast sky has been measured, it can generally be represented by $B_\theta = B(a + b \sin \theta)$, where B_θ is the sky brightness at an altitude θ , B is the sky brightness at the zenith, and a and b are constants. It is because of such facts that Class A conditions were selected as those for which the ratio of maximum-to-minimum vertical-surface illumination did not exceed about 1.5. Values of the constants a and b that have been used are $a = 0.4$, $b = 0.6$, and $a = \frac{1}{3}$, $b = \frac{2}{3}$. An integration of this expression for an unobstructed horizontal surface and for an unobstructed vertical surface gives a ratio for total horizontal- to total vertical-surface illumination of 2.42 and 2.52, respectively, for the two sets of constants. In table 4, such ratios are presented for

average values of horizontal- and vertical-surface illumination for Class A conditions and for the sum of conditions of Classes A, B, and C. It will be observed that these ratios for the summer months agree quite well with the theoretical values; however, for the winter months, the ratios are close to 2.0, which is the theoretical ratio for a sky of uniform brightness.

In the daylighting of buildings, the interior illumination is usually related to the exterior illumination of the surfaces containing the fenestrations. Some attempt has been made to establish average values for exterior illuminations due to overcast sky conditions; values of 500 and 1000 footcandles have been used for vertical surfaces, and 1000 and 2500 footcandles have been used for a horizontal surface. The data of this study indicate that, for strictly overcast sky conditions and with average foreground reflectance the average vertical-surface illumination, between 8:30 am and 3:30 pm is 1140 footcandles for the entire year and 960 footcandles for the school year. The corresponding figures for a horizontal surface are 2030 footcandles for the entire year and 1670 footcandles for the school year. For the period of 8:00 am to 5:00 pm, the figures, of course, will be somewhat lower. In any case, these data indicate that 1000 footcandles for a vertical surface and 2000 footcandles for a horizontal surface are reasonable averages for this location.

It should be realized, however, that minimum exterior illumination conditions do not only relate to overcast skies. Clear sky conditions for vertical surfaces not receiving direct sunlight or appreciable ground-reflected light should also be included. Comparison of Class D and Class A averages for north exposure, table 2, indicates that they are comparable. When the ground-reflected light is appreciable, the overcast sky conditions do represent the minimum.

One reason for establishing an average minimum exterior illumination is that for this value the interior illumination should be just adequate for the task involved. The percentage of time for which the exterior illumination, for all conditions, is above a specified level is given in figs. 3, 4, 5, 6, 7, and 8. In the case of 1000 footcandles for a vertical surface and 2000 footcandles for a horizontal surface, fig. 8 indicates that for the period 8:00 am to 5:00 pm for the entire year, these values will be exceeded 67 per cent

of the time for a horizontal surface and 75 per cent of the time for a vertical surface with south exposure.

In considering such figures, it should be realized that the data of this study are for one of the three districts in the United States having the lowest percentage of possible sunshine.

The U. S. Weather Bureau [9] extensively records solar radiation on a horizontal surface and collects illumination data at only a few geographical locations. More extensive data, showing total radiation and illumination for vertical surfaces, are required to obtain a correlation between solar heat and luminous-energy intensities and atmospheric conditions. Recording devices designed specifically for such research are needed to avoid the time-consuming methods of tabulation and analysis used in presenting the data of this study.

Acknowledgment. The collection and initial tabulation of the data of this study were accomplished through the use of funds supplied by the Kimble Glass Company, a subsidiary of Owens-Illinois. The author is grateful to this Company for its support and permission to use the data in this publication. The author also wishes to thank the Director of The University of Michigan Research Institute for making funds available for the preparation of the manuscript.

REFERENCES

1. Kimball, H. H., 1919: Variations in the total and luminous solar radiation with geographical position in the United States. *U. S. Weather Review*.
2. Kimball, H. H., and I. F. Hand, 1922: Daylight illumination on horizontal, vertical and sloping surfaces. *U. S. Weather Review*.
3. Kunerth, W., and R. D. Miller, 1932: Variations of intensities of the visible and of the ultraviolet in sunlight and in skylight. *Trans. I. E. S.*, **27**, 82-94.
4. Weston Electrical Instrument Corporation, 1944: *Technical data on Weston photronic cells*. Cir. B20B.
5. Kunerth, W., R. D. Miller, and H. Harley, 1937: The amount of luminous and of ultraviolet solar radiation received on certain vertical planes. *Trans., I.E.S.*, **32**, p. 315.
6. Kingsbury, H. F., H. H. Anderson, and V. U. Bizzaro, 1957: Availability of daylight. *Illum. Eng.*, **Feb.**, p. 77.
7. Smithsonian Institution, 1951: *Smithsonian meteorological tables* (Sixth ed. rev.). Washington, D. C., Govt. Printing Off.
8. Angström, A., 1928, *Medd. Stat. Met. Hydr. Astr.*, **4**, No. 3.
9. U. S. Weather Bureau, *Climatological data*. Washington, D. C., Govt. Printing Off.

PART IV: Transportation Engineering

COMPUTATION OF THE DISTRIBUTION OF MAXIMUM ALLOWABLE GROSS TAKEOFF WEIGHTS FOR AIRCRAFT

Irving Solomon and William C. Spreen

Air Weather Service

ABSTRACT

A method is presented whereby the distribution of maximum allowable gross takeoff weight can be computed for an aircraft from surface weather observations and runway length. The method involves the mathematical approximation of the aircraft manufacturer's performance nomographs. This permits a flexible interchange of meteorological factors with operational factors and the utilization of electronic computer capability to simulate operational conditions. Frequency distributions of maximum allowable gross takeoff weights are shown for the USAF Convair T-29C for Stead AFB at Reno, Nevada.

1. Introduction

One of the functions of the meteorological specialty known as applied climatology is to provide planning and operational departments with a quantitative basis for decisions regarding operations under their control. The meteorologist in this field must convert the pertinent climatological elements into the operational terms of the user so that this quantitative basis will be most intelligible. This conversion of meteorological variables to the requisite operational variable can be complex. The operational variate is a function of vehicular variates, some of which are functions of meteorological variates. The mathematical manipulations involved in this type of conversion would often represent a rather sterile effort without the support and capability provided by electronic computers which allow the investigator to process masses of meteorological data and simulate actual operational conditions. The usefulness of this union of climatology and electronics can be illustrated by a practical problem involving the U. S. Air Force Convair T-29C.

An Air Force operations group was experiencing difficulties in maintaining its planned flying schedules from some high-elevation bases, particularly during summer, with certain grade fuels and at high aircraft gross weights. Consultation with the operational personnel established that the most useful operational

term was the maximum allowable gross takeoff weight and that a frequency distribution of this variate, by months and hours, would provide a quantitative basis for evaluation and modification of their present schedules and for the formulation of future plans and schedules. A review of the Technical Order (operating instructions) for the aircraft [2] showed that the maximum allowable gross takeoff weight was a function of engine minimum performance torque pressure, wing-flap setting, desired aircraft rate of climb, and runway length. The meteorological elements involved were air temperature, dew-point temperature, pressure altitude, density altitude, and wind speed.

2. Pilot-preparation procedure

The Technical Order (operating instructions) for the USAF T-29C (Convair 440) [2] describes in detail the necessary pilot preparation for takeoff which must be simulated in order to provide the appropriate climatological basis for decision. The portion of the preparation that is pertinent to this discussion is the determination of whether the plane with a given gross weight (cargo plus aircraft weight plus fuel, etc.) can become airborne safely. An abridged version of this procedure follows (the various nomograms referenced will be discussed later).

(a) Establish the gross weight of the aircraft and desired initial rate of climb.

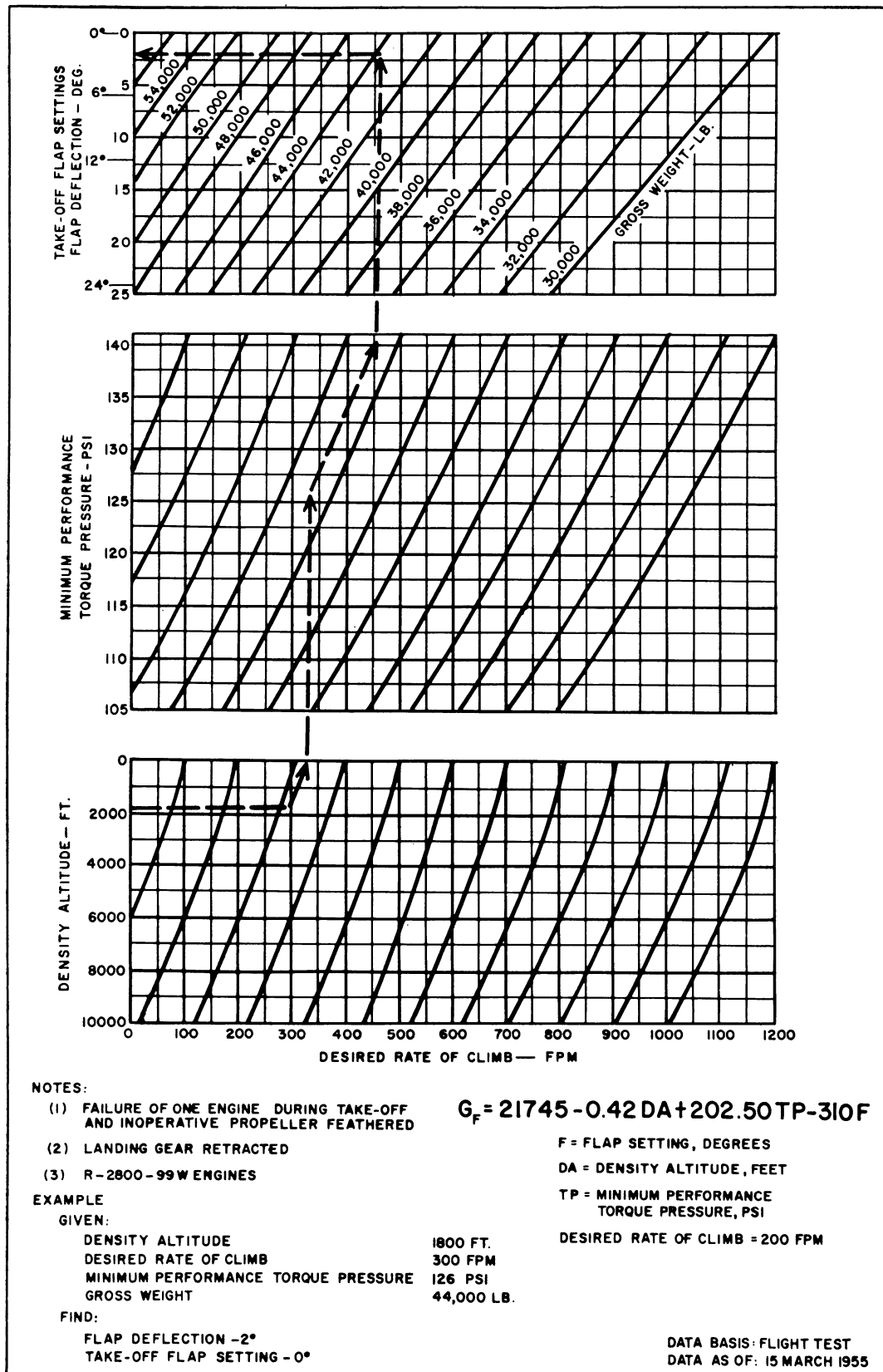


FIG. 1. Initial rate of climb nomograph.

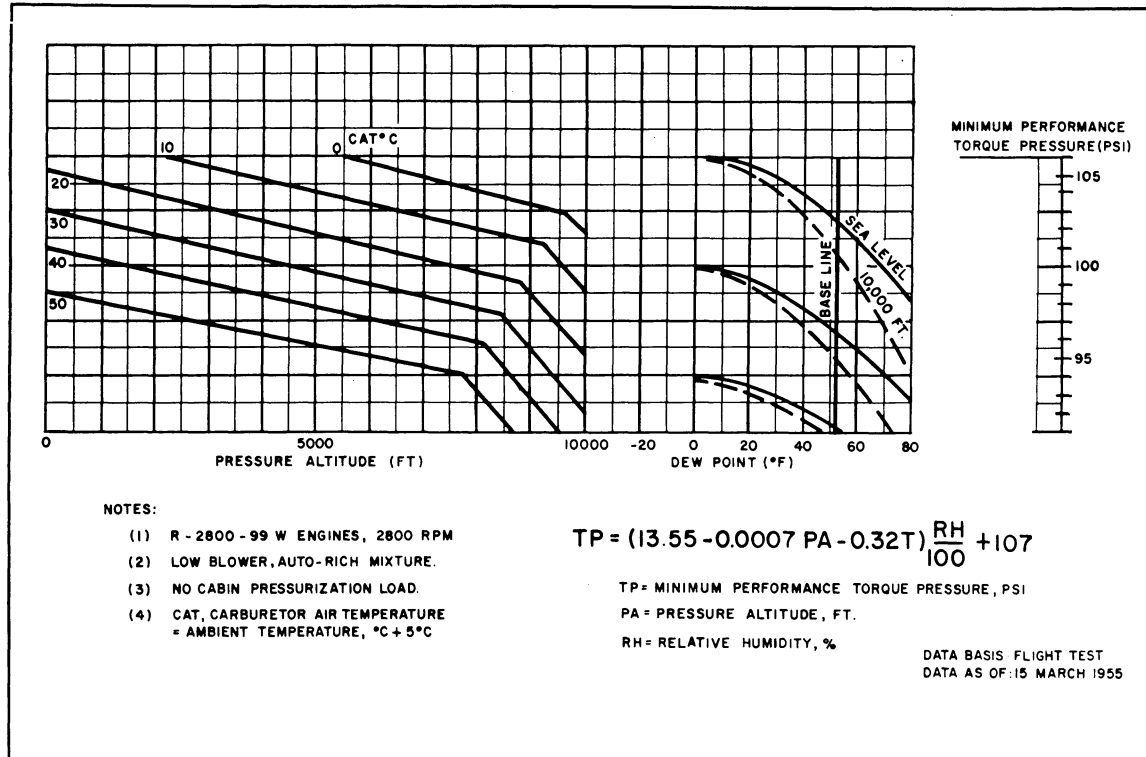


FIG. 2. Minimum performance torque pressure nomograph, dry takeoff power, 100/130 octane fuel.

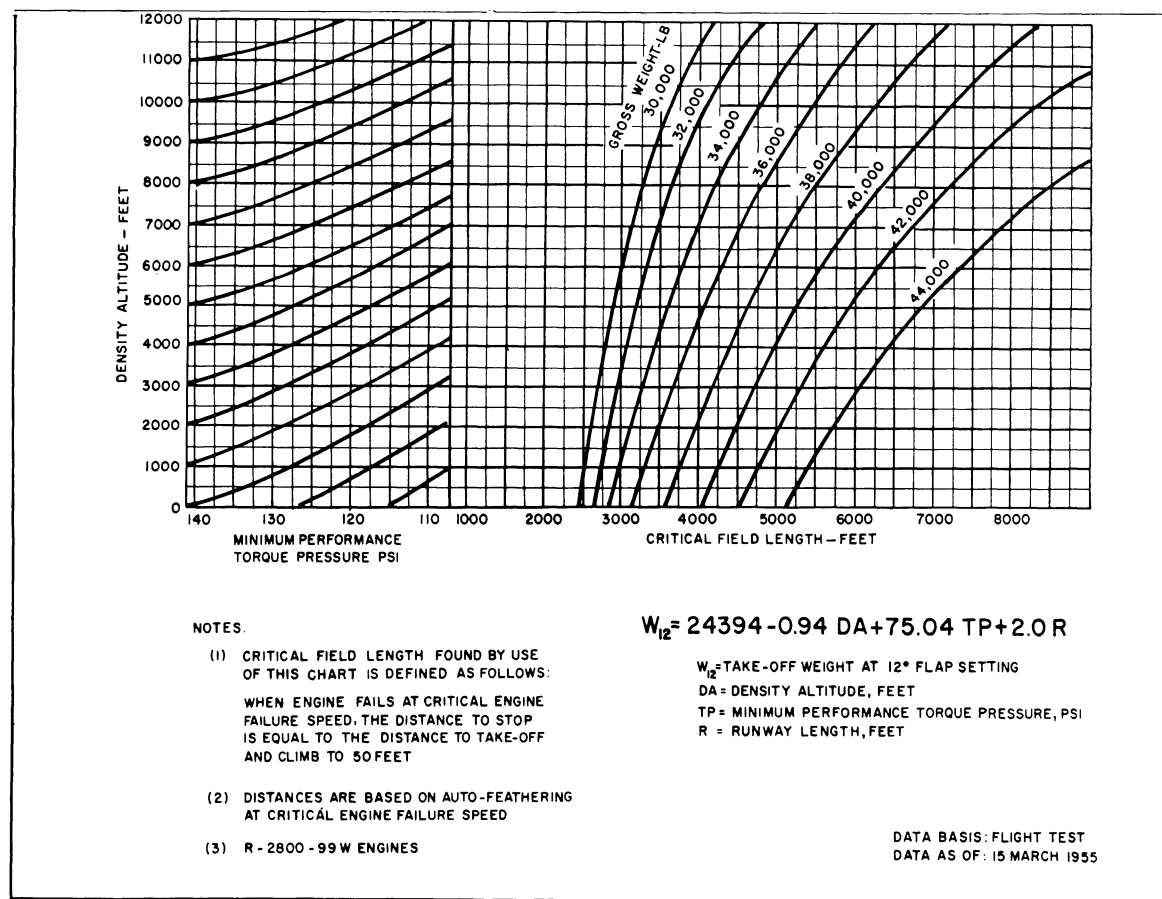


FIG. 3. Critical field length nomograph, 12° flap setting.

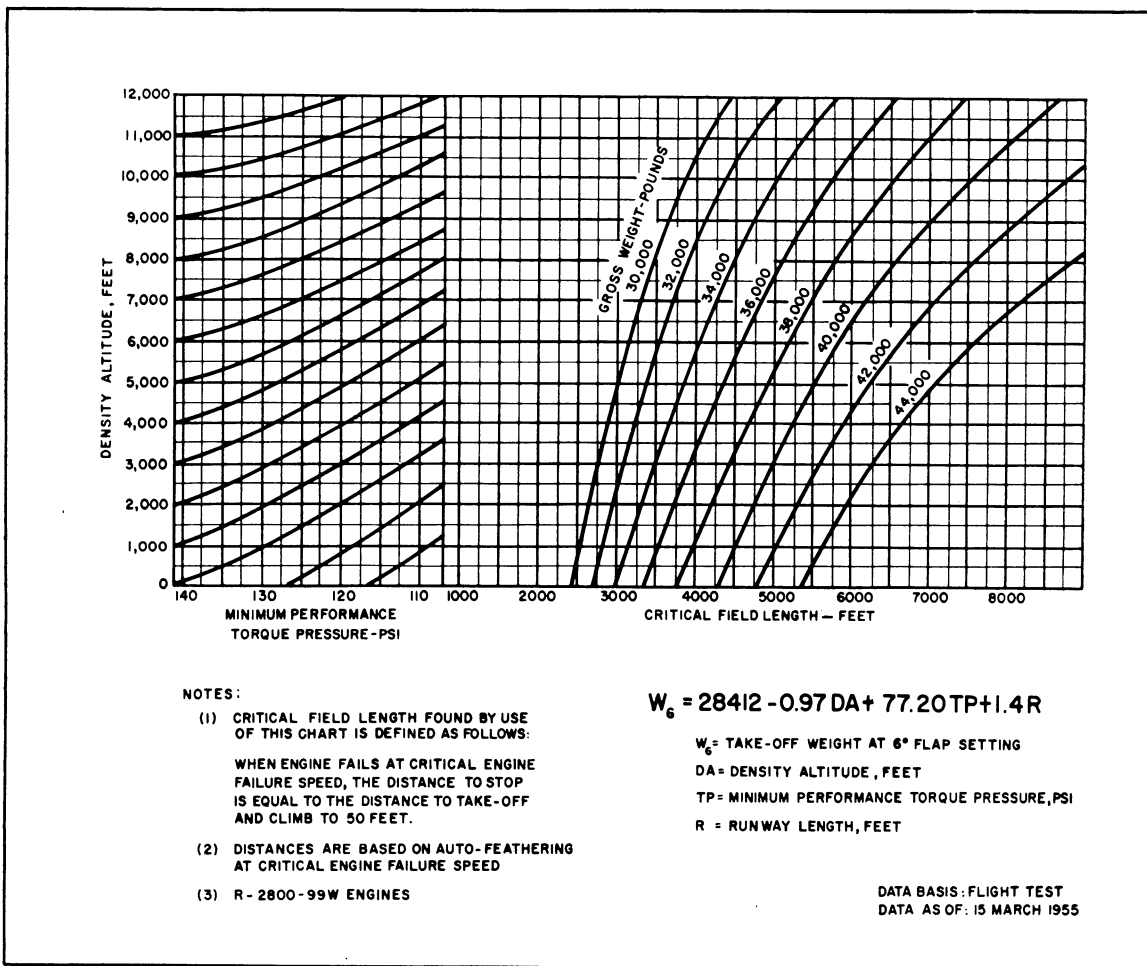


FIG. 4. Critical field length nomograph, 6° flap setting.

(b) Examine the Critical Field Length¹—24-deg Flap Chart (this chart has not been included because 24 deg of flap is not used by pilots in actual operations) to determine if the gross weight is acceptable. If so, examine Initial Rate of Climb Chart (fig. 1) for that weight and flap setting to determine if the initial rate of climb is acceptable for the torque pressure computed from fig. 2. If both conditions are satisfied, the takeoff can be accomplished with 24 deg of flaps.

(c) If either of the conditions in (b), above, is unacceptable, examine the Critical Field Length—12-deg Flap Chart (fig. 3) to determine if the gross weight of the aircraft is acceptable. If so, examine the Initial Rate of Climb Chart for that weight and flap setting to determine whether the desired rate of climb is acceptable. If both conditions are satisfied, takeoff can be accomplished with 12-deg flap settings.

(d) If either condition in (c), above, is unacceptable, repeat the process using the Critical Field Length—

6-deg Flap Chart (fig. 4) and the Initial Rate of Climb Chart to determine whether takeoff can be achieved with 6 deg of flap.

(e) If conditions in (d) are not satisfied, the process is repeated using the 0 deg of flap chart (fig. 5) and the Initial Rate of Climb Chart to determine the acceptability of a 0-deg flap setting.

(f) If conditions in (e) are not satisfied, the gross weight of the aircraft must be reduced. The procedure outlined above must then be repeated with a lesser gross weight, and so on, until an acceptable weight is determined.

3. Preparatory relationships

It might seem that the pilot's preparation procedure cannot be duplicated exactly since he knows the gross weight with which he would like to fly and the simulation procedure described herein computes the maximum gross weight for specified meteorological conditions. However, there is really no difference because the pilot can be assumed to start with the maximum possible gross weight, which he reduces until he reaches a gross weight at which the aircraft can be-

¹ Critical Field Length for this problem is defined as follows: that runway length which will permit acceleration to critical engine failure speed and, with an engine failure at that speed, the distance to stop is equal to the distance to takeoff and climb to 50 ft.

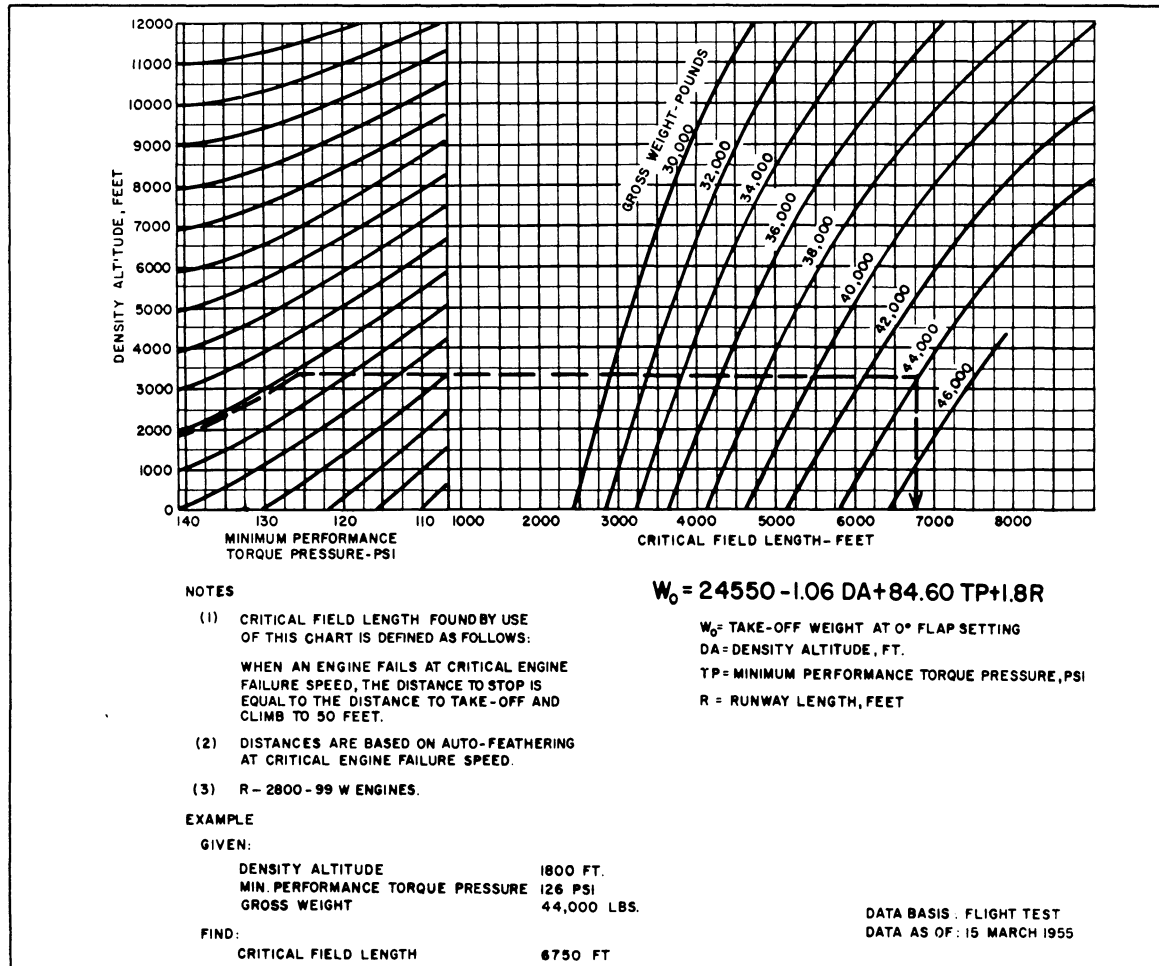


FIG. 5. Critical field length nomograph, 0° flap setting.

come safely airborne and can initiate a selected initial rate of climb. If this is equal to or greater than the actual gross weight, he has no problem; if it is less, cargo must be removed from the airplane. This, in effect, is what the simulation procedure will do, assuming that full advantage will be taken of the aircraft's capacity.

The variables which must be taken into account can be divided into three classes which are not mutually exclusive. They are vehicular variables, meteorological variables, and non-meteorological variables. Those in the first category are functions of the variables in the last two categories. These variables are listed in table 1, together with the symbols which will be used to designate them. The relationships among the various combinations of variables are shown graphically in figs. 1 through 5.

The operational variable, maximum gross weight, is the lesser of the two gross weights listed in the first column of table 1. These two gross weights, while functions of somewhat the same variables, react differently to them, especially with respect to flap setting. The gross weight (G_F) for a given combination

of the other variables (DA, TP, and C) is greater for the lesser flap settings (F); i.e., the less the flap setting, the greater the weight at which a desired rate of climb can be initiated. The gross weight (W_F), however, is greater for the larger flap settings when the other variables (DA, WS, TP, R and S) are specified; i.e., the greater the flap setting, the greater the weight at which takeoff can be accomplished. The optimum combination must be determined for these sets of conditions.

The next step is the conversion of the nomographs or performance charts (figs. 1 to 5) to mathematical expressions which can be used by the electronic computer. This conversion was somewhat simplified by the operational decision to require a rate of climb equal to 200 ft per min and the elimination of the use of 24-deg flap settings. It was also decided to assume that the runway has a 0-deg slope. Two meteorological conditions were omitted. They are wind velocity, and ceiling-visibility combination which close the field. The former element has a direct effect on the gross weight but would have required a considerably greater amount of computation and detail. Its omission here

TABLE 1. Variables in simulation computations.

Vehicular variables—function of—Meteorological variables—and—Non-meteorological variables		
Minimum performance torque pressure (TP)	Pressure altitude (PA) Air temperature (T) Relative humidity (RH)	
Gross weight limited by rate of climb (G_F)*	Density altitude (DA)	Minimum performance torque pressure (TP) Takeoff flap setting (F) Desired rate of climb (C)
Gross weight limited by runway length (W_F)*	Density altitude (DA) Wind speed (WS)	Minimum performance torque pressure (TP) Runway length (R) Takeoff flap setting (F) Runway slope (S)

* The subscript, F, refers to degrees of flap.

produced underestimates, or conservative estimates, of the maximum gross takeoff weights. The closed conditions, while not entering directly into the computation, are an obvious deterrent to operation. However, for the station being considered, their occurrence was too infrequent to be considered after the other simplifying assumptions had been made.

The conversion of the nomographs to a mathematical form began with minimum performance torque pressure (TP), since it affects both gross weights (G_F and W_F) and is itself a function of meteorological variables. Fig. 2 indicates that torque pressure is a function of ambient air temperature, dew-point temperature, and pressure altitude. Dew-point temperature was a problem, at first, but it was solved by expressing moisture content of the air in terms of relative humidity. After the change of variable, the equation shown in fig. 2 was derived. The family of curves on the extreme left of the chart has a discontinuity which is not permitted by the equation in fig. 2. This was deliberate avoidance of unnecessary complications. Even though the air base, Stead AFB, Nevada, is at a high elevation, the pressure and temperature variation would keep the computation to the left of this discontinuity. Otherwise, more than one equation would have been required.

Fig. 1 is the nomograph for computing gross weight limited by rate of climb (G_F). Since a 200-ft-per-min initial rate of climb is required, the equation shown is for that rate of climb and uses only density altitude, torque pressure, and flap settings. For illustrative purposes, torque pressure (TP) is kept as a variable rather than expressing it in terms of meteorological elements. Whether this is done in actual computations depends upon the machine facilities and program that is used.

The gross weight limited by runway length (W_F) has three nomographs, figs. 3, 4, and 5, to express its relation to the various variables; *i.e.*, there is one

chart for each of the three prescribed flap settings, 12 deg, 6 deg, and 0 deg. An equation was derived for each chart and is shown at the bottom of each nomograph with a subscript indicating the appropriate flap setting. Each equation involves the three variables: density altitude, torque pressure, and runway length. The actual runway length is used as the critical field length. Since the problem is to determine the maximum gross takeoff weight, it must be assumed that the maximum available runway length will be used. In these equations, the 8000-ft runway at Stead AFB was used.

Several other relations, in addition to those already derived, are necessary since the standard hourly weather observation includes temperature, pressure, and relative humidity but neither pressure altitude nor density altitude. Equations and/or tables for these last two elements can be found in many publications such as references [3] and [4]. Whether tables or equations are used for determining pressure altitude and density altitude depends upon the characteristics of the electronic computer that is available. Density is usually computed by one of the many formulae available.

4. Computer simulation procedure

The electronic-computer method, in duplicating or simulating the pilot's procedure, attempts to optimize the gross takeoff weight in accordance with the limiting effects of the weather elements, the initial rate of climb, and the runway length by varying the flap settings of the aircraft. For each flap setting, the procedure must consider the two weights (G_F and W_F) which have been discussed previously.

After computing the values of the various meteorological parameters, the procedure is a logical method by which the machine may objectively select the appropriate gross takeoff weight. The greatest flap

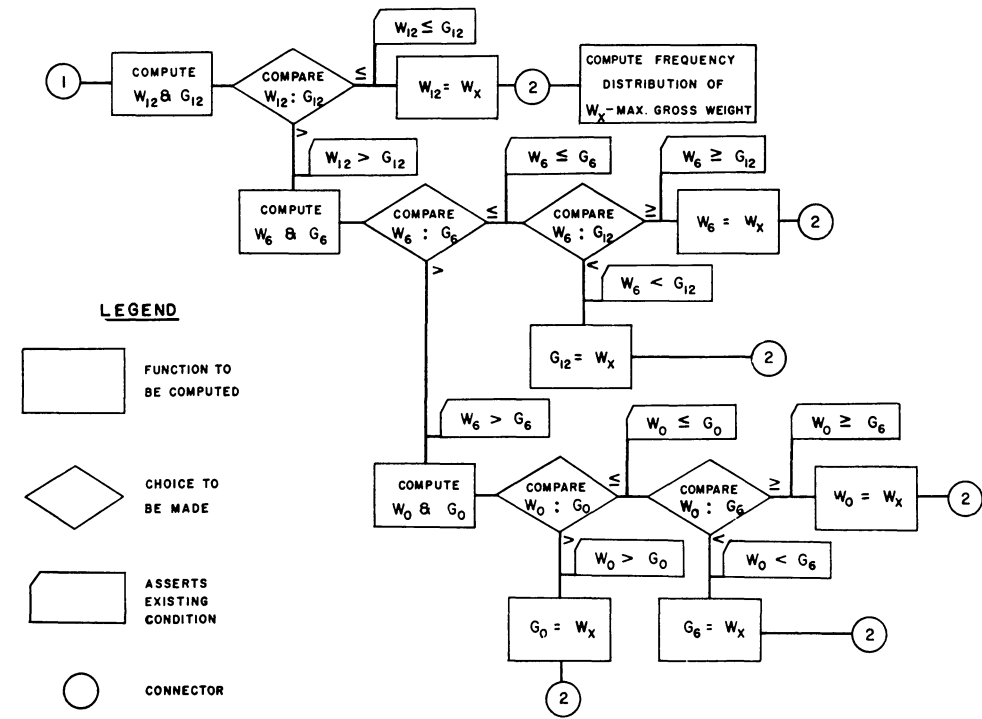
FIG. 6. Block diagram for selection of maximum gross take-off weight (W_x).

TABLE 2. Percentage frequency distribution of maximum allowable gross takeoff weights for T-29C, Stead AFB, Nevada. January

Weight (thsd of lbs)	Hours (LST)								
	01-03	04-06	07-09	10-12	13-15	16-18	19-21	22-24	01-24
39.5-40.0				0.9	0.4				0.2
40.0-40.5	1.1	1.1	1.7	3.7	10.3	8.4	3.0	1.7	3.9
40.5-41.0	13.1	12.3	11.0	20.9	32.9	27.3	16.3	13.3	18.4
41.0-41.5	19.1	19.1	18.5	26.9	34.4	35.1	27.7	20.2	25.1
41.5-42.0	16.8	16.8	17.6	22.4	15.1	20.4	23.2	23.4	19.5
42.0-42.5	19.8	17.8	14.4	12.9	5.8	6.0	16.8	16.8	13.8
42.5-43.0	11.0	10.1	14.4	8.4	1.1	2.6	7.7	13.5	8.6
43.0-43.5	11.4	11.8	8.4	3.2		0.2	5.2	6.5	5.8
43.5-44.0	6.0	7.5	10.8	0.4				4.5	3.7
44.0-44.5	1.7	3.2	2.8	0.2					1.0
44.5-45.0		0.2	0.4						0.1

TABLE 3. Percentage frequency distribution of maximum allowable gross takeoff weights for T-29C, Stead AFB, Nevada. July

Weight (thsd of lbs)	Hours (LST)								
	01-03	04-06	07-09	10-12	13-15	16-18	19-21	22-24	01-24
38.0-38.5							0.2		*
38.5-39.0	0.2	0.2	0.6	1.3	1.5	2.8	1.9	0.4	1.1
39.0-39.5	5.8	3.4	11.2	17.8	34.4	39.8	21.5	13.8	18.5
39.5-40.0	37.8	19.4	43.4	70.8	60.0	54.4	63.0	51.8	50.1
40.0-40.5	48.8	53.9	40.6	10.1	4.1	3.0	13.3	33.5	25.9
40.5-41.0	7.1	22.2	3.9					0.4	4.2
41.0-41.5	0.2	0.9	0.2						0.2

* Less than 0.05%

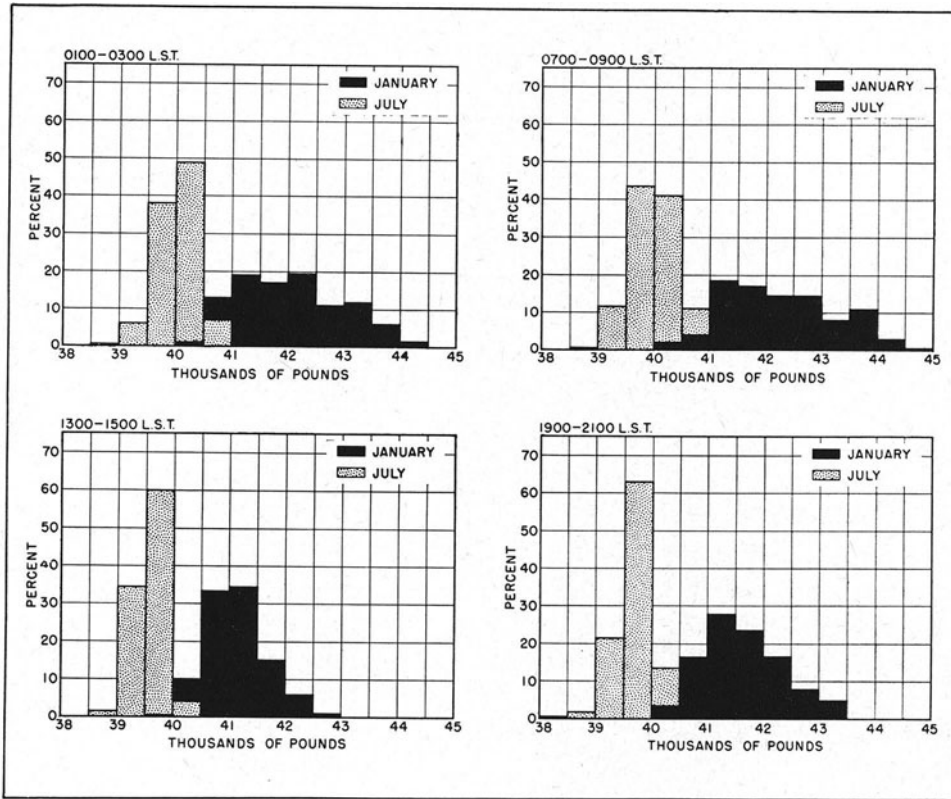


FIG. 7. Frequency distributions of maximum gross takeoff weights for T-29C, 100/130 octane fuel, dry takeoff power, Stead AFB, Reno, Nevada.

setting (12 deg) is considered first and the allowable takeoff weights with runway limitations (W_{12}) and with rate of climb limitations (G_{12}) are computed and compared (see figs. 2 and 3). If W_{12} is greater than G_{12} , it means that the aircraft can take off at that weight but cannot initiate a 200-ft-per-min rate of climb. In that case, it is necessary to consider lesser flap settings and lesser gross weights until a weight satisfying both conditions is obtained in much the same fashion as the pilot's procedure described previously.

The logical procedure, in diagrammatic form, is presented in fig. 6. The symbols and format used in this figure are taken from McCracken [1]. It shows essentially the decisions which the electronic computer must make in choosing the maximum gross takeoff weight.

5. Results

The computations and computational procedures described in the previous sections were made for a 5-yr period for Stead AFB from hourly surface weather observations. Thus, the pilot's procedure was simulated approximately 44,000 times. As a simple type of summarization, the results were grouped in percentage frequency distributions of maximum allow-

able gross takeoff weights, by month and by 3-hr groups (01-03, 04-06, 07-09, etc., LST). Tables 2 and 3 are examples of this type of summarization for January and July at Stead AFB (the takeoff weights are given in 500-lb class intervals). Fig. 7 presents these same data in the form of frequency histograms. Essentially, the data represent 5 yr of operational experience for the aircraft at that base, even though that aircraft type may never have been flown from that field.

This form of summarization is among the least complex of those which the electronic computer can perform. The type of summarization is dependent upon the aspects of the aircraft problem rather than upon the limitation of the computer. The data could have been presented as time changes, durations, waiting times, airfield comparisons, aircraft comparisons (if more than one aircraft type were involved), etc.

6. Conclusions

This example illustrates that the electronic computer in applied climatology, as in other fields, is an extremely powerful tool. It opens types of investigation and application which have been previously closed to the climatologist because of prohibitive requirements of manpower and time. The versatility of these

computers allows the simulation of operations, and it can accumulate and reproduce the experience of years of operation. In addition, a high-speed computer gives us the gift of hindsight, for with it we can go back and study the effects of alternative modes of operation.

This study further illustrates one of the basic precepts of applied climatology, which is translation of the problem into meteorological terms for processing and analysis, but presenting the results of the analysis in the operational terms of the user. The results of this example would have been indecipherable if this had not been done. Essentially, a complex multivariate frequency distribution of meteorological and non-meteorological elements was converted into a simple frequency distribution of maximum gross takeoff weight. The representation of this complex distribution would have required many tables and would have been practically unintelligible to both the planner and the meteorologist because of the sheer magnitude of the data.

Many uses of the approach exemplified here are obvious. More complicated plans can be evaluated in

terms of calculated risks, ability to meet operational commitments can be examined and standards formulated, and even recommendations for aircraft modifications are feasible. An extension of this study could be made to consider meteorological conditions affecting usability of an airfield (ceiling, visibility, gust, cross-winds, etc.) and route winds, in addition to those affecting aircraft performance. As an example, all of these conditions could be examined for an analysis of a recurring air operation such as a maximum-effort logistic operation.

REFERENCES

1. McCracken, D. D., 1957: *Digital computer programming*. New York, John Wiley & Sons, Inc., 87-97.
2. U. S. Department of the Air Force, 1958: *Flight handbook, USAF series T-29C aircraft*. T.O. 1T-29C-1.
3. U. S. National Advisory Committee for Aeronautics, 1955: *Standard atmosphere, tables and data for altitudes to 65,800 feet*. Rep. 1235, pp. 64-72.
4. Smithsonian Institution, 1951: *Smithsonian meteorological tables*. Misc. collection vol. 114, pp. 265-267.

THE CLIMATIC ENVIRONMENT AS A FACTOR IN BUILDING ROAD AND AIRPORT PAVEMENTS

O. L. Stokstad

Michigan State Highway Department

ABSTRACT

Climate is one of the basic considerations in designing and building road and airport pavements. Its influence is so general that a short paper can cover only a few phases of the complete subject. Therefore, this paper will attempt to discuss the subject matter under the following four headings:

- (1) A general statement regarding the climatic influence in the development of highway and airport needs.
- (2) Climate as it enters into the Michigan technique for pavement design; (this is often summed up in the statement "Traffic-wear controls surface design, and climate, together with its associated soil and drainage conditions, determine foundation design").
- (3) Climate as a factor in construction operations; (this phase becomes important, especially in connection with the timing of operations and in the development of equipment).
- (4) Climate as a factor in the service life of a pavement and in the cost of its proper maintenance.

The climate of an area is one of at least five dominant factors to be considered in the design, construction, and maintenance of highway and airport pavements. In the development of this thesis, it will first be quite important that the term "pavement" be defined and also that the broader engineering definition be kept in mind. In modern design practice, the term "pavement" is defined as including not only the wearing course but also the base and subbase courses used to support the wearing course. In other words, the pavement includes all parts of the road structure needed to transmit and distribute wheel loads to the underlying natural soil at a load concentration which will be within the strength capacity of that soil.

The five dominant pavement design controls mentioned above may be listed as follows:

- (1) the weight of wheel loads to be served,
- (2) The character and amount of traffic to be accommodated,
- (3) construction materials available for building the pavement,
- (4) soils over which the pavement is to be built, and
- (5) the climatic environment under which the pavement must be built and maintained.

The engineer is not only interested in each of these factors separately but also the influences which each will have on the others. He finds that a discussion of one cannot progress very far without involving the other four.

The need for the pavement in the first place is strongly influenced by climate. The greatest amount of pavement construction will be required in areas of greatest population concentrations, a situation for which climate is partially responsible either directly

or indirectly. For instance, a temperate climate produces an environment which permits the growth of a dense population without serious lowering of living standards. Such an environment not only tends to generate a vigorous people but it also produces the prairie soils, the world's most productive. This combination of circumstances, a favorable climate and good farm soils, has favored the development of population concentrations with transportation needs which have required extensive investments in highway and airport pavements.

There is a number of areas supporting numerous and prosperous populations and a typical one which will serve to illustrate the general influence of climate on the entire area complex is the population concentration around the lower end of Lake Michigan. Here is an area served by an inland sea of fresh water, the basin of which was mainly carved by climatically produced glaciers, served also by inland waterways roughed out by climatically produced glacial streams, supplied with building materials deposited by climatically produced glacial-melt waters, fed by the climatically produced prairie soils (corn belt), and stimulated by a climatically induced energetic brand of enterprise. This fortunate combination of circumstances placed in a convenient geographic position for transportation purposes has naturally resulted in rapid and extensive development which has required and will continue to require a tremendous program of pavement construction for roads, streets, runways, and railroads.

By visualizing the transportation needs of a community as described above, it is not too difficult to see the relationship between climate and the amount of freight to be moved, the character and volume of traffic to be provided for, and, in a glaciated state such

as Michigan, the character of construction materials available for building pavements.

Probably the fourth factor listed above (soils over which the pavement is to be built) is the basic factor in pavement design most sensitive to the climatic environment under which the pavement must serve. Early pavement studies conducted in Michigan 30 yr ago quickly demonstrated that foundation soils and climatic environment combined to exert a stronger influence on pavement life than did the wear and tear of traffic. Information gained during these early years of soil surveys and pavement-condition studies has guided Michigan's design philosophy. This is based on the proposition that traffic is the dominant factor in the design of the wearing course or pavement surface and that the combined influence of soil, drainage, and climate is the dominant factor in the design of pavement components below the wearing course. The design procedure, therefore, becomes one of fitting wearing-course dimensions to the volume and character of traffic, and then the development of adequate support for the wearing course to carry legal axle loads. It is the development of proper support for the pavement top course which especially calls for detailed soil surveys and a careful evaluation of foundation conditions in the light of climatic conditions involved.

There are three climatic factors which have special significance in the satisfactory performance of any pavement.

(1) Temperature and its variations in combination with other factors cause such engineering headaches as pavement disintegration, frost heaving, spring break-up, and frost boils. The number of frost degree days per year has been used as a means to estimate the extent of frost damage to be anticipated in the various regions of the northern states. A highway engineer in Michigan, for instance, knows that Lansing's 700 frost degree days require from $2\frac{1}{2}$ to 3 ft of undercutting through silty soils to control frost heaving and that the 1200 to 1800 frost degree days in the Upper Peninsula require from 3 to 4 or even 5 ft of undercutting under the same soil conditions. Because of the depth of frost penetration, pavement foundations must be well drained to depths of at least 5 ft if frost damage is to be prevented.

(2) Rainfall (its amount, distribution, and character) is of serious concern to the highway and airport engineer. The gentle, misty rains of Northern Europe, for instance, require much less in the way of storm sewers and ditches generally than the "gully washers" we sometimes experience in this area. Also, there is a relationship between precipitation, soil moisture, and soil foundation or subgrade strength. Clay soils especially can store considerable quantities of moisture

which serves to reduce its strength as a foundation material. This is especially true if the foundation soil is subjected to frost action. The seriousness of frost damage increases as subgrade soil-moisture content increases. Pavement mud pumping on fine textured soils is one of the more serious causes of pavement failure which can be traced directly to excessive amounts of subgrade moisture.

(3) Evaporation is a third climatic factor which functions in association with temperature and rainfall to influence pavement design and construction practice. This association determines the amount of soil moisture which in turn will control designs, construction techniques, and construction progress.

It may be seen from this very brief discussion that climatic-induced foundation conditions can seriously influence pavement performance. In many instances of pavement destruction where the damage has been laid to traffic, the real culprits have been frost heaving, mud pumping, subgrade displacement, or excessive elastic movement in the foundation. In other words, pavement failure could be traced to a structure inadequately designed for legal axle loads—a design inadequate usually because of failure to anticipate and provide for subgrade strength changes due to the influence of seasonal climatic changes.

Every region has its own peculiar climatic environments and associated engineering problems. In Michigan, frost-moisture-soil-aggregate associations are of front-rank importance. In other regions, important problems may involve differential foundation swell or foundation resilience.

It is this extremely important influence of the climatic factor on design practice which seriously limits the extent to which the results of pavement research from one area can be applied in another. The big question becomes what correction factor should be used in translating the research results of one climatic region into terms which will be applicable in another climatic region.

The comments above deal mainly with foundation conditions or pavement support. The climatic factor also is a very important one controlling highway-surface durability. In the cool, moist climate of Michigan, for instance, specifications controlling the character of construction materials must guard against materials which break down as a result of freezing and thawing.

Consideration of the climatic factor does not end with the completion of pavement designs. The construction stage comes next and here the weather is of prime importance, especially in connection with the timing of operations to fit the restrictions imposed by the changing seasons. Certain types of construction cannot be done during winter weather. Any operation

dependent on the evaporation of moisture or the use of water is difficult to manage under freezing conditions. Portland cement concrete, for instance, must be protected from frost until cured. Other operations such as asphaltic concrete require high temperatures during laying process to obtain good compaction and a smooth uniform surface.

Certain types of grading work can be effectively performed under winter conditions. Excavating and backfilling through peat swamps, for instance, is an operation which lends itself very well to winter construction. General grading work is more difficult, but sandy soils can be handled with fair success during winter weather. Not only is weather a very important factor in planning construction work, but it also enters into the design of construction equipment. Special equipment and materials for protecting freshly poured concrete from drying too fast, and also tire and track design to provide flotation under seasonal changes in soil and drainage conditions, are items which serve to illustrate this problem.

The engineer's concern with the weather does not

end with the completed pavement. The rate at which pavement riding quality and pavement soundness is maintained over the years depends on the use to which it is put, the character of the maintenance effort it receives, and the climatic conditions under which it must serve. Because of weather and wear, a pavement surface will eventually wear out. At this time, if it has been designed with proper consideration for foundation and climate, it may be retired as a surface and become the base for a new surfacing course. If proper consideration was not given to foundation and climate, it will be necessary to rebuild from the bottom up with little or no salvage value in the original structure.

In summary, it may be said that it is difficult to find any phase of highway and airport design and construction where climate does not form one of the controlling factors. It is, therefore, mandatory that the highway and airport engineer carefully consider information on the climatology of a site not only in the development of his designs but also in the transfer of engineering experience from one geographic complex to another.

WEATHERING TESTS OF PORTLAND-CEMENT CONCRETE FOR HIGHWAYS

F. E. Legg, Jr.

Michigan State Highway Department

ABSTRACT

In contrast to many types of construction, almost all of the product of the highway engineer is, or necessarily, dispersed across the open countryside and therefore vulnerable to destructive weathering action. Slow deterioration of bituminous road binders may result from prolonged high atmospheric temperatures and exposure to the sun's radiation. In northern climates, seasonal and daily temperature changes occur, frequently passing through the freezing point. These temperature changes in the presence of snow or rain may be highly destructive to portland-cement concrete.

The concrete technologist has, for some time, sought accelerated laboratory tests by which he may predict long-time field performance. Bridges and pavements are rightfully expected to be enduring. One of the prevalent means of evaluating concrete is by laboratory freeze-thaw tests. The uncertainty of knowledge with respect to properly assessing climatic effects is exemplified by the fact that the American Society for Testing Materials now has four tentative freeze-thaw methods. These vary greatly as to required temperature gradients and freezing media. Brief descriptions of these are given. One of the methods has been used for evaluating Michigan mineral aggregates in concrete.

Prediction is made that the disciplines of the meteorologist could well be helpful to the concrete technologist if mutual understanding of the problems were developed.

1. Introduction

In 1931, the distinguished engineer Thomas H. McDonald, Commissioner of the Bureau of Public Roads, made the following statement: "The roads are more destroyed really by climatic and soil conditions than they are by any use that is made of them."

Climatic effects on highway planning. It is necessary to reflect only briefly to realize how profoundly the weather affects the activities of the highway engineer. Before he is called upon to build a road between points A and B, the intervening terrain has been acted upon by centuries of weathering action putting rivers in his way, hills, valleys, peat bogs, and rock. If the rock is so accommodating as to be in the vicinity of his intended bridge foundations, he is lucky; otherwise, he may have to drive piles down to support the structure or spread out costly heavily reinforced footings. If the rock is in a hill, he may have to blast it out of the way to level the contour of the intended expressway. Again, to straighten out vertical alignment, he may have to fill in valleys or depressions. Soil sometimes misbehaves when disturbed, and the fill material will have to be carefully selected and compacted to provide a firm foundation for the intended surfacing. If the intended road goes over a peat deposit, his troubles may be more serious; jetting or deep excavation by dragline may be necessary, for in no case will the offending organic matter make a secure footing for the highway and must be entirely removed. During these cutting and filling operations, the natural drainage-

ways established over the ages will have been disturbed and the soils engineer and drainage engineer will have to coordinate their efforts to reestablish proper drainage. Costly installations must be put underground where the motorist will never see them.

So far, the engineer, in his planning, must adapt himself to what geologic history, as influenced by the weather, has provided him. This is unglamorous business and rarely reaches the newspapers, but actually it is a most vital part of road building.

Daily weather influences construction. When construction starts, the day-to-day weather becomes highly important to the operation. Sudden or prolonged rains, unexpected freezing or thawing, or any unusual weather behavior puts a burden on the contractor's operations and may catch him unprepared. Roofing over his work is unthinkable; his crew may be spaced out over several miles. Far up ahead, land is being cleared, and a little back of that, heavy grading is going on with installation of drainage structures; granular base and fine grading is following and finally the actual paving operation is reached. This is followed by clean-up and painting crews, by the sodding of slopes, etc. Twenty-four-hour and five-day weather forecasts are vital to all these activities and are carefully scrutinized. A recent job near Ann Arbor was estimated to have a daily labor-plus-overhead cost of \$5100.00 for the paving part of the operation alone. The annual salary of the average university professor could not stand many inclement days at this rate!



FIG. 1. Frost heave on highway near Ann Arbor. Upward movement of underlying frost-susceptible soil has cracked pavement transversely.

Effect of climate on roadway. After paving and clean-up is completed and the construction crews have left, traffic and mother nature take over. If the pavement and bridges are properly designed to withstand anticipated traffic densities and loads, a certain amount of wear and tear will result from this traffic, but nature itself will be the one to ultimately cause the greatest destruction.

Underlying soil. For instance, if the judgment of the soils engineer or vigilance of inspection has faltered such as to leave frost-susceptible soil in the road base, heaving of the road surface will result in the first season or may await later the proper combination of weather factors, just the right amount of moisture and freezing to cause formation of ice lenses in the soil to create severe volume change. Fig. 1 shows a frost heave on a highway near Ann Arbor. Upward movement of the underlying soil has cracked the pavement transversely. The flag on the pole warns the motorist of an unpleasant bump.

As a group, soils engineers appear to have studied weather factors more in detail than most associated with the highway industry. For instance, soils engineers have found cumulative degree days useful in predicting the depth of frost penetration which is in turn related to the depth below which they need not be so careful to remove frost-susceptible soils. Fig. 2 shows a plot of this index for one winter in New Jersey, for the severe 1947-48 season [5].

Pavement surface. The pavement surfaces, themselves, are acted upon by climatic factors. Bituminous pavements consist of mineral aggregate bound together by various types of asphaltic materials. The sun's radiation, coupled with wind and rain and high summer temperature, invariably cause a slow transfer of the bituminous binder from a plastic semi-solid to a weak brittle solid. In the last stages, the plastic

properties of the bituminous binder have been lost and the pavement crumbles under traffic, or even without traffic. Most of us have probably observed abandoned streets put in subdivisions by over-optimistic developers. Without any traffic, these will frequently be in poor condition after a relatively few years and show what nature alone can accomplish. The roofing and asphalt-shingle industry have long ago learned that protection of their products from the sun is essential, and so they cover built-up roofs with crushed rock, pebbles, or slag and imbed mineral granules on the surface of asphalt shingles. Without pinpointing the reaction to the complete satisfaction of the organic chemist, the weathering action on the bituminous hydro-carbons is one of slow oxidation, slow removal of the volatiles, and slow increase of the carbon-hydrogen ratio.

2. Weathering of portland-cement concrete

General. In the case of portland-cement concrete pavements and structures, weathering action is quite different and will be the subject of the remainder of this discussion. With a few, but nonetheless important exceptions, weathering here appears to be primarily a physical reaction. The exceptions where chemical reactions are important will be mentioned only briefly, as follows:

- (1) Concrete in contact with sulfate soils, such as occurs in California, may show chemical deterioration.
- (2) A few rock types used as aggregate in concrete react deleteriously with alkalies in the portland cement causing undue expansion of the concrete. Troubles from this source have been reported from many parts of the United States, Canada, and Australia. Generally, the rock types contain forms of amorphous silica—such as opal or chalcedony. Remedial measures are now well known and used.
- (3) In certain industrial applications, special protection may be given the concrete against chemical attack by strong alkalies or acids.

By far the most significant destructive agency of concrete exposed outdoors is the weather itself, particularly in northern climates. Freezing and thawing action in the presence of moisture may cause rapid breakdown of concrete. The use of chloride salts on highways for removal of ice and snow accelerates this destructive action. Concrete made under lax control of ingredient proportions or careless handling in placement and curing will be even more vulnerable to frost attack.

If the structure of hardened portland-cement concrete is considered for a moment, the reason for the

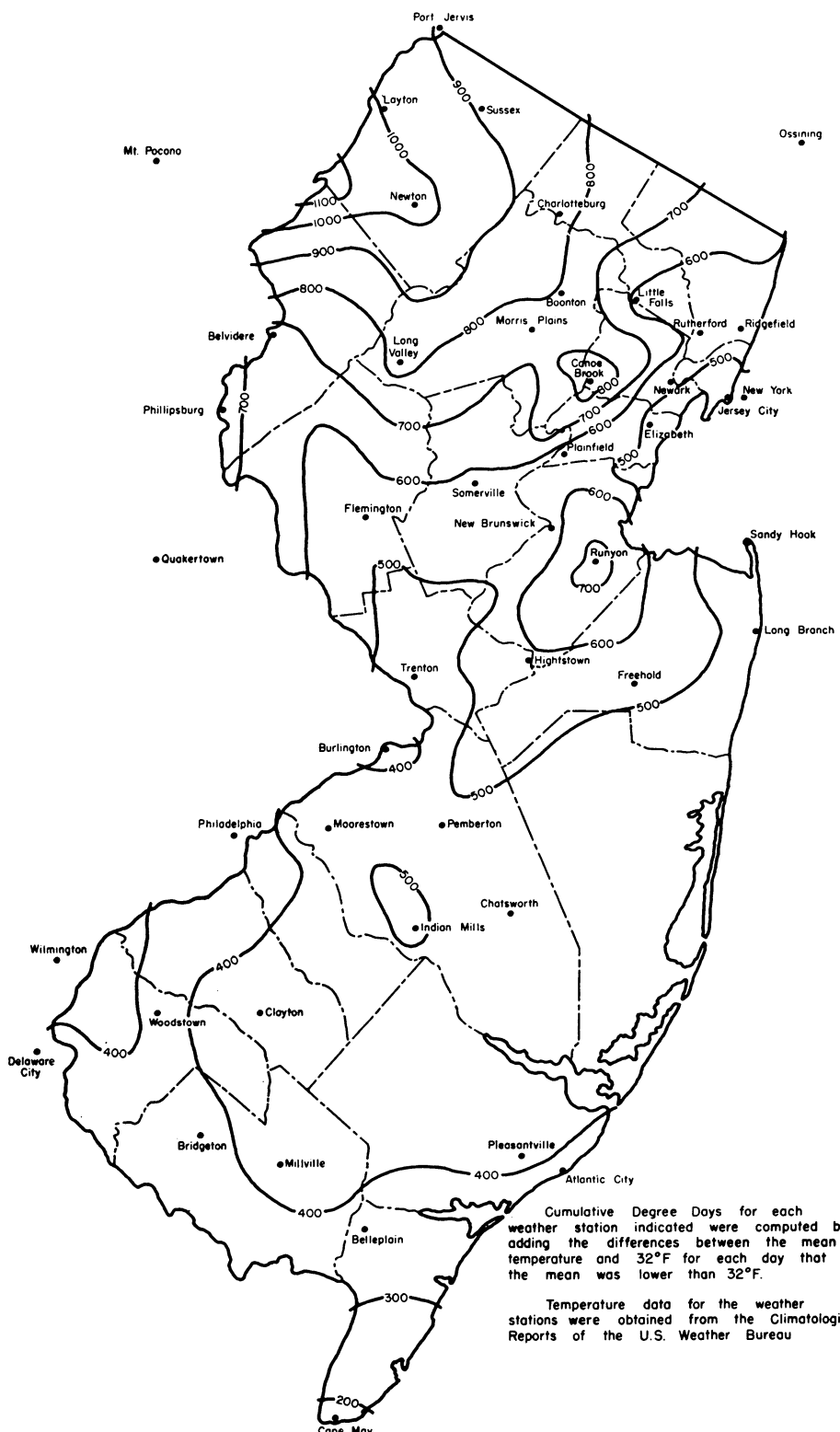


FIG. 2. Cumulative degree days for New Jersey. Severe winter of 1947-48. This index has proven useful to highway-soils engineers. (From [5]. Reproduced by courtesy of Highway Research Board.)

vulnerability of low quality concrete to frost attack, in the presence of moisture, should be apparent. At the time of mixing the concrete, water is added which combines chemically with the cement to bind together the mineral aggregates. Almost without exception, more water is added than necessary to complete this hydration reaction. This is done to promote workability of the plastic concrete for easy filling of the forms. The excess water forms capillary spaces since it will not be used in the hydration process. If these capillaries remain filled with water which freezes under adverse weather conditions, or if the concrete dries out and they later become filled, ice formation causes expansion action which may disrupt the concrete. The granular gel which imparts the characteristic hardness and rigidity to concrete itself contains some interstitial water. The latter water is classed as non-freezable, since it is contained in such sub-microscopic pore spaces that it cannot freeze at any temperature of interest [7]. The vulnerability of high-water-content concrete to frost attack has long been known and nearly all specifications place an upper limit on the allowable water-cement ratio. Minimum water content, consistent with required workability of the fresh concrete, is now insisted upon by all informed users.

Air entrainment. A development of the past twenty years which has had remarkable success in alleviating freeze-thaw problems of concrete is air-entrainment. By incorporating exceedingly small amounts of certain organic foaming agents in the concrete, a well dispersed system of minute air bubbles is created. Surrounding each air bubble is a zone of protected concrete highly resistant to frost action. For best protection, the average spacing of the bubbles must not exceed about 0.01 in. If the concrete is moist and contains water in the capillaries, the air bubbles provide escape boundaries for water forced ahead by the advancing ice front, thus dissipating dangerously high hydraulic pressures. All informed users and national specifications now require the use of air-entrained concrete where weather-exposure conditions are expected to be severe. Fig. 3 shows an accurate drawing of a polished section, $\frac{1}{10}$ in square, of air-entrained concrete. This was made using a camera lucida attachment on the microscope. Note that the air bubbles tend to be circular—*i.e.*, spherical in three dimensions, and are now considered a separate ingredient of concrete.

Laboratory weathering tests. Methods. Concrete technologists have for many years sought means by which they could accelerate weathering action simulating nature's cycles of freezing and thawing; the techniques used have varied from informal procedures of manually transporting specimens in and out of cold

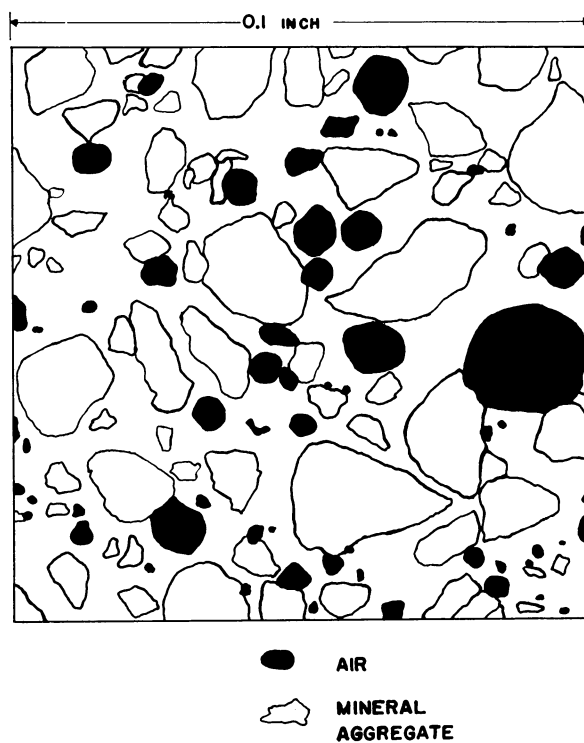


FIG. 3. Reproduction of 1/10-in-square plane section of air-entrained concrete showing distribution of generally spherical bubbles.

chambers or deep-freeze boxes to elaborate fully automatic devices to simultaneously carry many specimens through prescribed temperature and moisture cycles. Tidal variations of the sea providing thawing, coupled with the cold winters for freezing, have been used at Treat Island, Maine to provide nature's own automatic freeze-thaw apparatus for testing concrete [6].

Interpretation of the results of these accelerated weathering tests has provided a challenge to the best efforts of competent physicists, engineers, and chemists. Anomalous results have been frequent and most disconcerting. Concrete displaying good job performance, has on occasion, broken down rapidly in accelerated tests and, conversely, poor concrete has sometimes shown good behavior in accelerated tests. This anomalous behavior can be explained, at some risk of oversimplification, to different, and usually unknown, degrees of water saturation of the concrete under the procedures of different investigators. Water expands about 9 per cent upon freezing. Concrete, at about 91 per cent saturation, is therefore at a critical point with respect to freezing and thawing and may show anomalous behavior depending upon what might normally be expected to be insignificant changes in water content. Also temperature gradients and end temperatures of the cycles influence behavior of the concrete.

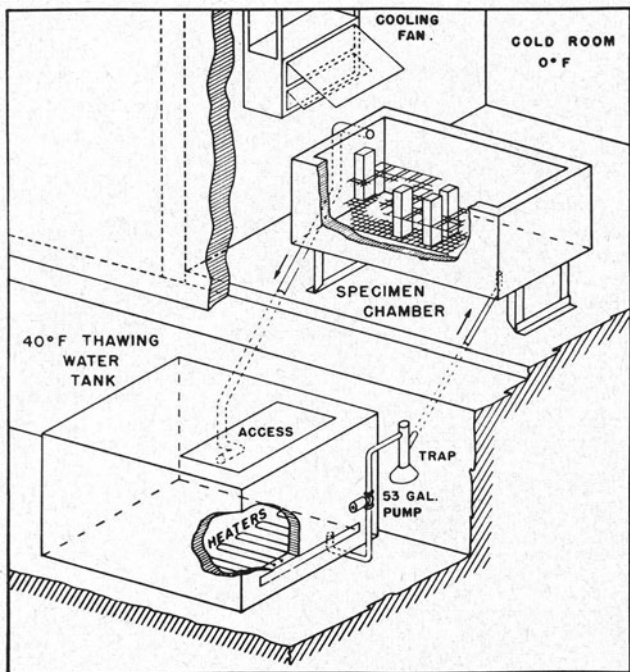


FIG. 4. Schematic diagram of automatic freeze-thaw apparatus for concrete being used at State Highway Laboratory at University of Michigan. (From [4]. Reproduced by courtesy of Highway Research Board.)

The American Society for Testing Materials, whose responsibility it is to prepare standard test methods, issued in 1952 four freeze-thaw methods for concrete [1]. It was thought that this would encourage standardization by means of which some concordance of results could be achieved. At present, most laboratories have patterned their procedures after one of these four methods. Two of the A.S.T.M. methods are "fast,"—*i.e.*, giving the concrete from six to twelve freeze-thaw cycles daily. In both cases, the specimens alternate between 0F and 40F. In one, the specimens are continuously submerged in water, and, in the other, water surrounds the specimens only during the thawing portion of the cycle. The other two A.S.T.M. methods provide "slow" cycles, giving either one or $\frac{1}{2}$ cycle per day. In one, the specimens are alternated between 0F and 73F when immersed in water or brine, and, in the other, between 0F and 40F. The latter procedure freezes the specimens in air and thaws them in water.

It should be obvious to the meteorologist that these four procedures by their repetitiveness and extremes of temperature at the low end of the cycle furnish a highly stylized facsimile of actual weather. Indeed, the concrete technologist is concerned lest he introduce such an exaggeration of nature that unrealistic variables are being inserted in the picture. Acceleration is desired and, in fact, mandatory, but it is hoped that side effects do not overshadow the main goal.

Fig. 4 shows a schematic diagram [4] of automatic freeze-thaw equipment being used at the Michigan State Highway Laboratory here at the University. This equipment has been used primarily for study of mineral aggregates in concrete and furnishes a cycle which complies with the requirements of A.S.T.M. Method C-291, "Resistance of Concrete Specimens to Rapid Freezing in Air and Thawing in Water." In the freezing and thawing cycle used for evaluation of aggregates, 3- by 4- by 16-in concrete specimens made with the test aggregate are placed in the specimen chamber on a rack which keeps them accurately positioned for uniform exposure to both the freezing air and thawing water. Freezing is accomplished by circulating cold room air at 0F to -5F around specimens. The temperature of the center of the specimens is brought from 40F to 0F in $2\frac{1}{2}$ hr and remains at this temperature for 30 min, at which time a switch turns on the centrifugal pump and rapidly circulates water at 42F around the specimens to thaw them. The water continues to recirculate by means of the overflow, the specimen centers rise to 40F in 45 min, thawing continues for an additional 15 min at which time the pump automatically stops, and the water in the specimen chamber then drains back by gravity through the pump into the thawing water storage tank. The equipment thus provides six complete cycles per day. Temperature loss of the thawing water (about 3F per cycle) is made up by five 1000-w thermostatically controlled immersion heaters in the thawing tank. Thirty-six specimens can be tested simultaneously.

Internal destruction of the concrete caused by expanding aggregate during the freeze-thaw tests is measured by the sonic apparatus shown in fig. 5. An oscillator drives the specimen under observation into flexural vibration and, by suitable adjustment of the frequency, the specimen can be made to vibrate in its first mode. Examination of the Lissajou figures on the oscillograph, one plate of which is connected to a phonograph pick-up which follows the transmitted vibrations at the other end of the specimen, helps identify that the specimen is being driven in its first mode. Since the change in modulus of elasticity is proportional to this frequency squared, destruction of the specimen can be traced by making this determination at suitable intervals as freezing and thawing progress. Diminished modulus of elasticity invariably accompanies internal breakdown.

Otherwise excellent concrete containing some Michigan mineral aggregates have been found to fail in as few as 15 or 20 cycles, whereas other aggregates of high quality may last more than 1000 freeze-thaw cycles. Fig. 6 shows a photograph of a Michigan pavement only a few years old showing surface defacement caused by an aggregate of low freeze-thaw durability.

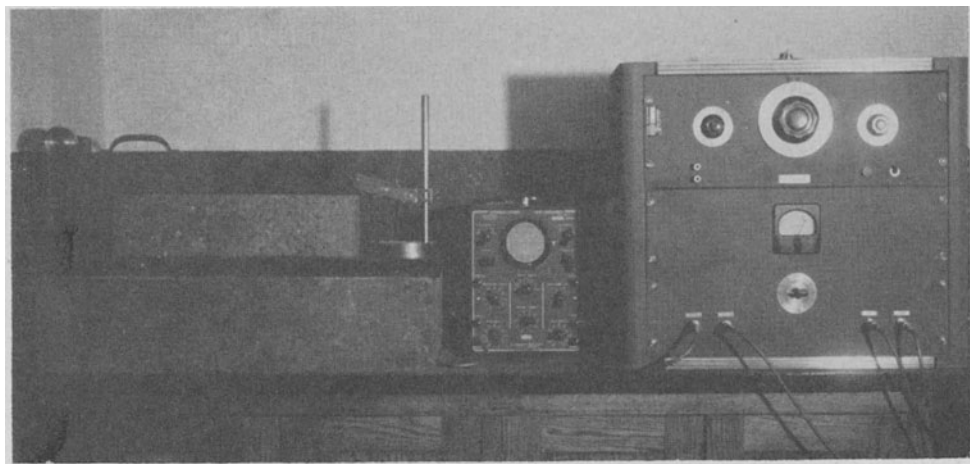


FIG. 5. Sonic modulus of elasticity apparatus used for measuring internal destruction of concrete due to freezing and thawing.

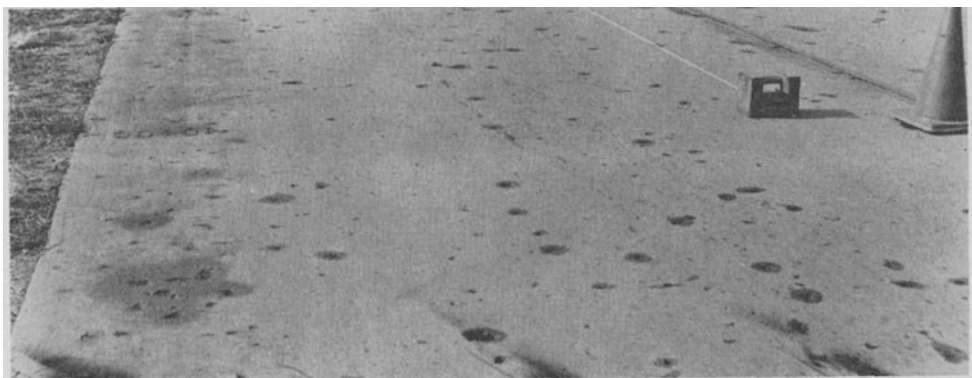


FIG. 6. Six-yr-old Michigan pavement defaced by freeze-thaw action on susceptible mineral aggregates, causing pitting of surface.

Expansive aggregates have popped out of the concrete surface causing the pitting.

Interpretation of results. The results of freeze-thaw tests of concrete from many investigators around the nation are voluminous. Each investigator is, of course, hopeful that these results will prove useful to him in predicting the behavior of concrete in actual service. He has been cautioned, however, by the scope written for each one of the aforementioned A.S.T.M. freeze-thaw test procedures wherein it is stated that "This method is not intended to provide a quantitative measure of the length of service that may be expected from a specific type of concrete." This pretty effectively reflects the committee's caution in assessing job variables.

At about this point, it appears that the meteorologist should be of assistance—at least in the viewpoint of a non-meteorologist. For instance, do differing weather factors permit the concrete technologists in Detroit, Michigan to compare freeze-thaw results with a fellow worker intending to place concrete in the high mountains of California? The marked difference in the

vegetation at the two points suggests that there must be substantial soil and weather differences. Can the meteorologist quantitatively characterize the climate differences so as to be helpful to the engineer?

Concrete technologists agree that there is an interplay of moisture content and freeze-thaw cycles which, under certain conditions, will deteriorate poor concrete or even good concrete containing poor mineral aggregates. It has been suggested that concrete in the summer months receives a reprieve under drying conditions which fortify it for the next winter's freeze-thaw situation [8]. Soil scientists have observed, however, that, under certain conditions of pore water pressure in base courses, hot summer days may instead cause rise of water to the surface of pavements [3]. Possibly some pavements do not receive this summer reprieve and tend toward saturation the year around.

At least one group of manufacturers and consumers has considered weather factors as influencing standard material acceptance tests. A tentative revision to American Society for Testing Materials Specification

Designation: C62-58, for "Building Brick (Solid Masonry Units Made from Clay or Shale)" [2], incorporates a map of the United States showing southern regions where it is unlikely that there will be high moisture saturation of exposed brick concurrently with cycles of freezing and thawing. In these areas, absorption and saturation coefficient requirements of the brick are proposed to be waived.

The monetary stake in the proper weathering behavior of concrete for highways is not small, and its mention may serve a purpose in putting this matter in better perspective. The Michigan State Highway Department alone, for instance, is now using concrete at the rate of roughly two million cubic yards per year. At a minimum cost of about \$18.00 per cu yd for paving concrete, this makes the annual investment thirty-six million dollars. Bridge concrete in place will have a unit cost much more than this, and although the annual volume consumption is relatively small, the dollar contribution will increase the above total estimate. The contributors to highway funds are entitled to use of the best engineering knowledge at such a rate of expenditure of their money.

3. Conclusions

In conclusion, the following observations are offered:

(1) The highway engineer inherits a terrain over which he must work which has been acted upon by centuries of weathering action. He must live with what he finds.

(2) During construction operations, climatic factors are important, and day-to-day weather forecasts are vital. Considerable progress appears being made in this regard.

(3) After construction, his product is at the mercy of traffic and climatic factors. The weather factors may well combine to be destructive to his handiwork. At least two construction groups have been mentioned as making attempts to quantitatively characterize climate differences in the United States—namely, highway soils engineers and those in the brick industry. Is help forthcoming for those in other fields, preferably from meteorologists trained in such matters? The question may be raised whether the investigator, intent on improving the weather resistance of a construction material for a certain climate, may only be shadow-boxing since he does not well know the tactics of his adversary.

REFERENCES

1. American Society for Testing Materials, 1955: *ASTM Standards*, Part 3, pp. 1339–1354.
2. American Society for Testing Materials, 1958: *ASTM Standards*, Part 5, pp. 31–37.
3. Barber, E. S., and G. P. Steffens, 1958: Pore pressures in base courses. *Public Roads*, **30**, No. 3, 53–62.
4. Legg, F. E., 1956: *Freeze-thaw durability of Michigan concrete coarse aggregates*. Highway Res. Board, Bull. 143, 13 pp.
5. Jumikis, A. R., 1956: *Cold quantities in New Jersey, 1901–1955*. Highway Res. Board, Bull. 135, 122 pp.
6. Kennedy, T. B., and K. Mather, 1953: Correlation between laboratory accelerated freezing and thawing and weathering at Treat Island, Maine. *Proc. Amer. Concrete Inst.*, **50**, 141–172.
7. Powers, T. C., and R. A. Helmuth, 1953: Theory of volume changes in hardened portland cement paste during freezing. *Proc. Highway Res. Board*, **32**, 286.
8. Powers, T. C., 1955: Basic considerations pertaining to freezing-and-thawing tests. *Proc. Amer. Soc. Testing Materials*, **55**, 1132–1155.

METEOROLOGICAL MONOGRAPHS

- Vol. 1, No. 1. *Wartime Developments in Applied Climatology* by W. C. Jacobs. August, 1947. \$1.00. Out of print.
- No. 2. *The Observations and Photochemistry of Atmospheric Ozone and Their Meteorological Significance* by R. A. Craig. September, 1950. \$2.50.
- No. 3. *On the Rainfall of Hawaii: a group of contributions* by L. B. Leopold; H. Landsberg; C. K. Stidd and L. B. Leopold; T. C. Yeh, C. C. Wallén, and J. E. Carson; and T. C. Yeh, J. E. Carson, and J. J. Marciano. June, 1951. \$2.50.
- No. 4. *On Atmospheric Pollution: a group of contributions* by J. H. Carter, C. A. Gosline, E. W. Hewson, H. Landsberg; M. L. Barad; G. W. Brier; W. C. L. Hemeton; P. H. Lowry; P. H. Lowry, D. A. Mazzarella, M. E. Smith; H. F. Poppendiek; H. Rouse; R. H. Sherlock; M. E. Smith. November, 1951. \$4.50.
- No. 5. *Forecasting in Middle Latitudes* by H. Riehl; and J. Badner; J. E. Hovde; N. E. La Seur; L. L. Means; W. C. Palmer; M. J. Schroeder; L. W. Snellman; and others. June, 1952. \$3.50. Out of print.
- Vol. 2, No. 6. *Thirty-Day Forecasting: a review of a ten-year experiment* by Jerome Namias. July, 1953. \$3.50.
- No. 7. *The Jet Stream* by H. Riehl, M. A. Alaka, C. L. Jordan, and R. J. Renard. August, 1954. \$3.50.
- No. 8. *Recent Studies in Bioclimatology: a group* by C. W. Thornthwaite and J. R. Mather; W. G. Wellington; J. D. Findlay; L. P. Herrington; H. F. Blum; C. Monge M.; G. and B. Duell; F. Sargent, II; H. Landsberg; K. Buettner; J. M. May; J. H. Foulger. Edited by F. Sargent, II and R. G. Stone. October, 1954. \$5.00.
- No. 9. *Industrial Operations under Extremes of Weather* by J. A. Russell; W. W. Hay; J. W. Waters; H. E. Hudson, Jr.; J. Abu-Lughod, W. J. Roberts, and J. B. Stall; A. W. Booth; and E. F. Taylor. Edited by J. A. Russell. May, 1957. \$6.00.
- No. 10. *Interaction of Sea and Atmosphere: a group of contributions* by A. C. Redfield, A. R. Miller; G. W. Groves; D. L. Harris; R. O. Reid; W. Marks and J. Chase. June, 1957. \$5.00.
- No. 11. *Cloud and Weather Modification: a group of field experiments* by S. Petterssen; J. Spar; F. Hall; R. R. Braham, Jr., L. J. Battan, and H. R. Byers; H. J. aufm Kampe, J. J. Kelly, and H. K. Weickmann. July, 1957. \$6.00.
- Vol. 3. *Meteorological Research Reviews: summaries of progress from 1951 to 1955*. July, 1957. \$7.00. (Numbers 12-20, Volume 3, are bound as one volume.)
- No. 12. *Review of Climatology, 1951-1955* by H. E. Landsberg.
- No. 13. *Meteorological Instruments* by J. C. Bellamy.
- No. 14. *Radiometeorology* by J. S. Marshall and W. E. Gordon.
- No. 15. *Weather Observations, Analysis, and Forecasting* by S. Petterssen.
- No. 16. *Applied Meteorology* by T. F. Malone.
- No. 17. *Physics of the Upper Atmosphere* by E. O. Hulbert.
- No. 18. *Physics of Clouds* by H. J. aufm Kampe and H. K. Weickmann.
- No. 19. *Physics of Precipitation* by H. K. Weickmann.
- No. 20. *Atmospheric Electricity* by H. J. aufm Kampe.
- Vol. 4, No. 21. *Studies of Thermal Convection in a Rotating Cylinder with some Implications for Large-Scale Atmospheric Motions* by Dave Fultz, Robert R. Long, George V. Owens, Walter Bohan, Robert Kaylor, and Joyce Weil. \$9.00.
- No. 22. *Topics in Engineering Meteorology* by J. M. Biggs, G. S. Vincent, A. K. Blackadar, H. E. Cramer, E. P. Segner, E. Cohen, C. C. Bates and M. A. Kohler, S. A. Changnon, F. A. Hoff and R. G. Semonin, M. K. Thomas, R. W. Gerdel, A. H. Murphy, R. A. Boyd, I. Solomon and W. C. Spreen, O. L. Stokstad, and F. E. Legg. \$8.00.

Orders for the above publications should be sent to:
THE AMERICAN METEOROLOGICAL SOCIETY
 45 BEACON ST., BOSTON 8, MASS.

Continued from Cover 2

number, pages. For a book: author(s), year, title of book (underlined), city of publication, publisher, pages.

8. Appendix. Essential material which is of interest to a limited group of readers should not be included in the main body of the text but should be presented in an appendix. It is sufficient to outline in the text the ideas, procedures, assumptions, etc., involved, and to refer the reader to the appendix for fuller details. For example, lengthy and involved mathematical analyses are better placed in an appendix than in the main text.

9. Legends. Each figure must have an adequate legend and a list of these legends must be supplied on a separate sheet of paper.

Illustrations. The illustrations should accompany the manuscript and be in final form. Each figure should be mentioned specifically in the text. Figure number and legend will be set in type and must not be part of the drawing. A separate list of legends should be provided. The following details should be observed:

1. Drawings should be done entirely in black India ink. It is often desirable to submit photographic copies

of original drawings, retaining the originals until the manuscript has been accepted and is ready to go to the printer. If the drawings are large, photographic copies should be no larger than $8\frac{1}{2} \times 11$ inches to facilitate reviewing and editing.

2. The width of a figure as printed is $3\frac{1}{8}$ inches or, less frequently, $6\frac{1}{2}$ inches. Original drawings are preferably about twice final size but in no case larger than five times or 22×32 inches.

3. Lettering must be large enough to remain clearly legible when reduced; after reduction the smallest letters should not be less than $1/16$ inch or 1 mm high.

4. Maps should be oriented so that the meridian through the center of the drawing is parallel to its sides.

Mathematical symbols and equations. It is preferable to enter all equations except the simplest ones by pen and ink rather than by typewriter. To permit marking for the printer, leave ample space above and below all centered equations and symbols within the equations. Explain ambiguous or uncommon symbols by marginal notes in pencil.